

Field and Laboratory Investigations of the Adsorption of Nitrogen Compounds on Estuarine Based Sediments

Fathia Abdulgawad
B.Sc., M.Sc

Thesis submitted for the degree of
Doctor of Philosophy

Division of Civil Engineering, Cardiff School of Engineering
Cardiff University

March 2010

UMI Number: U585348

All rights reserved

INFORMATION TO ALL USERS

The quality of this reproduction is dependent upon the quality of the copy submitted.

In the unlikely event that the author did not send a complete manuscript and there are missing pages, these will be noted. Also, if material had to be removed, a note will indicate the deletion.



UMI U585348

Published by ProQuest LLC 2013. Copyright in the Dissertation held by the Author.
Microform Edition © ProQuest LLC.

All rights reserved. This work is protected against
unauthorized copying under Title 17, United States Code.



ProQuest LLC
789 East Eisenhower Parkway
P.O. Box 1346
Ann Arbor, MI 48106-1346

ABSTRACT

Nitrogen plays a major role in the metabolism of aquatic eco-systems. However, at low concentrations it can affect primary productivity and rise to very high concentrations, leading to eutrophication problems. Nitrogen compound fluxes in the aquatic environment are in the form of nitrate, ammonium or nitrite. Ammonium is soluble in the water column and depending on the type of sediment it can be adsorbed onto the sediments. Ammonium adsorption processes have been the main focus of this study in both deionised and saline waters, and for clean clay and sand and natural sediments taken from the Loughor Estuary, in Wales. An equation for ammonium adsorption onto bed sediments has been developed and included in the DIVAST water quality model, which is based on the QUAL2E US EPA model. The adsorption coefficient was found for both fresh and saline water conditions. It was found that adsorption, and consequently the adsorption coefficient, decreases with increasing salinity. Nitrate adsorption was also studied in this research project and it was confirmed that nitrate can adsorb only to specific types of clay, such as Kaolinite and organic matter.

Salinity was found to influence nitrate adsorption on the clay and the types and amount of clay present in the bed sediments were found to have an impact on the nitrate mobility across the sediment water interface.

The results of the field study for the Loughor Estuary have shown that ammonium adsorption decreased with increasing salinity. The highest amount of ammonium adsorption was found during March, at site 1b at 80.3 $\mu\text{g/g}$. Dissolved inorganic nitrogen (DIN) was found to be dominated by nitrate and nitrite during autumn and spring, whereas the DIN was found to be dominated by ammonium in the summer. Ammonium and Nitrite concentrations of 4.25 mg/l and 10.23 mg/l respectively, were found to be the highest recorded in literature for UK estuaries. Nitrate concentrations were present on 30th June at all sampling sites and increased with incoming tide, indicating the coastal water source for nitrates during this time of the year. The suspended sediment present in the Loughor Estuary was found to be independent of the velocities present and not sensitive to the difference in velocities.

Acknowledgements

My thanks go to my supervisors Dr Bettina Bockelmann and Professor Roger Falconer for their assistance, and their continuous guidance through this period of study. Through their guidance I acquired immense knowledge which without them this study would not have come into fruition.

I grateful to the Libyan government to giving me the opportunity to acquire this degree.

I would like to thank Professor Keith Williams and Dr Devin Sapsford for their knowledge and assistance during my research studies. I would like to thank the Cleer lab staff especially Jeffery Rowlands and Ravi Mitha whos assistance has been helpful and essential throughout.

Many thanks to my parents and sibling for their encouragement love and advice in completing this degree.

Special thanks to the research office staff for their help and social behaviour.

At least not last, I would like to show my appreciation to all my friends especially Dr Richard March, Xiaoline Wang, James Littler, Suraya Sharil Asma Saidi for encouragement and support during my studies. Thank you.

TABLE OF CONTENTS

ABSTRACT	I
ACKNOWLEDGEMENTS	II
TABLE OF CONTENTS	III
NOTATION	VI
1 INTRODUCTION	1
1.1 EUTROPHICATION	2
1.2 EU WATER FRAMEWORK DIRECTIVE (WFD)	3
1.2.1 EU Nitrate Directive	4
1.2.2 EU Habitats Directive	5
1.3 THE NITROGEN CYCLE IN AQUATIC SYSTEMS	5
1.3.1 Ammonification (mineralisation)	5
1.3.2 Nitrification	6
1.3.3 Denitrification	7
1.3.4 Anammox (anaerobic ammonium oxidation)	8
1.3.5 Nitrogen fixation	9
1.4 AIMS AND OBJECTIVES	9
1.5 OBJECTIVES	10
1.6 ORGANISATION OF THE THESIS	10
2 LITERATURE REVIEW	13
2.1 SOURCES OF WATER POLLUTION	13
2.1.1 Diffuse source pollution	13
2.1.2 Atmospheric deposition	14
2.1.3 Runoff	14
2.1.4 Agriculture Impact	15
2.1.5 Irrigation impacts on surface water quality	16
2.1.6 Sources of nitrogen from agriculture	17
2.2 SEDIMENT ADSORPTION	19
2.2.1 Types of adsorption	20
2.2.2 Adsorption isotherms	21
2.2.3 Adsorption Isotherm Models	22
2.2.4 Kinetics of adsorption	26
2.2.5 Ammonium adsorption to sediments	27
2.2.6 Factors affecting ammonium adsorption	28
2.3 SETTLING VELOCITY OF SEDIMENTS	32
2.4 HYDRO-ENVIRONMENTAL COMPUTER MODELS	33
2.4.1 Surface water models	35
2.4.2 River, estuarine and coastal models	36
2.4.3 DIVAST	37
2.5 SUMMARY	39
3 WATER QUALITY MODELS	41

3.1	QUAL2E MODEL	42
3.1.1	<i>Nitrogen compound processes in QUAL2E</i>	43
3.2	QUAL2K MODEL.....	47
3.3	N-MODEL	48
3.4	WATER QUALITY ANALYSIS SIMULATION PROGRAMME (WASP)	50
3.4.1	<i>WASP Version 5 (WASP5)</i>	50
3.5	SUMMARY	51
4	LABORATORY EXPERIMENTS – MATERIALS AND METHODS	52
4.1	SAMPLE PREPARATION	52
4.1.1	<i>Water sample</i>	52
4.1.2	<i>Clays and sand</i>	53
4.2	PARTICLE SIZE DISTRIBUTION ANALYSIS OF CLAYS AND SAND	56
4.3	ADSORPTION EXPERIMENTS	57
4.3.1	<i>Adsorption isotherm experiments</i>	57
4.3.2	<i>Desorption experiments</i>	58
4.3.3	<i>Kinetic experiments using artificial sea water</i>	58
4.3.4	<i>Nitrate adsorption on Kaolinite</i>	59
4.4	SAMPLE ANALYSIS.....	60
4.4.1	<i>Use of HACH reagent to determine ammonium concentration</i>	61
4.4.2	<i>Use of HACH reagent to determine the nitrate concentration</i>	61
4.4.3	<i>Calibration curve for ammonium</i>	62
4.4.4	<i>Calibration curve for nitrate</i>	62
4.4.5	<i>pH and EC readings</i>	63
4.5	SUMMARY	64
5	LABORATORY EXPERIMENTS – RESULTS AND DISCUSSION	65
5.1	AMMONIUM ADSORPTION ISOTHERMS.....	65
5.1.1	<i>The Chi-square test (X^2)</i>	71
5.1.2	<i>Nonlinear regression (R^2)</i>	71
5.2	SALINITY AND AMMONIUM ADSORPTION ISOTHERM EXPERIMENT	79
5.2.1	<i>Salinity effect on ammonium adsorption coefficient</i>	82
5.3	DESORPTION KINETICS USING ARTIFICIAL SEA WATER.....	85
5.4	NITRATE ADSORPTION	88
5.5	CLAYS AND SAND PARTICLE SIZE	91
5.6	DISCUSSION	91
5.6.1	<i>Adsorption isotherms</i>	91
5.6.2	<i>Desorption kinetics using artificial sea water</i>	94
5.6.3	<i>Nitrate adsorption</i>	95
5.7	SUMMARY	97
6	CASE STUDY OF THE LOUGHOR ESTUARY	99
6.1	THE STUDY AREA.....	99
6.2	SAMPLE COLLECTION	99
6.3	MATERIALS AND METHODS.....	103
6.3.1	<i>Determination of the physico-chemical characteristics for the Loughor Estuary bed sediments</i>	103
6.4	FIELD SAMPLE EXPERIMENTS	109
6.4.1	<i>Ammonium adsorption of bed sediment</i>	110
6.4.2	<i>Ammonium adsorption isotherm of bed sediment</i>	111

6.4.3	<i>Fixed ammonium on the bed sediment</i>	111
6.4.4	<i>Salinity effect on ammonium adsorption</i>	112
6.4.5	<i>Dissolved ammonium concentration</i>	112
6.4.6	<i>Sediment and water nitrate and nitrite concentration</i>	112
6.5	SUMMARY	114
7	RESULTS AND DISCUSSION OF FIELD WORK	115
7.1	PHYSICO-CHEMICAL CHARACTERISTICS OF THE SEDIMENT	115
7.1.1	<i>Porosity, particle and bulk density of bed sediment samples</i>	115
7.1.2	<i>Inorganic, organic and total carbon content</i>	116
7.1.3	<i>Particle size distribution of the Loughor Estuary bed sediments</i>	117
7.1.4	<i>X-ray diffraction (XRD)</i>	120
7.1.5	<i>Adsorption isotherm results</i>	122
7.1.6	<i>Salinity effects on ammonium adsorption</i>	133
7.1.7	<i>Comparison of adsorption coefficients of field data and clean clays (Montmorillonite, Kaolinite) and sand (fine and coarse)</i>	137
7.1.8	<i>Field data from the Loughor Estuary</i>	138
7.2	DISCUSSION OF FIELD WORK	161
7.2.1	<i>Adsorption isotherms adsorption coefficients and the effect of physical parameters on the ammonium adsorption</i>	161
7.2.2	<i>Seasonal effects on ammonium adsorption</i>	164
7.2.3	<i>Salinity effect on ammonium adsorption</i>	165
7.2.4	<i>Sediment classification and composition</i>	166
7.2.5	<i>The influence of salinity on suspended sediment concentrations</i>	167
7.2.6	<i>Nitrogen compounds</i>	169
7.3	SUMMARY	175
8	CONCLUSIONS AND FUTURE WORK	179
8.1	AMMONIUM ADSORPTION EQUATION IN QUAL2E	179
8.2	LABORATORY EXPERIMENTS	179
8.3	RECOMMENDATIONS AND FUTURE WORK RESULTING FROM LABORATORY STUDY	182
8.4	FIELD EXPERIMENTS	183
8.5	RECOMMENDATIONS AND THE FUTURE WORK RESULTING FROM FIELD WORK	186
	REFERENCES	188
	APPENDIX 1 MINERALOGY OF THE SEDIMENT (XRD ANALYSIS)	204

NOTATION

α_4	Oxygen up take per unit of algal respiration/death(mg/O ₂ /mg-A)
p_2	Algal death rate (1/day)
A	Algal biomass (mg/l)
K_4	Bottom respiration rate of BOD (g O ₂ /m ² per day)
D	Average depth (m)
λ_2 and λ_1	oxygen production and consumption rate by plant respiration (O ₂ /m ² per day), respectively
\overline{Q}	Amount of adsorbate required to form a complete monolayer on the adsorbent surface
b	Constant related to the energy of adsorption
q_e	Amount of adsorbate adsorbed per unit weight of solid
C_e	equilibrium concentration of the solute remaining in solute
x	Mass of the adsorbate
m	Mass of the adsorbent
k and n	empirical constants
V	volume of solute
C_o	initial concentration
C_1	Concentration at a given time

N_4	Concentration of organic nitrogen, mg-N/L
β_3	rate constant for hydrolysis of organic nitrogen to ammonium nitrogen, temperature dependent, day ⁻¹
α_1	fraction of algal biomass that is nitrogen, mg-N/mg-A
ρ	Algal respiration rate, day ⁻¹
σ_4	rate coefficient for organic nitrogen settling, temperature dependent, day ⁻¹
N_1	Concentration of ammonium nitrogen, mg – N/L
N_3	Concentration of nitrate nitrogen, mg-N/L
N_4	Concentration of organic nitrogen, mg-N/L
β_1	rate constant for the biological oxidation of ammonium nitrogen, temperature dependent, day ⁻¹
σ_3	fraction of algal biomass which is nitrogen, mg-N/ft ² -day
d	mean depth of flow, m
F_1	fraction of algal nitrogen uptake from ammonium pool
μ	local specific growth rate of algae, day ⁻¹

F	fraction of algal nitrogen taken from ammonium pool
β_2	rate constant for the oxidation of nitrite nitrogen, temperature dependence, day^{-1}
EC_{riv}	river export coefficient (fraction N inputs to river that is exposed to estuary as nitrate)
$DINexp_{riv}$	sum of natural and anthropogenic DIN export by river to estuary (kg N Km^{-2} of watershed yr^{-1})
$Fert_{ws}$	fertilizer nitrogen (N) use (kg N Km^{-2} of watershed yr^{-1})
$NO3exp_{riv}$	sum of natural and anthropogenic nitrate export by river to estuary (kg N Km^{-2} of watershed yr^{-1})
Pop_d	population density (number of people per square kilometre of watershed)
$P_{sources}$	point sources sewage loading rates (kg N Km^{-2} of watershed yr^{-1})
$P_{pt\ ws}$	total atmospheric NO_y deposition (kg N Km^{-2} of watershed yr^{-1})
EC_{ws}	watershed export coefficient (fraction that is not retained)
Urb	fraction of population living in urban areas
Ws	watershed area (Km^2)

p_s	partition coefficient (l kg^{-1})
C	total chemical concentration (mg/l)
n	porosity of the sediment or 1 in the water column
$q_{e,m}$	equilibrium data obtained by calculated from model ($\mu\text{g/g}$)
q_e	experimental data of the equilibrium ($\mu\text{g/g}$)
SS_{reg}	unit of the Y-axis squared
SS_{tot}	sum of the square of the distances of the points from a horizontal line through the mean of all Y values
Q	amount of ammonium adsorbed by the different types of adsorbents ($\mu\text{g/g dry wt}$)
K^*	Slope of the regression line (ml/g) (adsorption coefficient)
K	dimensionless adsorption coefficient
C	ammonium ion equilibrium concentration in water (mg/l)
q	fixed ammonium content in the adsorbent ($\mu\text{g/g dry wt}$)
ρ	density of the sediment
S	salinity concentration (ppt)
Φ	porosity of the sediment

1 Introduction

The demand for water has increased with the increasing population of human beings and this has led to water scarcity in many parts of the world. The situation is aggravated by the problem of water pollution. Groundwater and surface water are an important part of the environment, and need to be protected from all sources of pollution because human survival depends on their sustainable use. Polluted groundwater can cause problems when it reaches the surface through seepage into surface water bodies or when it is pumped out for use as drinking water.

Coastal and estuarine ecosystems have been heavily influenced by human activity through pollution. However, human activity has caused accelerated eutrophication giving rise to problems in the affected water bodies. Eutrophication, the process characterised by an increase in phosphorus and nitrogen concentrations in the water frequently results in the development of undesirable biological populations.

Water quality can also be affected by climate and geology (DWAF, 1995; Boorman, 2003). Water pollution is related to human activity: e.g agriculture, cattle farming and urbanization. As a result, surface water and groundwater quality can be affected by both point sources, and diffuse sources of pollution. These pollutants can be both organic and inorganic.

A point source pollution is associated with domestic and industry discharge into estuaries and along the coast through a pipe or outlet. A diffuse source of pollution is defined as pollution arising from land use activities that are dispersed across a catchment or sub catchment. Agriculture is one of the main sources of diffuse pollution. In addition diffuse source pollution does not arise in the form of a process effluent, but as municipal sewage effluent. The diffuse sources of nutrient pollution to the aquatic environment vary largely throughout

the world's catchments due to variations in industry, population and agricultural practices (Pieterse et al., 2003).

Furthermore, this field of research can be impacted by large scale hydro-environmental projects, such as the proposed Severn Barrage. A barrage across the Severn would have large effects on the hydrodynamic processes and thus on the water quality. It would reduce suspended sediment concentrations in water column and thus turbidity and this would lead to more light penetrating into the water column, which would result in an increase in biodiversity. These would be seen as changes in nutrient concentrations and algal and fauna concentrations, which could lead to a decrease in eutrophication within the estuary. The main aim of this research project is to be able to predict more accurately nutrient transport process representation in estuarine and coastal waters. Representation can be achieved by including more realistic water quality process into water quality models.

1.1 Eutrophication

Eutrophication is the process caused by increases in the availability of nitrogen and phosphorus concentrations in surface waters. These nutrients are present in soil and water in the form of nitrate and phosphorus. However leaching of nutrients from agricultural soils is a significant source that has contributed to eutrophication of rivers and lakes. It has increased with the intensification of agriculture and the increased use of nitrogen fertilizers and manure.

The consequences of eutrophication can be an increased frequency of algal blooms (sometimes toxic), increased water turbidity, slime production, oxygen depletion in deep waters and mass fish and benthic fauna kills. In freshwaters phosphorus is considered to be limiting to algal growth, in marine waters this role is more likely to be caused by nitrogen and could be due either to nitrogen or phosphorus in brackish waters (Caddy, 1993). Algal production in transitional waters between fresh and fully saline waters (e.g in relatively enclosed coastal waters) can be limited by either nitrogen or phosphorus

depending upon whether the transitional area receives important freshwater supplies (Vollenweider et al., 1992). In estuaries factors such as water turbidity, light availability and retention time are equally important to nutrient concentrations and availability.

To prevent water quality problems all water resources must be protected and sustained. There are a number of legislations requirements and directives, which aim to prevent and decrease the contamination of surface water and groundwater from various sources of pollution.

1.2 EU Water Framework Directive (WFD)

Coastal, river and lake waters are crucial natural resources; they provide drinking water and vital habitats for many different types of wildlife. Significant proportions of them are under threat or environmental damage. Protecting the environment is an important part of achieving sustainable development.

The Water Framework Directive (2000/60/EC) aims to protect surface waters, including rivers, lakes, estuaries and coastal waters, and ground waters with regard to aquatic systems and to their water needs within the European Community. It highlights the need for integrated nutrient management strategies at catchment scale (Heathwaite, 2003). In the UK the Water Framework Directive is being implemented by the Environment Agency (EA) in England and Wales. The EA has been named the competent authority, and has statutory duties to investigate river basins and associated ground water bodies. The environmental objective of the Directive is to achieve good status for all groundwaters and surface waters by 2015; this might be sufficient time to implement the requirements of the directive, but the water supply and management infrastructure will have been required to be fully transformed. The Water Framework Directive (WFD) is the umbrella legislation to resolve the problems of water policy. The (WFD) is sets by following directives:-

1.2.1 EU Nitrate Directive

Increasing nitrogen inputs to the rivers and coastal waters through surface water runoff leads to eutrophication problems. Elevated concentrations of ammonium, through nitrates and nitrites derived from agricultural practice, can enhance the algal growth in surface waters, resulting in undesirable conditions in these aquatic systems and reducing the water quality of these waters. Agricultural practice can have a large affect on spreading of nitrate contamination in surface (river, lake and estuary) waters. In particular, inorganic and organic fertilisers applied on farmland are commonly responsible for nitrate pollution in estuaries and coastal waters. These pollutants are addressed by the EC Nitrate Directive.

The Nitrate Directive (91/676/EEC) aims to reduce the pollution of water caused by the application of inorganic fertilizer and manure on farmland. Overall, it has been designed to prevent ecological damage and ensure a safe drinking water resource. Also it establishes an upper limit of 50 mg/l nitrate in drinking water.

Eutrophication is defined in the Nitrates Directive as “the enrichment of water by nitrogen compounds, causing an accelerated growth of algae and higher forms of plant life to produce an undesirable disturbance to the balance of organisms present in the water and to the quality of the water concerned”. If waters are found to be eutrophic (high nutrient content), or might be become eutrophic, (i.e. high nutrient content) and a high amount of the nitrate present in the water comes from agricultural sources, then the Member State must designate the land draining into the affected waters as a vulnerable zone and put in place Action Programmes for reduced nitrate pollution.

The EU Nitrate Directive is implemented in the UK by the Environment Agency (EA) in England and Wales. Selected agricultural catchements in south west England have gained environmental benefits from changes in land use practices with particular emphasis on the eutrophic status of coastal waters. The EU Nitrate Directive has been applied in Wales particularly to limit the total amount of nitrogen from livestock manure that can be produced on a farm

within nitrate vulnerable zones to 170 kg of nitrogen per hectare per year (Nitrate Directive, 91/676/EEC).

1.2.2 EU Habitats Directive

Many coastal environments have undergone changes in their water quality and quantity caused by changes in annual and seasonal desertification, erosion and flooding, all of which have direct affect on habitats. The EU Habitats Directive (92/43/EEC) seeks to improve the quality of the environment and conserve natural habitats and wild fauna and flora. The Habitats Directive aims to ensure and maintain favourable conservation status of designated habitats and species by requiring member status to take measures to maintain natural habitats and wild species. The Water Framework Directive (2000/60/EC) aims to provide improved ecological status for river basins (Read et al., 2001).

1.3 The nitrogen cycle in aquatic systems

Most of the nitrogen enters rivers and coastal regions through runoff, which leads to increasing nitrogen input to the water body. Ammonium is a major component in the nitrogen loading to coastal areas. The processes of the nitrogen cycle in aquatic systems are: - Ammonification, Nitrification, Denitrification and Nitrogen fixation which will be covered in this section and an overview of the process is shown in Figure 1.1.

1.3.1 Ammonification (mineralisation)

When aquatic plants and animals (organic matter) die, bacteria decompose the organic nitrogen, forming ammonia, which rapidly converts to the ammonium ion (NH_4^+). This process is referred to as ammonification process, and occurs at a pH less than 7.5. Organic matter is abbreviated as compounds of carbon (C), nitrogen (N) and phosphorous (P). NH_3 is a gas which can be lost via volatilization. This process is shown in Figure 1.1.

1.3.2 Nitrification

Ammonium ions (NH_4^+) can be retained in sediments due to adsorption at cation exchange sites, which are present on the surface of organic matter and clay (Berner, 1980). Adsorbed NH_4^+ is available to microbes and plants but is essentially immobile with respect to water movement. Small amounts of NH_4^+ can desorb to the water column; a process which is increased by re-suspension of the sediment particles back into the water column by a hydrodynamic processes caused by currents and wave action.

Nitrification is a microbial process, in which ammonium ions are sequentially oxidized to nitrite (NO_2^-) and nitrate (NO_3^-) by nitrifying bacteria. Nitrate, in contrast to ammonia, is very soluble and moves freely through soils or sediment with subsurface waters. Nitrate is the most highly oxidized form of nitrogen and is usually the most abundant form of inorganic nitrogen (NH_4^+ , NO_3^- and NO_2^-) in streams and lakes (Horne & Goldman, 1983).

The nitrification process occurs in oxygenated sediments. This aerobic reaction is carried out by autotrophic bacteria, i.e. able to make its own food, that obtain all carbon required for biosynthesis from inorganic sources. Maximum nitrification rates occur at neutral pH levels and high temperatures, (i.e. between 15 and 25°C). This process is indicated in Figure 1.1.

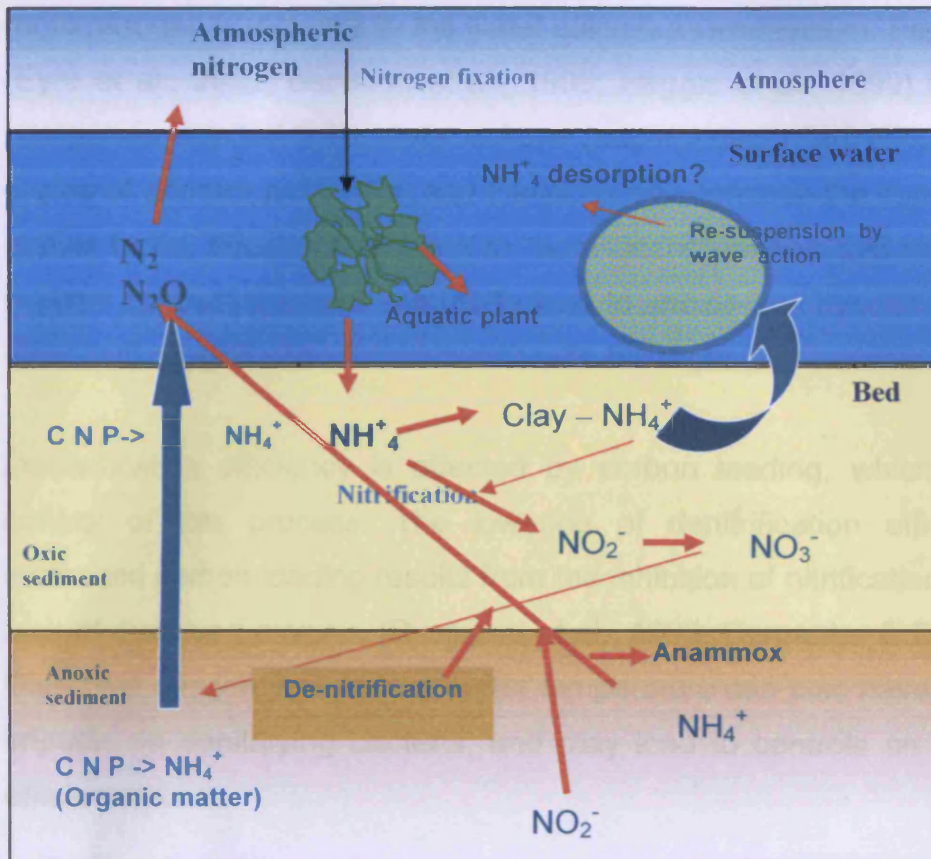


Figure 1.1: A schematic of the nitrogen cycle in the aquatic system.

1.3.3 Denitrification

The denitrification process occurs in anoxic sediments, i.e. oxygen-depleted. It is the process by which nitrate is reduced to nitrogen (N_2) gas, which is important because it removes bio-available nitrogen and returns nitrogen gas to the atmosphere.

Bacterial denitrification is the microbial reduction of NO_3^- to N_2O or N_2 . For example, pseudomonas bacteria use NO_3^- instead of O_2 (a terminal electron acceptor) to obtain oxygen from nitrate for use in respiration at low oxygen levels.

This process occurs under anaerobic conditions, when sediment nitrate is used as an acceptor during the oxidation of organic matter. Some of the N_2 produced during denitrification leaves the water through outgassing and some is fixed by algae and bacteria. When denitrification efficiencies are lowered,

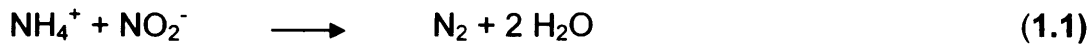
more nitrogen is recycled to the water column as ammonium. Previous studies (Eyre et al., 2002; Berelson et al., 1998; Heggie et al., 1999) indicated that nitrogen is recycled to the water column (and not denitrified) stimulating further cycles of primary production and therefore can continue the supply of organic matter to the sediments leading to more decomposition and more dissolved oxygen consumption and potentially lead to anoxic and hypoxic, (i.e. reduced dissolved oxygen of water column by aerobic organisms) events.

Denitrification efficiency is affected by carbon loading, which is the main control of this process. The lowering of denitrification efficiencies with increased carbon loading results from the inhibition of nitrification caused by a lack of dissolved oxygen, (Rysgaard et al., 1999; Carpenter & Durham, 1985). Dissolved oxygen, salinity and water temperature can also have physiological impacts on denitrifying bacteria, and may lead to controls on denitrification efficiencies.

1.3.4 Anammox (anaerobic ammonium oxidation)

Ammonium oxidation is another stage in the nitrogen cycle. The anammox reaction is anaerobic oxidation of ammonium, coupled with nitrite reduction under anoxic conditions. In addition ammonium is converted to nitrogen gas under anoxic conditions with nitrate as the electron acceptor. It is called anaerobic ammonium oxidation (Anammox) because ammonium is oxidized in the absence of oxygen. In this biological process, nitrate and ammonium are converted directly into dinitrogen gas (N_2) (Jianlong et al., 2004). Up to 50% of the nitrogen gas produced in the oceans is caused by this process.

The bacteria that perform the anammox process belong to bacterial phylum and are called planctomycetes. They are aquatic bacteria found in marine, brackish and fresh water. Equation (1.1) shows the anammox reaction where ammonium is oxidized by nitrite to produce nitrogen gas in the absence of oxygen (Margesin, 2008).



1.3.5 Nitrogen fixation

The earth's atmosphere contains about 78% nitrogen. Nitrogen is essential for many biological processes, and it is crucial for any life on earth. Fixation is necessary to convert gaseous nitrogen into forms that can be used by living organisms; most fixation is done by symbiotic bacteria. Biological nitrogen fixation occurs when atmospheric nitrogen is converted to ammonium by bacteria (nitrogenise) and blue – green algae.

Aquatic plants such as azola (a blue green algae) float on the surface of water, like leaves with their roots hanging in the water. They form a symbiotic relationship with the blue green alga (Azola – water fern), which fixes atmospheric nitrogen, giving the plant access to the essential nutrient (John Postgate, 1987).

1.4 Aims and objectives

Nutrients such as nitrogen and phosphorus are among the most important elements in the metabolism of aquatic systems. However, high concentrations can lead to eutrophication processes as described in section 1.1.

This study will focus on nitrogen compounds, in particular nitrate and ammonium pollution in river and estuarine water systems. Sediment-nutrient-water interaction will be addressed. In particular ammonium adsorption processes will be considered for both fresh and saline water conditions. The effect of salinity and other factors such as organic matter and sediment size on the adsorption processes and therefore on the adsorption coefficients of ammonium will be determined.

The QUAL2E model, which is included in the Depth Integrated Velocities And Solute Transport (DIVAST), hydrodynamic model has been used for solving

many environmental problems. The adsorption processes of ammonia are not included in the water quality model QUAL2E. This study will investigate these processes and introduce the ammonium adsorption equation into QUAL2E thus providing a complete picture of the nitrogen cycle processes in this water quality model. The knowledge gained will be added to the DIVAST model through the water quality model QUAL2E.

This study aims to improve knowledge of nitrogen transport processes in river and estuarine waters. This study focuses on two types of investigation:

- 1- Idealised laboratory experiments using different types of clean sediment (Montmorillonite and Kaolinite) clays and fine and coarse sand.
- 2- Investigation of nitrogen in real estuarine water with sediment samples taken from the field, namely the Loughor Estuary in South West Wales.

1.5 Objectives

The main objectives of this study can therefore be summarized as follows:

- 1- To determine the adsorption coefficients of ammonium onto sediments for both fresh and saline waters with various concentrations of salinity.
- 2- To determine the adsorption coefficients of ammonium onto sediments of different mean particle size and for different total carbon contents.
- 3- To improve the representation of ammonium adsorption processes as investigated and the interaction with sediments (bed sediments) in numerical models.

1.6 Organisation of the thesis

The first chapter introduce the nitrogen related eutrophication problem in the aquatic system. The environmental legislation requirements and directives have been addressed with the important role to aim to prevent and decrease water pollution. The motivation of the research undertaken has been discussed. The rest of thesis consists of seven chapters which can be outlined as follows:-

Chapter 2 describes the sources of water pollution that can have negative effect on water quality. A comprehensive literature review was carried out investigating the different source of pollution from agriculture that leads to increase nitrogen in the surface water and subsequently to the ground water arising nitrate levels. A review of literature to investigate the water quality deals with pollution of surface water is details in this chapter.

Chapter 3 Details are given of ammonium adsorption processes on sediment and the adsorption isotherm model. This chapter describes water quality model QUAL2E and gives details of the nitrogen processes in the water column. Details of the adsorption equation are developed and are described by including the ammonium bed sediment adsorption processes in the QUAL2E model.

Chapter 4 describes the methods of ammonium adsorption and desorption experiments for using clean clay and sand (Montmorillonite, Kaolinite and coarse and fine sand. Details of adsorption isotherm and nitrate adsorption are also given here.

Chapter 5 presents the results of the ammonium adsorption isotherms for Montmorillonite, Kaolinite and fine and coarse sand for both conditions deionised and artificial sea water. The results of desorption kinetics is also presented for the clays and sands investigated.

Chapter 6 presents the case study area of the Loughor Estuary and describes the field work. Details are given for collecting bed sediment and water samples during arising and falling tides.

Chapter 7 presents the results of physical and biochemical parameters of the bed sediments and water samples from the Loughor Estuary. Details of the results of ammonium adsorption and adsorption isotherm and the effect of salinity are given. The results and then discussed in terms of the impact of

physical and biochemical parameters on the nitrogen compound concentrations and the adsorption coefficient.

Chapter 8 present the conclusion and recommendation for future work compiled from the current study.

2 Literature Review

2.1 Sources of water pollution

There are various sources of pollution which can have negative effects on water quality, such as point source and diffuse pollution. Point source pollution enters rivers courses at specific sites such as pipe discharge whereas diffuse pollution arises mainly from to agricultural practises and human activities and is input at arbitrary locations along water courses. Agriculture is an important source of diffuse pollution. Increasing populations and land use activities have caused the use of extensive quantities of fertilizer and pesticides in an attempt to increase agricultural production. This has caused pollution of both ground and surface waters. Increased nitrogen inputs to the soil are mainly caused by chemical fertilizers, animal manure, crop residues, atmospheric deposition and nitrogen fixation by legumes. This manifests itself mainly by non-point runoff and groundwater flow draining agricultural land, sewage discharges and atmospheric deposition, which all increase nitrogen inputs to rivers and marine systems (Galloway et al., 1995).

2.1.1 Diffuse source pollution

Diffuse source or non-point pollution is the contamination of the environment from different sources, often associated with land use, as opposed to individual point sources. Point sources are easily identified and controlled. However, diffuse source pollution is a major problem for freshwater resources as it is hard to attribute it to one activity and a combination of sources might be causing the pollution (DEFRA, 2004). The release of natural contaminants including nitrogen compounds depends on the agricultural practices. Increasing the nutrients in receiving fresh waters can lead to eutrophication, which can lead to oxygen deficiency in the aquatic ecosystem causing a decrease in aquatic habitat quality.

2.1.2 Atmospheric deposition

Atmospheric deposition occurs when pollutants in the air deposit on the land or surface waters. Pollution deposited through rain, fog or snow is called wet deposition, while the deposition of pollutants as dry particles or gases is called dry deposition. Air pollution can be deposited into water bodies either directly from the air and the surface of the water or through indirect deposition where the pollutants settle on the land and are then carried into the water body by rainfall or by movement of ground water through the soil. Any chemical that is emitted into the air can cause air deposition problems. Some of the common air pollutants include different forms of nitrogen, mercury, copper, polychlorinated biphenols (PCBs), polycyclic aromatic hydrocarbon (PAHs) chlordan, dieldrin, lead, lindane, polycyclic organic matter (POM), dioxins, furans, toxaphene, hexachlorobenzene, hexachlorocyclohexane, and diazanon (Erisman et al., 1995)

2.1.3 Runoff

As with all aspects of the water cycle, the interaction between precipitation and surface runoff varies according to time and geography. Surface runoff is affected by both meteorological factors and the physical geology and topography of the land.

Runoff occurs when the amount of water falling on the ground is greater than the infiltration rate through the surface. Runoff specifically refers to the water leaving an area and flowing across the land surface to points of lower elevation. Runoff depends on two variables relative to the rainfall event:

- 1 The intensity of rainfall, which dictates the amount of infiltration if other parameters are kept constant.
- 2 The duration of the rainfall event in combination with the rainfall intensity.

As the world's population increases and as more development occurs, then more of the natural landscape is replaced by impervious surfaces, such as roads, houses, car parks, and buildings that reduce infiltration of water into the ground and accelerate runoff to ditches and streams (Campbell et al., 2004).

2.1.4 Agriculture Impact

The impact of agriculture on water quality is diverse, and water pollution from agricultural activities is a serious problem and remains of major concern for countries applying intensive agricultural practise. The main agricultural water pollutants are nutrients and fertilizers (Ayers and Westcot, 1985). The different impacts of agriculture on water quality of groundwater and surface water are summarised in Table 2.1.

Table 2.1 Agricultural impact on water quality

Agricultural activity	Impacts	
	Groundwater	Surface water
Use of fertilizers	Leaching of nitrate to groundwater which can later feed surface waters, resulting in increased eutrophication; exceedance of drinking water levels is a threat to human health.	High concentrations of nutrients, particularly of nitrate and phosphate are leading to eutrophication of surface waters; excess algae growth is leading to oxygen deficiency in the water and fish and benthic fauna kills.
Manure spreading	Pollution of ground-water, especially by nitrogen which can worsen eutrophication when groundwater is recharged by receiving waters.	Used as fertilizer, excess manure spreading on ground results in high levels of pollution of receiving waters with pathogens, phosphorus and nitrogen leading to eutrophication.

Agricultural activity	Impacts	
	Groundwater	Surface water
Pesticides	Some types of pesticides may leach into groundwater causing human health problems from polluted wells used for drinking water production.	Pesticides are carried as dust by wind over very long distances and can contaminate aquatic systems. Run off of fertilizers and pesticides to surface waters leads to contamination of surface water and ecological systems in surface waters by loss of top predators due to growth inhibition and reproductive failure; public health impacts from eating contaminated fish and from drinking water.
Irrigation	Increased salinity of groundwater and increased levels of nutrients; particularly nitrates.	Runoff of salts is leading to salinisation of surface waters.
Animal husbandry	Potential leaching of nitrogen and bacteria to groundwater; same health risks as for surface waters pollution of wells used for drinking water treatment.	Pollution of surface waters with various faecal organisms and nutrients leading to health risks.

2.1.5 Irrigation impacts on surface water quality

There are several problems that affect irrigated areas, such as water logging, salinisation, desertification and erosion. It also leads to the downstream degradation of water quality by adding salts, agrochemicals and toxic leaches. It has become apparent that trace toxic constituents, such as selenium (Se), molybdenum (Mo) and arsenic (As) in agricultural drainage waters may cause

pollution problems that threaten the continuation of irrigation in some areas (Letey et al., 1993).

2.1.6 Sources of nitrogen from agriculture

Pollution from agriculture occurs on cultivated fields or on grazed or cut grassland. It is caused by nitrogen losses from animal excreta, application of animal manure slurry, from mineral fertilizer or from N-fixation (Binkley et al., 1999). Depending on the local conditions, (i.e. soil type, temperature, humidity, bacterial activity and N-dynamics) nitrogen losses or fluxes are in the form of nitrate ammonium or nitrous oxide (Townsend, 1998). Nitrate is very mobile in soil solution and can enter the subsurface flow, which may enter streams and rivers. Nitrogen is also lost from agricultural land use through volatilization or evaporation of NH_3^- which relatively quickly reacts to give NH_4^+ . Such losses mainly originate from animal husbandry, either directly from the animal excreta or through losses in collecting, storing and applying animal manure or slurry, or from inadequate disposal practices.

2.1.6.1 Nitrate

The World Health Organisation (WHO) reports that nitrogen levels in groundwater have increased in many parts of the world as result of agricultural practice (WHO, 1993). The nitrate level in drinking water is extremely important with regard to infants because of their high intake of water with respect to body weight. High nitrate levels in water can cause methemoglobinemia or blue baby disease. This condition is found particularly in infants less than six months old due to the level of stomach acid in infants being less than in adults. This causes an increase in bacteria that can readily convert nitrate to nitrite, which is then absorbed into the blood stream. This converts haemoglobin to the methemoglobin that does not carry oxygen efficiently. These results in reduced oxygen supply to important tissues, such as the brain and can result in brain, damage and death (Avery, 1999).

Nitrate is one of the most common water pollutants in the world. There are many studies indicating that nitrate levels have increased in some countries in

drinking water to the point where more than 10% of the population is exposed to nitrate levels in drinking water that are above 10 mg/l (WHO ,1993).

High nitrate levels occurred in groundwater as a result of high fertilizer use, particularly nitrogen fertiliser that is not taken up by the plants but volatilized, or carried by surface runoff, and then leaches to the ground water in the form of nitrate. The nitrogen is then not available to plants but causes an increase in the nitrate concentration in the groundwater above peak acceptable levels desirable for drinking water.

Other important sources for nitrogen entering into bodies of water are industrial wastewater, animal waste and discharges from car exhausts, which can also elevate the nitrate concentrations in water.

2.1.6.2 Ammonia and Ammonium

Typically references do not distinguish between ammonia and ammonium and often discuss them interchangeably, which is technically imprecise. Ammonia and ammonium are forms in which nitrogen occurs. Ammonia is a compound with formula NH_3 and is a gas at room temperature. It is toxic and harmful to aquatic life because it is neutral (un-ionized) and is therefore able to diffuse cross biological membranes more readily than other forms. However, ammonia is mainly present in water in the form of ammonium ion NH_4^+ and desirable for algae and aquatic animals. Equation 2.1 gives the reaction of ammonia and water, ionising to ammonium and a hydroxyl ion.



In addition ammonia which is present in aquatic systems mainly as the dissociated ion NH_4^+ (ammonium), is a more reactive compound due to its higher chemical energy.

From the reversible arrow it can be seen that the reaction can go either way and hydroxyl ions and ammonium ions could combine to form ammonia and water.

Ammonia is highly toxic, whereas the ammonium ion is significantly less toxic.

This shifting balance is dependent upon the pH of the water. If the pH value rises, then toxic ammonia will tend to be dominant. Conversely, at pH 7 the ammonium ion will prevail. Figure 2.1 indicates the percentage of NH_4^+ and NH_3 as a function of pH. Ammonium is produced by the decomposition of organic matter. Its positive charge enables it to form bonds with negatively charged clays.

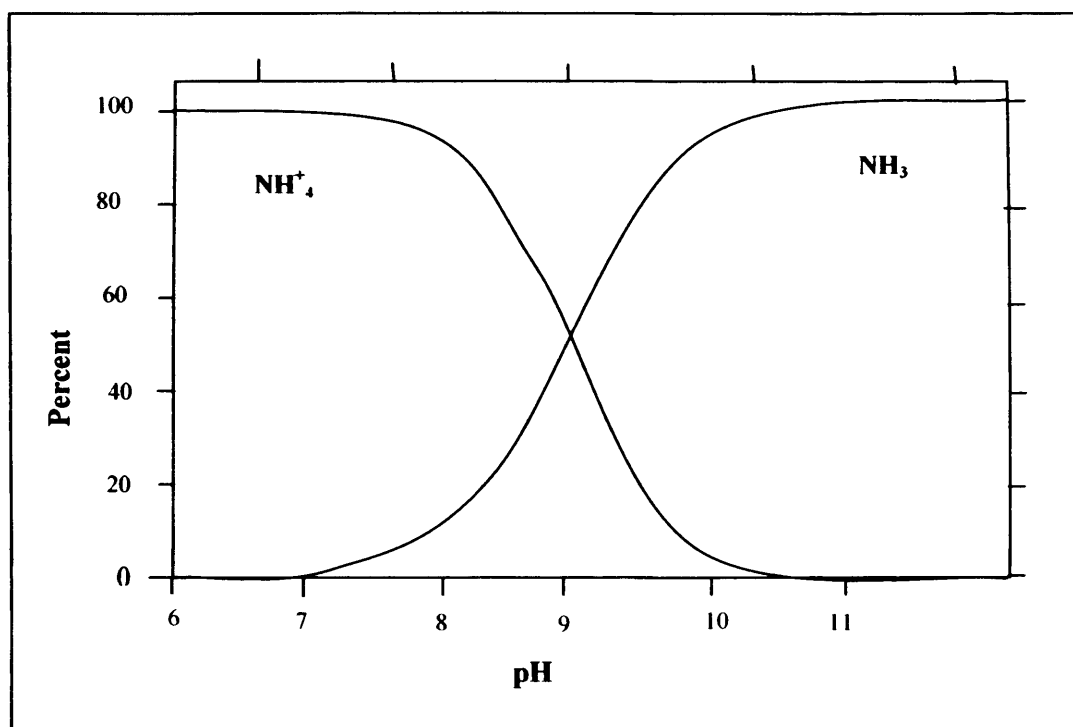


Figure 2.1: Percentage of NH_4^+ and NH_3 as a function of pH

2.2 Sediment adsorption

Adsorption by solids is defined as the phenomenon of taking up of molecules from the fluid phase by a solid surface; the term 'surface' includes both the outer geometric surface and inner the surface bounding such as the capillaries, cracks and crevices (Kirk et al., 1947). The solid material (clay or sand) is defined as the adsorbent. The contaminant (ammonium ion) is defined as the adsorbate. The positively charged ammonium ion in fresh water and marine sediments is adsorbed to negatively charged surfaces of clay and organic matter (Martens et al., 1974). The driving force of solute mass transfer

from the solvent to the surface of solid adsorption may be the lyophobic (i.e. solvent-rejecting) character of the solute or the affinity of the solute for the solid or the combination of both (Casey et al., 1992; Kirk et al., 1947).

2.2.1 Types of adsorption

There are three general types of adsorption: Physical, chemical and exchange.

2.2.1.1 Physical adsorption

Physical adsorption is relatively nonspecific and due to the operation of weak forces of attraction, such as Van der Waals' forces and electrostatic forces between adsorbate molecules, and the atoms which compose the adsorbent surface. A small particle in close proximity to a solid surface is subjected to either electrical attraction or repulsion, depending on the surface charges developed by both the particle and the surface when in contact with the fluid and to the attraction caused by Van de Waals' forces. It is also subjected to the hydraulic forces resulting from the movement of the fluid (Weber, 1972; Ludersen, 1983). Here, the adsorbed molecule is not affixed to a particular site on the solid surface, but is free to move about over the surface.

2.2.1.2 Chemical adsorption

Chemical adsorption (or chemisorption) is adsorption accompanied by a chemical reaction or chemical bonding (Ludersen, 1983). It involves electron transfer or sharing, or the adsorbed species (the adsorbate) breaks up into atoms as radicals which are bonded separately. Chemical adsorption is seldom reversible – the adsorbent must generally be heated to higher temperatures to remove the adsorbed material. Physical adsorption can involve the formation of a multi-molecular layer, while pure chemisorption is completed in a mono-layer and gives a stronger bond (Ludersen, 1983).

2.2.1.3 Exchange adsorption

This type of adsorption is used to describe adsorption characterized by electrical attraction between the adsorbent and the adsorbate, known as ion exchange. Ions with greater charge are attached more strongly toward a site of

opposite charge than molecules with a lesser charge. In addition, the smaller the size of the ion, the greater the attraction with the adsorbent surface (Rao, 1994; Ludersen, 1983). For instance ammonium adsorbed on the surface of the sediment particles due to the cation exchange sites, which is present on the surface of the clay (Berner, 1980). Ammonium is a weak anion and has a positive charge, binding it to the negatively charged clay. This weak force between the ammonium and the clay sediment particle can be replaced with another cation. In addition, the ammonium ion is weakly bound to the clay or soil particles and as such can be replaced with another cation.

2.2.2 Adsorption isotherms

The affinity of the adsorbate for an adsorbent is quantified using adsorption isotherms. These are used to describe the amount of adsorbate that can be adsorbed onto an adsorbent at equilibrium and at a constant temperature. Positive adsorption in solid-liquid systems results in removal of the solute from solution and an increase in concentration at the surface of the solid. This process continues until the concentration of the solute remaining in solution reaches a dynamic equilibrium with the concentration at the surface (Weber et al., 1972).

A liquid phase isotherm shows the distribution of adsorbate (that which is absorbable) between the adsorbed phase and the solution phase at equilibrium. It is a plot of the amount of adsorbate adsorbed per unit weight of solid adsorbent, (q_e) versus the concentration of the adsorbate remaining in solution (C) (Martin et al., 1972; Chermisinoff et al., 1978).

The isotherm results indicate the amount of solid that is adsorbed or desorbed (Lucas et al., 2002). The amount of adsorbed material per unit weight of adsorbent increases with increasing concentrations but is not necessarily proportional as shown in Figure 2.2.

Curves I and III indicate curvilinear dependence of adsorption on the amount of concentrate at the solid surface, with the amount remaining in the solute

phase for favourable and unfavourable separation patterns respectively. Curve II represents a linear adsorption pattern (Weber et al., 1972).

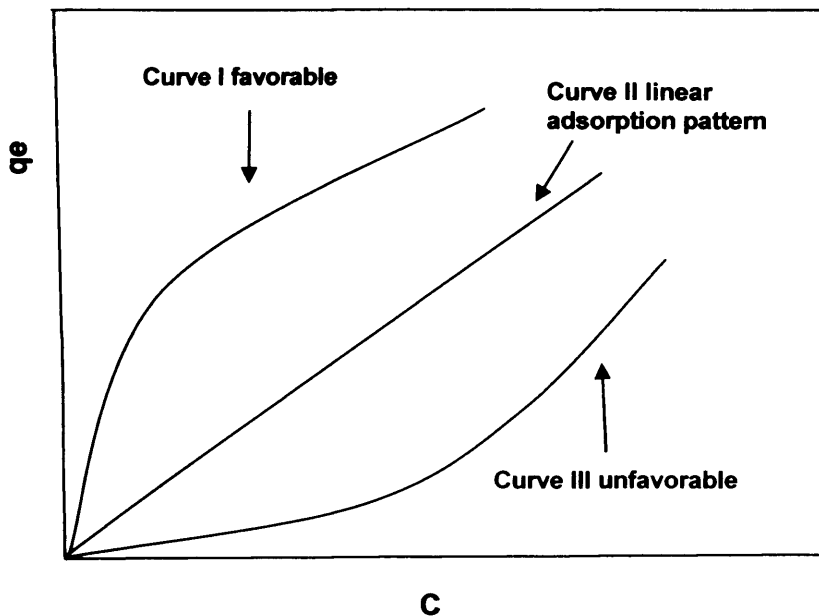


Figure 2.2: Types of adsorption isotherms

2.2.3 Adsorption Isotherm Models

2.2.3.1 Langmuir Model

The Langmuir isotherm developed by Langmuir in 1915 is used to describe monolayer adsorption. The Langmuir equation can be used for describing equilibrium conditions for adsorption and for providing parameters Q (which is the amount of adsorbate) and b (which is a constant related to the energy of adsorption). This can be used to compare adsorption behaviour in different adsorbent–adsorbate systems or conditions within any given system (Langmuir, 1918; Grittenden et al., 1998).

The Langmuir isotherm is used most frequently to describe adsorption data. The basic assumptions underlying the Langmuir model, which is also called the ideal localized monolayer model, are:

- Solute molecules are adsorbed on definite sites on the adsorbent surface.

- Each site can accommodate only one molecule (monolayer).
- The area of each site is a fixed quantity, determined solely by the geometry of the surface.
- The adsorption energy is the same at all sites.
- The adsorbed molecules cannot migrate across the surface or interact with neighbouring molecules.
- Adsorption is reversible (Sarkar and Acharya, 2006).

The Langmuir equilibrium adsorption equation has the form

$$qe = x / m = \bar{Q}bC_e / (1 + bC_e) \quad (2.2)$$

$$C_e / q_e = 1 / \bar{Q}b + C_e / \bar{Q} \quad (2.3)$$

where:

\bar{Q} and b are Langmuir constants related to adsorption capacity and energy of adsorption respectively.

b is the Langmuir constant and adsorption coefficient (K_L).

q_e is the amount of adsorbate adsorbed per unit weight of solid.

C_e is the equilibrium concentration of the solute remaining in solute (Weber et al., 1972; Luderse et al., 1983).

A plot of (C_e/q_e) versus the equilibriums concentration gives a straight line, the slope of which gives the value $(1/\bar{Q})$ and with intercept with the (C_e/q_e) axis is the value of $(1/\bar{Q}b)$ being as shown in Figure 2.3.

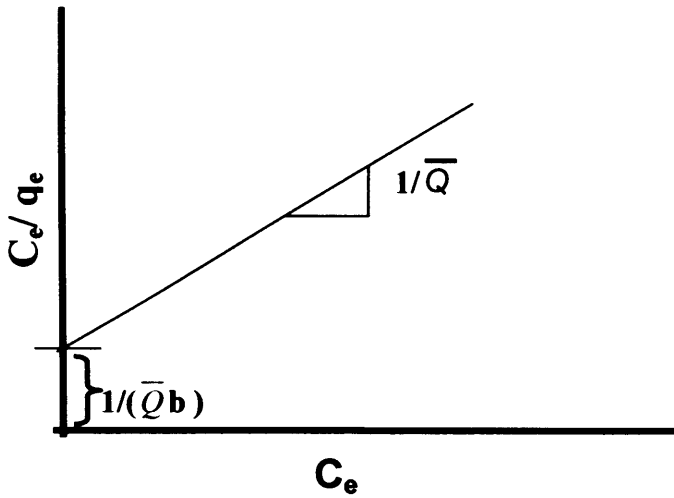


Figure 2.3: A linear Langmuir isotherm

The Langmuir equation can be used for describing equilibrium for adsorption and for providing parameters \bar{Q} and b . This can be used to compare adsorption behaviour in different adsorbent–adsorbate systems or conditions within any given system (Langmuir, 1918; Grittenden et al., 1998).

2.2.3.2 The Freundlich isotherm model

The Freundlich adsorption isotherm has been widely used for many years as an empirical equation. This equation is used to describe the data for heterogeneous adsorbent surfaces, in which the energy term (b) in the Langmuir equation varies as a function of surface coverage (q_e), strictly due to variation of heat of adsorption (Weber and Walter, 1972).

The Freundlich equation has the form (Freundlich, 1906; Casey et al., 1992; Luderse et al., 1983) of :-

$$q_e = x/m = k C_e^{1/n} \quad (2.4)$$

where:

x is the mass of the adsorbate

m is the mass of the adsorbent

C_e is the equilibrium concentration of the solute remaining in the solute

k and n are empirical constants (Lucas, 2004)

The equation is more useful in the logarithmic form, expressed by (Martin et al., 1972) to give:-

$$\log q_e = \log(x/m) = \log k + 1/n \log C_e \quad (2.5)$$

A plot of (x/m) versus the concentration on a logarithmic scale results in a straight line of slope $(1/n)$ and intercept (k) and is roughly an indicator of the adsorption capacity of the solid. Experimental data are often plotted in this manner as a convenient way of determining the removal of a material from the solution by adsorption and as a means of evaluating the constants (k) and (n) , see Figure 2.4. K is the adsorption coefficient of Freundlich isotherm (K_F).

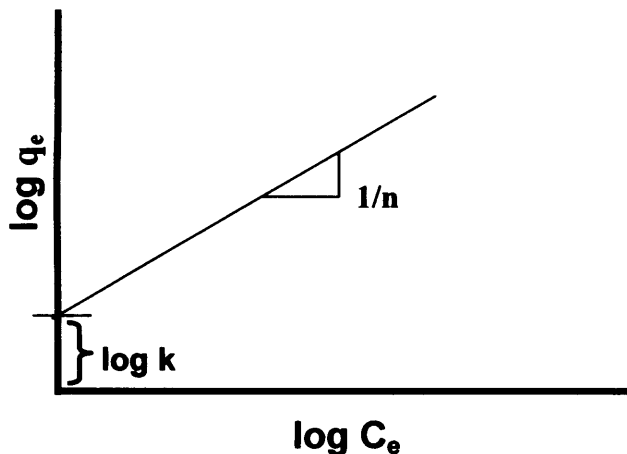


Figure 2.4: A linear Freundlich isotherm

The Freundlich equation generally agrees with Langmuir equations for data over a moderate range of concentrations. Martin et al (1979) found that the equilibrium capacity of one solute will be affected adversely by the presence of another solute.

Poots et al (1976), found that adsorption of dye (acid blue 25) on peat and wood conforms to both Freundlich and Langmuir equations, which show an increase in the adsorption capacity with decreasing particle size. Casey (1992) carried out different tests which are useful indications of the potential of the adsorption process for a particular application, but the design data are preferably obtained from pilot plant operation.

2.2.3.3 Combination of Langumuir and Freundlich isotherm models

Sips (1948) combined the two adsorption models and expected to describe heterogeneous surfaces much better at low sorbate concentrations, and derived the following combined equation 2.6:

$$q_e = \frac{b q_m C_e^{1/n}}{1 + b C_e^{1/n}} \quad (2.6)$$

2.2.4 Kinetics of adsorption

When an adsorbent comes into contact with a fluid the number of molecules in the fluid decreases. During their motion in the fluid, molecules strike the surface of the solid and some remain attached to the surface for a certain time before they become adsorbed. The rate at which the number of molecules in the fluid decreases depends on the velocity at which they reach the site on the surface at which they are adsorbed (Milan et al., 1970).

For chemisorption the process of binding can be slow and complex. But for physical adsorption the mechanism of binding of the molecules has a very high rate. The factor controlling the decrease in the number of molecules in the fluid phase, (i.e. the overall rate of adsorption) is usually the rate of transport of the adsorbate to the sites on the surface at which they become bound (Milan et al., 1970).

For investigations of adsorption kinetics and diffusion into the solid phase from the liquid solute, the constant volume method for measuring the diffusion

coefficient has distinct experimental advantages (Suzuki et al., 1974). Batch-type contact operation is a process in which a quantity of adsorbent (e.g. clays and sand) is mixed continuously with a specific volume and concentration of the adsorbate, e.g. ammonium (C_0), until the concentration in this solute decreases to a desired level (C_1).

The concentration profile decreases with time as shown in Figure. 2.5

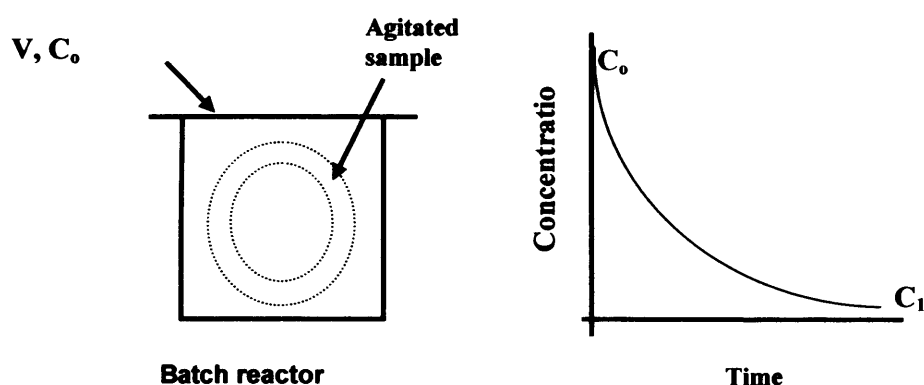


Figure 2.5: Schematic illustration of the experimental batch process

where:

V is the volume of solute

C_0 is the initial concentration and C_1 is the concentration at a given time.

For this case the concentration of solute in contact with a specific quantity of adsorbent will quickly decrease followed by a larger slower decrease in the liquid concentration. As the solute and adsorbent contact time increases the adsorbent becomes less effective in adsorbing. (Weber, 1972).

2.2.5 Ammonium adsorption to sediments

Ammonia is adsorbed to sediment particles following ammonification. The ammonium ion is a major component in the nitrogen loading to coastal areas, particularly since nitrogen is the limiting nutrient in many coastal waters. Sediments are a major component controlling the cycling and availability of nitrogen (ammonium, nitrate and nitrite). Ammonium ions can be desorbed and diffuse to overlying surrounding water or be denitrified (Nixon et al., 1996).

Ammonium produced during decomposition of organic matter can be retained in sediment due to physical adsorption at cation exchange sites. These sites are present on the surface of organic matter and clay minerals (Berner, 1980). Figure 2.6 shows a sketch of the adsorption reaction of ammonium on the surface of clay particles.

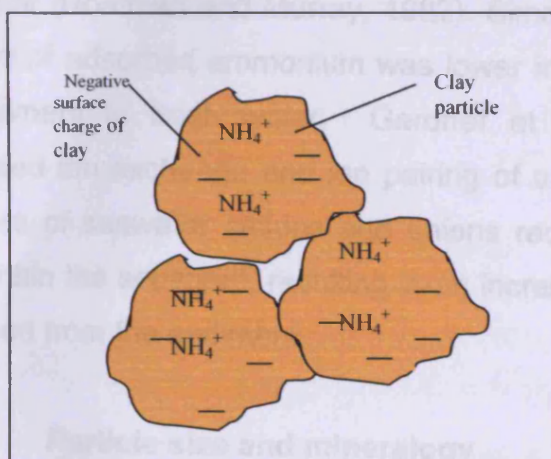


Figure 2.6: Sketch of ammonium ions adsorbed on clay particles

2.2.6 Factors affecting ammonium adsorption

There are several factors that have an effect on ammonium adsorption including salinity, temperature, pH and particle size, which will be discussed in the following:

2.2.6.1 Salinity

Salinity can influence ammonium adsorption during the mixing of freshwater and seawater in estuarine systems. Seawater cations (e.g, Mg^{++} , Na^+ , K^+) have been shown to interfere with the ammonium ion on the surface particles of clay and ammonium adsorption decreases with increasing salinity (Hou et al., 2003; Seitzinger et al., 1991; Wang et al., 2002). In contrast, increasing ammonium desorption as well as increasing salinity in estuarine systems can potentially affect the nitrification due to decreasing residence time of ammonium on the surface of the clay (Boynton et al., 1985; Gardner et al.,

2006). The potential nitrification rates were markedly lower at higher salinity (Rysgaard et al., 1999).

This can also be due to harsher conditions for nitrifying bacteria in the saline water environment. Changing and fluctuating salinity in estuarine sediments plays a major part in the control of the ammonium adsorption capacity of the sediment (Boatman and Murray, 1982). Simon et al. (1987) reported that the amount of adsorbed ammonium was lower in estuarine sediments compared to sediment in fresh water. Gardner et al. (1991) suggested that the increased ion exchange and ion pairing of ammonium caused by increasing numbers of seawater cations and anions reduces the ammonium residence time within the sediment, resulting in an increase of ammonium that becomes desorbed from the sediment.

2.2.6.2 Particle size and mineralogy

There are many earlier studies indicating that grain size, mineralogy, and organic matter content can affect ammonium adsorption (Rosenfeld, 1979; Boatman and Murray, 1982). The rate of achievement of equilibrium in exchange reactions is fastest when clay-sized materials are involved and sorbate ions can directly contact surface sites. Clay mineralogy plays an important role in ammonium adsorption since each type of clay has specific composition and ability for ammonium adsorption, due to the difference in cation exchange capacity of the clays. Adsorption occurs on the surface of the clay, which is negatively charged, and attracts the positively charged ammonium (Rosenfeld, 1979). Cation exchange capacity (CEC) has a potential effect on ammonium adsorption. Clay with comparatively large cation exchange capacity favours adsorption. In general, cation exchange capacity is inversely proportional to the particle size of the clays.

For materials with larger sized particles, including rock fragments and in rock matrices, adsorption equilibrium is limited by a much slower rate of diffusion of sorbing species into and out of rock pores (Jenne, 1995). There are several types of clay that dominate estuary and river sediments, which are presented

in Table 2.2. Each type of clay has a different structure and cation exchange capacity.

As can be seen from the table, Montmorillonite has the largest CEC (80 – 150 meq / 100g) compared to Illite (15 – 40 meq / 100g) and Kaolinite (2 – 15 meq / 100g).

Table 2.2 Properties of clays (Sparks, 1995)

Type of clay / mineral	Composition	Cation exchange capacity (CEC) (meq/100g)
Kaolinite (1:1)	$\text{Al}_2 \text{Si}_2 \text{O}_5 (\text{OH})_4$	2 – 15
Montmorillonite (2:1)**	$\text{K}_{0.3} \text{Al}_{1.9} \text{Si}_4 \text{O}_{10} (\text{OH})_2$	80 – 150
Illite (2:1)**	$\text{K}_{1.5} \text{Al}_4 (\text{Al}_{1.5} \text{Si}_{6.5} \text{O}_{20} (\text{OH})^+_4$ $\text{K}_{0.8} \text{Al}_{1.9} (\text{Al}_{0.5} \text{Si}_{3.5}) \text{O}_{10} (\text{OH})_2$	15 – 40

* Kaolinite is a 1:1 type of clay mineral with one silica tetrahedral and one gibbsite octahedral.

**Illite and Montmorillonite are 2:1 type clay minerals with two silica tetrahedral attached to one gibbsite octahedral

2.2.6.3 Charge density

Charge density is defined as the number of charges on the cation divided by its surface area. The attraction force of the water to a cation is therefore varied and specific to each cation. The charge density is inversely proportional to the radius of the cation in its crystal state. The charge density of the clay is very significant in determining the amount of cations that can be adsorbed to the surface. The strength of the bond between the clay and the cation, relative to its bond with water, will determine which cations will be adsorbed to the clay. During the adsorption process, water molecules close to the sediment are lose their hydration shell, compared to the cations, which do not lose their hydration shell near the clay surface. A cation might be replaced from its adsorbed site by another cation. The selectivity of cations on the clay surface is influenced by the hydration forces (Kafkafi, 2007).

In comparing the concentrations of lithium, sodium and potassium near the clay, and cations being attached to the clay without their water shell, lithium has the smallest crystalline radius.

This means that lithium bonds with water more strongly than sodium and potassium, therefore lithium has the lowest concentration of these ions attached to the solid.

Potassium has weaker hydration energy than ammonium which means that it can replace other cations much faster, which is due to its higher charge density. It is common in ammonium adsorption studies to use potassium chloride as a replacement cation of ammonium on the clay surface.

In marine water, there are monovalent and divalent cations. Monovalent cations (one charge) such as Na^+ and K^+ , have less opportunity to adsorb on the sediment than the divalent cations (two charges) such as Ca^{++} , Mg^{++} . Mg^{++} cations can be replaced by K^+ cations because K^+ has higher charge density. For example, in terms of charge density, NH_4^+ is stronger than K^+ , which is stronger than Na^+ . In contrast potassium can replace ammonium on the sediment because of its higher charge density but sodium can not because of its smaller charge density (Toth, 1964).

2.2.6.4 Organic matter

Organic matter in the sediment can increase the efficiency of ammonium adsorption in the sediment. Studies of natural soils have shown that ammonium is adsorbed not only by clay mineralogy but also by organic matter, particularly clay-humic complexes. These complexes dominate the behaviour of ammonium adsorption in sediments rich in organic matter, whereas the clay minerals control ammonium adsorption in the organic-poor sediment (Boatman et al., 1984).

Rosenfeld (1979) undertook laboratory experiments and found that more ammonium is adsorbed by mangrove sediments than mud sediments because sediment from around mangroves contained more organic matter. This is of particular interest in estuarine waters where flocculate is a natural process occurring when fresh water and sea water mix (Harris et al., 1996).

2.2.6.5 Temperature

Temperature dependence of cation adsorption in clay suspensions and marine sediments is significant but comparatively small over 20° C where it varies between 10 and 25% (Mangelsdorf et al., 1969; Sayles et al., 1975). Ammonium is a minor constituent in sea water, its adsorption behaviour as a function of temperature in general depends on the absolute concentration of ions with which NH_4^+ exchanges, and on the type of particular ions for adsorption sites (Boatman and Murray, 1982), with temperature playing a much less significant role. In the temperature range 6° – 26° C which encompasses the typical values around the UK coast, the effect of temperature on ammonium adsorption is negligible compared to the precision of the extraction method. This is due to ammonium being a minor constituent and therefore the effect of temperature on adsorption being hard to predict (Mackin et al., 1984).

Landen et al. (1998) suggested that temperature has an indirect effect on adsorption because bioturbation is stimulated by increased temperature and the dwelling fauna enhances the reworking of the sediment which provides new sites for adsorption. This aspect will be of interest with predicted enhancement of bioactivity in the Severn Estuary upstream of a potential barrage site where turbidity would reduce, thus enabling more light into the water, which could enhance bioactivity.

2.3 Settling velocity of sediments

Sediment transport in river estuaries plays an important role in water quality assessment and prediction. Resuspension and deposition of the sediment can be a source of water pollution and eutrophication. The influence of sediment resuspension to water quality has been studied extensively in the past decades (James et al. 1997) partly because it is a source of heavy metal pollution and partly because it increases the possibility of eutrophication in river estuaries and coastal areas, where large amounts of nitrogen and phosphorus adsorbed by the sediment particles can move into the overlying

water with the sediment resuspension (Anggara-Kasih and Kitada 2004; Fevre and Lewis 2003).

The settling velocity of sediment is one of the key variables in the study of sediment transport, especially when suspension is the dominant process. It serves to characterize the restoring forces opposing turbulent entraining forces acting on the particle. It depends not only on the size, shape, and density of particles and the density and viscosity of the fluid, but also on the number of, or concentration of, the particles.

Much experimental and analytical information on the settling velocity of a single particle is available to guide practical application, though the problem is far from being completely solved. However, the case most frequently encountered in analyses and predictions on sediment transport is one where more than a solitary particle falls through a fluid. The presence of other grains will modify the settling velocity of an individual particle in the fluid, due to mutual interference among particles. For example, a few closely spaced particles in a fluid will fall faster than a single particle. On the other hand, the settling velocity of the particles uniformly dispersed throughout a fluid will be less than that of an identical isolated particle in a clear fluid. The second instance appears most commonly in practice. Past investigations regarding the influence of sediment particle concentration on the settling velocity were carried out by Choklitsch [see Bogardi (1974)] and McNown and Lin (1952). Their results, while being quantitatively inconsistent with each other, show that increasing sediment concentration results in reducing the settling velocity of particles.

2.4 Hydro-environmental computer models

Hydro- and geo-environmental computer models can be used to simulate a range of the processes within the hydrological system. Analytical models are limited only to simple systems and are not appropriate for the type of sites being considered herein. In contrast numerical models have been developed to deal with complex basins and are widely used, at present, to investigate surface water flow, ground water flow and contaminant transport processes in

water systems. Lumped parameter (or black box) models regard the catchment as a single unit (Sokrut et al., 2001). Parameters are averaged over the whole area and the models are calibrated by curve-fitting estimates to historical data (Beven, 1989). Such models have little provision for the representation of spatially distributed characteristics and separate hydrological processes across the catchments or for different contributions within the modelled system. Physically based distributed models use parameters with a physical interpretation. They attempt to model more precisely the hydrological system through subdividing it into separate processes and simulating these processes accordingly.

The variety of hydro- and geo-environmental computer models available on the market and in the research community mirror the breadth of their possible applications. These models have been used widely as research tools to better understand the processes that occur in the hydrological system and contribute to water quality problems in surface waters. In recent years computer modelling tools have been increasingly used to aid in policy making (Burt and Johnes, 1997). The results they provide can be used to design best techniques for example for the application of fertilizers. In this situation the models can be used to trace a chosen representative nutrient through the systems such as flow the pollution from a fertilizer such is transported through the water courses to the receiving water.

It has been shown (Schroder et al., 2003) that selecting the appropriate ion or compound of the nutrient to represent the pollution within a catchment is crucial. This is because different types of compounds can be goal orientated (where the environmental quality is of greatest concern), or means orientated (when certain inputs of farming are used as indicators governed by laws and governmental schemes).

2.4.1 Surface water models

In order to investigate the fate of contaminants once discharged into the water body, surface water models can be used. In this section hydrological river, estuary and coastal models have been investigated.

2.4.1.1 Hydrological models

Hydrological models are designed to estimate the runoff regarding the rainfall intensity, the topography and the soil moisture content. A typical such model relating to information is: Chemicals, Runoff and Erosion from Agricultural Management Systems (CREAM) is a surface response model which incorporates some root processes (Knisel et al, 1992). It combines the hydrology, erosion and chemistry of the surface water to predict surface runoff and percolation as well as the chemistry. The model incorporates nitrogen and phosphorus cycles, which simulate all the major reactions determining the chemical specification and their occurrence along different pathways.

The Soil and Water Assessment Tool (SWAT) model is another example of a surface runoff model. It was developed by the United States Department of Agriculture in the 1990s. SWAT is a basin – scale continuous time model that operates on a daily time step and is designed to predict the impact of management on water, sediment and agricultural chemical yield in watersheds. SWAT is a hydrological model including component of; weather, surface runoff, return flow, percolation, evapotranspiration, transmission losses, pond and reservoir storage, crop growth and irrigation, ground water flow, nutrient and pesticide loading and water transfer. SWAT can be considered as a watershed hydrological transport model.

Applications of SWAT have expanded worldwide over the past decade. Many of the applications have been driven by the needs of various agencies, particularly in the US and the European Union, which require direct assessments of climate change, anthropogenic and other influences on a wide range of water resources.

One of the first major applications performed with SWAT was within the Hydrological Unit Model of the United States (HUMUS). This is a modelling system which was implemented to support the United States Department of Agriculture (USDA), as discussed by Arnold et al (1999). SWAT has also been used in Europe. Several modelling studies have used SWAT to quantify the impacts of climate change for different watersheds in Europe within the climate hydrochemistry and economics of surface water systems. The goal of these projects was to assess the ability of the models to estimate nonpoint nitrogen and phosphorus losses to both fresh water stream and coastal waters (EUROHARP, 2006).

2.4.2 River, estuarine and coastal models

Surface water models exist for river, estuarine and coastal waters where they are typically characterised as follows:-

2.4.2.1 One dimensional (1-D) models

One dimensional models have been widely used to model the flow and solute transport processes in rivers and open channels. These types of models are efficient when dealing with large and complex river / channel systems and various hydraulic structures. One dimensional models become less applicable when applied to floodplain flows and estuarine and coastal waters, which are dominated by two dimensional (2-D) and 3-D flow processes. (Lin et al, 2005).

2.4.2.2 Two dimensional (2-D) models

2-D models have been applied widely to estuaries and coastal waters that are tidally dominated. They are generally 2-D depth- averaged and are assumed to be well mixed vertically. They have been developed to estimate river and estuarine flows at high spatial and temporal resolutions. The models have advanced to the discretisation of the floodplain into a network of simulated river branches and spills linked with the main river channels. This approach has been practised successfully for many studies but the accuracy of the predictions is varied and also depends upon the initial model setup which can be a time consuming process. Two dimensional models are frequently based

on the Alternative Directive Implicit (ADI) scheme, which has been shown to be computationally efficient (by avoiding solving a full two dimensional matrix) and generally very stable, robust and accurate (Lin et al, 2005). The model can also be linked to 1-D characterise river systems, thereby giving a better representation of the estuarine water systems and with river and estuary being studied together.

The linking of 1-D models and 2-D models has been undertaken for many hydrodynamic and water quality modelling studies to predict. flood flows, faecal coliform and heavy metal concentration distributions etc (Lin et al, 2005). 2-D models are used as estuarine and coastal models when 2-D flow processes are dominant. These models involve solving the depth integrated 2-D flow and sediment transport equations to describe the governing flow and suspended transport processes (Falconer and Owens, 1990). Considering that 2-D models need less data and computer resources in comparison with full 3-D models, these models are still useful for many practical engineering applications.

2.4.2.3 Three dimensional (3-D) models

3-D models can successfully reproduce complex three dimensional coastal and floodplain velocity distributions. Measured 3-D velocity data or dye tracing experiments for say a 100 – year return period are used to calibrate and verify the 3-D model. These models are used for problems such as sediment transport and flow vegetation interaction, where this dimensionality of representation is important (Paul et al, 2005).

2.4.3 DIVAST

The Hydraulic Research Centre's (HRC) Depth Integrated Velocity And Solute Transport (DIVAST) model is an example of a two dimensional, depth integrated, time-variant model, which has been developed for estuarine and coastal waters (Lin and Falconer, 2005; Falconer, 1992; Lin et al 1996). This study relates to the DIVAST model, since the QUAL2E model pollutant transport formulations have been used in the DIVAST model to study water

quality problems. This study aims to improve the nitrogen processes used in the water quality model DIVAST. These processes will be investigated in relation to sediment-nutrient-water interactions with the aim being to develop an adsorption equation and coefficient for ammonium fluxes through the various zone. As yet sediment-nutrient-water interactions, especially the adsorption processes of ammonium have not been included in the model. The work carried out here in DIVAST and QUAL2E aims to increase the range of applicability of the DIVAST model by adding the ammonium adsorption equation in the corresponding transport formulation.

This model is suitable for simulating flow and pollutant transport within water bodies that are dominated by horizontal, unsteady flow and do not display significant vertical stratification. The model simulates the two dimensional distribution of currents, water surface elevations and various water quality constituents within the modelling domain and as functions of time taking into account the hydraulic characteristics governed by the bed topography and open and closed boundary conditions.

The DIVAST model is based on the finite difference method and uses the Alternative Directive Implicit (ADI) method to solve the differential flow equations and compute the changes in water velocity, etc with time. Fluxes are calculated for each grid cell in the longitudinal (x) and lateral (y) directions, with the model ensuring conservation of mass throughout the domain (Falconer, 1992). The ADI method thus involves the prediction of the fluxes in the x and y directions at the end of each time step. The method involves dividing the time step in two and solving the equations for the flux in the x direction for the middle of the time step and the flux in y direction for the beginning of the time step generating a set of linear equations. The process is then repeated for the flux in the second half of the time step.

The aim of this project is to refine the governing biochemical formulations for nutrients, particularly nitrogen compounds (ammonium nitrate and nitrite) such as adsorption processes for ammonium ions, according to the QUAL2E standards (Brown and Barnwell, 1987) which form the basis of the water

quality formulations in the DIVAST model. These refinements have been achieved through combined field sampling and laboratory studies see section (4.3 below). The existing water quality models have mainly been developed for rivers and lakes and not for estuarine and coastal waters, which are impacted by sea water ions. Also, the original formulations of QUAL2E have not included all of the processes occurring in nutrients cycle, especially the sediment nutrient interactions.

2.5 Summary

This chapter has investigated nitrogen in connection with environmental problems and the sources of nitrogenous water pollution, such as point source and diffuse source pollution. All of these pollutants are products of human activities of agricultural practice. These impacts have caused pollution of both ground and surface waters. The main contaminants which have been addressed in this thesis are nitrogen compounds. The presence of these pollutants is increased by chemical fertilizers, animal manure, crop residues etc. The increase in nitrogen inputs in river estuarine and coastal water systems can lead to eutrophication problems. Nitrogen compound losses or fluxes occur in the form of nitrate, ammonium or nitrous oxide. Nitrate is mobile in the water column and can enter the ground water system through leaching. Ammonium is soluble in the water column and, depending on the type of sediment, it can be adsorbed onto sediment. Ammonium is the major source of nitrogen in the environment and ammonium adsorption has been investigated in this study for both deionised and saline waters.

The adsorption processes of ammonium to the sediments has been investigated. The positively charged ammonium ion is adsorbed by the negatively charged surface of the sediment (clay or organic matter).

Adsorption isotherms and the adsorption isotherm model of Langmuir and Freundlich have been introduced in this chapter in order to be compared to the experimentally determined adsorption isotherms from this study. These types of theoretical models have been compared to the experimental adsorption isotherm in order to determine which model provides the best fit with these

ammonium adsorption isotherms. These comparisons enable an assessment of whether the Langmuir or Freundlich theoretical isotherm provides the best fit to the data and can inform as to whether ammonium adsorption is a mono-layer or multi-layer process (see Chapter 2). Salinity has been found in the literature to have a big influence on the ammonium adsorption and one of the main objectives of this study has also been to determine the adsorption coefficients of ammonium for both fresh and saline waters and also for different sediment particle sizes and total carbon content of the sediment.

Hydro-environmental computer models, which can be used to simulate the processes within the hydrological system, have been discussed in section 2.3. Numerical models have been designed to investigate surface water and ground water flow and contaminant transport processes in a water body. These models have been widely used to better understand the processes that occur in the hydrological system and to contribute to predicting the water quality characteristics of surface waters. A brief review of surface water models is has been carried out in section 2.3, including one-dimensional, two-dimensional and three-dimensional models. The depth integrated velocity and solute transport (DIVAST) model has been included in this study with its inclusion of the water quality formulations QUAL2E to model water quality problems. This study aims to improve on representation the nitrogen transport process in the DIVAST model and in particular for the adsorption processes of ammonium. These processes are investigated further in terms of developing an adsorption equation for ammonium, which has not previously been included in the DIVAST model. This new adsorption equation will increase the completeness of the water quality model DIVAST.

3 Water quality models

The growing concern of diffuse source pollution has resulted in the increasing application of water quality models to coastal waters in an attempt to assess and predict the impact that catchment-wide land use practices can cause on receiving water pollution. Many uncertainties are linked to water quality modelling, including uncertainties of both the hydrodynamic and biochemical processes occurring in coastal and estuarine waters. As well as the uncertainties there is also often a lack of data, which are unavailable for many coastal water basins.

Water quality modelling involves the prediction of water pollution processes using mathematical formulations and computational simulation techniques. A typical water quality model consists of a collection of formulations representing physical and biochemical processes that determine the fate and transport of pollutants in a water body. Water quality modelling is a complicated task because of the inherent randomness and uncertainties associated with various processes and variables throughout the receiving water environment and the frequent lack of suitable data (Abrishamchi et al, 2005). This study aims to improve our understanding of the behaviours of nitrogen compounds (nitrate and ammonium) and especially ammonium adsorption process for both fresh and saline water conditions. The study focuses on representing adsorption process of ammonium in the water quality model DIVAST by developing and adding new equations for ammonium adsorption. This equation provides a more complete representation of the ammonium adsorption process in this water quality model. The complete process of ammonium adsorption will be presented in this chapter.

The QUAL2E and QUAL2K water quality models which will be presented in Sections 3.1 and 3.2, have been widely used to form the basis of many coastal models to help predict and manage water quality problems such as eutrophication. However, there are limitations resulting from a lack of

knowledge of the model coefficients used to represent water quality processes, especially for estuarine and marine waters and these coefficients and representations have been refined herein.

3.1 QUAL2E model

The water quality model QUAL2E was developed by Brown and Barnwell (1987). It is a one-dimensional mathematical model, developed by Laboratory of Environmental Research of the United States Environmental Protection Agency (USEPA). This model has been widely used to evaluate surface water quality and is based on a series of bio-chemical formulations for water quality. It has been used in the Hydro-environmental Research Centre at Cardiff University as part of their DIVAST (Falconer et al, 2001) and HEMAT (Bockelmann et al, 2007). These models have been used for many applications, including for sample modelling flow and water quality processes in Carmarthen Bay, which is located in Pembrokeshire, West Wales. The DIVAST model is written in FORTRAN and includes the basic equations from the QUAL2E (Schnauder et al, 2007) model. Access to the water quality equations through the FORTRAN code allows the bio-chemical reactions for the nitrogen processes to be refined. Figure 3.1 shows the processes of the nitrogen cycle that are included in this model. QUAL2E is related to water quality processes present in the water body only and does not cover the processes of sediment water interaction which are important for adsorption processes.

One of the aims of this study has been to better represent sediment nutrient interactions in the DIVAST model especially the adsorption processes of ammonium in the sediment. This has been achieved by refining the governing biochemical formulations for nutrients, particularly nitrogen compounds (ammonium, nitrate and nitrite), and adsorption processes for ammonium ions in this case. This study investigates the adsorption processes for ammonium in the sediment in order to refine the adsorption equations and the adsorption coefficients for ammonium. The ammonium adsorption coefficient was

measured for both fresh and saline water conditions to give a better understanding of the sediment nutrient interaction as a function of this parameter.

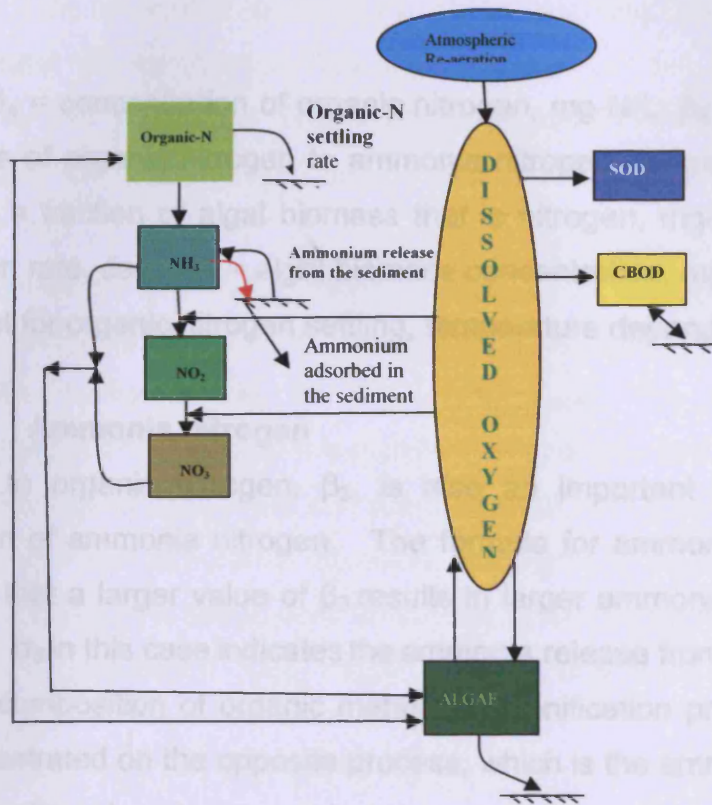


Figure 3.1: The concept of nitrogen cycle as indicated in QUAL2E-MODEL; the red arrows represent the ammonium adsorption processes in the sediment

3.1.1 Nitrogen compound processes in QUAL2E

3.1.1.1 Organic nitrogen

The biochemical reactions of organic nitrogen as represented in QUAL2E are indicated in Equation 3.1. The rate constant of the hydrolysis β_3 for organic nitrogen in converting to ammonium nitrogen is β_3 , which is the rate at which organic nitrogen breaks down due to the reaction with water at the correct temperature and pH. In addition to this, at high temperature and high pH the reaction of organic nitrogen will lead to ammonia production as a gas, rather than production of ammonium ions.

The ammonium ion in the model is referred to as ammonia, which is technically inaccurate (see Chapter 2).

$$\frac{dN_4}{dt} = \alpha_1 * \rho * A - \beta_3 * N_4 - \sigma_4 * N_4 \quad (3.1)$$

Where: N_4 = concentration of organic nitrogen, mg-N/L; β_3 = rate constant for hydrolysis of organic nitrogen to ammonia nitrogen, temperature dependent, day⁻¹; α_1 = fraction of algal biomass that is nitrogen, mg-N/mg-A; ρ = Algal respiration rate, day⁻¹; A = algal biomass concentration, mg-A/L; and σ_4 = rate coefficient for organic nitrogen settling, temperature dependent, day⁻¹

3.1.1.2 Ammonia nitrogen

Similarly to organic nitrogen, β_3 , is also an important coefficient for the production of ammonia nitrogen. The formula for ammonia in equation 3.2 indicates that a larger value of β_3 results in larger ammonium concentrations over time. σ_3 in this case indicates the ammonia release from the sediment due to the decomposition of organic matter (ammonification process). This study has concentrated on the opposite process, which is the ammonium adsorption onto the sediment.

$$\frac{dN_1}{dt} = \beta_3 * N_4 - \beta_1 * N_1 + \frac{\sigma_3}{d} - F_1 * \alpha_1 * \mu * A \quad (3.2)$$

Where:

N_1 = the concentration of ammonium nitrogen, mg-N/L; N_3 = the concentration of nitrate nitrogen, mg-N/L; N_4 = the concentration of organic nitrogen, mg-N/L; β_1 = rate constant for the biological oxidation of ammonia nitrogen, temperature dependent, day⁻¹; σ_3 = the benthos source rate for ammonia nitrogen, mg-N/ft²-day, d = mean depth of flow, ft; F_1 = fraction of algal nitrogen uptake from ammonium pool; μ = the local specific growth rate of algae, day⁻¹; and A = algal biomass concentration, mg-A/L

3.1.1.3 Ammonium adsorption processes

Ammonium adsorption has also been investigated in this study and has been included in the nitrogen cycle of the DIVAST model. The concentration of ammonium (N1) is produced during the decomposition of organic matter in the sediments. This amount of ammonium can be released from the sediment or adsorbed onto the sediments. This study focuses on the ammonium that is adsorbed by the sediments. The ammonium adsorption process can occur before ammonium oxidizes to nitrite and subsequently to nitrate (nitrification).

The ammonium nitrogen in the water column can be classified as a dissolved phase, and in the sediment as the adsorbed phase, with the concentrations of each phase being written as C_{wN1} and C_{sN1} . The adsorbed phase concentration depends on both the sediment ammonium concentration and the ammonium concentration of the surrounding water. It can be expressed as the following ammonium adsorption equation, developed in this study.

Where: the equation is based on a linear relationship between the equilibrium ammonium concentration (C_{wN1} mg/l) and the adsorbed ammonium (C_{sN1} mg/g) giving:

$$C_{sN1} = K_p * C_{wN1} \quad (3.3)$$

Where: K_p = adsorption coefficient (partitioning coefficient) (l/g), which describes the ammonium concentration distribution between dissolved and adsorbed phase; C_{wN1} = equilibrium concentration of ammonium (mg/l); and C_{sN1} = adsorbed ammonium (mg/l)

The total concentration of the ammonium can then be written as:

$$C = C_{wN1} + C_{sN1} = C_{wN1} + K_p * C_{wN1} * S \quad (3.4)$$

Where: C = total concentration of ammonium (mg/l); S = the sediment concentration (mg/l); the fraction of dissolved and adsorbed concentration can therefore be derived as:

$$f_{wN1} = \frac{C_{wn1}}{C} = \frac{1}{1 + K_p S} \quad (3.5)$$

$$f_{sN1} = \frac{C_{sN1}}{C} = \frac{K_p S}{1 + K_p S} \quad (3.6)$$

Sediment porosity and particle density can be included to calculate the dimensionless partition coefficient (K_{pd}). The dimensionless partition coefficient equation can then be written as:

$$K_{pd} = \frac{1 - \phi}{\phi} * \rho * k_p \quad (3.7)$$

Where: Φ = porosity of the sediment (%); and ρ = density of the sediment (g/cm^3)

This part of the nitrogen cycle includes: new variables related to the adsorption process of ammonium; the dissolved ammonium concentration; the adsorbed ammonium and the total ammonium. The partitioning coefficient and the dimensionless partition coefficient (K_{pd}) were determined both for fresh and saline water conditions.

3.1.1.4 Nitrite

The most sensitive parameters in the nitrite equation are β_1 and β_3 , which both cause changes in the nitrite concentration (see equation 3.8).

$$\frac{dN_2}{dt} = \beta_1 N_1 - \beta_2 N_2 \quad (3.8)$$

Where: N_2 = the concentration of nitrite nitrogen, mg-N/L; and β_2 = rate constant for the oxidation of nitrite nitrogen, temperature dependent, day^{-1}

3.1.1.5 Nitrate

As shown in equation 3.9, the nitrate equation in QUAL2E does not include denitrification.

$$\frac{dN_3}{dt} = \beta_2 N_2 - (1 - F)\alpha_1 \mu A \quad (3.9)$$

Where: F = fraction of algal nitrogen taken from ammonium pool; α_1 = fraction of algal biomass that is nitrogen, mg-N/mg-A; and μ = local specific growth rate of algae, day⁻¹

3.2 QUAL2K model

The QUAL2K model (Chapra et al, 2005) is a more advanced version of the water quality model QUAL2E. It includes a more detailed representation of some of water quality processes in QUAL2K. QUAL2K additionally covers sediment water interaction such as denitrification, which occurs in anoxic (oxygen-depleted) sediments. However it does not include ammonium adsorption processes. Most of the model equations included in QUAL2K are similar to those in QUAL2E except for the Dissolved equation for Oxygen (DO) and the Biological Oxygen Demand (BOD). Sediment water interaction processes, such as denitrification have also been included. Figure 3.2 shows the processes of the nitrogen cycle which are included in the QUAL2K model.

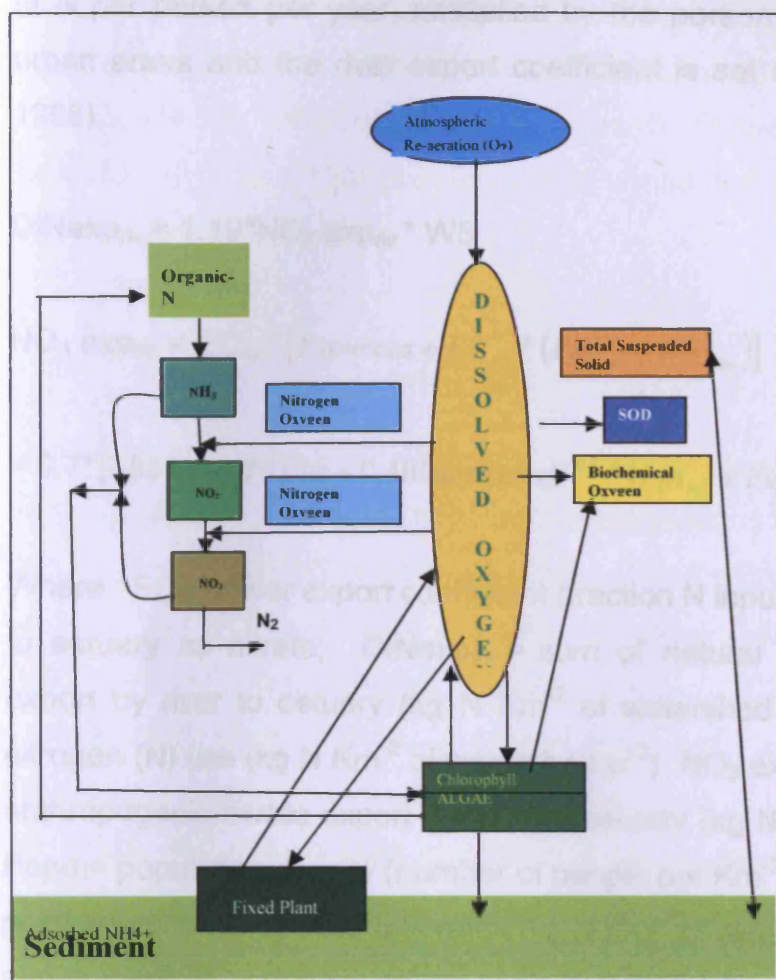


Figure 3.2: Representation of the nitrogen cycle in QUAL2K

3.3 N-model

The N-model is another surface water quality model that considers eutrophication problems in surface waters (including coastal, estuary and river waters). The N-model was developed by Caraco and Cole (1999). The model is based on regression analysis, revealing the relationship between measured nitrate export for up to 35 rivers ($NO_{3exp_{riv}}$) as a function of point source N inputs to those rivers from human sewage and non-point N inputs from fertilizer use and atmospheric deposition to the soils in the watershed as indicated in equation 4.11. Dissolved inorganic nitrogen (DIN) exported by rivers is calculated by the N-model as a function of fertilizer use, sewage production and atmospheric deposition in the watersheds (Kroeze and Seitzinger, 1998) as shown in equation 4.10. As indicated in equation 4.12, sewage loading, or point source inputs ($P_{sources}$), are calculated as 1.85 kg

of N per person per year, multiplied by the portion of population that live in urban areas and the river export coefficient is set to 0.7 (Caraco and Cole, 1998).

$$\text{DINexp}_{\text{riv}} = 1.19 \cdot \text{NO}_3 \text{ exp}_{\text{riv}} \cdot \text{WS} \quad (3.10)$$

$$\text{NO}_3 \text{ exp}_{\text{riv}} = \text{EC}_{\text{riv}} \cdot [P_{\text{sources}} + \text{EC}_{\text{ws}} \cdot (P_{\text{pt}_{\text{ws}}} + \text{Fert}_{\text{ws}})] \quad (3.11)$$

$$= 0.7 \cdot [1.85 \cdot \text{Popd} \cdot \text{Urb} + 0.4 \cdot \text{WaterRunoff}^{0.8} \cdot (P_{\text{pt}_{\text{ws}}} + \text{Fert}_{\text{ws}})] \quad (3.12)$$

Where : EC_{riv} = river export coefficient (fraction N inputs to river that is exposed to estuary as nitrate); $\text{DINexp}_{\text{riv}}$ = sum of natural and anthropogenic DIN export by river to estuary (kg N Km^{-2} of watershed yr^{-1}); Fert_{ws} = fertilizer nitrogen (N) use (kg N Km^{-2} of watershed yr^{-1}); $\text{NO}_3 \text{ exp}_{\text{riv}}$ = sum of natural and anthropogenic nitrate export by river to estuary (kg N Km^{-2} of watershed yr^{-1}); Popd = population density (number of people per Km^{-2} of watershed); P_{sources} = point sources sewage loading rates (kg N Km^{-2} of watershed yr^{-1}); $P_{\text{pt}_{\text{ws}}}$ = total atmospheric NOy deposition (kg N Km^{-2} of watershed yr^{-1}); EC_{ws} = watershed export coefficient (fraction that is not retained); Urb = fraction of population living in urban areas; WaterRunoff = water runoff ($\text{m}^3 \text{m}^{-2} \text{yr}^{-1}$); and WS = watershed area (Km^{-2})

The N-model determines the dissolved inorganic nitrogen export by rivers to the sea. Dissolved inorganic nitrogen (DIN) is exported as calculated by the N-model as a function of watershed area atmospheric deposition (NOy), water runoff, population, urbanization and fertilizer use. The goal of that study was to quantify nitrogen fluxes into and out of the sea as well as possibilities to reduce nitrogen related to environmental problems (e.g. eutrophication) in the sea. The N-model has been used in the US and in Europe since its development. The N-model calculates DIN input to estuaries from river nitrate export assuming that 84% of DIN in the river water is nitrate (Kroeze and Seitzinger, 1998). The N-model has calculated the highest point source input for the River Thames. This high value reflects both the high population densities in this

watershed, which is about 400 individuals km^{-2} and the high degree of urbanization, which is 92%. Nitrate export by the Thames River per year was 1120 (kg N Km^{-2} of watershed yr^{-1}). Thus, the NO_3 export was higher in the Thames with a very high population and a moderate runoff (Caraco and Cole, 1999).

3.4 Water quality analysis simulation programme (WASP)

In the WASP water quality model emphasis is given to the simulation of the biogeochemical transformation that determines the fate of nutrients, in particular the simulation of the aquatic cycles of nitrogen and phosphorus compounds. This model also includes procedures for determination of growth and death of phytoplankton (Zhang et al., 2008). WASP is a dynamic compartment model that can be used to analyse a variety of water quality problems in such diverse water bodies as streams, lakes, reservoirs, rivers, estuaries, and coastal waters. WASP is a dynamic compartment-modelling programme for aquatic systems, including both the water column and the underlying benthos. This model allows the user to investigate 1, 2, and 3 dimensional systems, and a variety of pollutant types.

3.4.1 WASP Version 5 (WASP5)

This refined version of the WASP model was developed by Ambrose et al. (1993a,b). It can simulate the transport and transformations of organic and inorganic ammonium, nitrate and nitrite nitrogen, phosphorus organics, algae oxygen and carbonaceous oxygen demand. This model can be linked with hydrodynamic and sediment transport models that can provide as output: velocities, water depths, temperature, salinity and sediment fluxes. A study by James et al (1997) investigated the influence of sediment resuspension on the water quality of shallow lakes. The WASP5 model was used in that study to simulate algal dynamics and nitrogen, phosphorus and oxygen cycles and inorganic suspended solids were also included in the study. Therefore, the inclusion of sediment resuspension to the WASP model in this study improved the accuracy of nutrient and chlorophyll predictions as it included fluxes of

organic and inorganic nutrients and inorganic suspended solids between sediments and the water column.

3.5 Summary

This chapter discussed the main water quality models. Water quality modelling involves the prediction of water pollution transport processes using mathematical formulations and computational simulation techniques. Typically, water quality models consist of a collection of formulations representing physical and biochemical processes that determine the fate and transport of pollutants in the water body, but still there are limitations in using these models due to the uncertainties associated with various processes and variables throughout the receiving water environment and the lack of data. The ammonium adsorption equation that is developed in this study is described in this chapter in section 3.1.1.3. The adsorption equation of ammonium is based on the linear relationship between equilibrium concentration of ammonium and adsorbed ammonium. The total concentration of ammonium is calculated and presented in individual equations by adding the concentration of equilibrium ammonium to the concentration contributed by the adsorbed ammonium.

4 Laboratory experiments – Materials and Methods

This chapter deals with the materials and procedures used in the ammonium (NH_4^+) adsorption isotherm experiments, NH_4^+ desorption experiments, the NH_4^+ kinetics test of adsorption / desorption, and also the nitrate adsorption experiments. The objective of these experiments was to find the adsorption coefficients of ammonium for clays (Kaolinite and Montmorillonite) and two grades of sand (coarse and fine). This study was conducted using both deionised water and artificial sea water. Three different concentrations of artificial sea water were prepared and used: including 35, 25 and 17 parts per thousand (ppt). In the nitrate adsorption experiments, which were carried out for Kaolinite only, two conditions were tested (using distilled water and artificial sea water) to determine the respective adsorption coefficients.

4.1 Sample preparation

Before starting the adsorption experiments and to achieve the actual adsorption processes, sample preparation was carried out using the following methods.

4.1.1 Water sample

Deionised water and artificial sea water were used in this study. Artificial sea water was prepared according to the Scottish Association for Marine Science (MASM, 2007) standard. Concentrations of salts were prepared using artificial seawater solution (35ppt) and giving:

- $\text{MgSO}_4 \cdot 7\text{H}_2\text{O}$ -24.4g
- KCl -6.0g
- NaNO_3 -10.0g
- $\text{CaCl}_2 \cdot 2\text{H}_2\text{O}$ - 3.0 g
- KH_2PO_4 -0.5g
- NH_4Cl - 2.67 g
- NaCl - 30.0 g

Each of the salts were dissolved into 100 ml of distilled water, agitated and made up to 1 litre using deionised water. The pH of this solution was measured with a Seven Multi pH meter and found to be 8.5. Prior to measurements the meter was calibrated using pH buffers of 4 and 7 as indicated in Section 4.4.5. The same procedure was used to prepare the other artificial sea water concentrations.

4.1.2 Clays and sand

Commercially available Kaolinite, Montmorillonite and sand were obtained. Sand was crushed in order to prepare fine samples; this was done using a Labtech Essa LM1-P ring mill.

4.1.2.1 Washing clays and sand

The commercial clay and sand were treated with chemicals during manufacture, therefore they were washed prior to use in experiments carried out as a part of this study. There are several steps to obtain clean clays and sands. This study closely followed the method of Jeon et al. (2001).

Kaolinite, Montmorillonite and sand (coarse and fine) were prepared by washing of 400 g samples. These samples were washed for 24 hours with 0.1 N NaOH and then washed twice with deionised water. The suspension was subsequently washed with 0.1 HCl solution for 24 hours and then 6 times with deionised water, until the desired electronic conductivity (EC) was reached, i.e. close to the EC of distilled water.

Following each wash the suspension was centrifuged at 3000 rpm for 20 minutes. Electronic conductivity and pH were measured by a Seven Multi instrument (range 0.0 to 14.0 pH) with an accuracy ± 0.2 pH and a range from 0 to 1990 $\mu\text{S}/\text{cm}$ for conductivity. The meter was calibrated using pH buffers of 4 and 7 and 0.01 M KCl solutions to adjust the EC to 1413 at 25 °C. The pH and EC were measured after each washing as indicated in Figures 4.1 - 4.4. These figures are included to show the properties of each material at each

washing stage, and in order to illustrate how the washing process affected the material.

4.1.2.2 Chemical preparation

In this step in the experiments the chemical concentration of ammonium chloride and sodium nitrate were separately varied in order to measure the adsorption coefficients for ammonium and nitrate at varying concentrations of ammonium and nitrate. Ammonium chloride (NH_4Cl_2) was varied in concentrations of 2, 4, 6, 8, 10, 20 and 30 mg/l NH_4^+ . Sodium nitrate (NaNO_3) was varied in concentrations of 2, 4, 10, 20 and 30 mg/l NO_3^- .

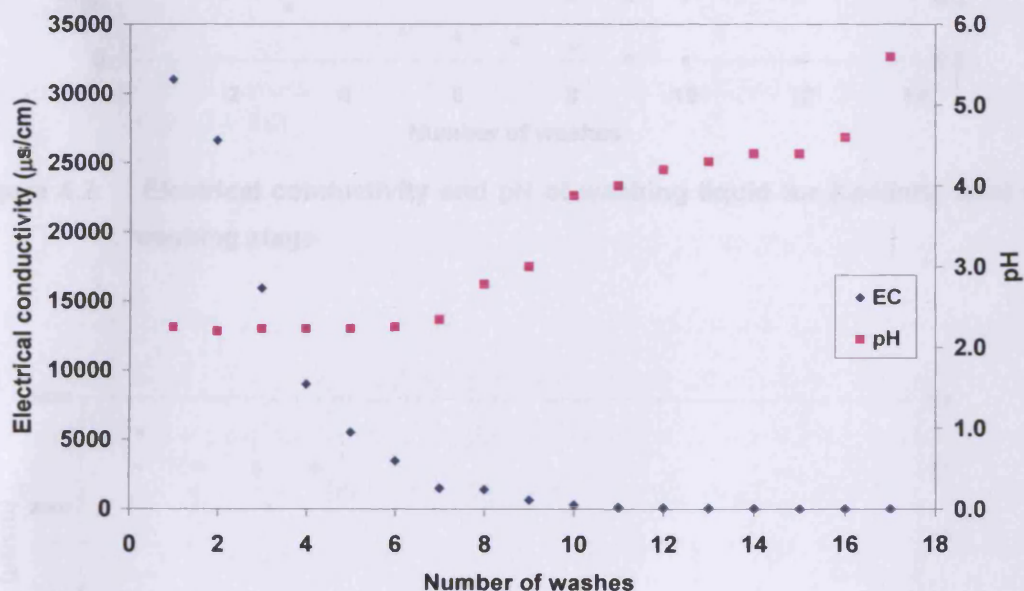


Figure 4.1: Electrical conductivity and pH of washing liquid for Montmorillonite after each washing stage

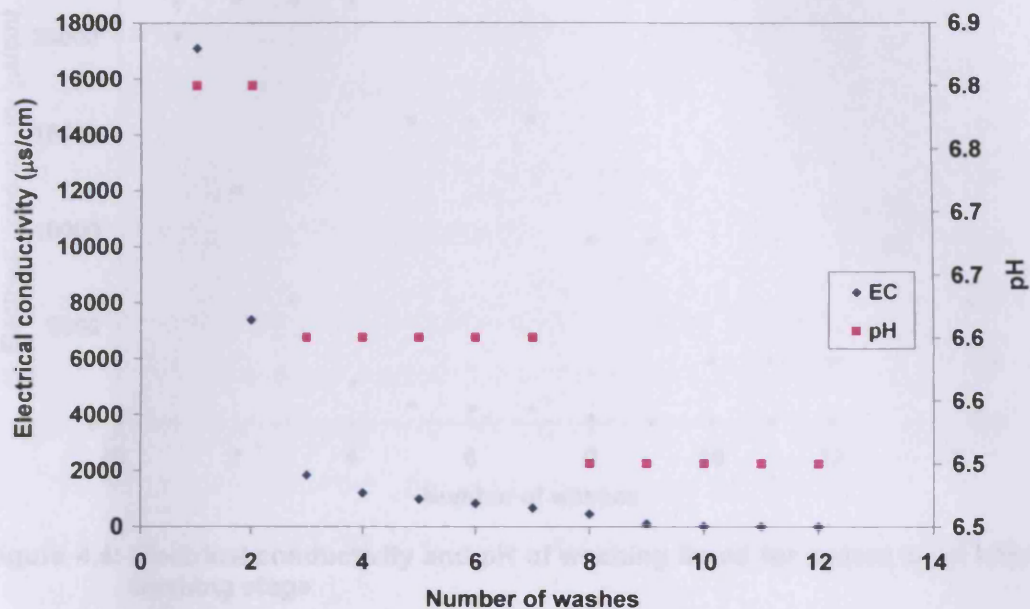


Figure 4.2: Electrical conductivity and pH of washing liquid for Kaolinite after each washing stage

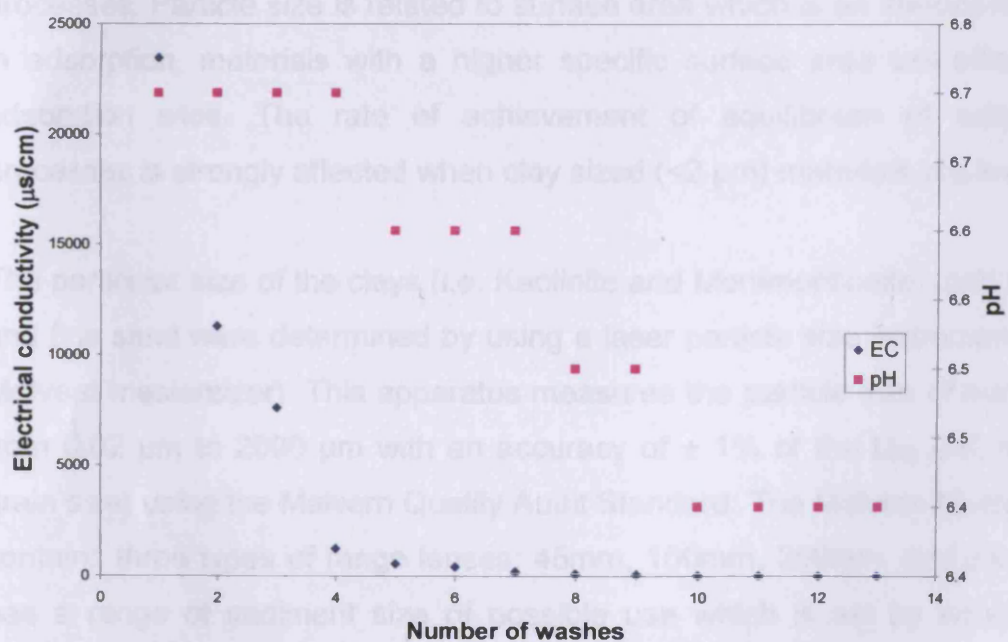


Figure 4.3: Electrical conductivity and pH of fine sand after each washing stage

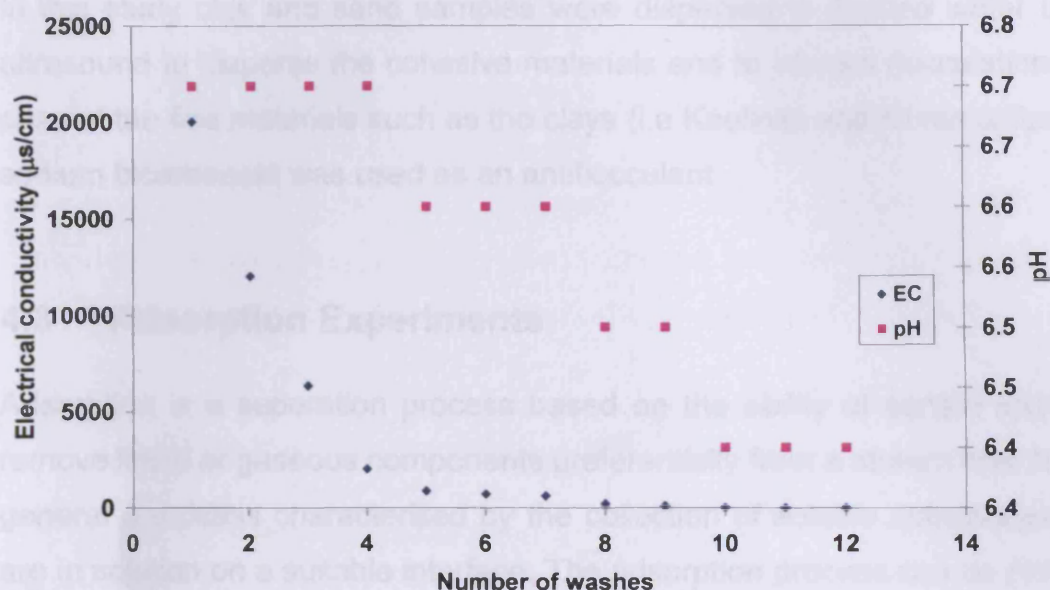


Figure 4.4: Electrical conductivity and pH of washing liquid for coarse sand after each washing stage

4.2 Particle size distribution analysis of clays and sand

It is important to know the size of material in order to study adsorption processes. Particle size is related to surface area which is an important factor in adsorption, materials with a higher specific surface area will offer more adsorption sites. The rate of achievement of equilibrium of adsorption processes is strongly affected when clay sized ($<2\ \mu\text{m}$) materials are involved.

The particular size of the clays (i.e. Kaolinite and Montmorillonite), and coarse and fine sand were determined by using a laser particle size instrument (i.e a Malvern mastersizer). This apparatus measures the particle size of materials, from $0.02\ \mu\text{m}$ to $2000\ \mu\text{m}$ with an accuracy of $\pm 1\%$ of the D_{50} (i.e. median grain size) using the Malvern Quality Audit Standard. The Malvern Mastersizer contains three types of range lenses: 45mm, 100mm, 300mm, and each one has a range of sediment size of possible use which is set by whether its aperture is large enough to collect the scattering angles needed. In the case of fine material, such as clay, the 100mm lens was used and for the coarse material, such as sands the 300mm lens was used. The material density and

obscuration settings were defined prior to the test. The density of the soil mineral particles usually varied from 2.6 to 2.7 gm/cm³ (Wild, 2001).

In this study clay and sand samples were dispersed in distilled water using ultrasound to disperse the cohesive materials and to prevent flocculation. For case of the fine materials such as the clays (i.e Kaolinite and Montmorillonite), sodium bicarbonate was used as an antiflocculant.

4.3 Adsorption Experiments

Adsorption is a separation process based on the ability of certain solids to remove liquid or gaseous components preferentially from a stream flow. It is in general a process characterised by the collection of soluble substances that are in solution on a suitable interface. The adsorption process can be pictured as one in which molecules leave solution and are held on the solid surface (Wark and Warner, 1976).

4.3.1 Adsorption isotherm experiments

The goal of these experiments was to perform ammonium adsorption isotherm experiments for 24 hours, as this was found to be sufficient for equilibrium to be reached. Deionised water and artificial sea water of different concentrations were used in this study. A 0.8 g sample of each material, including Kaolinite, Montmorillonite, coarse and fine sand were placed in a centrifuge tube containing 40 ml of NH₄⁺Cl, at varying concentrations of NH₄⁺. Covering 2, 4, 6, 8, 10, 20 and 30 mg/l NH₄⁺. The centrifuge tube was placed on a shaker with continuous agitation for 24 hours, at standard room temperature, as shown in Figure 4.5. The samples were then centrifuged at 3000 rpm for 20 minutes. The supernatant was then collected, filtered through a 2 µm cellulose filter paper and analysed for NH₄⁺. This was undertaken using a Lambda EZ150 Spectrophotometer in conjunction with HACH reagent as described in 4.4.1. The wavelength was set at 640 nm. The wavelength accuracy of this device was ± 1 nm and the wavelength range was 200 to 1100 nm.

4.3.2 Desorption experiments

The adsorption isotherm experiment was followed by desorption experiments. Wherein 40ml of 2 M KCl solution was added to the clays and sand remaining in the centrifuge tubes and replaced on the shaker. After 2 hours agitation by shaking, the solutions were centrifuged at 3000 rpm for 20 minutes. The supernatant was removed and analysed with the spectrophotometer. This procedure was repeated until NH_4^+ was removed from the clays and sand. In this way desorption and adsorption phenomena were studied for NH_4^+ .

4.3.3 Kinetic experiments using artificial sea water

The purpose of these tests was to ascertain the time it took for the clays and sand samples to reach desorption equilibrium. The kinetic tests were performed at standard room temperature. In this experiment three different concentrations of ammonium chloride (NH_4Cl_2) were prepared including 2, 6 and 10 mg/l NH_4^+ . The sediments samples in the kinetic experiments consisted of two types of clays (Kaolinite and Montmorillonite) and coarse and fine sand. These were all weighed into 0.8 g portions. Each sample was then placed in 3 polyethylene centrifuge tubes containing 40 ml of 3 concentrations of ammonium, i.e. 2, 6 and 10 mg/l NH_4^+ made from deionised water. The samples were placed in a shaker, with continuous agitation for 24 hours as shown in Figure 4.5.

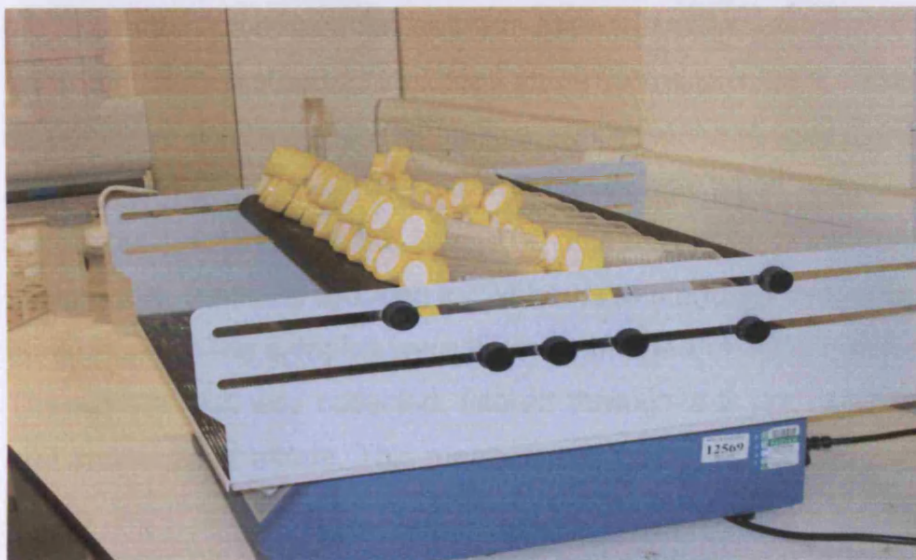


Figure 4.5: Set of samples in the shaker

The samples were left for 24 hours to reach equilibrium. The supernatant was then removed and filtered. The solutions were analysed using the spectrophotometer and the NH_4^+ concentration measured. 40 ml of artificial sea water was then added to the remaining clays and sand slurries. The tubes were replaced on the shaker and every 10 minutes a tube of each concentration was removed. The removed solution was then centrifuged, filtered and the supernatant was extracted for NH_4^+ analysis. This procedure was continued for 1 hour and 20 minutes. After this time there was one remaining set of solutions at each concentration, to serve as a control set. This set was left on the shaker for 24 hours in order to be certain that the solutions had reached equilibrium. These samples were then analysed with the same procedure. The amount of NH_4^+ adsorbed by the clays and sand was calculated and plotted against time. The filtered solution was analyzed for ammonium concentration, using a spectrophotometer and HACH reagent as explained in Section 4.4.1. Experiments were conducted in triplicate for each concentration of ammonium for all sediment samples.

4.3.4 Nitrate adsorption on Kaolinite

The main aim of this experiment was to establish if adsorption of nitrate on Kaolinite was taking place and consequently to measure nitrate adsorption on

the Kaolinite. The adsorption isotherm experiment was performed for 24 hours, using the same method as indicated above in Section 4.3.1. Deionised water and different concentrations of artificial sea water were used in this study.

A 0.8 g of Kaolinite was placed in 8 centrifuge tubes, containing 40 ml of NaNO_3^- at 2, 4, 6, 20, 30, 40, 50 and 60 mg/l NO_3^- . The tubes were placed on a shaker, with continual agitation for 24 hours at standard temperature (i.e. room temperature). The samples were then centrifuged at 3000 rpm for 15 minutes. The supernatant was collected, filtered through a 2 μm cellulose filter paper and analysed for nitrate. This measurement was undertaken using a Lambda EZ150 Spectrophotometer again using HACH reagent with the wavelength set at 543 nm. The NO_3^- was considered as being at equilibrium concentration. The adsorption experiment was followed by a desorption procedure in order to remove NO_3^- from the surface of the Kaolinite. A 40 ml of 0.5 K_2SO_4^- solution was added to the clay remaining in the centrifuge tubes, and the solution replaced on the shaker. After 30 minutes agitation the solutions were centrifuged at 3000 rpm for 15 minutes. The supernatant was removed and analysed with the spectrophotometer and HACH reagent as indicated in Section 5.4.2. This procedure was repeated until NO_3^- was removed from the surface of the Kaolinite.

4.4 Sample analysis

The ammonium and nitrate concentrations for the above experiments were analysed using a Lambda EZ150 Spectrophotometer and HACH reagent as shown in Figure 4.6. The principle how a Spectrophotometer works is that it sends light at a set wavelength coming through a sample and a detector determines the percentage of light that is not absorbed by the sample. The adsorbed percentage of the light and the resulting concentration of NH_4^+ were then calculated.



Figure 4.6 : Spectrophotometer device (Lambda EZ 150)

4.4.1 Use of HACH reagent to determine ammonium concentration

The reagents used in these experiments were ammonia salicylate reagent powder, ammonia cyanurate reagent powder and ammonia ammonia ver diluent reagent vials. A 0.1 ml sample was added to the dilution reagent vials and then salicylate and cyanurate were added and mixed together. This solution was left for 20 minutes until any changes in colour were complete. After the colour change was complete 10ml of the final solution was transferred to a cuvette using a syringe. The cuvette was placed into the spectrophotometer and the sample was analyzed at 640nm (Eaton et al.,1995).

4.4.2 Use of HACH reagent to determine the nitrate concentration

The reagent used was Nitra Ver 5 Nitrate powder pillow. A 10 ml sample was added to the test container. One powder pillow reagent of nitra ver 5 nitrate was added to the sample and the solution was left for 5 minutes until a change of colour occurred. After the colour changed 10 ml of solution was placed into a cuvette using a syringe. The cuvette was placed into the

spectrophotometer and the sample was analysed at 543 nm (Eaton et al., 1995).

4.4.3 Calibration curve for ammonium

Different concentrations of ammonium were prepared for calibration of the spectrophotometer used in this study. Ammonium chloride (NH_4^+Cl) was used as a source of ammonium. The sorption of ammonium occurs at a wavelength of 640 nm. Figure 4.7 shows the concentrations of ammonium (mg/l) and the spectrophotometer readings. The calibration was acceptable, given that the coefficient of determination (R^2) was 0.9973. In order to obtain accurate results the standard curve was prepared each time a new experiment was carried out. The error bars represent the maximum and minimum values in X which is ammonium concentration (mg/l), and Y is absorbance (nm) over three replicates. No error bars are visible, as the distribution of data around each point is small.

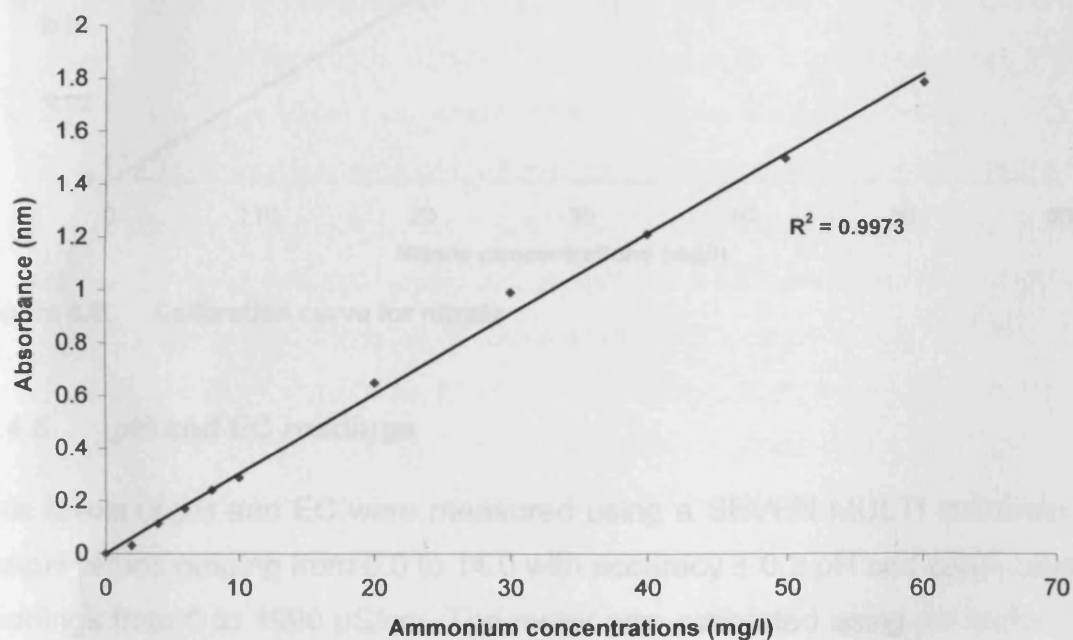


Figure 4.7: Calibration curve for ammonium

4.4.4 Calibration curve for nitrate

Different concentrations of nitrate were prepared to set up the calibration curve for nitrate. Sodium nitrate (NaNO_3^-) was used as source of nitrate. The

absorption of nitrate occurs at a wavelength of 543 nm. Figure 4.8 shows the concentrations of nitrate (mg/l) and the spectrophotometer readings. The calibration was acceptable, given that the coefficient of determination (R^2) was 0.9947. The error bars over three replicates represent the maximum and minimum values of X, which is nitrate concentration (mg/l), and Y is absorbance (nm) of measured absorbance of different concentration of nitrate solutions. Error bars are not visible as the distribution of data around each point is small.

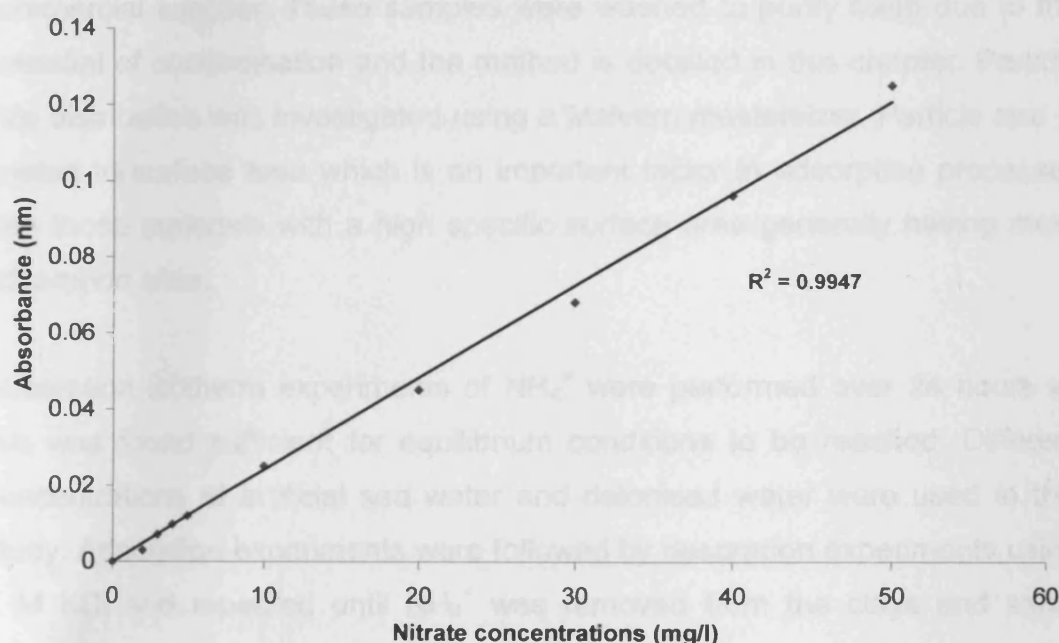


Figure 4.8: Calibration curve for nitrate

4.4.5 pH and EC readings

The levels of pH and EC were measured using a SEVEN MULTI instrument, for pH values ranging from 0.0 to 14.0 with accuracy ± 0.2 pH and conductivity readings from 0 to 1990 $\mu\text{S}/\text{cm}$. The meter was calibrated using pH buffers 4 and 7 and 0.01 M of KCl solution to adjust EC to 1413 at 25 °C.

4.5 Summary

This chapter has addressed the materials and methods for ammonium adsorption and desorption experiments, the kinetics test of desorption and nitrate adsorption experiments. Two types of water were used in these experiments; these were deionised and artificial sea water. These were prepared with different concentrations in order to study the effect of salinity on the NH_4^+ adsorption onto Montmorillonite, Kaolinite and coarse and fine sand samples. The clay and sand used in these experiments was obtained from a commercial supplier. These samples were washed to purify them due to the potential of contamination and the method is detailed in this chapter. Particle size distribution was investigated using a Malvern mastersizer. Particle size is related to surface area which is an important factor in adsorption processes with those materials with a high specific surface area generally having more adsorption sites.

Adsorption isotherm experiments of NH_4^+ were performed over 24 hours as this was found sufficient for equilibrium conditions to be reached. Different concentrations of artificial sea water and deionised water were used in this study. Adsorption experiments were followed by desorption experiments using 2 M KCl and repeated until NH_4^+ was removed from the clays and sand. Kinetic experiments are addressed in this chapter which were carried out using artificial sea water and the goal of these experiments was to find out the time required for the Montmorillonite, Kaolinite and coarse and fine sand samples to reach desorption equilibrium. NO_3^- adsorption on Kaolinite was investigated in this chapter to determine the adsorption of nitrate on kaolinite. This experiment was performed over 24 hours using the same method as for NH_4^+ . The Spectrophotometer was used in conjunction with HACH reagents to determine the concentrations of both NH_4^+ and NO_3^- , at specific wavelengths, of 640nm and 543nm, respectively.

5 Laboratory experiments – results and discussion

This chapter presents the results of ammonia adsorption isotherms for Montmorillonite, Kaolinite and fine and coarse sand for both deionised and artificial sea water conditions, the ammonium kinetics test of adsorption / desorption. Also the results of nitrate adsorption isotherm for Kaolinite under deionised and artificial sea water are considered in this chapter. The results of isotherm experiments for ammonium and nitrate were conducted using two types of water, i.e. deionised and artificial sea water of different salinities, in order to determine the adsorption coefficients for both conditions and to determine the effect of salinity on the adsorption coefficient. Duplicate experiments were conducted for each experiment and the average was taken.

5.1 Ammonium adsorption isotherms

The results of adsorption isotherm of ammonium in deionised water and artificial sea water on Montmorillonite, Kaolinite, coarse and fine sand are presented in this section. Different concentrations of ammonium were used (2, 4, 6, 8, 10, 20, 30, 40, 50 and 60 mg/l NH_4^+) in order to determine the Freundlich and Langmuir adsorption isotherms of ammonium for these sediments.

Figures 5.1- 5.8 show comparisons between the experimental and theoretical results, using the Langmuir and Freundlich adsorption isotherm equations (2.2, 2.3) and (2.4, 2.5) respectively, which were presented in section 2.2.3. All points on these figures were carried out following the methods described in Chapter 4, thus representing an equilibrium concentration. The amount of adsorbed ammonium was calculated by dividing the ammonium equilibrium concentration as a unit of mass by the weight of clay and sand in the samples, with the result being displayed in a form that can be compared with the theoretical isotherms (Langmuir and Freundlich isotherms). Figures 5.1-5.8 indicate the theoretical adsorption coefficients (Langmuir and Freundlich) presented as K (Freundlich coefficient) and b (Langmuir coefficient). The

adsorption coefficient for Montmorillonite for both theories (Langmuir and Freundlich) at deionised and artificial sea water was higher compared to other sediment samples. The values of adsorption coefficient for Freundlich were higher than the Langmuir values. The Langmuir adsorption coefficient (b) ranged between (0.0027 to 0.171) and the Freundlich values adsorption coefficient (K) ranged between (4 to 316). The theoretical adsorption coefficient was lower at artificial sea water than deionised water. The results indicated that the Freundlich model did not fit well with experimental data the ammonium adsorption for Montmorillonite, Kaolinite, coarse and fine sand for the experimental data for the two types of water (deionised and artificial sea water) and the high ammonium equilibrium concentrations were respectively (1.13, 1.12), (1.07, 1.10), (1.08, 1.05), (1.12, 1.09) times lower than the Freundlich isotherm model. In contrast the results showed good agreement between the experimental and theoretical treatment. The Langmuir model fits was found to the data reasonably well for all samples tested, according to the error analysis that was performed for all the samples. The error bars represent the maximum and minimum values (in X which is ammonium equilibrium concentration (mg/l) and Y is adsorbed ammonium ($\mu\text{g/g}$)) over three replicates of measured ammonium adsorption on the sediments. No error bars are visible, as the distribution of data around each point is small.

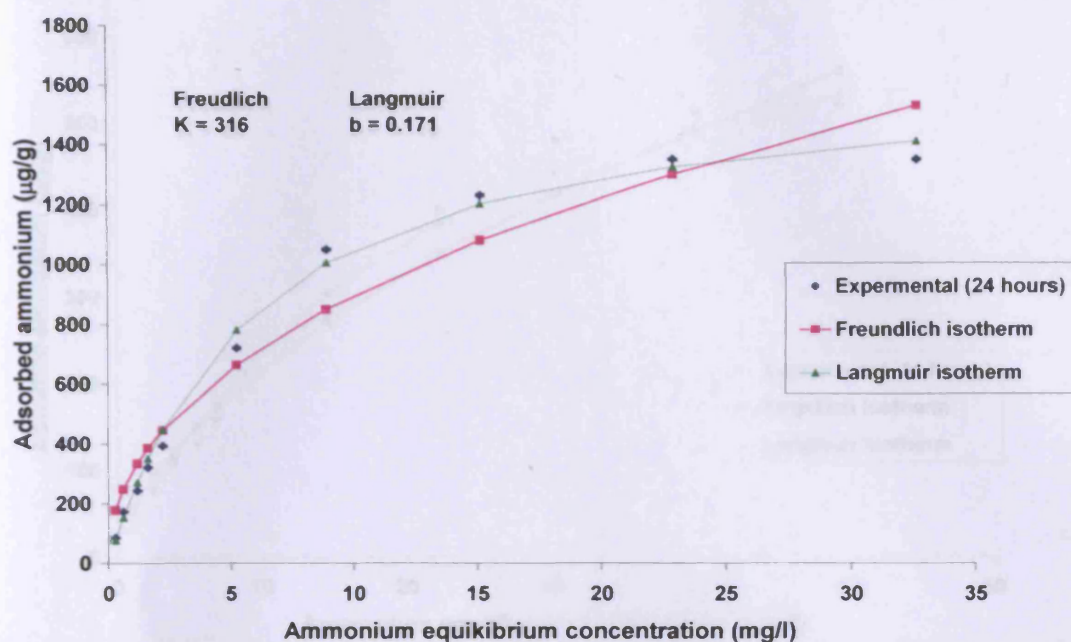


Figure 5.1: Experimental results and theoretical (Langmuir and Freundlich) adsorption isotherms for ammonium on Montmorillonite in deionised water, (b) is the Langmuir constant and adsorption coefficient, K is the Freundlich constant and adsorption coefficient

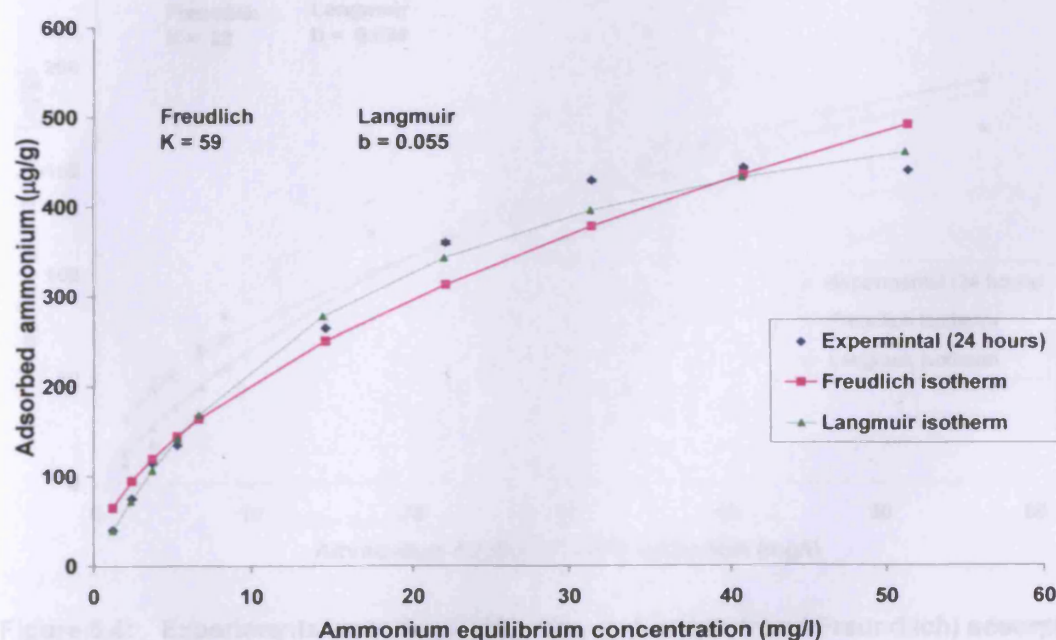


Figure 5.2: Experimental results and theoretical (Langmuir and Freundlich) adsorption isotherms for ammonium on Montmorillonite in artificial sea water, (b) is the Langmuir constant and adsorption coefficient, K is the Freundlich constant and adsorption coefficient

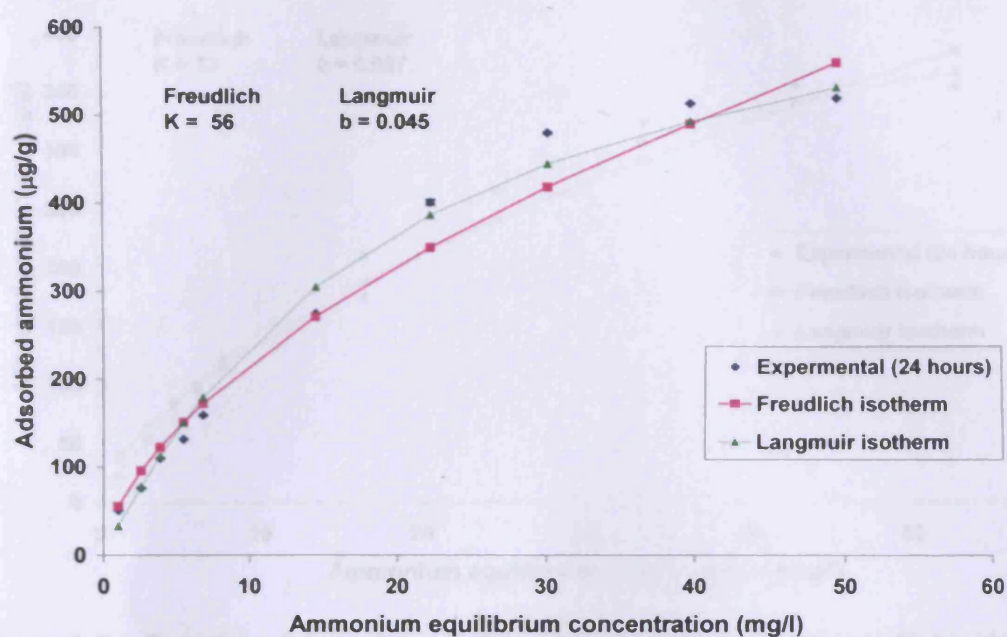


Figure 5.3: Experimental results and theoretical (Langmuir and Freundlich) adsorption isotherms for ammonium on Kaolinite in deionised water.

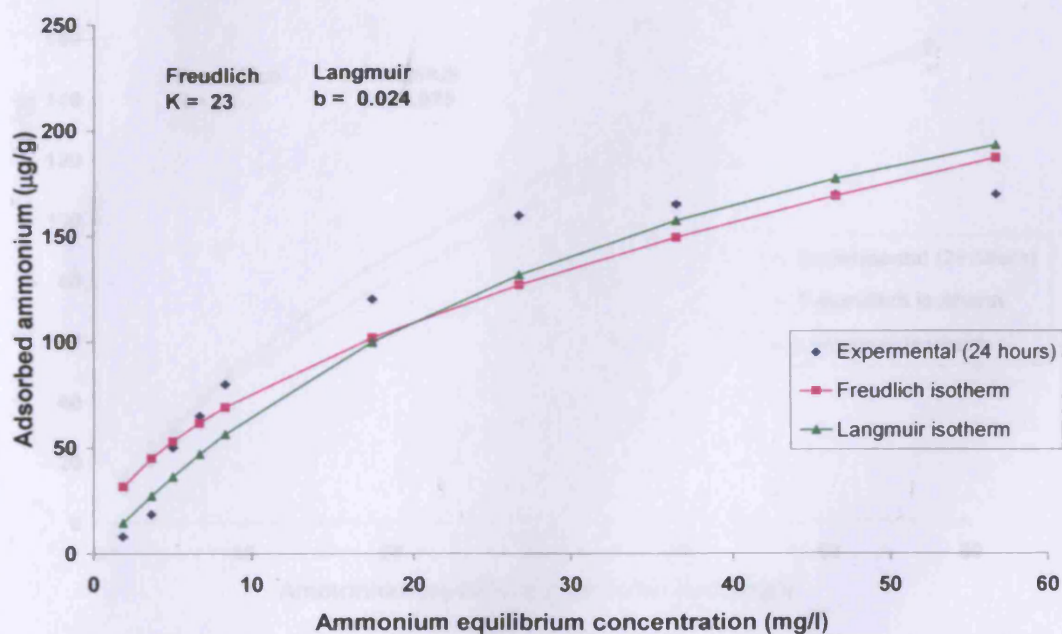


Figure 5.4: Experimental results and theoretical (Langmuir and Freundlich) adsorption isotherms for ammonium on Kaolinite in artificial sea water.

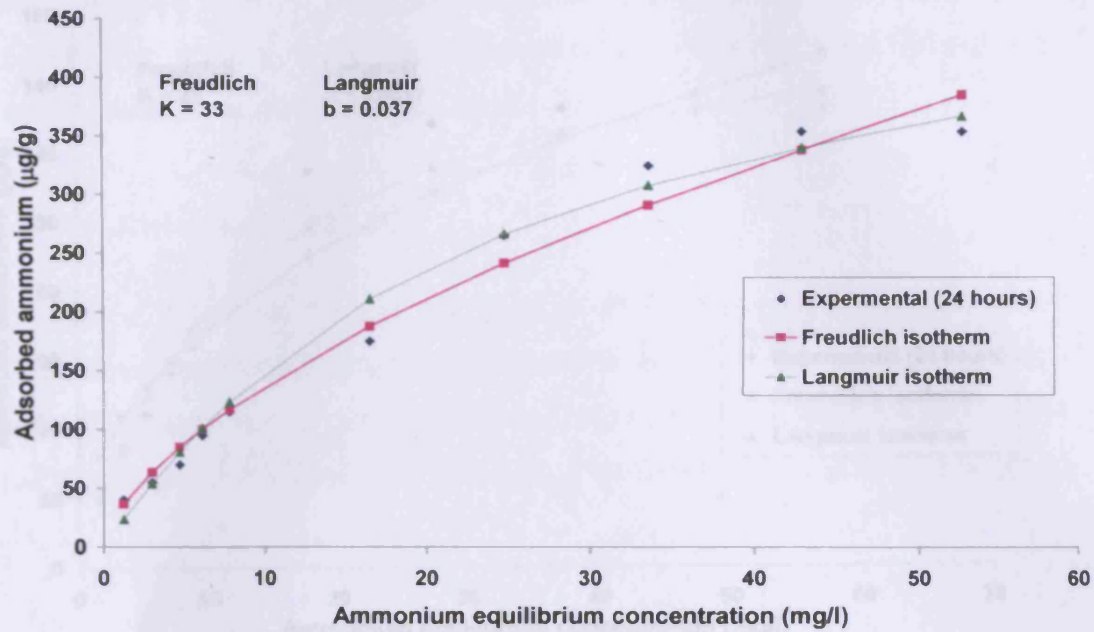


Figure 5.5: Experimental results and theoretical (Langmuir and Freundlich) adsorption isotherms for ammonium on fine sand in deionised water.

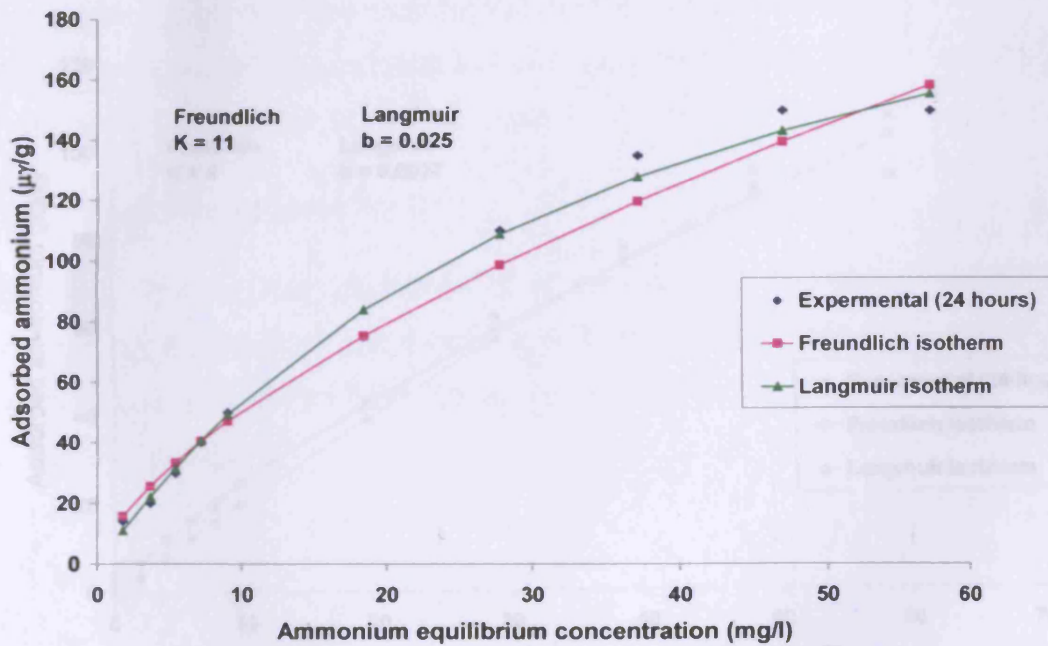


Figure 5.6: Experimental results and theoretical (Langmuir and Freundlich) adsorption isotherms for ammonium on fine sand in artificial sea water.

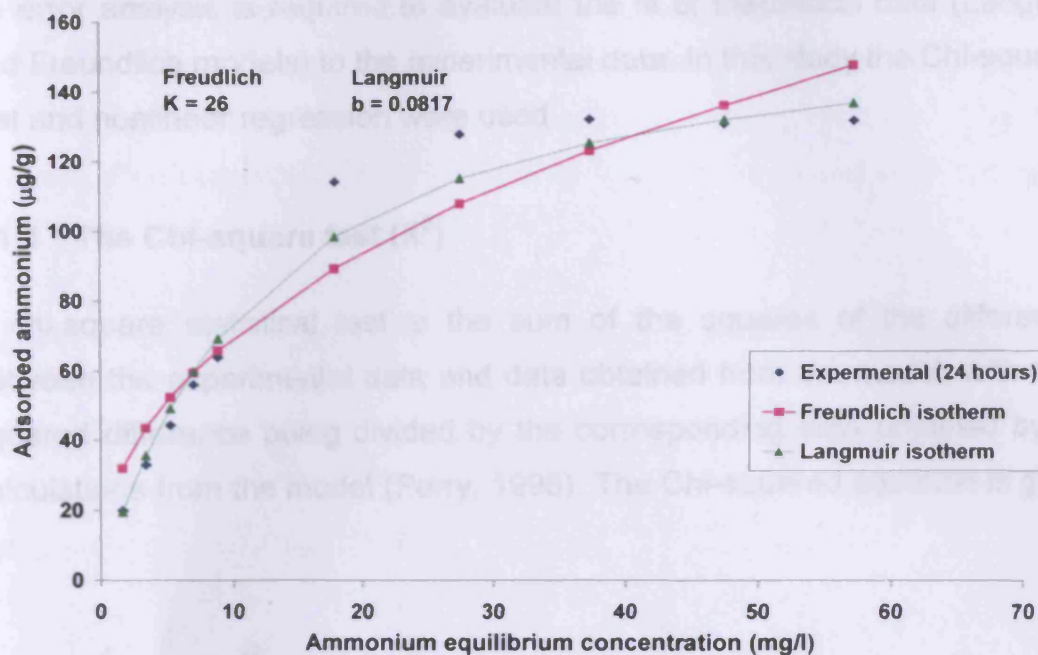


Figure 5.7: Experimental results and theoretical (Langmuir and Freundlich) adsorption isotherms for ammonium on coarse sand in deionised water.

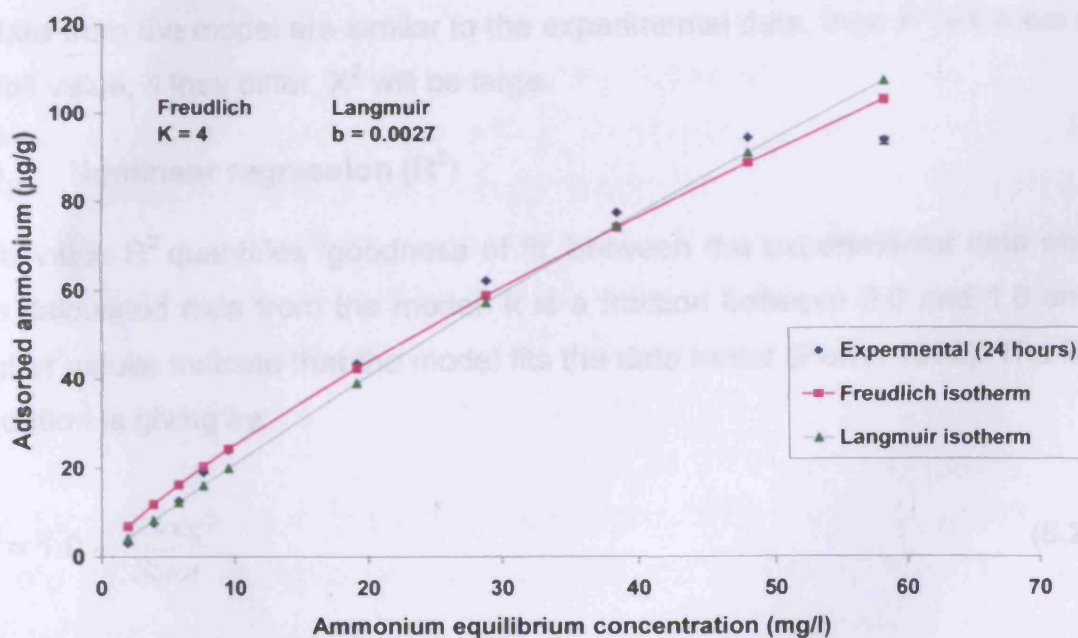


Figure 5.8: Experimental results and theoretical (Langmuir and Freundlich) adsorption isotherms for ammonium on coarse sand in artificial sea water.

An error analysis is required to evaluate the fit of theoretical data (Langumir and Freundlich models) to the experimental data. In this study the Chi-squared test and nonlinear regression were used.

5.1.1 The Chi-square test (X^2)

A chi-square statistical test is the sum of the squares of the differences between the experimental data and data obtained from the model, with each squared difference being divided by the corresponding data obtained by the calculations from the model (Perry, 1995). The Chi-squared equation is giving by:

$$X^2 = \sum \frac{(q_e - q_{e,m})^2}{q_{e,m}} \quad (5.1)$$

where: X^2 is chi square; $q_{e,m}$ is equilibrium data obtained by calculatation from model ($\mu\text{g/g}$); q_e is experimental data for equilibrium ($\mu\text{g/g}$)

If data from the model are similar to the experimental data, then X^2 will have a small value, if they differ, X^2 will be large.

5.1.2 Nonlinear regression (R^2)

The value R^2 quantifies 'goodness of fit' between the experimental data and the calculated data from the model. It is a fraction between 0.0 and 1.0 and higher values indicate that the model fits the data better (Perry. 1995). The R^2 equation is giving by:

$$R^2 = 1.0 - \frac{SS_{reg}}{SS_{tot}} \quad (5.2)$$

where: R^2 is nonlinear regression; SS_{reg} is the unit of the Y-axis squared; SS_{tot} is the sum of the square of the distances of the points from a horizontal line through the mean of all Y values. SS_{reg} will be much smaller than SS_{tot} .

Table 5.1 shows the error analysis for Langmuir and Freundlich adsorption isotherms. The Chi-squared test and nonlinear regression were used to evaluate the fit of the theoretical data to the experimental data. The error analysis was applied for all experiments for both deionised and sea water conditions.

Table 5.1 Error Analysis for Langmuir and Freundlich adsorption isotherms using Chi-squared test (X^2) and nonlinear regression (R^2).

Type of Water	Samples	Langmuir Isotherm		Freundlich Isotherm	
		X^2	R^2	X^2	R^2
Deionised water	Montmorillonite	23.00	0.99	205	0.94
	Kaolinite	22.50	0.99	37.0	0.97
	Fine sand	16.40	0.97	21.0	0.95
	Coarse sand	5.50	0.97	31.4	0.90
Artificial sea water	Montmorillonite	12.20	0.98	49.4	0.91
	Kaolinite	42.06	0.92	87.2	0.70
	Fine sand	3.035	0.99	5.38	0.98
	Coarse sand	5.00	0.97	8.27	0.95

The Langmuir model fits the data reasonably well for all samples (i.e. for both deionised and artificial sea water), with X^2 ranging from 5.50 to 23.0 and 5.00 to 42.06 respectively and R^2 values ranging from 0.97 to 0.99 and 0.92 to 0.99 respectively. In contrast the Freundlich model fits the data less well for all samples and for deionised and artificial sea water with, X^2 ranging from 21.0 to 205 and 5.38 to 87.2 respectively and R^2 values ranging from 0.90 to 0.97 and 0.70 to 0.98 respectively.

The Langmuir model appears to be the better fitting model for ammonium adsorption on Montmorillonite, Kaolinite, fine and coarse sand for deionised and artificial sea water conditions as reflected by its small values of X^2 and higher values from the nonlinear regression.

Figures 5.9 - 5.13 show a comparison of ammonium adsorption by clays (Montmorillonite and Kaolinite) and sand (coarse and fine) in both deionised and artificial sea water (35ppt). These figures show the difference in salinity

dependence of ammonium adsorption on the 4 sets of sediments, in both deionised and artificial sea water. The results show an almost linear relationship between ammonium equilibrium concentration and adsorbed ammonium, within the controlled range of ammonium concentration tested in the laboratory experiments. Different concentrations of ammonium were used, including 2, 4, 6, 8, 10, 20 and 30 mg/l NH_4^+ . The adsorption isotherm equation for ammonium is given below in the form of a the linear regression equation

$$Q = K^* \cdot C + q \quad (5.3)$$

Where Q (mg/g dry wt) is the amount of ammonium adsorbed by the different types of adsorbents (i.e. Montmorillonite, Kaolinite, coarse and fine sand),, K^* is the slope of the regression line (adsorption coefficient), C (mg/l) is the ammonium ion equilibrium concentration in water, q is fixed ammonium content in the adsorbent which is zero in this case because clean commercial clays and sand were used

From Figures 5.9 to 5.13 and also table 5.2 it can be seen that the adsorption coefficient is lower in artificial sea water (35 ppt) than deionised water for all samples. Comparing the adsorption coefficients it was found that Montmorillonite had the highest adsorption coefficient compared to Kaolinite, fine and coarse sands for both conditions i.e,for deionised water and artificial sea water. The adsorption coefficients were found to be 85%, 66%, 62%, 63% respectively.

The adsorption onto Montmorillonite was the highest compared to the other materials, both when using deionised water and artificial sea water. The results indicated that ammonium adsorption on Montmorillonite, Kaolinite, fine and coarse sand in deionised water were respectively 2.6, 2.5, 2.4, and 2 times higher than the ammonium adsorbed using artificial sea water. The adsorbed ammonium reduced by 63% of its original value from 1050 $\mu\text{g/g}$ to 390 $\mu\text{g/g}$ for Montmorillonite from freshwater conditions to full sea water conditions (35ppt); whereas the same reduction for Kaolinite, fine and coarse sand, was only 60%, 58%, 51% respectively.

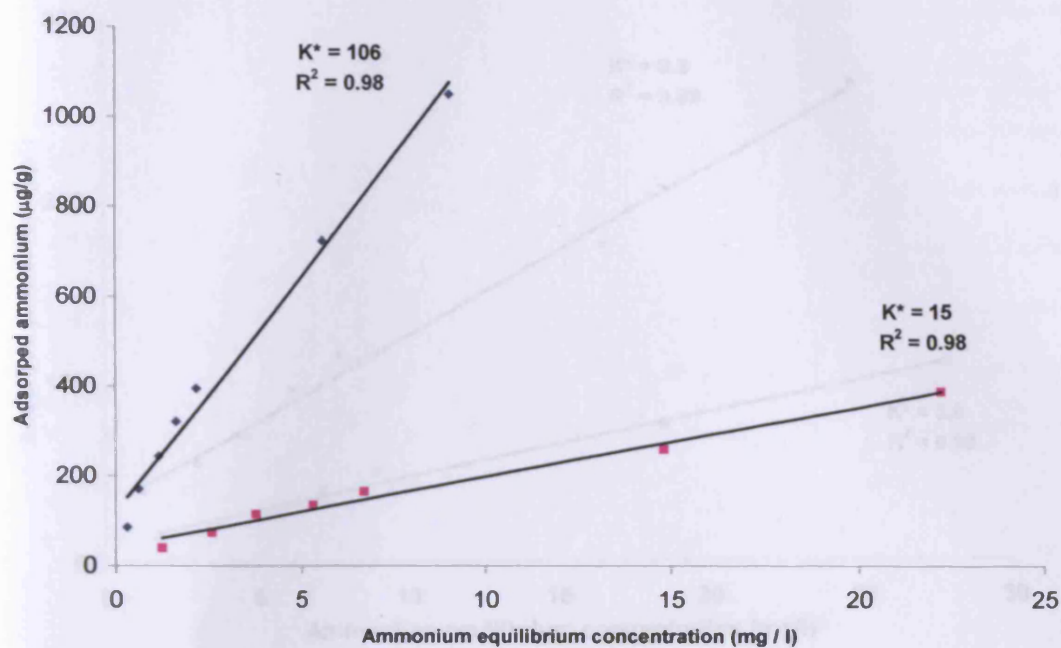


Figure 5.9: Adsorption isotherm of ammonium on Montmorillonite in deionised water and artificial sea water (35ppt)

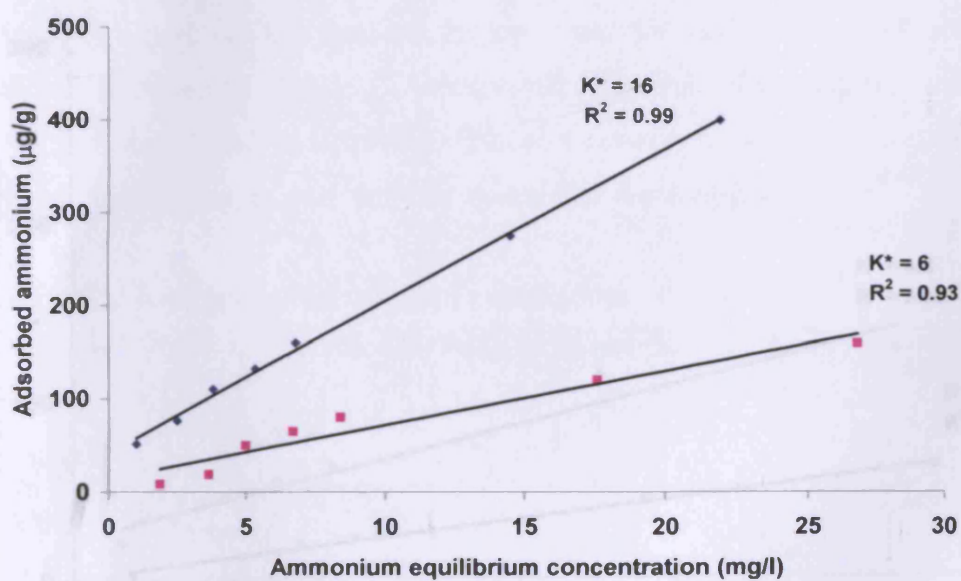


Figure 5.10: Adsorption isotherm of ammonium on Kaolinite in deionised water and artificial sea water (35ppt)

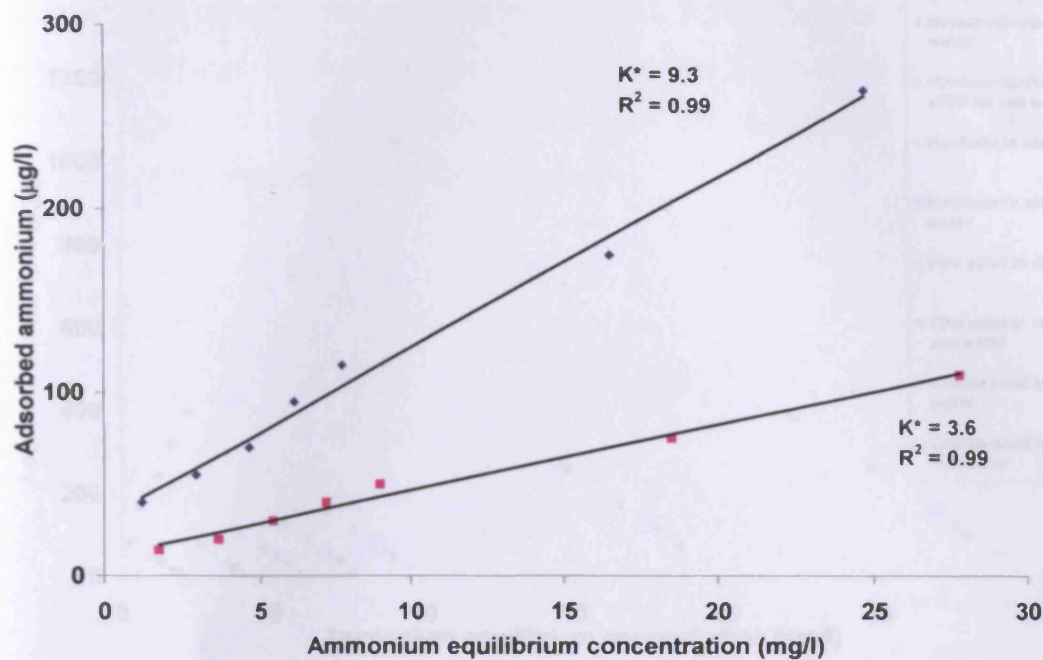


Figure 5.11: Adsorption isotherm of ammonium on fine sand in deionised water and artificial sea water (35ppt)

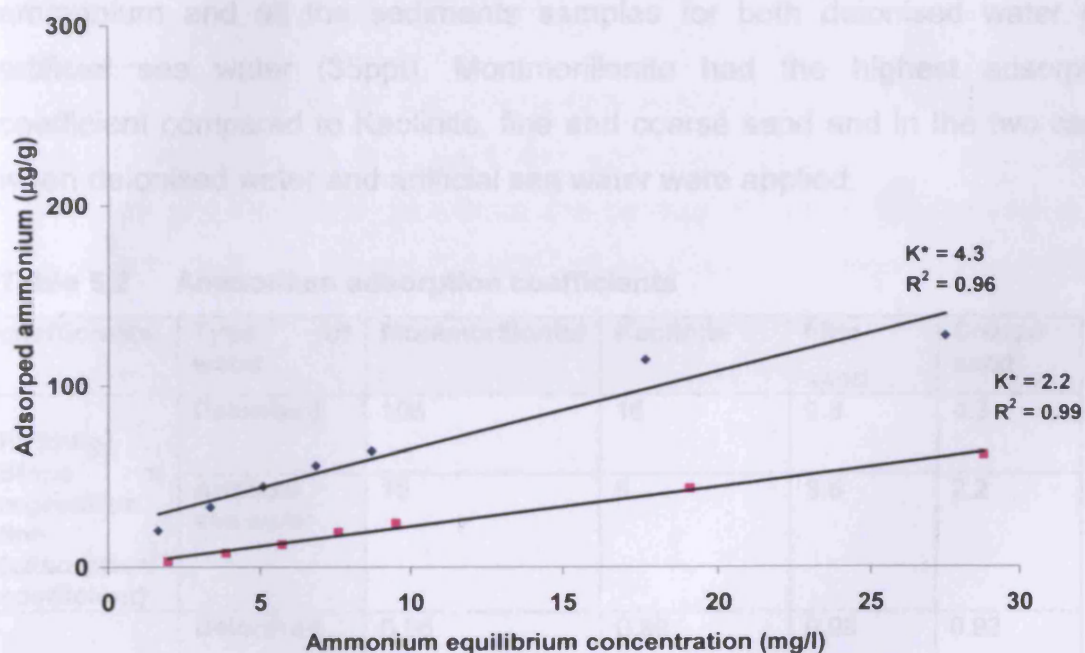


Figure 5.12: Adsorption isotherm of ammonium on coarse sand in deionised water and artificial sea water (35ppt)

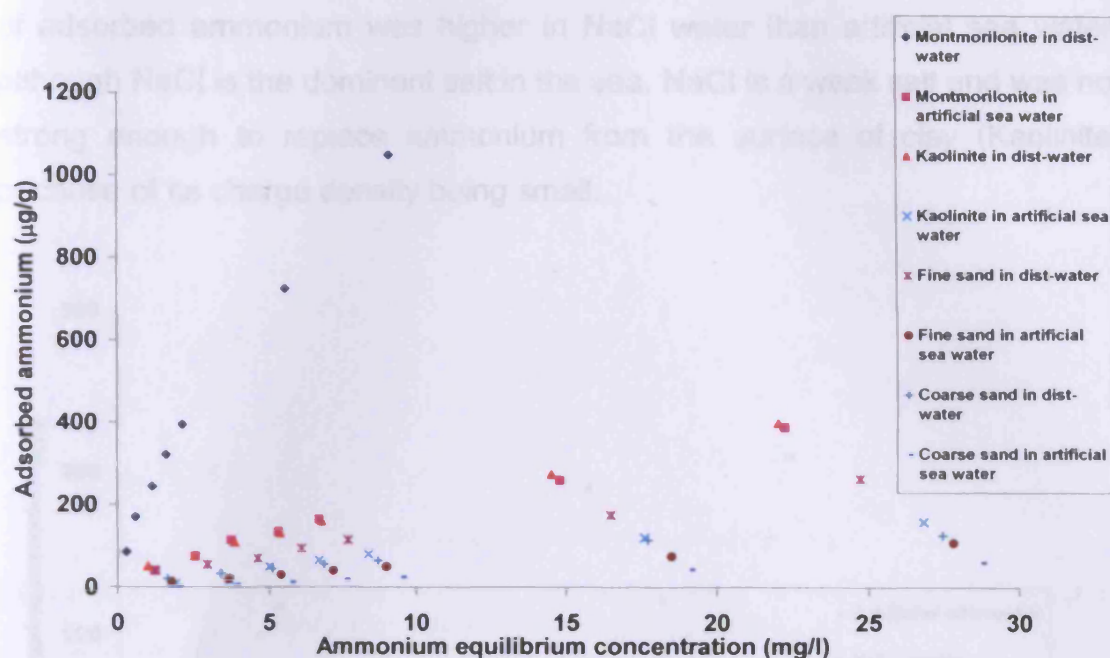


Figure 5.13: Comparison of ammonium adsorption on the Montmorillonite, Kaolinite and fine, coarse sand in deionised water and artificial sea water (35ppt)

Table 5.2 indicates the adsorption coefficients found in this study for ammonium and all the sediments samples for both deionised water and artificial sea water (35ppt). Montmorillonite had the highest adsorption coefficient compared to Kaolinite, fine and coarse sand and in the two cases when deionised water and artificial sea water were applied.

Table 5.2 Ammonium adsorption coefficients

coefficients	Type of water	Montmorillonite	Kaolinite	Fine sand	Coarse sand
K* (ml/g) Slope of regression line (adsorption coefficient)	Deionised	106	16	9.3	4.3
	Artificial sea water	15	6	3.6	2.2
R ² correlation coefficient	Deionised	0.98	0.99	0.99	0.92
	Artificial sea water	0.98	0.93	0.99	0.96

Figure 5.14 shows the comparison between artificial sea water and sodium chloride water (NaCl) for the ammonium adsorption on Kaolinite. The amount

of adsorbed ammonium was higher in NaCl water than artificial sea water, although NaCl is the dominant salt in the sea. NaCl is a weak salt and was not strong enough to replace ammonium from the surface of clay (Kaolinite) because of its charge density being small.

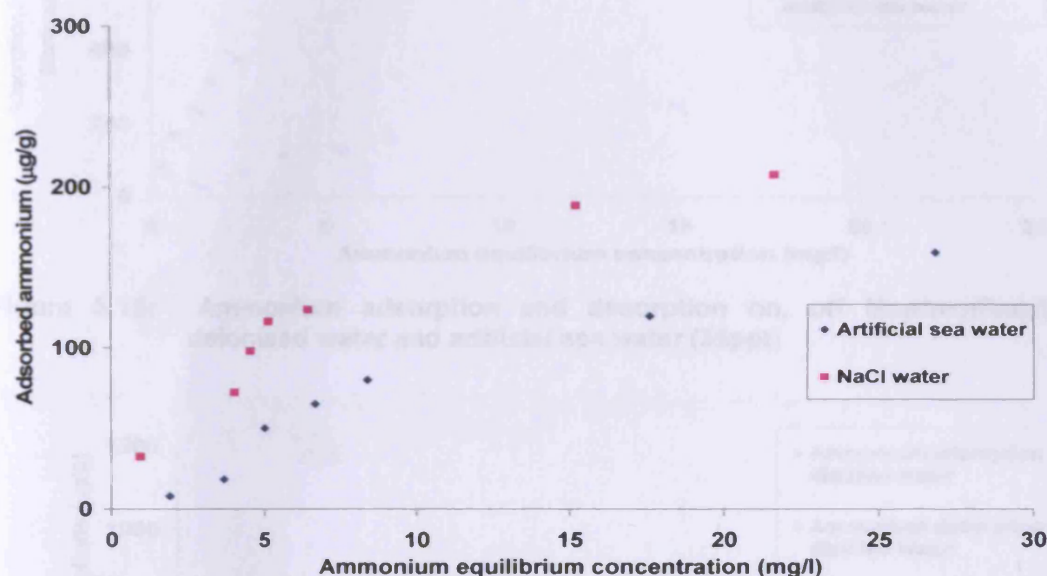


Figure 5.14: Comparison of ammonium adsorbed on Kaolinite in artificial sea water (35ppt) and NaCl water (35ppt)

Figures 5.15 - 5.18 show the ammonium adsorption and desorption for the clays (Montmorillonite and Kaolinite) and sand (fine and coarse), using potassium chloride (KCl) to extract the ammonium from the surface of the sands and clays. The figures indicate that the amount of desorbed ammonium, compared to adsorbed ammonium, was similar for all samples for both the deionised and artificial sea water.

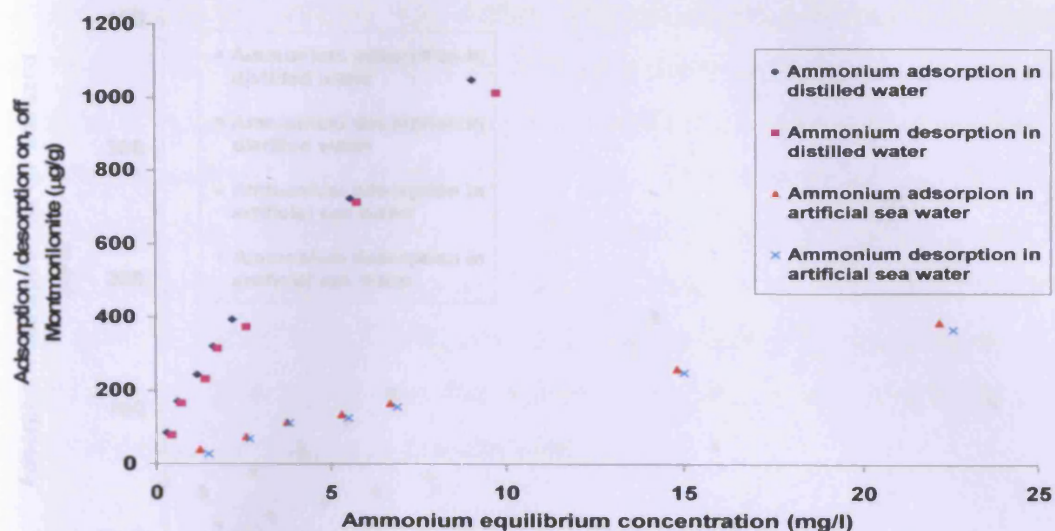


Figure 5.15: Ammonium adsorption and desorption on, off Montmorillonite in deionised water and artificial sea water (35ppt)

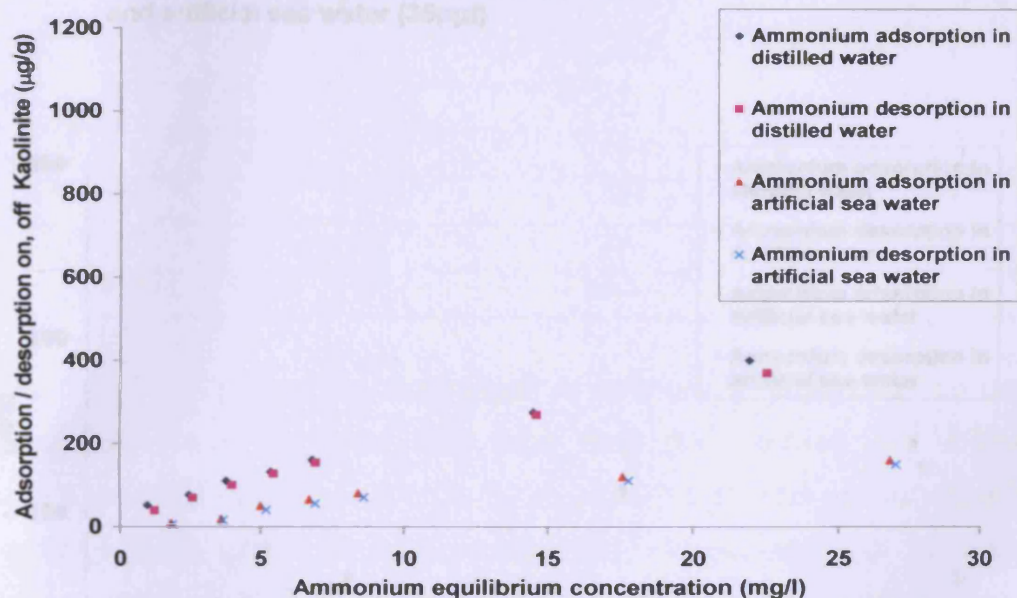


Figure 5.16: Ammonium adsorption and desorption on, off Kaolinite in deionised water and artificial sea water (35ppt)

5.2 Salinity and ammonium adsorption isotherm experiment

This section presents the results of an ammonium adsorption isotherm on clays (Montmorillonite and Kaolinite) and sand (fine and coarse) for different

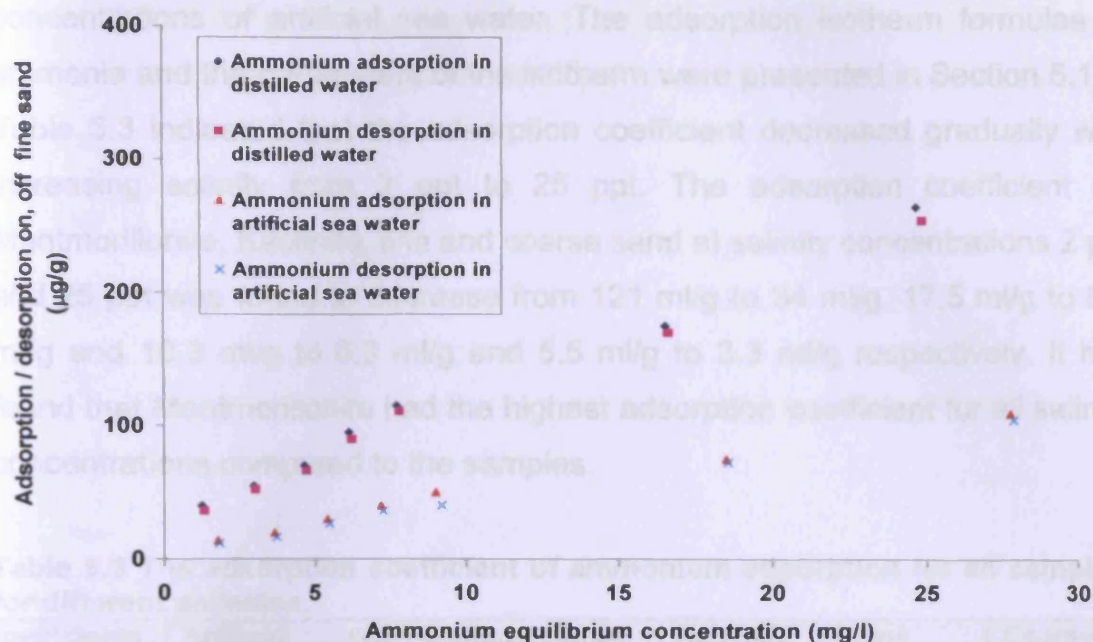


Figure 5.17: Ammonium adsorption and desorption on, off fine sand in distilled water and artificial sea water (35ppt)

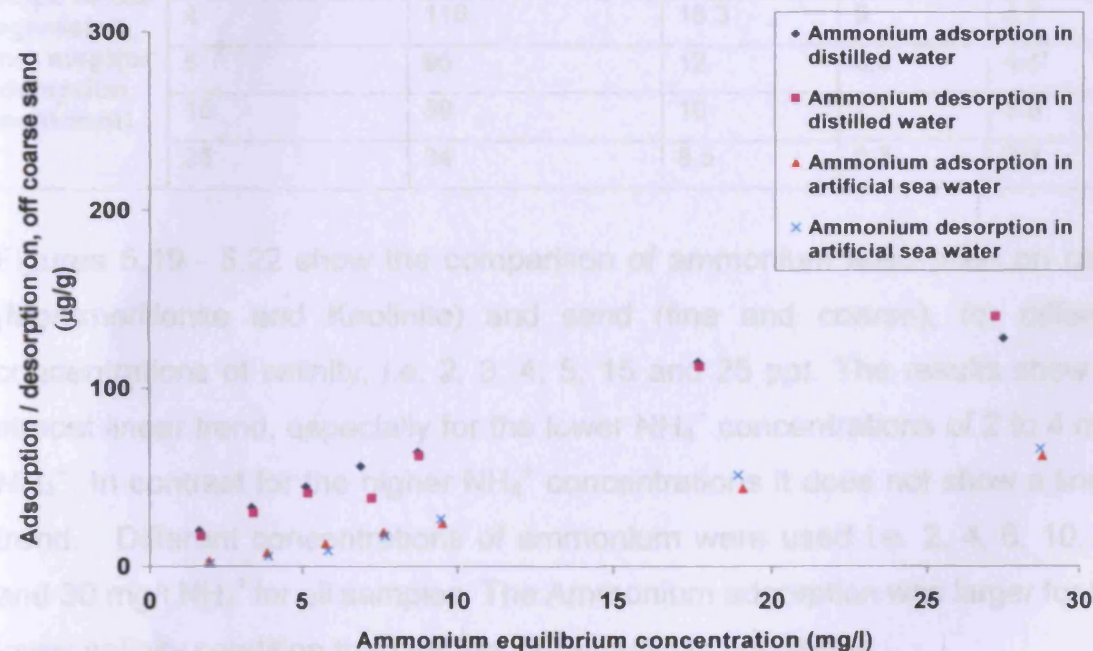


Figure 5.18: Ammonium adsorption and desorption on, off coarse sand in deionised water and artificial sea water (35ppt)

5.2 Salinity and ammonium adsorption isotherm experiment

This section presents the results of ammonium adsorption isotherm on clays (Montmorillonite and Kaolinite) and sand (fine and coarse) for different

concentrations of artificial sea water. The adsorption isotherm formulae of ammonia and the parameters of the isotherm were presented in Section 5.1.

Table 5.3 indicated that the adsorption coefficient decreased gradually with increasing salinity from 2 ppt to 25 ppt. The adsorption coefficient for Montmorillonite, Kaolinite, fine and coarse sand at salinity concentrations 2 ppt and 25 ppt was found to decrease from 121 ml/g to 34 ml/g, 17.5 ml/g to 8.5 ml/g and 10.3 ml/g to 6.3 ml/g and 5.5 ml/g to 3.3 ml/g respectively. It has found that Montmorillonite had the highest adsorption coefficient for all salinity concentrations compared to the samples.

Table 5.3 The adsorption coefficient of ammonium adsorption for all samples, for different salinities.

Coefficients	Artificial sea water salinity concentrations (ppt)	Montmorillonite	Kaolinite	Fine sand	Coarse sand
K* (slope of the regression line ml/g)(or adsorption coefficient)	2	121	17.5	10.3	5.5
	3	118	17	9.4	5.0
	4	116	16.3	9	4.7
	5	95	12	8.6	4.4
	15	59	10	7.7	3.8
	25	34	8.5	6.3	3.3

Figures 5.19 - 5.22 show the comparison of ammonium adsorption on clays (Montmorillonite and Kaolinite) and sand (fine and coarse), for different concentrations of salinity, i.e. 2, 3, 4, 5, 15 and 25 ppt. The results show an almost linear trend, especially for the lower NH_4^+ concentrations of 2 to 4 mg/l NH_4^+ . In contrast for the higher NH_4^+ concentrations it does not show a linear trend. Different concentrations of ammonium were used i.e. 2, 4, 6, 10, 20 and 30 mg/l NH_4^+ for all samples. The Ammonium adsorption was larger for the lower salinity condition than for the higher salinity conditions.

The adsorption onto Montmorillonite was highest for all concentrations of salinity considered and, compared to the other samples. At low concentrations of salinity (i.e. 2ppt), Montmorillonite has the highest NH_4^+ adsorption compared to Kaolinite, fine and coarse sand with respective of values of 44%,

41%, 32%, 27% higher than the adsorbed level for a salinity concentration of 25ppt, which is the highest typical salinity concentration in estuarine waters.

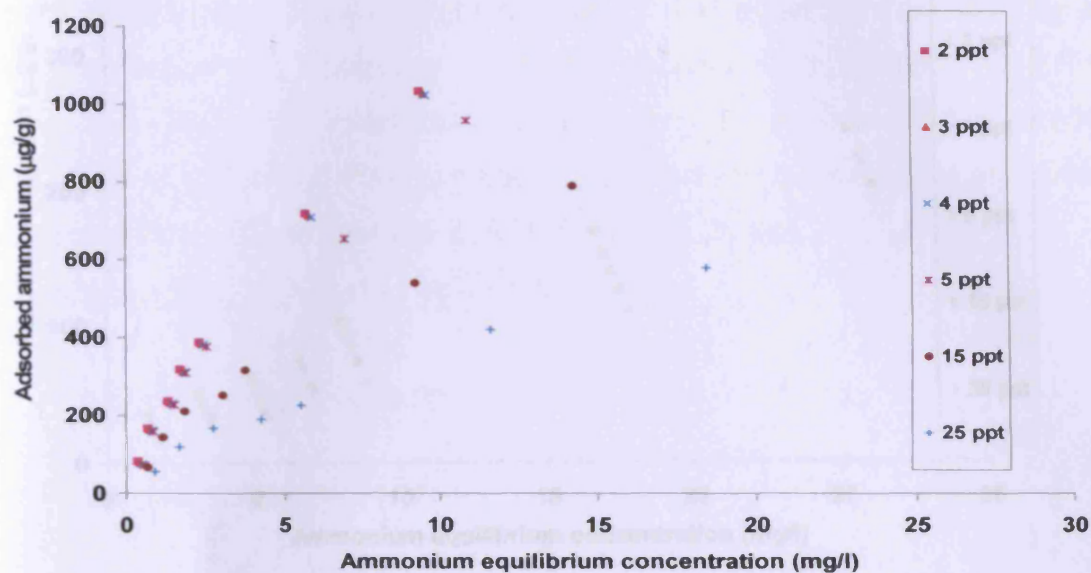


Figure 5.19: Comparison of ammonium adsorption on Montmorillonite for different salinities

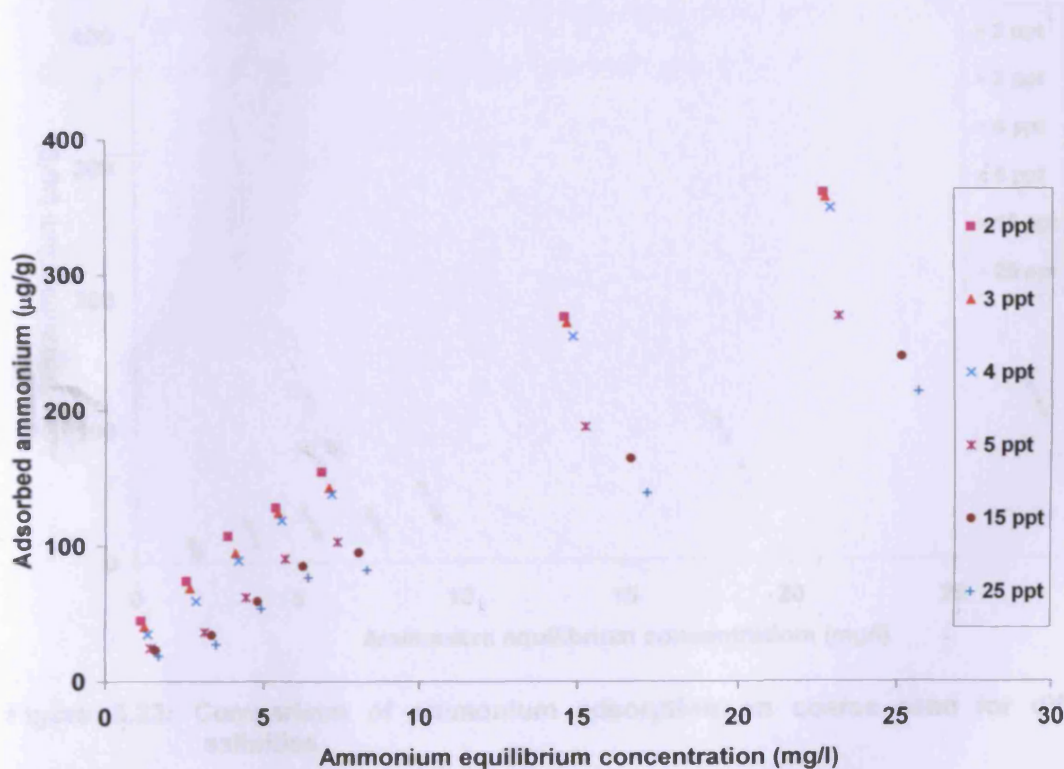


Figure 5.20: Comparison of ammonium adsorption on Kaolinite for different salinities

5.2.1 Salinity effect on ammonium adsorption coefficient

The results of the effect of salinity on the adsorption coefficient are covered in this section. Figures 5.23 – 5.26 show the change of the ammonium

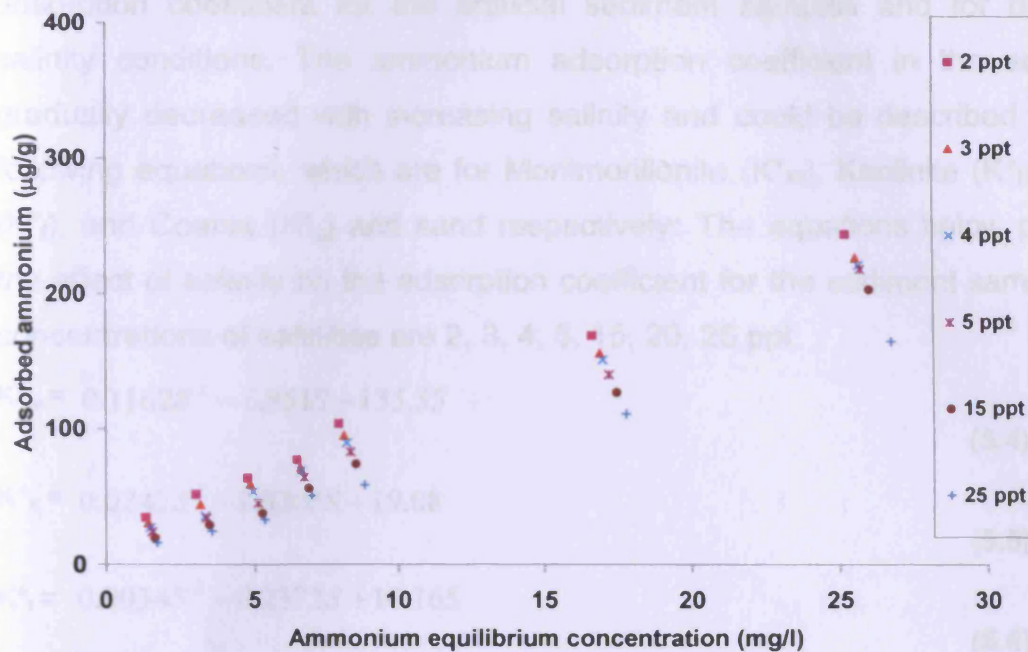


Figure 5.21: Comparison of ammonium adsorption on fine sand for different salinities

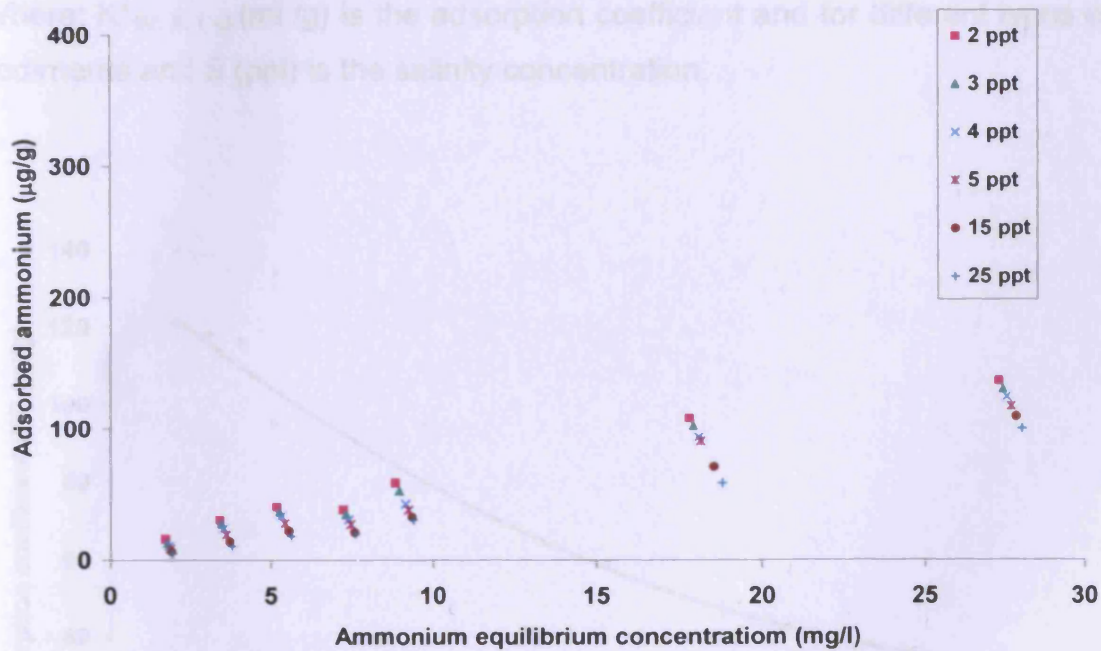


Figure 5.22: Comparison of ammonium adsorption on coarse sand for different salinities

5.2.1 Salinity effect on ammonium adsorption coefficient

The results of the effect of salinity on the adsorption coefficient are covered in this section. Figures 5.23 - 5.26 show the change of the ammonium

adsorption coefficient for the artificial sediment samples and for different salinity conditions. The ammonium adsorption coefficient in the samples gradually decreased with increasing salinity and could be described by the following equations, which are for Montmorillonite (K^*_M), Kaolinite (K^*_K), Fine (K^*_f), and Coarse (K^*_c) and sand respectively: The equations below present the effect of salinity on the adsorption coefficient for the sediment samples at concentrations of salinities are 2, 3, 4, 5, 15, 20, 25 ppt.

$$K^*_M = 0.1162S^2 - 6.951S + 135.55 \quad (5.4)$$

$$K^*_K = 0.0242S^2 - 1.0205S + 19.08 \quad (5.5)$$

$$K^*_f = 0.0034S^2 - 0.2372S + 10.165 \quad (5.6)$$

$$K^*_c = 0.0035S^2 - 0.1834S + 5.586 \quad (5.7)$$

Where: $K^*_{(M, K, f, c)}$ (ml /g) is the adsorption coefficient and for different types of sediments and S (ppt) is the salinity concentration.

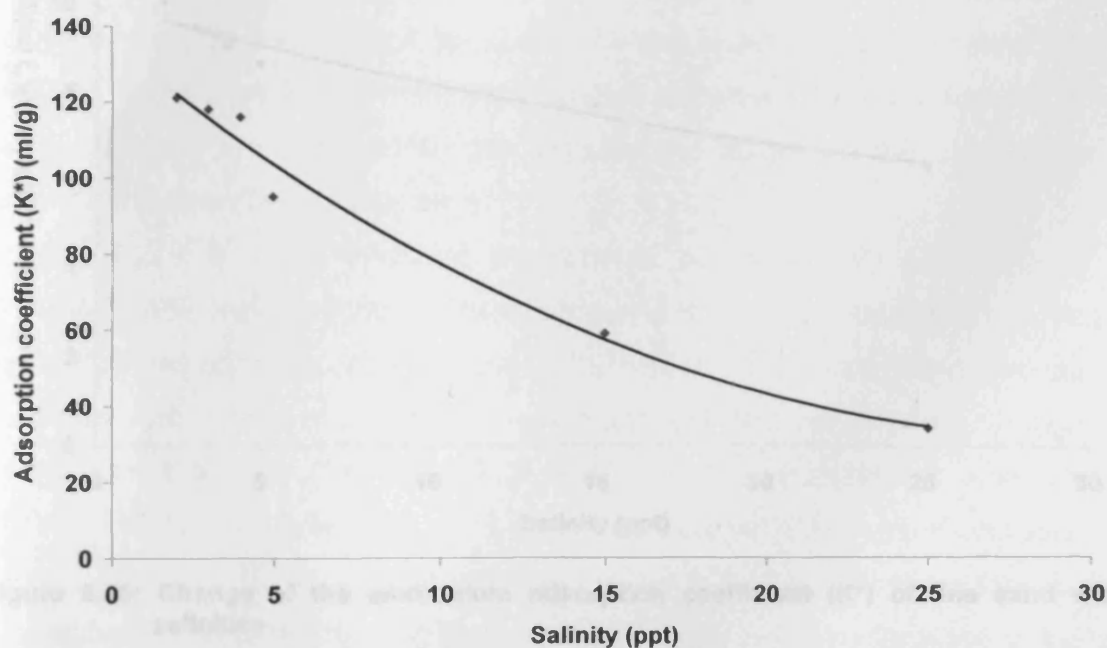


Figure 5.23: Change of the ammonium adsorption coefficient (K^*) of Montmorillonite with salinities

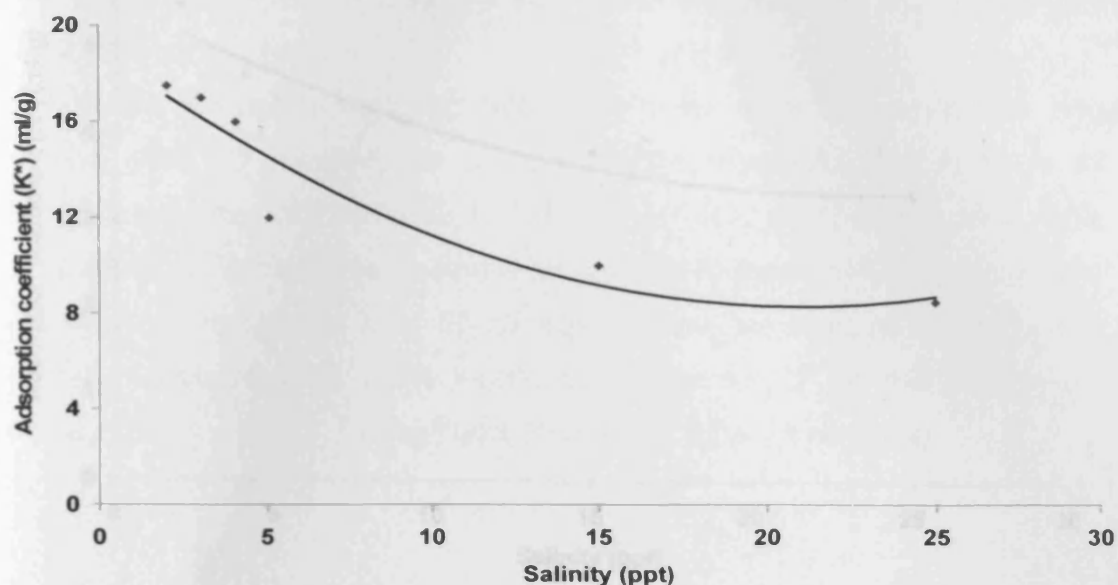


Figure 5.24: Change of the ammonium adsorption coefficient (K^*) of Kaolinite with salinities

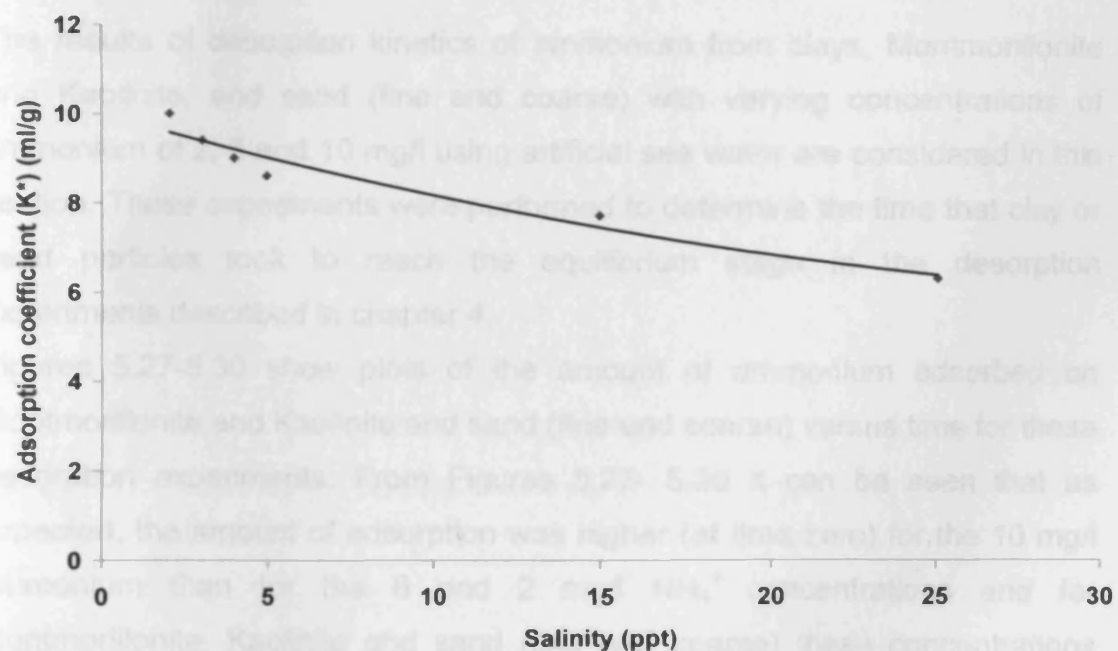


Figure 5.25: Change of the ammonium adsorption coefficient (K^*) of fine sand with salinities

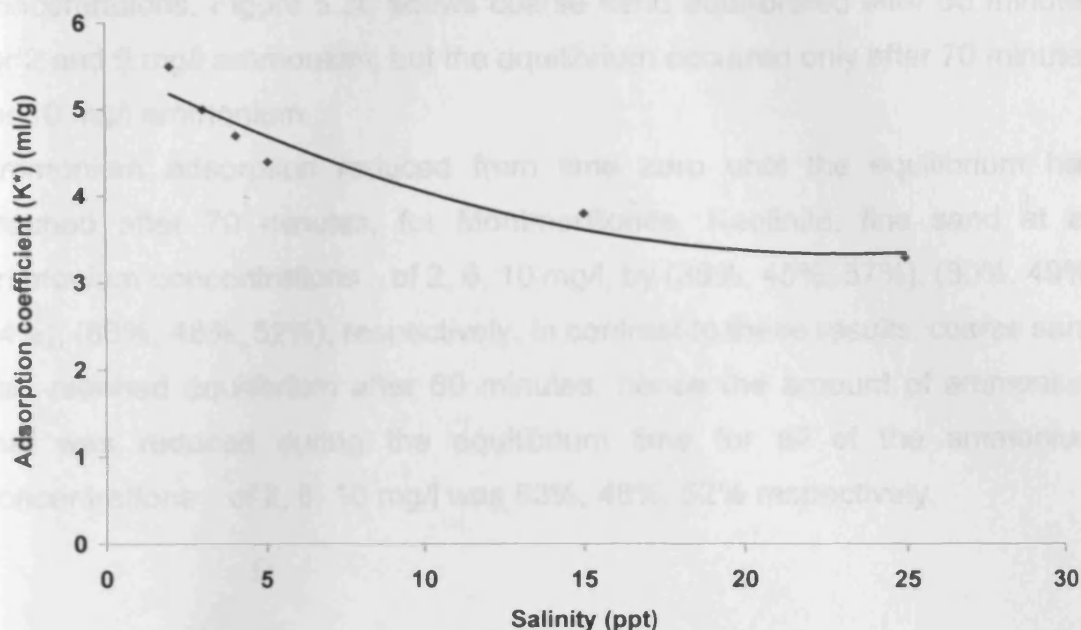


Figure 5.26: Change of the ammonium adsorption coefficient (K^*) of coarse sand with salinity

5.3 Desorption kinetics using artificial sea water

The results of desorption kinetics of ammonium from clays, Montmorillonite and Kaolinite, and sand (fine and coarse) with varying concentrations of ammonium of 2, 6 and 10 mg/l using artificial sea water are considered in this section. These experiments were performed to determine the time that clay or sand particles took to reach the equilibrium stage in the desorption experiments described in chapter 4.

Figures 5.27-5.30 show plots of the amount of ammonium adsorbed on Montmorillonite and Kaolinite and sand (fine and coarse) versus time for these desorption experiments. From Figures 5.27- 5.30 it can be seen that as expected, the amount of adsorption was higher (at time zero) for the 10 mg/l ammonium than for the 6 and 2 mg/l NH_4^+ concentrations and for Montmorillonite, Kaolinite and sand (fine and coarse) these concentrations were, 390, 160, 115, 64 $\mu\text{g/g}$ respectively. Figures 5.27 - 5.30 show that the adsorption rate was decreasing over time and the equilibrium for none of the samples was achieved in less than 60 minutes. It can be seen from Figures 5.27 and 5.29 that the equilibrium concentration for Montmorillonite, Kaolinite and fine sand was not reached until 70 minutes and for all of the ammonium

concentrations. Figure 5.30 shows coarse sand equilibrated after 60 minutes for 2 and 6 mg/l ammonium, but the equilibrium occurred only after 70 minutes for 10 mg/l ammonium.

Ammonium adsorption reduced from time zero until the equilibrium had reached after 70 minutes, for Montmorillonite, Kaolinite, fine sand at all ammonium concentrations of 2, 6, 10 mg/l, by (38%, 45%, 57%), (80%, 49%, 44%), (63%, 48%, 52%), respectively. In contrast to these results, coarse sand had reached equilibrium after 60 minutes, hence the amount of ammonium that was reduced during the equilibrium time for all of the ammonium concentrations of 2, 6, 10 mg/l was 63%, 48%, 52% respectively.

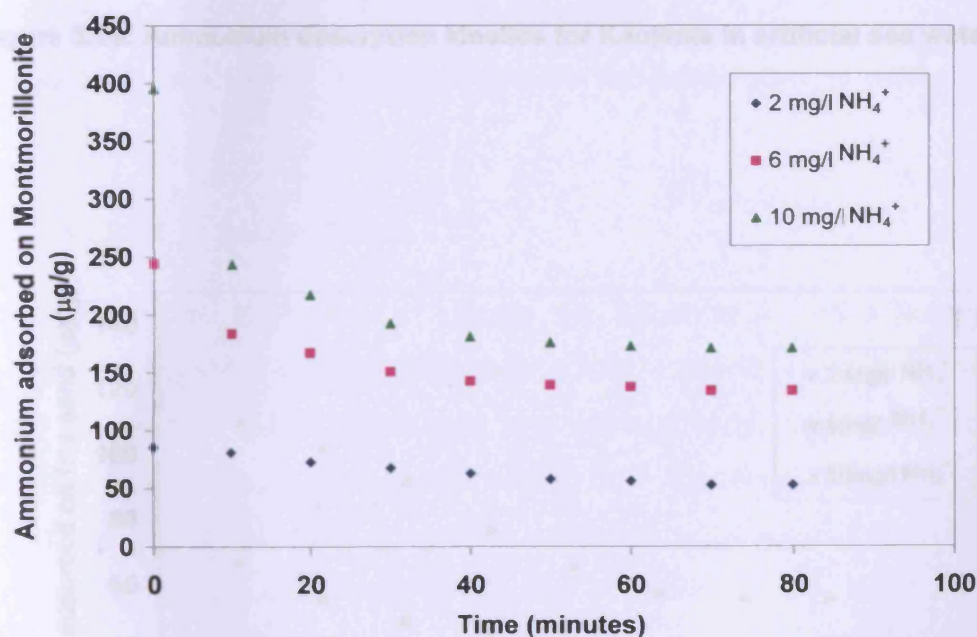


Figure 5. 27: Ammonium desorption kinetics for Montmorillonite in artificial sea water (35ppt)

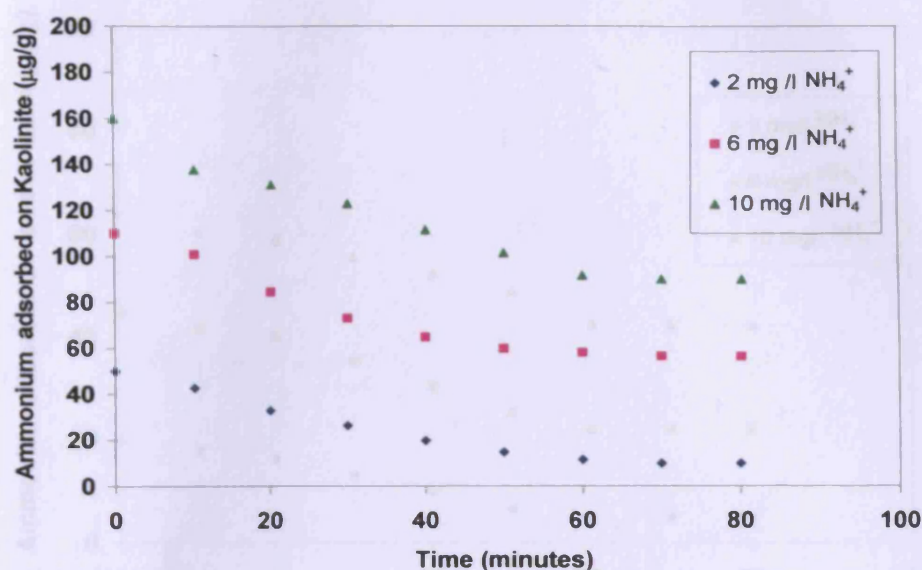


Figure 5.28: Ammonium desorption kinetics for Kaolinite in artificial sea water (35ppt)

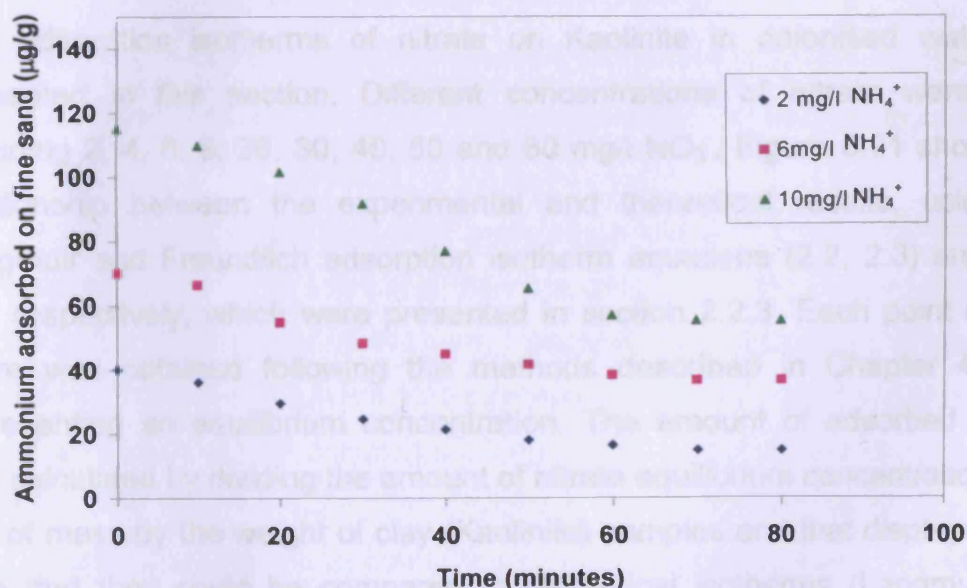


Figure 5.29: Ammonium desorption kinetics for fine sand in artificial sea water (35ppt)

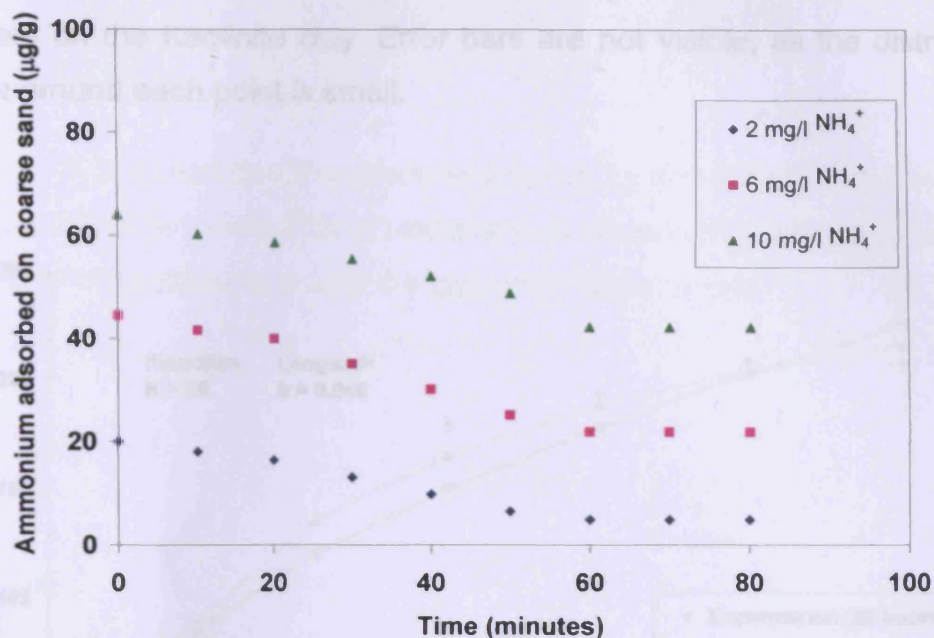


Figure 5.30: Ammonium desorption kinetics for coarse sand in artificial sea water (35ppt)

5.4 Nitrate adsorption

The adsorption isotherms of nitrate on Kaolinite in deionised water are presented in this section. Different concentrations of nitrate were used including 2, 4, 6, 8, 20, 30, 40, 50 and 60 mg/l NO_3^- . Figure 5.31 shows the relationship between the experimental and theoretical results, using the Langmuir and Freundlich adsorption isotherm equations (2.2, 2.3) and (2.4, 2.5) respectively, which were presented in section 2.2.3. Each point on this figure was obtained following the methods described in Chapter 4, thus representing an equilibrium concentration. The amount of adsorbed nitrate was calculated by dividing the amount of nitrate equilibrium concentration as a unit of mass by the weight of clay (Kaolinite) samples and that displayed in a form that they could be compared to theoretical isotherms (Langmuir and Freundlich isotherms). The results show good agreement between experimental and theoretical concentrations. However at high equilibrium nitrate concentrations the Freundlich model was shown to give a poorer fit, as shown in Figure 5.31, with the data being up to 1.13 times lower than

Freundlich isotherm model. The error bars represent the maximum and minimum values (in X and Y) over three replicates of measured adsorbed nitrate on the Kaolinite clay. Error bars are not visible, as the distribution of data around each point is small.

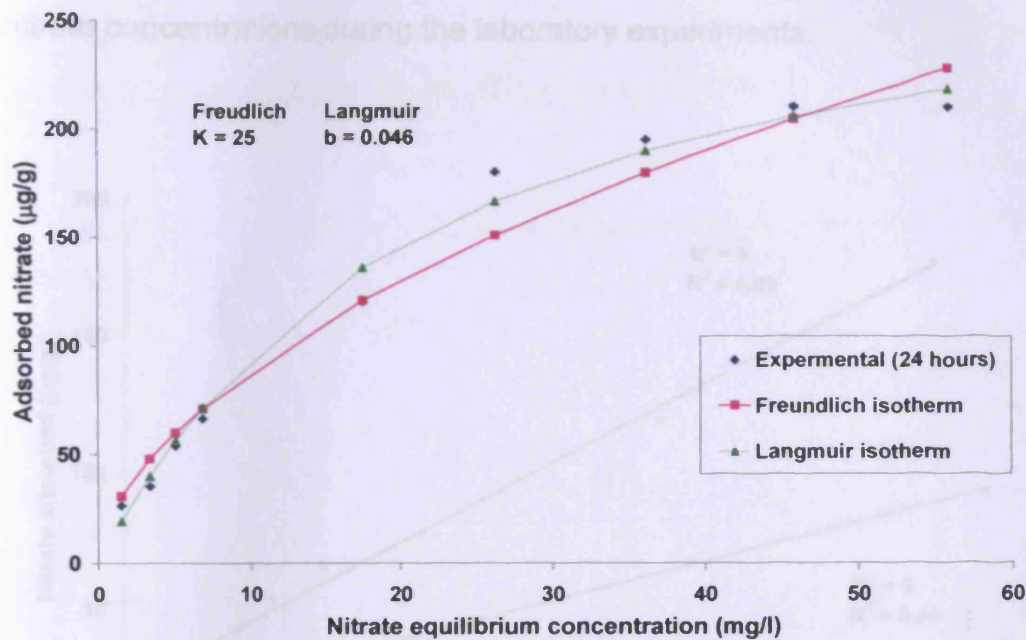


Figure 5.31: Experimental results and theoretical. : Experimental results and theoretical (Langmuir and Freundlich) adsorption isotherms for nitrate on Kaolinite in deionised water, (b) is the Langmuir constant and adsorption coefficient, and K is the Freundlich constant and adsorption coefficient

The Langmuir model fits the data well, since the errors derived from the Chi-squared and R^2 tests are lower than the errors from the Freundlich model, see table 5.4. The results of the errors analysis indicated that the Langmuir model fits the data well for the Kaolinite samples in deionised water, with $X^2 = 11.00$ and $R^2 = 0.99$. In contrast the Freundlich model fits the data less well with $X^2 = 11.5$ and $R^2 = 0.94$. The Langmuir model appears to be the better fitting model for nitrate adsorption on Kaolinite for deionised water, as reflected by its small values of X^2 and higher values from the R^2 .

Table 5.4 Error analysis result for Langmuir and Freundlich:

Kaolinite	Langmuir		Freundlich	
	X^2	R^2	X^2	R^2
	11.00	0.99	11.5	0.94

Figure 5.32 shows that the nitrate adsorption by Kaolinite in both distilled water and artificial sea water (35ppt) were almost linear within the controlled range of nitrate concentrations during the laboratory experiments.

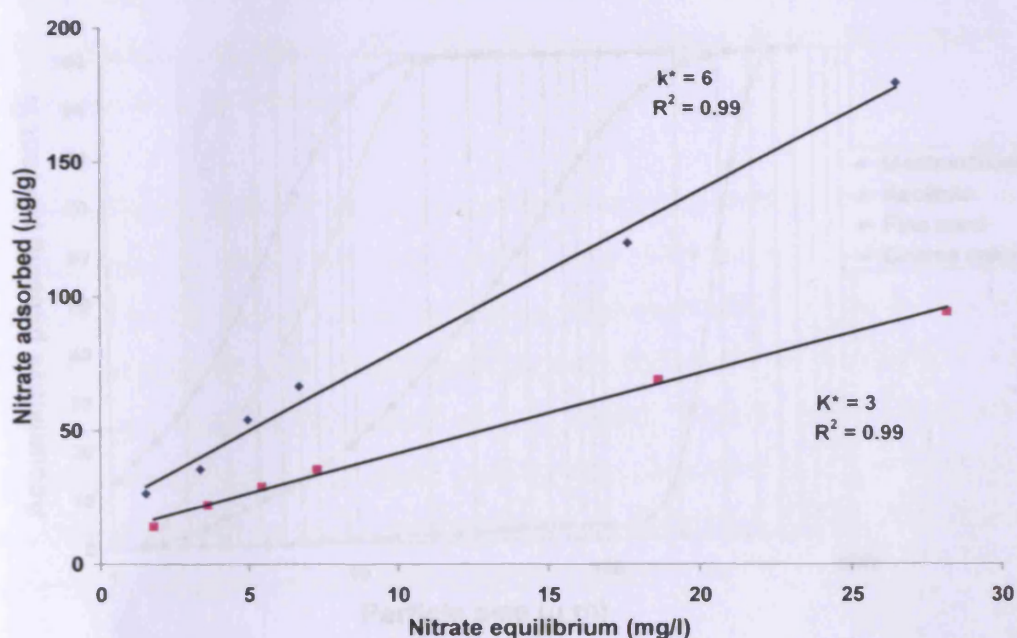


Figure 5.32: Adsorption isotherm of nitrate on Kaolinite in deionised water and artificial sea water (35ppt).

From Figure 5.32 presented nitrate adsorption by clay (Kaolinite) in both deionised water and artificial seawater, were almost linear with a controlled range of nitrate concentration during the laboratory experiments. Different concentrations of nitrate were used, including 2, 4, 6, 8, 20, 30, mg/l. It can be seen that the amount of nitrate adsorption was higher in deionised water than in artificial sea water. The adsorbed nitrate reduced by 47.5% of its original value, from 180 µg/g to 94.5 µg/g. The figure shows that the amount of nitrate equilibrium was lower in deionised water than artificial sea water, with the concentration being reduced by 3.6 mg/l and 1.86 mg/l of its initial concentration, which was 30 mg/l.

5.5 Clays and sand particle size

Figure 5.33 shows the particle size distributions of the four types of sediment (namely Montmorillonite, Kaolinite, fine and coarse sand), with the size distributions being determined by using a Laser particle size instrument (Malvern Master Sizer). The figure shows a comparison of the particle size and cumulative percent distributions mass for all of the samples. Montmorillonite has the smallest d_{50} compared to Kaolinite, fine and coarse sand with d_{50} values of $3.5\mu\text{m}$, $6.75\mu\text{m}$, $30\mu\text{m}$, $270\mu\text{m}$) respectively.

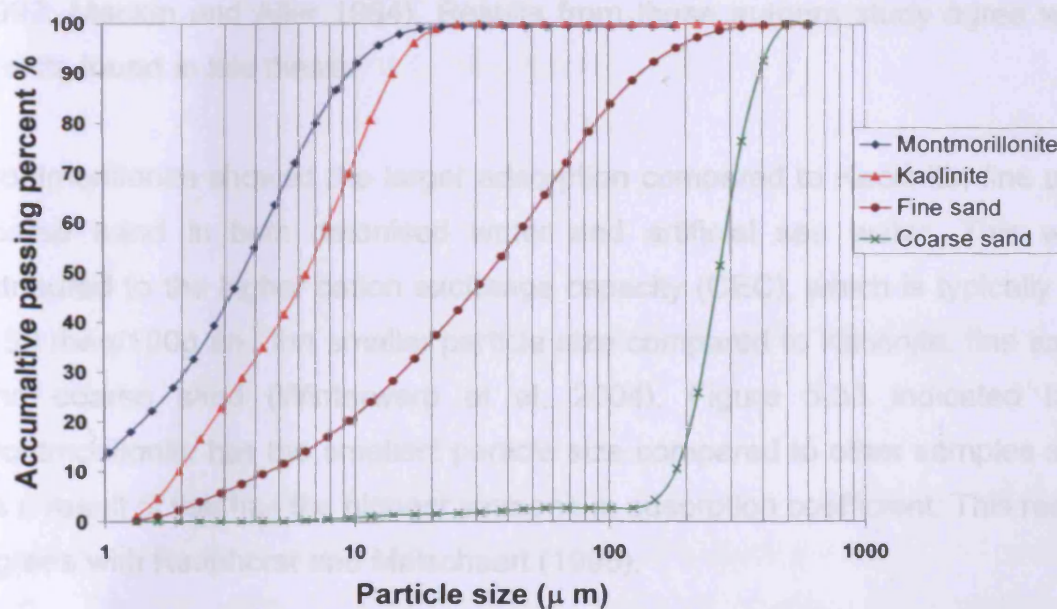


Figure 5.33: Comparison of particle size of samples (Montmorillonite, Kaolinite, fine and coarse sand)

5.6 Discussion

5.6.1 Adsorption isotherms

The ammonium adsorption on Montmorillonite, Kaolinite, coarse and fine sand in deionised water and artificial sea water was found to obey the Langmuir adsorption isotherm. The Freundlich and Langmuir adsorption isotherm formulae were presented in section 2.2.3. The Langmuir model fits the data well since the errors derived from the Chi-squared and R^2 tests are lower than the errors from the Freundlich model. The theoretical adsorption coefficients

(Langmuir and Freundlich) at two conditions of water (deionised and artificial sea water) were higher for Montmorillonite compared to other sediment samples presented. Both the adsorption coefficients (Langmuir and Freundlich) were higher at deionised water than artificial sea water for all sediment samples.

The results of this study showed that the ammonium adsorption by clays (Montmorillonite, Kaolinite) and sand (coarse, fine) were almost linear at ammonium concentrations (2, 4, 6, 8, 10, 20, 30mg/l) in both deionised water and artificial sea water. Studies by previous authors have shown that clay mineral and organic matter content influence adsorption of ammonium (Sugai 1992; Mackin and Aller 1984). Results from these authors study agree with results found in this thesis.

Montmorillonite showed the larger adsorption compared to Kaolinite, fine and coarse sand in both deionised water and artificial sea water. This was attributed to the higher cation exchange capacity (CEC), which is typically 80 -150 meq/100g and the smaller particle size compared to Kaolinite, fine sand and coarse sand (Winterwerp et al, 2004). Figure 5.33 indicated that Montmorillonite has the smallest particle size compared to other samples and as a result of that has the highest ammonium adsorption coefficient. This result agrees with Raaphorst and Malschaert (1996).

Montmorillonite has the smallest particle size and as a result is shown to have the highest ammonium adsorption characteristics compared to the other sediments investigated in this study. The ammonium adsorption on Montmorillonite, Kaolinite, fine and coarse sand was tested at different concentrations of artificial sea water (0, 2, 3, 4, 5, 15 and 25 ppt). The ammonium adsorption was found to successively decrease with increasing salinity and in (2, 3, 4, 5, 15 and 25 ppt).

Hou et al, (2003) and Boatman and Murray (1982), indicated that ammonium adsorption on the sediment was higher under lower salinity conditions than higher salinity conditions, which agrees with the findings from this study. Ammonium adsorption was affected not only by particle size of the sediments

but also by salinity of the water. The total amount of cations (primarily Na^+ and Mg^{2+}) increases with salinity resulting in a higher molecular competition with NH_4^+ .

The amount of adsorbed ammonium was calculated by dividing the amount of ammonium equilibrium concentration as a unit of mass by the weight of the clays and the sand samples. The ammonium adsorption coefficient expresses the characteristics of ammonium adsorption. The adsorption coefficient (K^*) was calculated in this experiment from the regression line of adsorbed ammonium plotted against the ammonium equilibrium concentration. K , the dimensionless equivalent of K^* , is calculated for the real sediment (samples from the field), using the formula from Berner (1980).

$$K = \frac{1-\phi}{\phi} * \rho * k^* \quad (5.8)$$

Where Φ = porosity of the sediment, ρ density of the sediment and K^* adsorption coefficient.

In this experiment K , the dimensionless adsorption coefficient was not calculated for clean sediments (Montmorillonite, Kaolinite, fine and coarse sand). For field samples K is calculated because physical soil parameters, such as sediment porosity and particle density, are not known. Hou et al (2003) indicated that adsorption coefficient of ammonium was higher under low salinity and lower under high salinity which was consistent with the findings of these experiments.

The results presented in Table 5.3 show that the adsorption coefficient decreased gradually with increasing salinity. Hou et al 2003 indicated the adsorption coefficient of ammonium was higher under low salinity and lower under high salinity which was consistent with the findings of these experiments. In addition Montmorillonite had the highest adsorption coefficient for all salinity concentrations among the samples presented in this study which was Kaolinite, fine and coarse sand.

Figures 5.23 to 5.26 present the change of ammonium adsorption coefficients for Montmorillonite, Kaolinite, fine and coarse sand under different salinities. The adsorption coefficient was affected by different concentrations of artificial sea water which was greater under low salinity than under high salinities because lower salinity is more favourable to ammonium adsorption by the samples tested. The first derivative equations present the adsorption coefficient for salinity range 2, 3, 4, 5, 15, 20, 25 ppt.

The adsorption coefficient for these samples under different concentrations of artificial sea water was fitted to equations 5.9, 5.10, 5.11 and 5.12. The first derivative equations were:

$$dk/dS = 0.2324S - 6.951 \quad \text{for Montmorillonite} \quad (5.9)$$

$$dk/dS = 0.0484S - 1.0205 \quad \text{for Kaolinite} \quad (5.10)$$

$$dk/dS = 0.0068S - 0.2372 \quad \text{for fine sand} \quad (5.11)$$

$$dk/dS = 0.007S - 0.1834 \quad \text{for coarse sand} \quad (5.12)$$

Where:

dk/dS (ml/g ppt) is the rate of change of the ammonium adsorption coefficient; S is the concentration of artificial sea water and ranged from 2, 3, 4, 5, 15, to 25, ppt).

From these first derivative equations, the rate of change of the ammonium adsorption coefficient can be calculated for the Montmorillonite, Kaolinite and coarse and fine sand. It can be seen how it gradually decreases with increasing salinity. The rate of change of ammonium adsorption coefficient is larger within the lower range of salinity, indicating that a little variation of salinity can have a dramatic effect on ammonium adsorption to sediment.

5.6.2 Desorption kinetics using artificial sea water

The purpose of these experiments was to mimic the situation that occurs in estuaries where fresh water is mixed with sea water and sediment

re-suspension occurs. Wave and tidal action cause re-suspension of sediment and ammonium release into the water column. Ammonium has a shorter residence time in estuarine sediments compared with fresh water sediment, due to competition for exchange sites from sea water cations (Seitzinger et al., 1991). Results from this study agreed with this. Ammonium adsorption on Montmorillonite, Kaolinite, and fine and coarse sand decreased gradually during the time during mixing of the samples with artificial sea water.

Kinetic experiments indicated that Montmorillonite, Kaolinite and fine sand reached equilibrium after 70 minutes. Coarse sand had reached the equilibrium after 60 minutes. This process occurs slower than for some of the sediment types that were investigated in this study since the particle size is comparatively small. The results show that the amount of ammonium that reduced or released from the surface of the sediment particles during mixing with artificial sea water was higher for Kaolinite than other samples at ammonium concentrations 2, 6 mg/l at 80% and 49% respectively. Montmorillonite has the highest ammonium reduction at ammonium concentration 10 mg/l, at 57%. This experiment showed that equilibrium of ammonium in artificial sea water had occurred after 70 minutes and 60 minutes in a few cases.

In the estuary during high tide when sea water and fresh water mix, sea water cations replace ammonium ions on the surface of the sediment particles. This process will continue until all the surface exchange sites will be occupied by the sea water cations, at which point equilibrium occurs. The equilibrium time (the time that sediment particles take to reach an equilibrium stage) depends on the sediment type as indicated in this study.

5.6.3 Nitrate adsorption

The nitrate adsorption on Kaolinite in deionised water was found to correspond to the Langmuir adsorption isotherm. The Langmuir equation was highlighted in Section 2.2.3. The Langmuir model fits the data well since the errors derived



from the Chi-squared and R^2 tests are lower than the errors from the Freundlich model.

This study showed that the nitrate adsorption by Kaolinite it was almost linear at nitrite concentrations (2, 4, 6, 8, 20 and 30 mg/l) in deionised water. Kaolinite mineral clay was used in the nitrate adsorption isotherm experiment, rather than other types of clay due to the positive charges on the edges of Kaolinite particles which can facilitate adsorption of the negatively charged nitrate ions. The positive charge on the edge of Kaolinite is caused by dissociation of the gibbsite octahedral structure at low pH, and becomes a negative charge when pH exceeds 7 (Winterwerp and Van Kesteren., 2004). Kaolinite affects NO_3^- mobility in anion adsorption. Anion adsorption happens when negatively charged NO_3^- ions attach to the positively charged Kaolinite surface. If anion adsorption is a dominant process, NO_3^- mobility in the water is reduced. The type of clay minerals present can influence anion adsorption, which is the dominant mechanism affecting NO_3^- movement through the water column. Kinjo and Pratt (1971) indicated nitrate adsorbed on the positive charge presented on the Kaolinite and other oxides such as ferric oxide that are created by protonation (where hydrogen ions (H^+) are accepted more than hydroxyl ions (OH^-) in excess of OH^- ions adsorbed). Allred et al (2007) found that NO_3^- anion adsorption will occur if pH is low and the clay mineral Kaolinite is available.

It was found in this study that salinity can influence nitrate adsorption on Kaolinite during mixing of fresh water and sea water in estuaries. Sea water anions (e.g. Cl^- , SO_4^{2-} , HCO_3^- , Br^-) interfere with the NO_3^- ion on the Kaolinite clay mineral, and nitrate adsorption decreases with increasing salinity. Kinjo and Pratt (1971) studied nitrate adsorption, in competition with chloride, sulphate and phosphate, stating that nitrate has a low capacity to compete with sea water anions on the anion exchange sites presented on the surface of clay minerals or organic matter as a result of high replacement of OH^- ions by Cl^- compared to NO_3^- . Sulphate and Phosphate also have more replacement ability than nitrate. Phosphate has a high capacity to adsorb on the anion exchange sites on clay minerals. The adsorption of anions increases in the

following order, $\text{NO}_3^- < \text{SO}_4^{2-} < \text{PO}_4^-$. Hingston et al (1972) found that stronger retention / adsorption of sulphate onto the sediment and soils containing organic matter and smectite clays was due to the sulphate ions high charge density compared with the monovalent chloride ion. Overall the types and the amounts of clay minerals present will impact highly on nitrate mobility within the sediments and between the sediments and the water column.

5.7 Summary

This chapter shows the results of the ammonium adsorption isotherms for Montmorillonite, Kaolinite and fine and coarse sand for conditions including deionised and artificial sea waters. The ammonium adsorption on Montmorillonite, Kaolinite and fine and coarse sand in deionised water and artificial sea water is found to obey the Langmuir adsorption isotherm. In addition, based on Chi-squared and R^2 tests which show lower errors than resulting from the Freundlich model. The results indicate that Montmorillonite shows larger ammonium adsorption compared to Kaolinite and fine and coarse sand in both deionised water and artificial sea water. The results indicate that NH_4^+ adsorption on Montmorillonite, Kaolinite, fine and coarse sand in deionised water was respectively 2.6, 2.5, 2.4 and 2.0 times higher than NH_4^+ adsorbed in artificial sea water of 35 ppt salinity. The results in this chapter also show that the adsorption coefficients decreases gradually with increasing salinity. From the first derivative equations the rate of change of ammonium adsorption coefficient is calculated for Montmorillonite, Kaolinite and fine and coarse sand. The rate of change of ammonium adsorption coefficient is larger within the lower range of salinity.

Desorption kinetics results mimicked the situation that occurs in estuaries where fresh water is mixed with sea water and sediment re-suspension occurs. The results indicate that Montmorillonite, Kaolinite and fine sand had reached equilibrium after 70 minutes. Coarse sand had reached the equilibrium after 60 minutes. Also the results of NO_3^- adsorption on Kaolinite in deionised water are shown in this chapter. The results indicate that the Langmuir model fits the data well and that salinity effectes the nitrate adsorption on Kaolinite. The

amount of nitrate adsorption was higher in deionised water than artificial sea water. This is believed to be caused by interfere sea water anions with the NO_3^- ion in the Kaolinite minerals and this can impact on the nitrate mobility within the sediment and in the sediment and water column.

6 Case study of the Loughor Estuary

6.1 The study area

The Loughor Estuary is located in South West Wales and is one of the main tributaries discharging into Carmarthen Bay and the Bristol Channel, Figure 6.1. The Bristol Channel is located on the west coast of the UK, is a funnel shaped estuary and has the second highest tidal range in the world (up to 14.5m at Avonmouth). As for most macro-tidal estuaries, the tides in the Bristol Channel and Carmarthen Bay play a major role in mixing fresh and salt water and in re-suspending sediments from the bed and transporting the suspended sediments landwards or seawards (Schnauder et al, 2007; Bockelmann et al, 2008). The changes in the environmental factors, particularly salinity, are very intense and can influence the ammonium adsorption rate and nutrient concentrations as a result of the interaction between the riverine freshwater and the seawater (Hou et al, 2003; Abdulgawad et al, 2008).

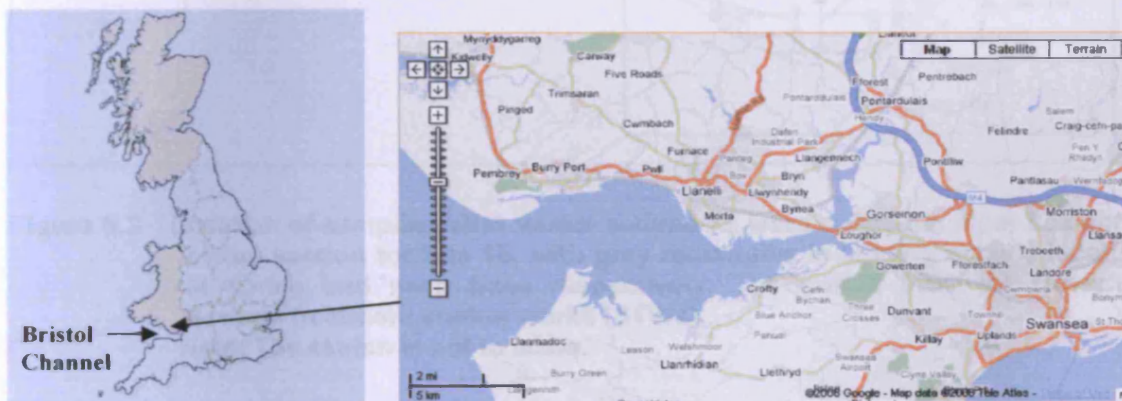


Figure 6.1 Location of Loughor Estuary, UK. (Base image courtesy of Google Earth, 2008)

6.2 Sample collection

Samples (water and bed sediments) were obtained from cross-sections at four sites along the Loughor Estuary, as shown in Figure 6.2. These samples were

taken as part of an ongoing research project, sponsored by the Environment Agency (EA) Wales. These samples were used for laboratory analysis.

These sites are designated as: 1a, 1b, 2, and 3 and are illustrated in Figures 6.3, 6.4, 6.5 and 6.6 respectively. The seasonal sampling programme ran from 6th November 2007 to 30th June 2008. Both water samples and sediment samples were collected on 6th November 2007, 14th December 2007, 13th March 2008, 2nd June and 30th June 2008. Water and sediment samples were collected over 6 hour periods during rising or falling tides.

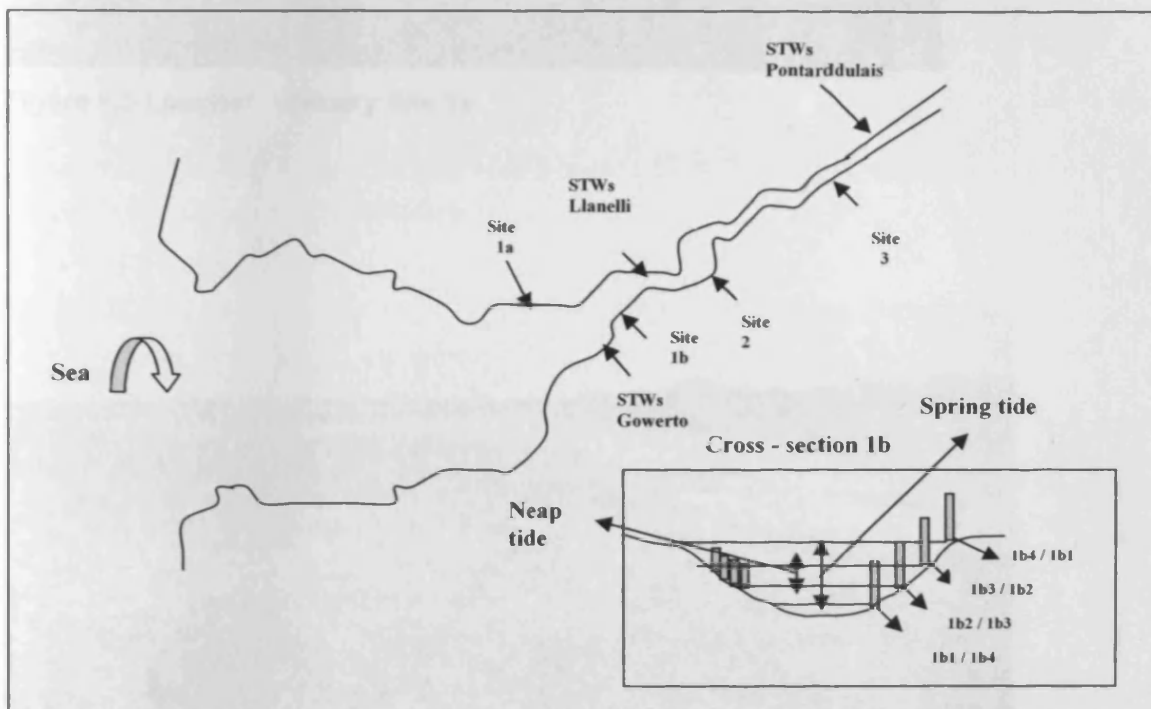


Figure 6.2 Location of sampling sites where sediments were collected. Inner box shows cross- section for Site 1b, with grey rectangles indicating sample locations at spring and neap tides respectively. The outfall from the Gowerton. Sewage treatment station works (STWs).
Note: The sketch is not to scale.



Figure 6.3 Loughor Estuary Site 1a

Figure 6.3 Loughor Estuary Site 2



Figure 6.4 Loughor Estuary Site 1b

Figure 6.4 Loughor Estuary Site 3

Samples were collected at each site at approximately hourly intervals. Bed sediment samples were taken close to the water's edge (at depths of 0–3 cm) below the surface. Sediment samples were collected along cross-sections for sites 1a and 2 along the Loughor Estuary (see Figure 6.3). Plastic bags were used for collecting the bed sediments, with samples being stored in a



Figure 6.5 Loughor Estuary Site 2



Figure 6.6 Loughor Estuary Site 3

Samples were collected at each site at approximately hourly intervals. Bed sediment samples were taken close to the water's edge (at depths of 0-3 cm) below the surface. Sediment samples were collected along cross-sections for sites 1b and 2 along the Loughor Estuary (see Figure 6.2). Plastic bags were used for collecting the bed sediments, with samples being stored in a

refrigerator at 4 °C over the next day before undertaking a series of adsorption/ desorption experiments. Plastic bottles (1 litre capacity) were used to collect the water samples (see section 6.4).

6.3 Materials and methods

This section contains details of the materials and procedures used to determine the physico-chemical characteristics of the sediments, the fixed ammonium on the bed sediments and the ammonium adsorption isotherm. The objective of these experiments was to determine the adsorption coefficient of ammonium. This study was conducted using real bed sediments from the Loughor Estuary. Artificial sea water, with different concentrations of salinity, was prepared to study the effects of salinity on the ammonium adsorption and on the adsorption coefficient for ammonium.

6.3.1 Determination of the physico-chemical characteristics for the Loughor Estuary bed sediments

The apparatus sediments and procedures used to measure the physico-chemical parameters of the bed such as density, porosity, organic carbon and particle sediment size, are explained in this section.

6.3.1.1 Bulk density and porosity of bed sediments

The bulk density was evaluated for different types of sediment, using a pycnometer with a cover. The pycnometer and cover were weighed, followed by the weight of the pycnometer, cover and distilled water, in order to find the weight of water and to calculate the volume of the pycnometer (see Figure 6.7).



Figure 6.7 Measuring bulk density using a pyknometer

The pyknometer was dried and filled with the sample, then covered and weighed again to find the weight of the sample. The bulk density was calculated using the following formula:

$$\text{Bulk density} = \frac{\text{Mass of the sample}}{\text{Volume of the sample}} \quad (6.1)$$

Particle density evaluation

The bottle with the stopper was weighed to the nearest 0.001 g (m1). The first sediment sample was transferred to the density bottle, directly from its sealed container. The contents, bottle and stopper were weighed to the nearest 0.001 g (m2). Sufficient air-free distilled water was added, just to cover the sample in the bottle and without disturbing the sample excessively. The bottle and the contents were then placed, without the stopper, in the vacuum desiccator (see Figure 6.8). The desiccator was evacuated gradually, reducing the pressure to about 20 mm of mercury. Care was taken during this operation to ensure that air trapped in the soil did not bubble too violently, which could have led to small drops of the suspension being lost through the mouth of the bottle.

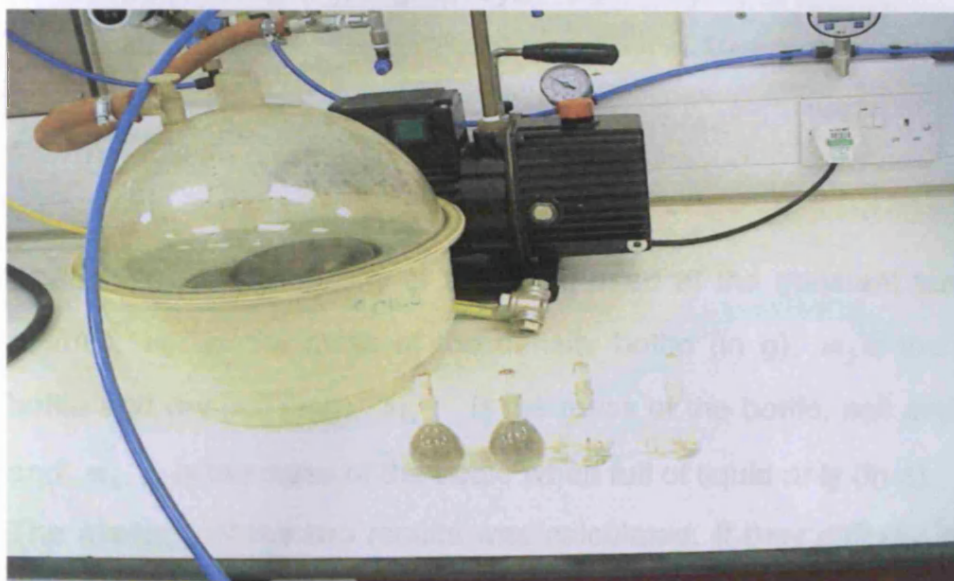


Figure 6.8 Measuring particle density using a vacuum desiccator

The bottle in the evacuated desiccator was left for at least 1 hour until no further loss of air was apparent. The vacuum was released and the lid of the desiccator removed. The sample was carefully stirred in the bottle by shaking it by hand. Particles of sediment adhering to the blade were washed off with a few drops of water. The lid of the desiccator was replaced and evacuated again. This was repeated until no more air from the sample. The density bottle and its contents were removed from the desiccator and more water was added to fill the bottle. The stopper was inserted in the bottle and the sealed bottle then immersed up to the neck in a constant-temperature bath (room temperature). The bottle was left in the bath for at least 1 hour, or until the contents had attained the constant temperature of the bath. When an apparent decrease in the volume of the liquid occurred, the stopper was removed and more liquid added to fill the bottle and the stopper then replaced. The bottle was returned to the bath, and again the contents were allowed to attain a constant temperature. The bottle was taken out of the bath, carefully wiped dry with minimum handling and again weighed to the nearest 0.001g (m_3). The bottle was cleaned, filled completely with de aerated water, wiped dry and again weighed to the nearest 0.001 g(m_4). This procedure was repeated using the second specimen of the same sample so that two values of particle density

were obtained. The equation for the particle density of the sample particles, ρ_s (in mg/m^3), is given by:

$$\rho_s = \frac{\rho_L(m_2 - m_1)}{(m_4 - m_1) - (m_3 - m_2)} \quad (6.2)$$

where: ρ_L is the density of the liquid used at the constant temperature (in mg/m^3), m_1 is the mass of the density bottle (in g), m_2 is the mass of the bottle and dry soil (in g), m_3 is the mass of the bottle, soil and liquid (in g), and m_4 is the mass of the bottle when full of liquid only (in g).

The average of the two results was calculated. If they differed by more than 0.03 mg/m^3 then the test was repeated.

Porosity

The porosity of the sediment samples from the Loughor Estuary was calculated using the following formula:

$$\text{Porosity}(\%) = 1 - \frac{\text{Bulk density}}{\text{Particle density}} \quad (6.3)$$

The determination of the bulk and particle density is indicated above.

6.3.1.2 Measurement of total carbon and inorganic carbon

Total carbon content was determined by combustion, using a Leco SC 144 total carbon analyzer as shown in Figure 6.9.



Figure 6.9: Leco total carbon analyzer

A dry sample of weight 0.350 g was inserted into a combustion boat (a specific sample container for combustion). The sample was placed in a pure oxygen environment, typically regulated at 1350°C. The combination of the furnace temperature and then oxygen flow caused the sample to combust. Sample materials contained in the combustion boat go through an oxidative-reduction process that causes carbon and sulphur bearing compounds to break down, thereby freeing the carbon and sulphur. The sample gases were first swept through the boat and stopped at the back of the inner combustion tube. They were then swept forward, between the inner and outer combustion tubes, allowing the sample gases to remain in the high temperature zone for a longer period and permit efficient oxidation.

From the combustion system, the gases flowed through two anhydrous tubes to remove moisture, through a flow controller that sets the flow of sample gases to 3.5 l/min, and then through the infrared detection cell. The carbon IR (infra-red) cell measured the concentration of sulphur dioxide gas. The instrument converted these values to a percentage by mass value. Sensitivity of the instrument ranged between 10 to 100 ppm at the lower end to greater than 10 000ppm (1%) at the higher end.

Measurement of inorganic carbon

The inorganic carbon content was determined after acidification with phosphoric acid this converted the inorganic carbon into carbon dioxide CO₂, and was obtained using a SHIMADZU SSM-5000 A (TOC-5000(A)/5050(A)) analyser as shown in Figure 6.10.



Figure 6.10 SHIMADZU analyser in use for inorganic carbon analysis

The sample was weighed and placed in the sample boat. Phosphoric acid was added and the reaction commenced. If the sample contained a high percentage of carbonate, such as sodium carbonate, then this could cause effervescence, causing part of the sample to scatter outside the sample boat. For such a case this type of sample was first moistened with a small amount of water before starting the process. Concentrated phosphoric acid was used to determine the inorganic carbon. The reaction did not occur unless the entire sample in the sample boat was dipped in the phosphoric acid. If undiluted, phosphoric acid could not enter the sample because of its high viscosity, thus the phosphoric acid was diluted with approximately two parts of water to allow all of the sample to be in contact with the acid. Injection of acid into the sample caused an immediate reaction with the inorganic carbon in the sample to produce CO_2 . Thus after closing the sample port cover and waiting for about two minutes, the sample boat was introduced into the inorganic carbon furnace, immediately after the acid was injected. The instrument converted the inorganic carbon values to percentage value. Sensitivity range in between 10 to 100 ppm at the lower end to greater than 10 000ppm (1%) at the higher end

6.3.1.3 X-ray diffraction (XRD) (mineralogical identification of sample)

X-ray diffraction (XRD) is a technique for determining the type and quantity of crystalline minerals in solid samples. Tests were carried out with a Philips PW

3830 X-ray generator, using the X pert industry software. Samples were dried at 105°C for 24 hours and crushed to a particle size of less than 0.5mm; this was done using a Labtech Essa LM1-P ring mill. A small amount of the sample was compacted into the sample holder and placed inside the x-ray chamber and a scan then run. On completion of the scan the data were exported to the X pert high-score software for analysis. The background of the plot was determined and peaks identified. The search and match functions were then used to identify the composition of the crystalline minerals. The sensitivity of the XRD was 0.1%.

6.3.1.4 Suspended sediment concentration

The simplest way of taking a sample of suspended sediment is to dip a container into the stream at a point where the sediment and water are well mixed. The sediment contained in a measured volume of water is filtered, dried and weighed.

A water sample with its suspended sediment was measured in a volumetric cylinder and filtered through 0.45 µm cellulose filter paper, then left to dry. The difference between the weight of the filter paper containing the samples and the weight of the empty filter paper, divided by the volume of the water sample (in litres), gave the weight of suspended sediment as given below:-

$$\text{Suspended sediment (mg/l)} = \frac{(B - A) * 1000 \text{ mg / g}}{V} \quad (6.4)$$

where: A = filter paper weight (in g), B = filter paper weight and sediment weight (in g), V = volume of sample filtered (in l)

6.4 Field sample experiments

This section deals with the laboratory apparatus and methods used for the laboratory experiments i.e. a series of adsorption experiments), for the field samples that were collected from the Loughor Estuary. Plastic bags were used

for collecting the bed sediments, which were then stored in a refrigerator at 4 °C for the next day (or night).

The experiments conducted were ammonium adsorption isotherm experiments, which were undertaken to investigate fixed ammonium and salinity effects on ammonium adsorption. Ammonium and nitrate concentrations in the water sample were also measured.

6.4.1 Ammonium adsorption of bed sediment

Bed sediment samples were taken from the field at Sites 1b and 2 and first weighed. A 50:50 mixture of sediment and water was prepared, agitated on the shaker for 1 hour and then centrifuged at 3000 rpm for 15 min. The supernatant was removed and the ammonium concentration analysed by using the Lambda EZ150 spectrophotometer, set at 640 nm (Eaton et al., 1995) and HACH reagent as indicated in section 4.4.1. 40 ml of 2 M KCl solutions were added to the remaining sediments (0.8 g) in the centrifuge tubes and these sediments were then replaced on the shaker with continuous agitation for 2 hours. The samples were then centrifuged at 3000 rpm for 15 minutes. The supernatant was removed and analysed using a spectrophotometer. This procedure was performed once to allow the adsorbed ammonium on the surface of the sediments to be removed. Another method of determining the ammonium adsorption was based on using dry sediments instead of wet sediments. This method was conducted by drying the sediments in the oven at 70°C for 24 hours. A dry sediment sample of weight 0.8 g was placed in a centrifuge tube, containing 2 M KCl, and the centrifuge tube was then placed on a shaker with continuous agitation for 2 hours. The same methodology above was used for the wet sediment adsorption. This method (using dry sediments) was undertaken to investigate if there was any difference in the amount of ammonium adsorption for the two types of sediments (i.e. dry and wet).

6.4.2 Ammonium adsorption isotherm of bed sediment

Ammonium adsorption studies were undertaken using bed sediments taken from the bed at surface depths of between 0 to 3 cm. Wet homogenised sediments were taken at each site, and then dried in the oven at 70°C for 24 hours. A sample of dry sediment weighing 0.8 g was placed in a centrifuge tube, containing 40ml of NH_4^+Cl , at varying concentrations of NH_4^+ (2, 4, 6, 10, 20 and 30 mg/l). The centrifuge tube was placed on a shaker with continuous agitation for 24 hours, at a temperature of 20 °C +/- 2 °C. The samples were then centrifuged at 3000 rpm for 15 min. The supernatant was collected, filtered through a 0.45 µm cellulose filter paper and then analysed for NH_4^+ . The determination of ammonium concentration in the supernatant was undertaken using a Lambda EZ150 Spectrophotometer, set at 640 nm (Eaton et al., 1995) and HACH reagent (see Section 4.4). The ammonium concentration in the supernatant was considered as being the equilibrium concentration for the sediment / water sample.

The adsorption isotherm experiments were followed by a desorption procedure, in order to remove ammonium ions from the solids. 40ml quantity of 2 M KCl solution was added to the sediments remaining in the centrifuge tubes and these sediments were then replaced on the shaker. After 2 hours of agitation the solutions were centrifuged at 3000 rpm for 15 min. The supernatant was removed and analysed using the spectrophotometer. This procedure was repeated until all of the NH_4^+ was removed from the sediments.

6.4.3 Fixed ammonium on the bed sediment

A 0.8g portion of dry sediments was placed in the centrifuge tubes and 40ml of 2 M KCl was added. The centrifuge tube was placed on the shaker with continuous agitation for 2 hours, then the supernatant collected and centrifuged at 3000 rpm for 15 min. The supernatant was removed and analysed using the spectrophotometer and HACH reagent, to determine the fixed ammonium (see Section 4.3). This procedure was repeated five times until all of the NH_4^+ was removed from the sediments.

6.4.4 Salinity effect on ammonium adsorption

This study was conducted using artificial sea water. Four different concentrations of artificial sea water were prepared using salinities of 2, 10, 15, 20 and 25 parts per thousand (ppt). Artificial sea water was prepared according to the Scottish Association for Marine Science procedure (MASM, 2007) (see Section 4.1), with the pH value of the artificial sea water being set to 8. Concentrations of ammonium were, 2, 4, 6 and 10 mg/l NH_4^+ . The same methodology was used as that outlined for the above mentioned isotherm adsorption experiments (see Section 6.4.2).

6.4.5 Dissolved ammonium concentration

Water samples were collected from the field for each site in order to analyse the dissolved ammonium concentration. For each case 0.1 ml of sample was added to the dilution reagent vials (i.e. ammonium reagent) (see Section 4.3).

6.4.6 Sediment and water nitrate and nitrite concentration

This section deals with the method and experiments to determine the concentrations of nitrate and nitrite present in the sediments and dissolved in the water for the field samples.

6.4.6.1 Determination of nitrate and nitrite concentrations in the sediment

Nitrate and nitrite concentrations were measured using sediments taken from the bed surface. Wet homogenised sediments were taken from each site 50:50 mixtures of sediment and water being prepared. The sediment water mixtures were placed on the shaker for 1 hour, then centrifuged at 3000 rpm for 15 min. The supernatant was removed and nitrate and nitrite concentrations were analysed by using Lambda EZ150 spectrophotometer, set at 543 and 540 nm respectively (Eaton et al., 1995) and HACH reagent as indicated in Section 4.4. These experiments were followed by a desorption procedure in order to remove nitrate and nitrite from the surface of the sediments. 40 ml of 2 M KCl and 0.5 N K_2SO_4 solution respectively were

added to the sediments remaining in the centrifuge tubes and placed back on the shaker for 30 minutes. The solutions were then centrifuged at 3000 rpm for 15 minutes. The supernatant was removed and analysed with a spectrophotometer and using HACH reagent as described above. Nitrite concentration was measured using NitrVer, powder pillows HACH reagent.

Procedure of the nitrite reagent

10 ml of the sample was added to the test container. One powder pillow reagent of Nitr1 Ver 2 Nitrite was added to the sample and the solution was left for 5 minutes until a change of colour occurred. After the colour changed, 10 ml of solution was placed into a cuvette using a syringe. The cuvette was placed into the spectrophotometer and the sample was analysed at 540 nm (Eaton et al., 1995).

Calibration curve for nitrite

In the test of creating a calibration curve for nitrate, different concentrations of nitrite were prepared. Sodium nitrite was used as a source of nitrite. Figure 6.11 shows the concentrations of nitrite (mg) and the spectrophotometer readings. The absorption of nitrite occurs at a wavelength of 540 nm.

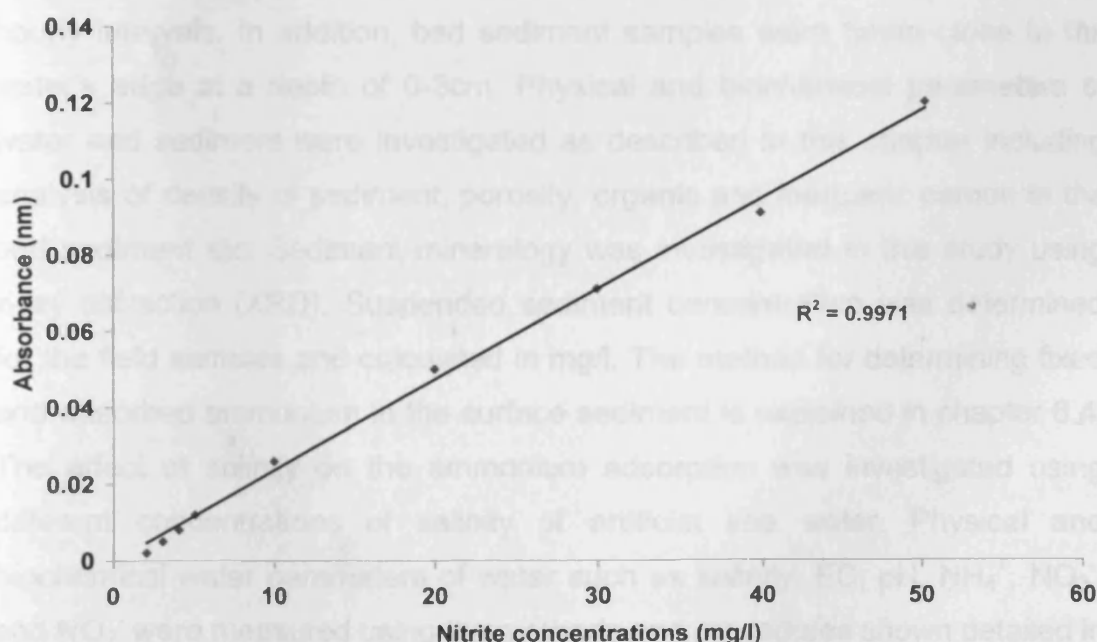


Figure 6.11 Calibration curve for nitrite

6.4.6.2 Dissolved nitrate and nitrite concentrations

Water samples were taken from the field for each site to the laboratory in order to analyse dissolved nitrate and nitrite concentrations. 10 ml from each sample was taken and added to the test container. Nitrate and nitrite reagent were then added and two different tests were carried out, as indicated in Sections 4.4.2 and 6.4.6.1.

6.5 Summary

This chapter introduces the case study area, namely the Loughor Estuary, which is located in south Wales and is one of the main tributaries discharging into Carmarthen Bay and the Bristol Channel. The field work carried out is described including the set of samples collected (water and bed sediment) from across the cross-sectional area at four sites along the Loughor Estuary. Samples were taken as part of an ongoing research project sponsored by the Environment Agency, Wales (EA). The sampling occurred during several seasons running from 7th November 2007 to 30th June 2008.

Water and bed sediment samples were collected over 6 hour periods during rising and falling tides. Samples were collected at each site at approximately hourly intervals. In addition, bed sediment samples were taken close to the water's edge at a depth of 0-3cm. Physical and biochemical parameters of water and sediment were investigated as described in this chapter including analysis of density of sediment, porosity, organic and inorganic carbon in the bed sediment etc. Sediment mineralogy was investigated in this study using x-ray diffraction (XRD). Suspended sediment concentration was determined for the field samples and calculated in mg/l. The method for determining fixed and adsorbed ammonium in the surface sediment is explained in chapter 6.4. The effect of salinity on the ammonium adsorption was investigated using different concentrations of salinity of artificial sea water. Physical and biochemical water parameters of water such as salinity, EC, pH, NH_4^+ , NO_3^- , and NO_2^- were measured using the methods and procedures shown detailed in this chapter.

7 Results and discussion of field work

7.1 Physico-chemical characteristics of the sediment

The results of an analysis of the physico-chemical characteristics of the sediments of the Loughor Estuary are given in this section and include: porosity, bulk and particle density and organic and inorganic carbon. Sediment samples were collected from Sites 1b and 2 at depths 0-3 cm below the bed, with samples being collected at each site at approximately hourly intervals (see Figure 6.2).

7.1.1 Porosity, particle and bulk density of bed sediment samples

In order to calculate the adsorption coefficient for the ammonium adsorbed on the sediments of the Loughor Estuary, it was first important to determine the related parameters such as bulk density, particle density, and porosity. The particle and the bulk density typically ranged from 1.0 to 1.6 mg/m³ and 2.6 to 2.7 mg/m³ respectively (Wild, 1993). The particle and bulk density are variable between the samples and also the sites. Particle density and bulk density are influenced by the mineralogy of the sediments and the organic matter content. The density of organic matter is much lower than the mineral solids density. Sediments high in organic matter, and also some clay minerals, have a low bulk density (Hillel, 1998). The particle density and bulk density for sediments from both Sites 1b and 2 ranged from between 1.10 to 1.50 mg/m³ and 2.63 to 2.69 mg/m³ respectively, see Table 7.1.

The particle density for a quartz dominated sediment is normally expected to be close to 2.65 mg/m³; the slight variation of the particle density between the samples was believed to be due to the organic carbon and clay minerals content; see Section 7.1.4 for the sediment mineralogy.

The porosity of sediment depends on a number of factors including the roundness, packing and the size distribution of the grains. The grain size also has an effect on the porosity of the solids sample, as was the case for the various grain sizes investigated in this study, such as coarse sand, fine sand and clay. The porosity of coarse sand, fine sand and clay ranged typically between 31 to 46%, 26 to 53%, and 34 to 60% respectively (Winterwerp., 2004).

Sediments from the sampling sites consisted mainly of fine sand as indicated in Section 7.1.3. However, their measured porosities ranged from 43% to 58%, which falls into the finer fractions of fine sand and even clay. Sample 1b₁ had the highest porosity value of 58%, attributed to the amount of organic carbon contained in the sample. Sample 2₂ had the low porosity value of 51%, due its low content of organic carbon. Overall, the difference between the results of sampling sites for density (including bulk and particle) and porosity are attributed to the sediment mineralogy and organic carbon content.

Table 7.1: Results of sediment samples for bulk density, particle density and porosity of bed sediment samples, 1b and 2 refer to the site locations. The subscript numbers refer to the sampling time as indicated in Figure 6.2. These samples were taken on 14th December 2007.

Sample Sites	Bulk density (ρ_b)(mg/ m³)	Particle density (ρ_s)(mg/ m³)	Porosity (Φ) (%)
1b₁	1.10	2.65	0.58
1b₂	1.30	2.67	0.51
1b₃	1.30	2.69	0.52
2₁	1.50	2.65	0.43
2₂	1.30	2.68	0.51
2₃	1.20	2.63	0.54

7.1.2 Inorganic, organic and total carbon content

Sediments from Site 1b were found to be higher in carbon content, ranging from 1.53% to 3.74%, when compared to the sediment samples taken from Site 2, which ranged from 1.29% to 4.81%, (see Table 7.2). Sample 2₁ had the

highest amount of organic carbon (4.81%) among the samples for both sites 1b and 2. This sample was collected at high tide. In contrast, sample 2₃ had the lowest amount of organic carbon at 1.29%, which was collected at low tide compared to the other samples from sites 1b and 2.

Table 7.2: Inorganic, organic and total carbon content of sediment samples. 1b and 2 refer to the site locations. The subscript numbers refer to the sampling time as indicated in Figure 6.2. These samples were taken on 14th December 2007

Samples sites	Total carbon (TC) %	Inorganic carbon (IC) %	Organic carbon (OC) %
1b₁	4.1	0.36	3.74
1b₂	2.92	0.1	2.82
1b₃	2.31	0.78	1.53
2₁	5.19	0.38	4.81
2₂	1.60	0.21	1.39
2₃	1.33	0.04	1.29

7.1.3 Particle size distribution of the Loughor Estuary bed sediments

The sediments in the Loughor Estuary from sites 1b and 2 comprised mainly of fine sand, with mean particle sizes (D_{50}) of 83 to 130 μm and 130 to 170 μm respectively (see Figure 7.1 and Table 7.4). Samples were collected when the tidal range was greater than a neap tide on 14th December with samples taken along the cross sections 1b and 2 (See Figure 6.2) and with depth of 7.9m at 8:48 am to 2.1m at 3:12 pm, See Table 7.10. Sample 1b₁ had the largest mean particle size of 130 μm at site 1b. The mean particle diameter for the site 1b samples (i.e. 1b₁, 1b₂, 1b₃) decreased, declining gradually in cross-sectional area and with diameters of the order of 130, 100, 83 μm respectively. In addition the mean grain diameter decreased during the out-going tide. Sample 2₂ had the largest particle size among the samples for both sites (170 μm), and was collected in the middle of the cross-sectional area, see Figure 6.2. This was also collected during the out-going tide. At 2₃, i.e. the position furthest

going down along the cross-section, sediment samples had the lowest mean particle size at 130 μm among the samples of site 2.

Site 1b was located closer to the sea along the Loughor estuary, than either Sites 2 or 3, and was typically of the area most affected by the interaction of sea water and fresh water along the estuary. Site 2 was located further up the estuary and further from the sea, as shown in Figure 6.2. The channel width at site 2 was larger than at site 1b, thus typically the water velocity at site 1b was generally higher than that at site 2. Samples collected from site 2 had a measured particle size higher than site 1b due to the water velocity being lower at site 2. Around high tide flocculation occurred resulting in small particles of sediments and organic matter accumulating to create flocs, thereby leading to increased particle size which were then partly deposited on the bed. Some of these sediments were resuspended from the bed of the channel, depending on the flow velocities and the resulting bed shear stresses. Furthermore at high tide the velocity decreased and largest particles were not entrained and settled to the channel bed.

Collection of samples at both sites 1b and 2 commenced during the out going tide. Table 7.4 and Figure 7.1 show that there was a relationship between the tidal cycle and the particle size at both sites, i.e. for the samples collected during the out-going tide; the resulting particle size was comparatively larger. The sediment size and sorting (i.e. the difference between the large and small particle) changed along the length of the estuary and downstream the smallest particles were generally recorded. This was as a result of a reduction in the transport capability and due to the reduction in slope (Middleton et al, 2003).

Sample 1b₃ had the lowest mean particle diameter among the samples for both sites with a value of 83 μm . This was collected furthest along the cross-section area, compared with sample 2₃ which, at the same position had a mean particle size of 130 μm . This was thought to be due to the width of the channel, which was wider at site 2 compared to site 1b, thus the water velocity was lower at site 2. The velocity at which a moving particle in motion cannot be transported further (and thus falls to the channel bed) is known as the fall velocity. This depends not just on the particle size but on the density and shape, as well as on the viscosity and density of water. This is because the

viscosity and density of water changes with the amount of sediment in the stream. As the flow velocity reduces, the coarser particles start to fall out, whilst the finer particles remain in suspension (Huggett., 2007).

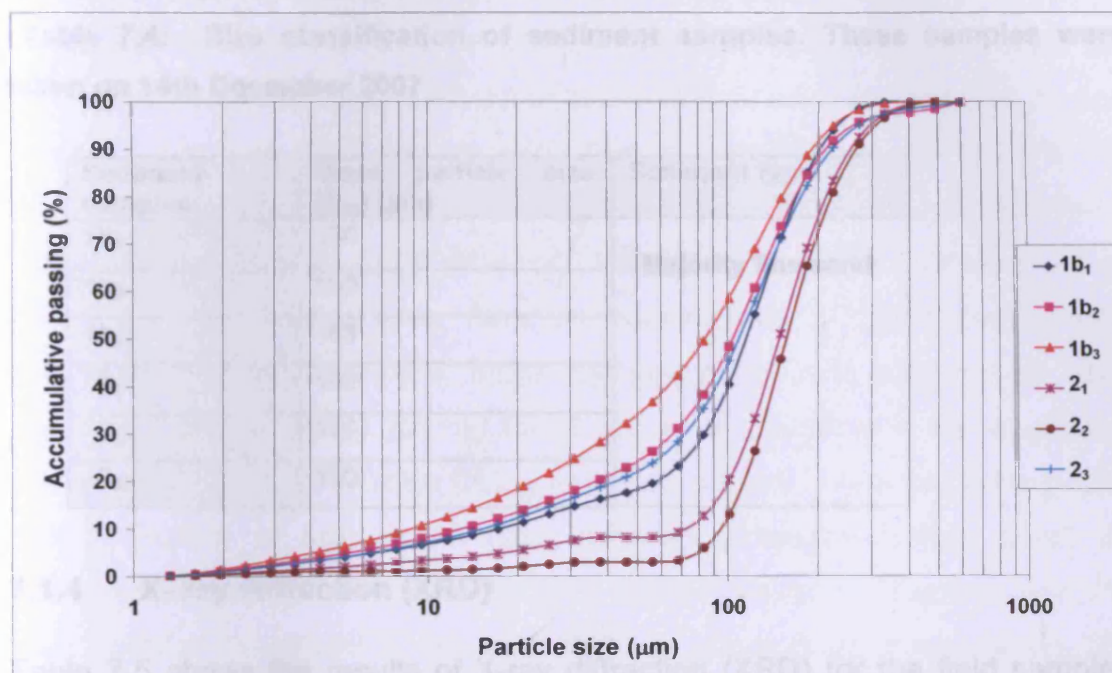


Figure 7.1 Particle size distribution of the Loughor Estuary sediment samples at sites 1b and 2. The subscript numbers refer to the sampling time (3 hours). These samples were taken on 14th December 2007

Table 7.3 shows the classification of mean particle sizes according to the British Standard (Winterwerp et al, 2004). The table shows the sediment types such as sand, silt and clay and the particle size range for each type of sediment. Coarse sand has the largest particle sizes, followed by fine sand, silt and clay respectively.

Table 7.3: Classification of sediment by particle size

Types of particles	Particle size (μm)
Coarse sand	600 – 2000
Fine sand	90 – 200
Silt	60 - 2
Clay	< 2

The field bed sediment samples can all be classified as majority fine sand, related to the British Standard as shown in Table 7.3. Table 7.4 shows sediment samples from 14th December, 2007 data and their mean particle sizes and respective classification.

Table 7.4: Size classification of sediment samples. These samples were taken on 14th December 2007

Sediment samples	Mean particle size (D_{50}) (μm)	Sediment type
1b ₁	130	Majority fine sand
1b ₂	100	
1b ₃	83	
2 ₁	160	
2 ₂	170	
2 ₃	130	

7.1.4 X- ray diffraction (XRD)

Table 7.5 shows the results of X-ray diffraction (XRD) for the field samples collected at sites 1b and 2. The results of XRD indicate that the sediments from both sites mainly comprise quartz, (66.1 to 88.3%), followed by calcite (9.9 to 17.5%), with minor amounts of halloysite (0.02 to 8.4%) and kaolinite (0.7 to 7.9%). Sample 1b₂ had the highest amount of quartz at 81.3% among the samples taken from site 1b. This sample was taken from the middle of the cross-section and collected during out-going tide. It was found that there was a slight difference in the amount of quartz for samples 1b₁ and 1b₃, with values of 87.6% and 78.9% respectively. These samples (i.e. 1b₁ and 1b₃) were collected during out-going tide and at position furthest up and down along the cross-section respectively. Sample 2₂ had the largest amount of quartz at 88.3% of the samples at both sites, which occurred for the sample collected in the middle of the cross-section. In contrast sample 2₃ had the smallest amount of quartz at 66.1% amongst the samples taken from sites 1b and 2. This sample was taken furthest down the cross-section, see Figure 6.2. The highest amount of Calcite among sites 1b and 2 was found to occur in the sediment sample 2₃. This sample was collected furthest down the cross-section at 17.5%. In contrast the smallest amount of Calcite among the samples at both

sites (i.e. 1b and 2) was measured in the sample 2₂ that was collected in the middle of the cross-section area. At site 1b, which was further down the estuary, sample 1b₃ had the largest amount of Calcite among these samples, at 15.7%. This sample was collected further down the cross-section area.

Sediment samples for sites 1b and 2 had small amounts of Kaolinite and Halloysite compared to the amount of quartz contained in the samples for both sites. The amount of Kaolinite for sites 1b and 2 ranged from 0.7 to 7.9%. The largest amount of Kaolinite among all of samples for sites 1b and 2 was found to occur in sample 2₃ with a value of 7.9%, and which was collected furthest along the cross-section area. Since the settling rate of suspended particles depends upon their diameter, small particles particularly clay and silt settle more slowly than larger grains, thereby then in suspension for longer and therefore with these particles taking longer to deposit. As would be expected the proportion of fine grains (clay mineral) increases further down the cross-section area. In contrast and the smallest amount of Kaolinite at 0.7%, was found in the sample 2₁, was collected furthest up along cross-section. This sample was collected during the out-going tide.

Sediment samples for sites 1b and 2 contained small amounts of Halloysite ranging from 0.1 to 8.4%. Sample 2₃ had the highest amount of Halloysite at 8.4% of all the of the samples taken at sites 1b and 2. This sample was collected further down along the cross-section area. In contrast the smallest amount of Halloysite was measured for sample 2₁ which was collected further – up the cross-section. Sample locations and cross – sections for sites 1b and 2 can also be seen in Figure 6.2.

Table 7.5: Mineral content determined by X-Ray diffraction (XRD) for field samples. These samples were taken on 14th December 2007

Samples	Mineral content (%)			
	Quartz (SiO ₂)	Calcite (CaCO ₃)	Kaolinite (Al ₂ Si ₂ O ₅ (OH) ₄)	Halloysite (Al ₂ Si ₂ O ₅ (OH) ₄)
1b ₁	87.6	10.2	1.5	0.3
1b ₂	81.3	15.0	1.7	0.3
1b ₃	78.9	15.7	4.2	1.0
2 ₁	87.8	11.4	0.7	0.1
2 ₂	88.3	9.9	1.8	0.0
2 ₃	66.1	17.5	7.9	8.4

Figure 7.2 shows the percentage of quartz increase with increasing mean particle size (D_{50}). It was found that samples with a smallest mean particle size had a smallest percentage of quartz and vice versa. This correlation is shown in Figure 7.2. The Loughor Estuary sediment was classified as fine sand (see Table 7.4), thus quartz dominates the minerals in the sediment for both sites 1b and 2.

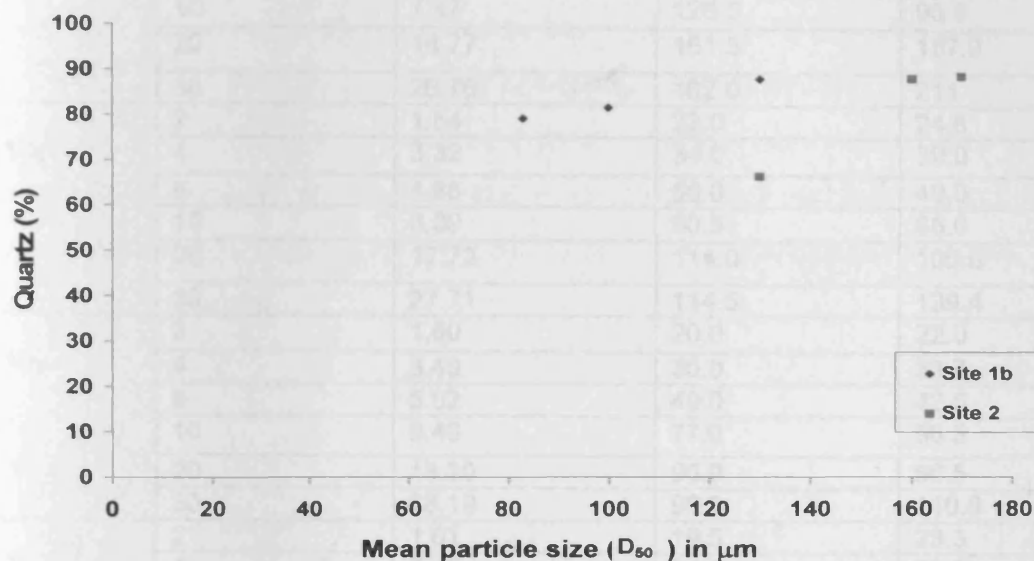


Figure 7.2 Correlation of quartz content with mean particle size

7.1.5 Adsorption isotherm results

During out-going tides over a period of 3 hours at sites 1b and 2, samples were collected at regular interval (i.e. samples 1b₁, 1b₂, 1b₃ and 2₁, 2₂, 2₃), as shown in Figure 6.2. Table 7.6 shows the amount of adsorbed ammonium ions for the two types of adsorption methods used for different ammonium concentrations, giving: (i) an experimental adsorption isotherm, and (ii) the Freundlich and Langmuir adsorption isotherms.

Table 7.6: Measured and theoretical amounts of adsorbed ammonium

Sediment samples	Ammonium concentration		Ammonium adsorption ($\mu\text{g/g}$)		
	Initial concentration (mg/l)	Equilibrium concentration (mg/l)	Experimental	Freundlich isotherms	Langmuir isotherms
1b ₁	2	1.51	24.5	35.5	35.1
	4	2.81	59.5	52.1	57.5
	6	4.27	86.5	67.6	77.0
	10	7.47	126.5	95.6	107.0
	20	16.77	161.5	157.9	150.2
	30	26.76	162.0	211	171.0
1b ₂	2	1.54	23.0	24.6	22.2
	4	3.32	34.0	39.0	41.3
	6	4.88	56.0	49.0	54.2
	10	8.39	80.5	68.0	75.0
	20	17.72	114.0	106.6	104.4
	30	27.71	114.5	139.4	119.6
1b ₃	2	1.60	20.0	22.0	20.9
	4	3.40	30.0	33.7	37.2
	6	5.02	49.0	42.0	47.8
	10	8.46	77.0	56.3	63.2
	20	18.20	90.0	86.5	84.4
	30	28.19	90.5	110.6	94.1
2 ₁	2	1.61	19.5	23.3	22.3
	4	3.32	34.0	36.2	39.6
	6	4.91	54.5	45.9	52.0
	10	8.31	84.5	63.3	70.6
	20	17.90	105.0	101.1	98.0
	30	27.89	105.5	132.5	111.2
2 ₂	2	1.63	18.5	19.9	18.8
	4	3.42	29.0	34.3	36.2
	6	4.98	51.0	45.2	49.0
	10	8.33	83.5	65.7	71.4
	20	17.48	126.0	113.0	110.8
	30	27.48	126.0	157.2	135.5
2 ₃	2	1.61	19.5	20.5	19.5
	4	3.39	30.5	34.8	37.1
	6	5.04	48.0	46.1	50.7
	10	8.22	89.0	65.2	71.5
	20	17.54	123.0	111.4	109.2
	30	27.54	123.0	153.2	131.4

Figures 7.3 – 7.8 show comparisons between the experimental or field data and the theoretical results, using the Langmuir and Freundlich adsorption isotherm equations. In general, the results show good agreement between the experimental or field and theoretical results. The Langmuir model fits the data particularly well for all of the samples tested, according to the error analysis which was performed for all samples. The Langmuir and Freundlich adsorption isotherm formulae are presented in Section 2.2.3. The Langmuir adsorption coefficient (b) for samples from both sites 1b and 2 ranged between 0.056 to 0.182 and the Freundlich adsorption coefficient (K), ranged from 20.7 to 42.6. The error bars represent the maximum and minimum values in both x , which is ammonium equilibrium, and y , which is adsorbed ammonium, over the three replicates. Error bars are not visible as the distribution of data around each point is small.

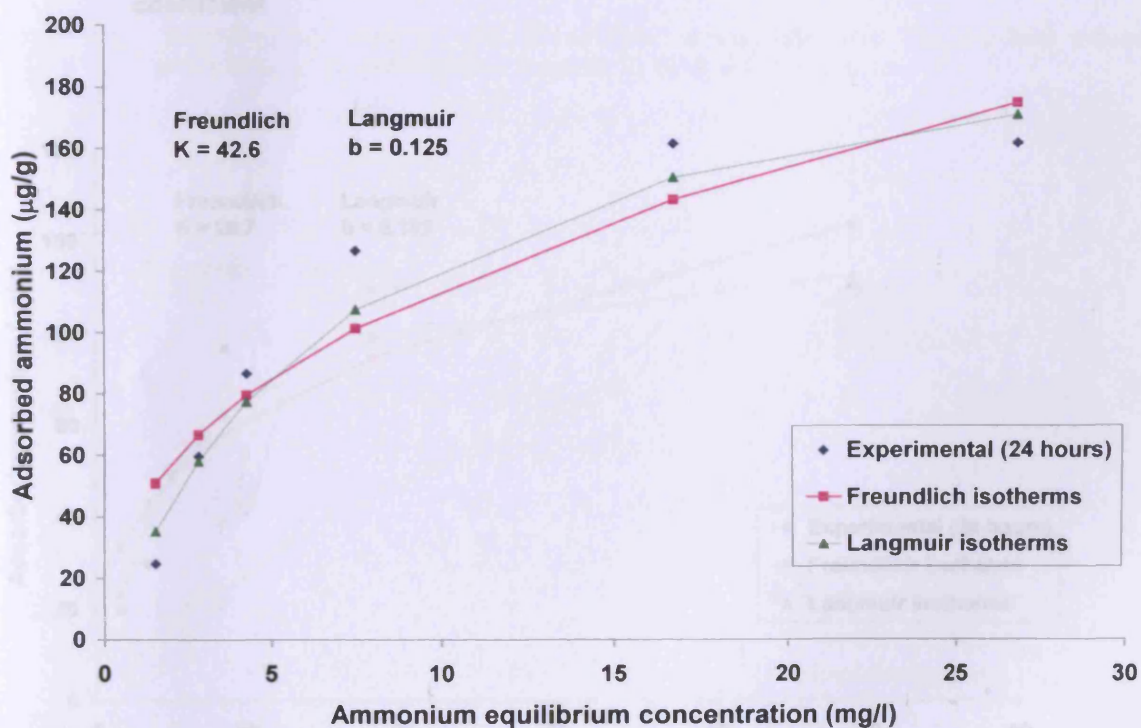


Figure 7.3 Experimental results and theoretical (Langmuir and Freundlich) adsorption isotherms of ammonium for sample 1b₁ in deionised water. b is the Langmuir constant and adsorption coefficient, K is the Freundlich adsorption coefficient,

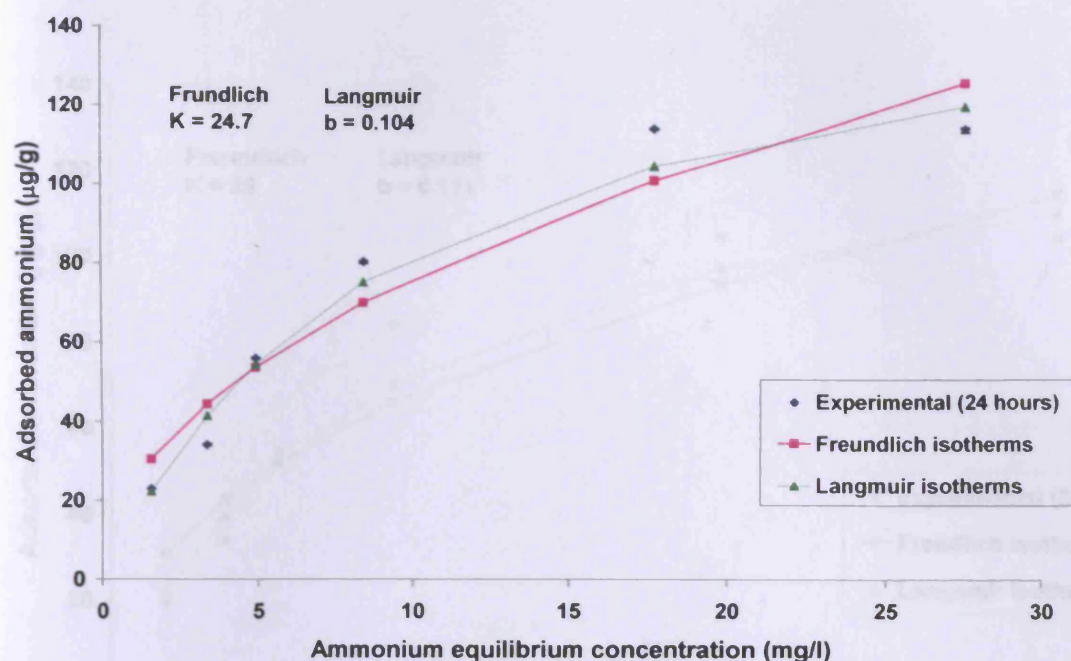


Figure 7.4 Experimental results and theoretical (Langmuir and Freundlich) adsorption isotherms of ammonium for sample 1b₂ in distilled water. b is the Langmuir constant and adsorption coefficient, K is the Freundlich adsorption coefficient

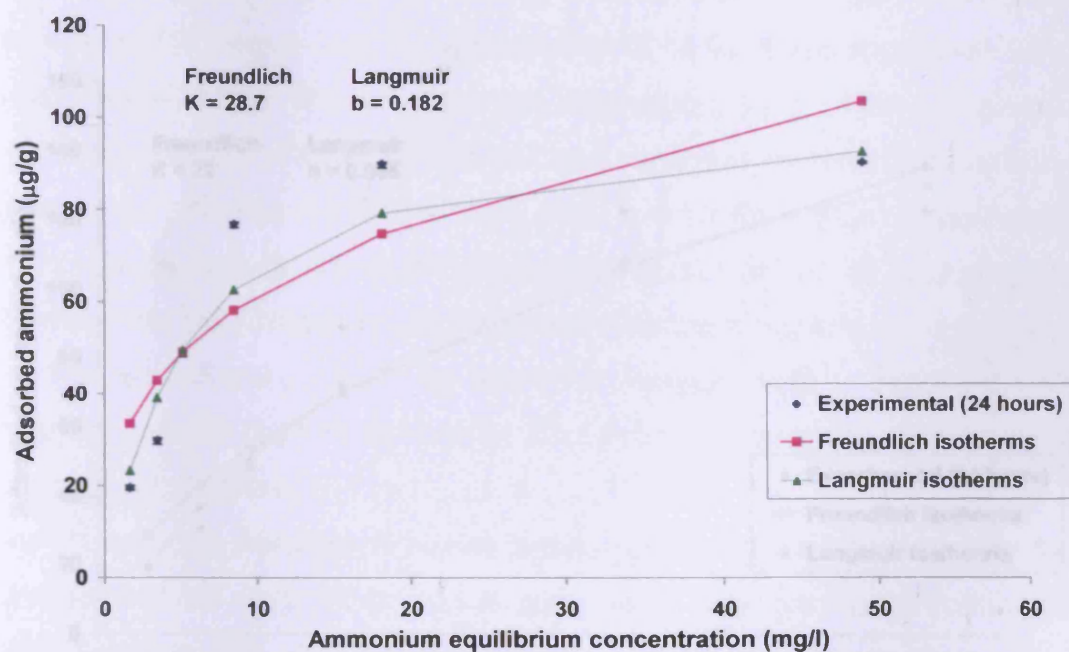


Figure 7.5 Experimental results and theoretical (Langmuir and Freundlich) adsorption isotherms of ammonium for sample 1b₃ in distilled water

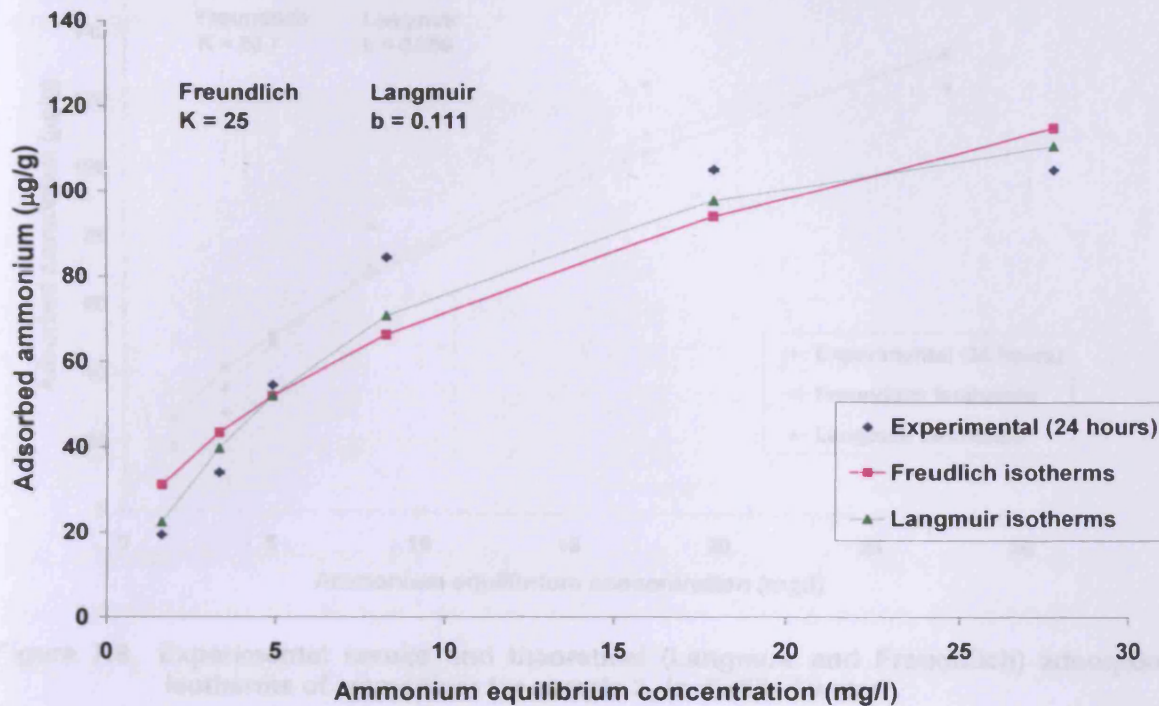


Figure 7.6 Experimental results and theoretical (Langmuir and Freundlich) adsorption isotherms of ammonium for sample 2₁ in distilled water

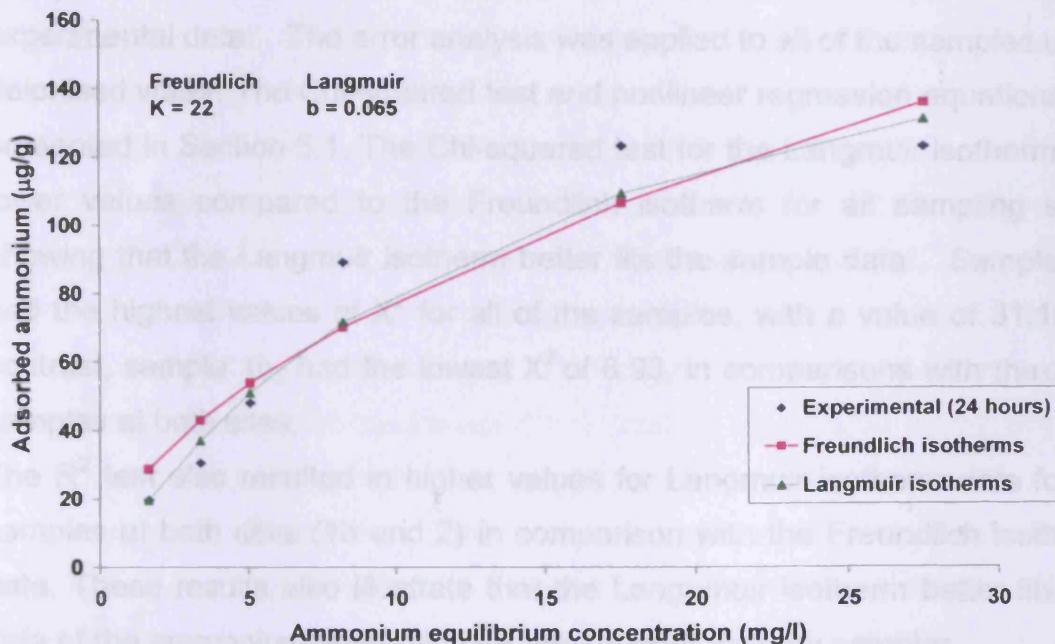


Figure 7.7 Experimental results and theoretical (Langmuir and Freundlich) adsorption isotherms of ammonium for sample 2₂ in distilled water

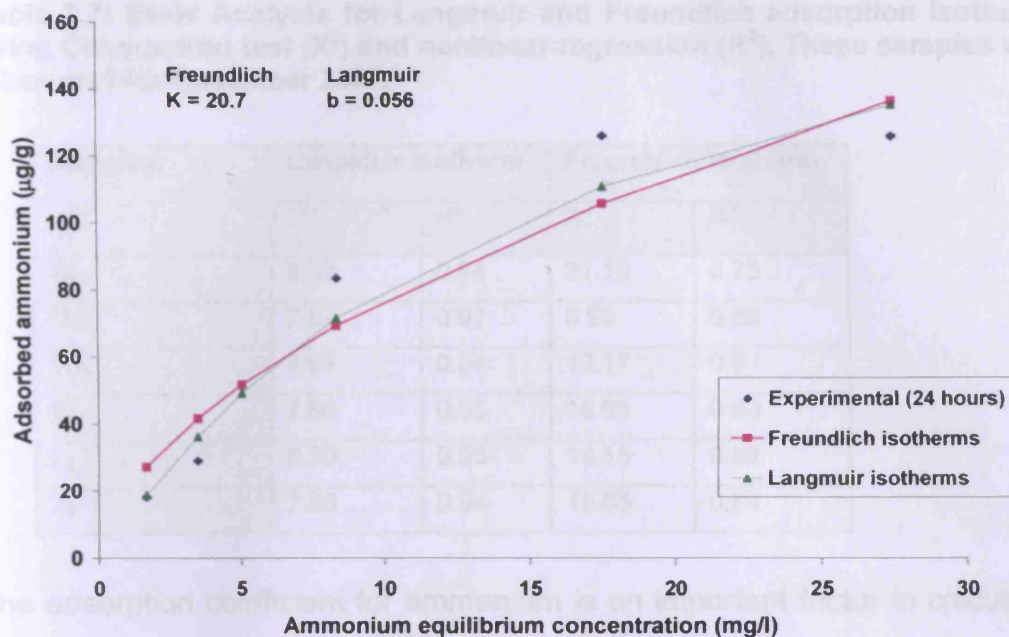


Figure 7.8 Experimental results and theoretical (Langmuir and Freundlich) adsorption isotherms of ammonium for sample 2₃ in distilled water

Table 7.7 shows a summary of the error analysis for the Langmuir and Freundlich adsorption isotherms. The Chi-squared test (X^2) and nonlinear regression (R^2) were used to evaluate the fit of the theoretical data with the experimental data. The error analysis was applied to all of the samples using deionised water. The Chi-squared test and nonlinear regression equations are presented in Section 5.1. The Chi-squared test for the Langmuir isotherm has lower values compared to the Freundlich isotherm for all sampling sites, showing that the Langmuir isotherm better fits the sample data. Sample 1b₁ had the highest values of X^2 for all of the samples, with a value of 31.10. In contrast, sample 1b₂ had the lowest X^2 of 8.93, in comparisons with the other samples at both sites.

The R^2 test also resulted in higher values for Langmuir isotherm data for all samples at both sites (1b and 2) in comparison with the Freundlich isotherm data. These results also illustrate that the Langmuir isotherm better fits the data of the ammonium adsorption for the Loughor Estuary samples.

Table 7.7: Error Analysis for Langmuir and Freundlich adsorption isotherms using Chi-squared test (χ^2) and nonlinear regression (R^2). These samples were taken on 14th December 2007.

Samples	Langmuir isotherm		Freundlich isotherm	
	χ^2	R^2	χ^2	R^2
1b₁	9.30	0.94	31.10	0.75
1b₂	2.87	0.97	8.93	0.88
1b₃	4.99	0.94	13.17	0.81
2₁	7.86	0.95	15.65	0.80
2₂	6.30	0.95	14.15	0.86
2₃	7.80	0.94	15.65	0.84

The adsorption coefficient for ammonium is an important factor in calculating the concentration of nitrogen in the sediments. The formula of ammonium adsorption coefficient of the sediments for the Loughor Estuary is indicated in Section 5.1.

Table 7.8 summarises the relative parameters of ammonium adsorption coefficient, such as the porosity Φ (%), particle density ρ_s (mg/cm³) and total organic carbon (TOC %) and the adsorption coefficient of ammonium (k^*). These parameters are important to calculate the dimensionless adsorption coefficient of ammonium (K) for the sediments of the Loughor Estuary as indicated in the equations presented in Section 5.6.1. The table shows that the values of the dimensionless adsorption coefficient (K) for ammonium ranged from 23.0 to 36.5. The highest dimensionless adsorption coefficient was found in the sediment containing the highest amount of total organic carbon, which was in the sample 2₁ and with values of 36.5 and 4.81% respectively. In contrast the lowest dimensionless adsorption coefficient was found in the sediment samples 1b₃ and 2₃ which contained smallest amounts of total organic carbon. The corresponding adsorption coefficient and TOC values were 23, 23 and 1.53 (%). 1.29 (%) respectively. These results indicate that total organic carbon is an important factor affecting the adsorption of ammonium onto the sediments in the Loughor Estuary. However, the results did not show any influence for other parameters namely Φ and ρ_s .

Table 7.8: Ammonium adsorption coefficients of the Loughor Estuary, its relative parameters and total organic carbon content (TOC). These samples were taken on 14th December 2007.

Parameters	Sampling sites					
	1b ₁	1b ₂	1b ₃	2 ₁	2 ₂	2 ₃
K	34.5	26.2	23.0	36.5	25.7	23.0
Φ	0.58	0.51	0.52	0.43	0.51	0.54
K*(ml/g)	18	10.20	9.3	10.4	10	10.3
ρ_s (g/cm³)	2.65	2.67	2.69	2.65	2.68	2.63
TOC (%)	3.74	2.82	1.53	4.81	1.39	1.29

Figures 7.9 - 7.14 show that the ammonium adsorption by sediments in distilled water were approximately linear within the controlled range of ammonium concentrations considered the laboratory experiments. Correlation coefficient (R^2) values ranged from 0.94 to 0.99 as shown in Table 7.9. Ammonium was used with concentrations varying in the range 2, 4, 6, 8 and 10 mg/l NH_4^+ . Comparatively low concentrations of ammonium were used in this experiment due to the low concentrations of ammonium that were found at sites 1b and 2 on 14th December 2007, with values ranging from 0.089 to 2.35 mg/l. The adsorption formula of ammonium is indicated in Section 5.1.

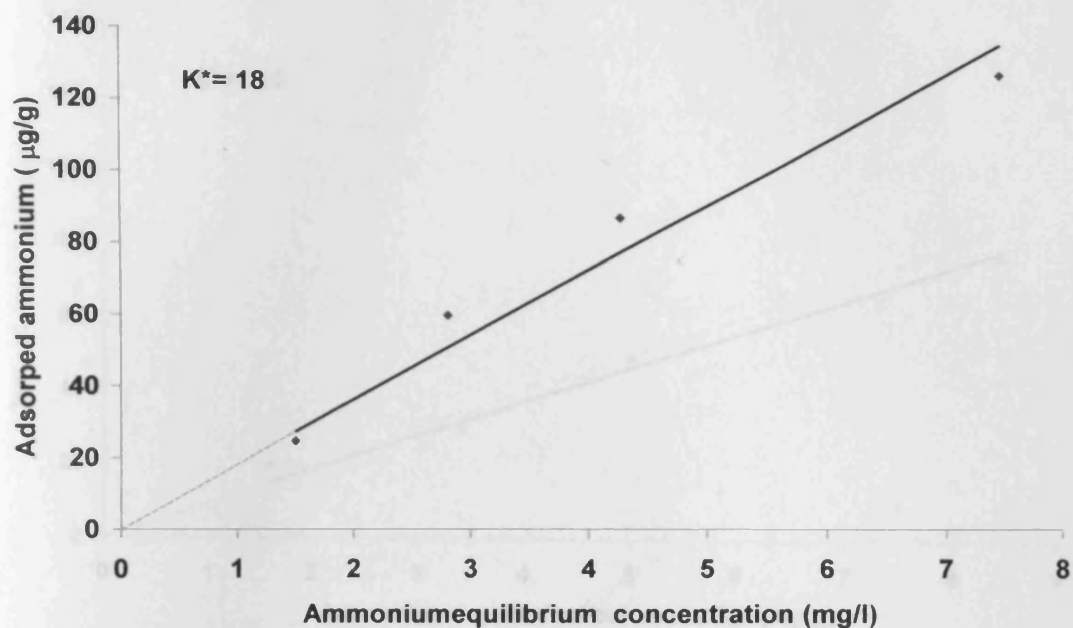


Figure 7.9 Adsorption isotherm of ammonium for Loughor Estuary sediment sample 1b₁, K^* is the slope of the regression line or the adsorption coefficient (ml/g)

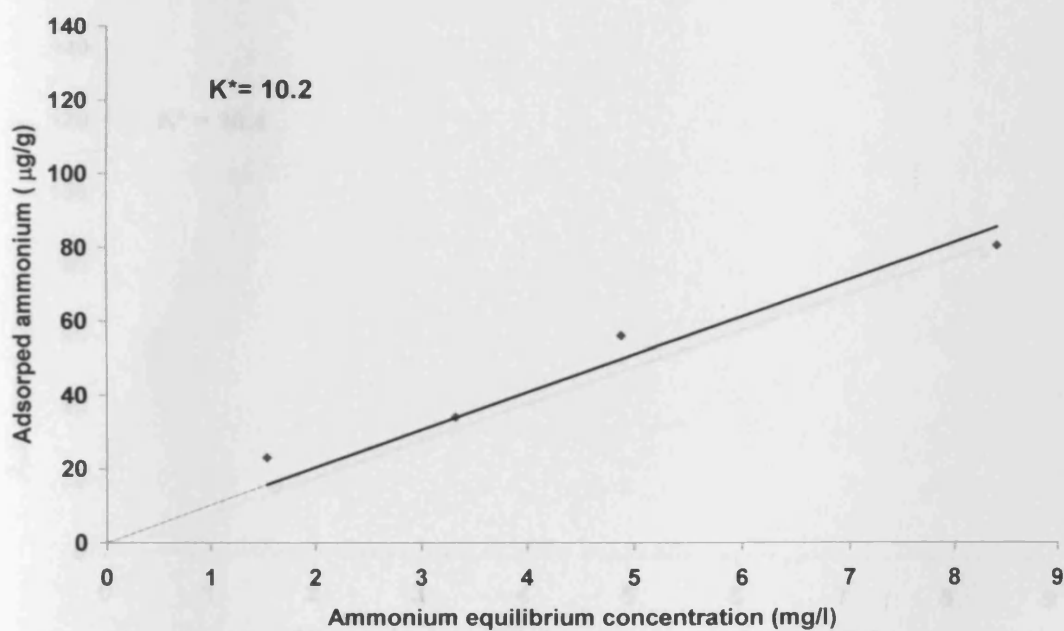


Figure 7.10 Adsorption isotherm of ammonium for Loughor Estuary sediment sample 1b₂

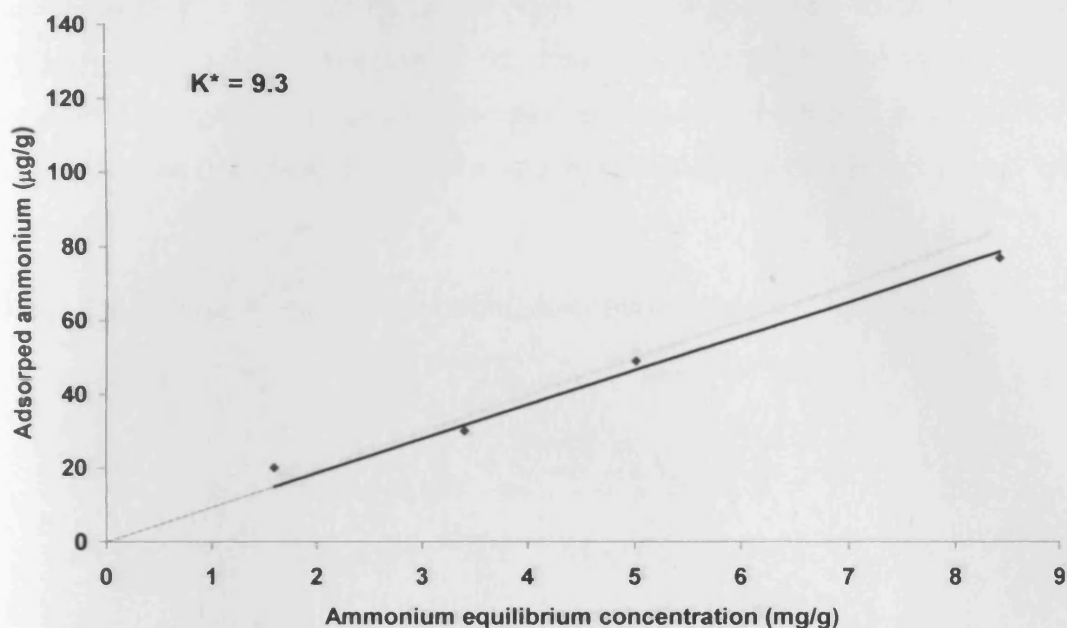


Figure 7.11 Adsorption isotherm of ammonium on sediment for Loughor Estuary sediment sample 1b₃

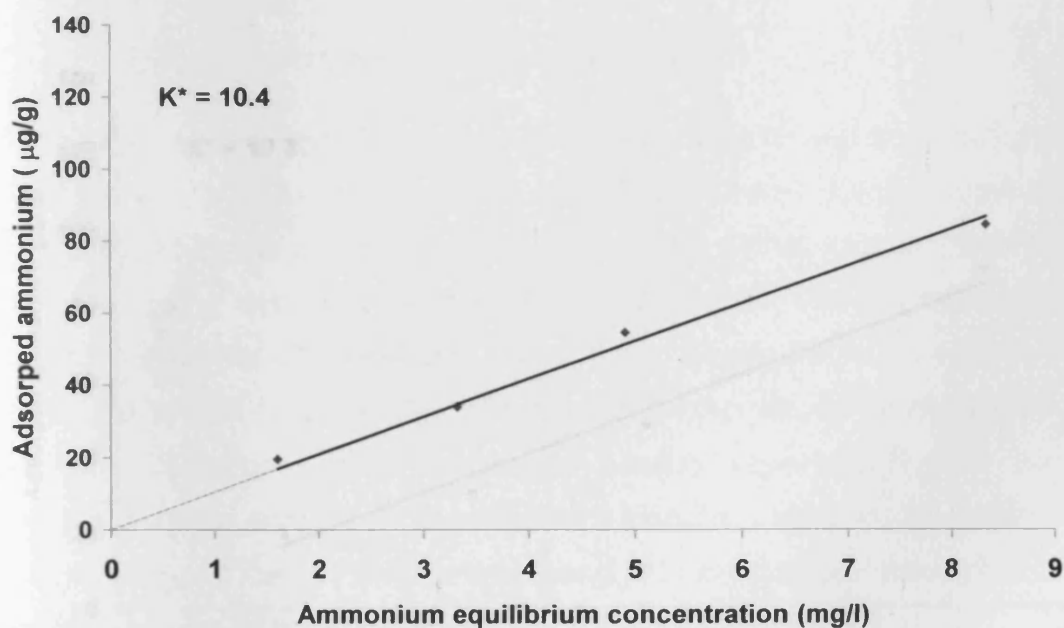


Figure 7.12 Adsorption isotherm of ammonium on sediment for Loughor Estuary sediment sample 2₁

Table 7.1 summarises the parameters K^* and R^2 of the ammonium adsorption isotherms, with the fixed ammonium levels in the sediments being zero. In general, sample 1b₃ had a higher adsorption coefficient among the samples.

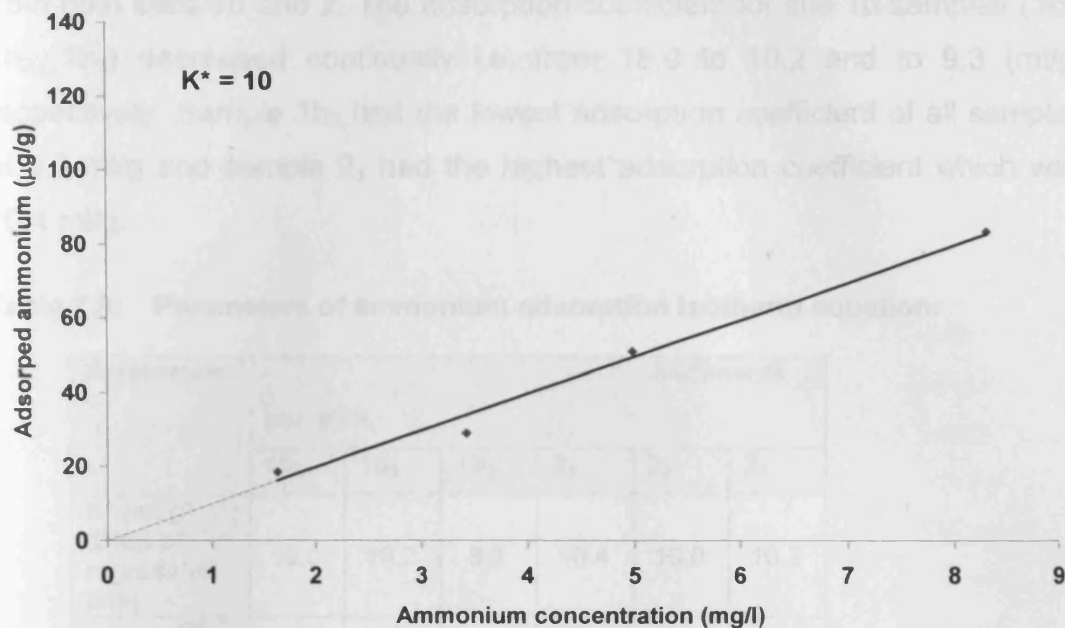


Figure 7.13 Adsorption isotherm of ammonium on sediment for Loughor Estuary sediment sample 2₂

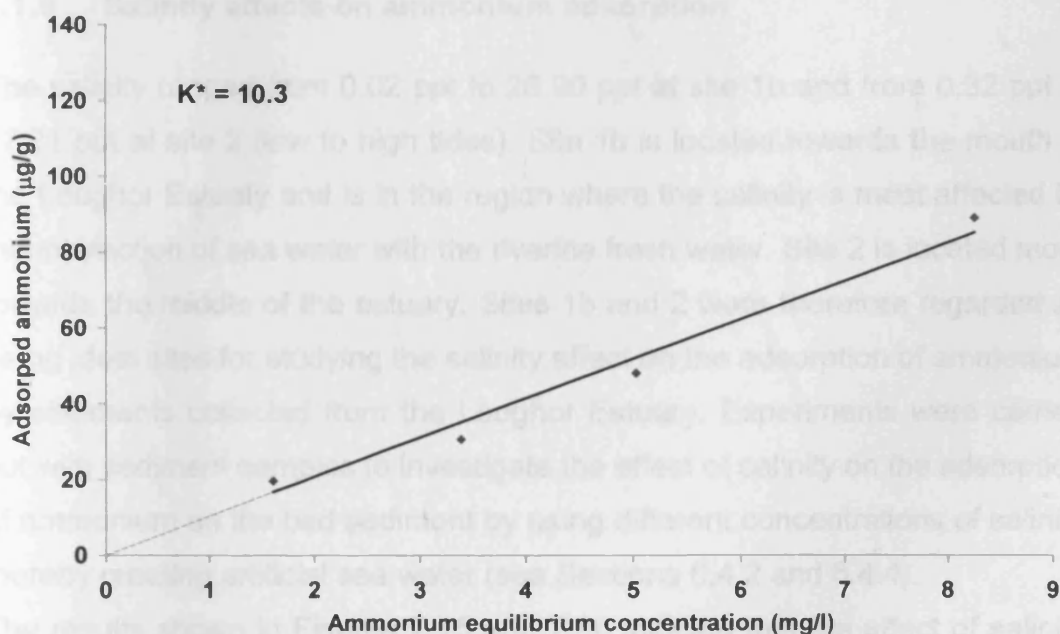


Figure 7.14 Adsorption isotherm of ammonium on sediment for Loughor Estuary sediment sample 2₃

Table 7.9 summarises the parameters K^* and R^2 of the ammonium adsorption isotherms, with the fixed ammonium levels in the sediments being zero. In general, sample 1b₁ had a higher adsorption coefficient among the samples

from both sites 1b and 2. The adsorption coefficient for site 1b samples ($1b_1$, $1b_2$, $1b_3$) decreased continually i.e. from 18.0 to 10.2 and to 9.3 (ml/g) respectively. Sample $1b_3$ had the lowest adsorption coefficient of all samples of 9.3 ml/g and sample 2_1 had the highest adsorption coefficient which was 10.4 ml/g.

Table 7.9: Parameters of ammonium adsorption isotherm equation.

Parameters	Sediments					
	samples					
	$1b_1$	$1b_2$	$1b_3$	2_1	2_2	2_3
K^* (ml/g) (Slop of regression line)	18.0	10.2	9.3	10.4	10.0	10.3
R^2 (correlation coefficient)	0.95	0.94	0.98	0.99	0.98	0.79

7.1.6 Salinity effects on ammonium adsorption

The salinity ranged from 0.02 ppt to 26.90 ppt at site 1b and from 0.32 ppt to 17.21 ppt at site 2 (low to high tides). Site 1b is located towards the mouth of the Loughor Estuary and is in the region where the salinity is most affected by the interaction of sea water with the riverine fresh water. Site 2 is located more towards the middle of the estuary. Sites 1b and 2 were therefore regarded as being ideal sites for studying the salinity affect on the adsorption of ammonium by sediments collected from the Loughor Estuary. Experiments were carried out with sediment samples to investigate the effect of salinity on the adsorption of ammonium on the bed sediment by using different concentrations of salinity thereby creating artificial sea water (see Sections 6.4.2 and 6.4.4).

The results shown in Figures 7.15 and 7.16 indicate that the effect of salinity on ammonium adsorption for samples $1b_1$ and 2_1 decreased gradually with increasing salinity concentrations, with the concentrations considered being: 2, 5, 10, 15, 20 and 25ppt. The ammonium adsorbed was reduced by 27% of its original value, i.e. from 84.5 $\mu\text{g/g}$ to 61.5 mg/g for sample 2_1 between

salinity levels of 0 ppt and 25 ppt. in contrast the reduction for sample 1b₁ was only 14% between salinity levels of 0 ppt and 25 ppt.

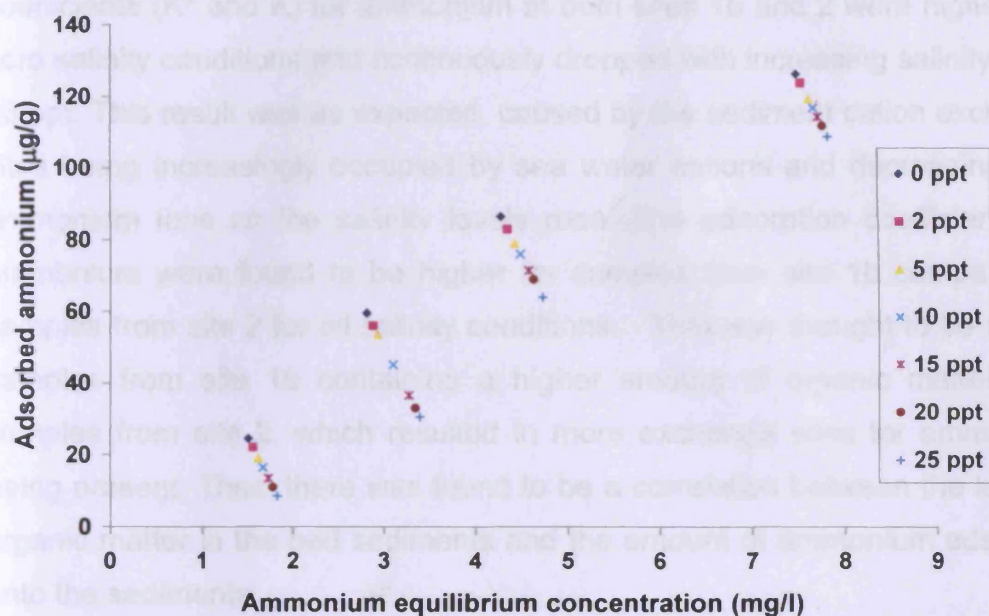


Figure 7.15 Ammonium adsorption for sample 1b₁ from site 1b for varying salinity concentrations

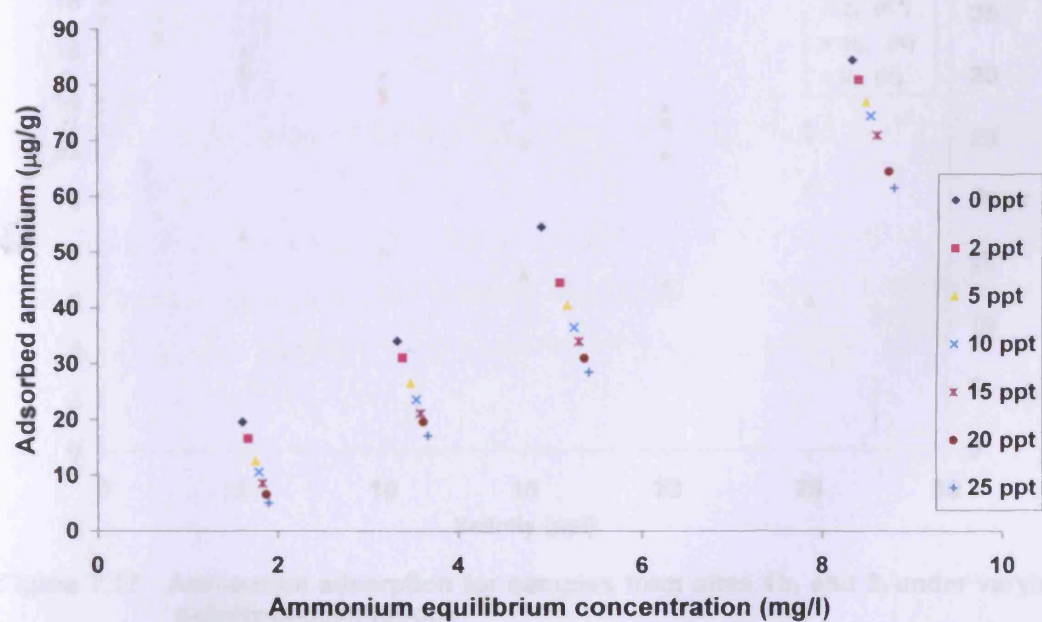


Figure 7.16 Ammonium adsorption for sample 2₁ from site 2 for varying salinity concentrations

The results shown in Figure 7.17 indicate the salinity effect on the adsorption coefficient (K^*) and the dimensionless adsorption coefficient for samples from sites 1b and 2. The results shown in the figure indicate that the adsorption coefficients (K^* and K) for ammonium at both sites 1b and 2 were highest for zero salinity conditions and continuously dropped with increasing salinity up to 25 ppt. This result was as expected, caused by the sediment cation exchange sites being increasingly occupied by sea water cations and decreasingly by ammonium ions as the salinity levels rose. The adsorption coefficients for ammonium were found to be higher for samples from site 1b compared to samples from site 2 for all salinity conditions. This was thought to be due to samples from site 1b containing a higher amount of organic matter than samples from site 2, which resulted in more exchange sites for ammonium being present. Thus, there was found to be a correlation between the level of organic matter in the bed sediments and the amount of ammonium adsorbed onto the sediments.

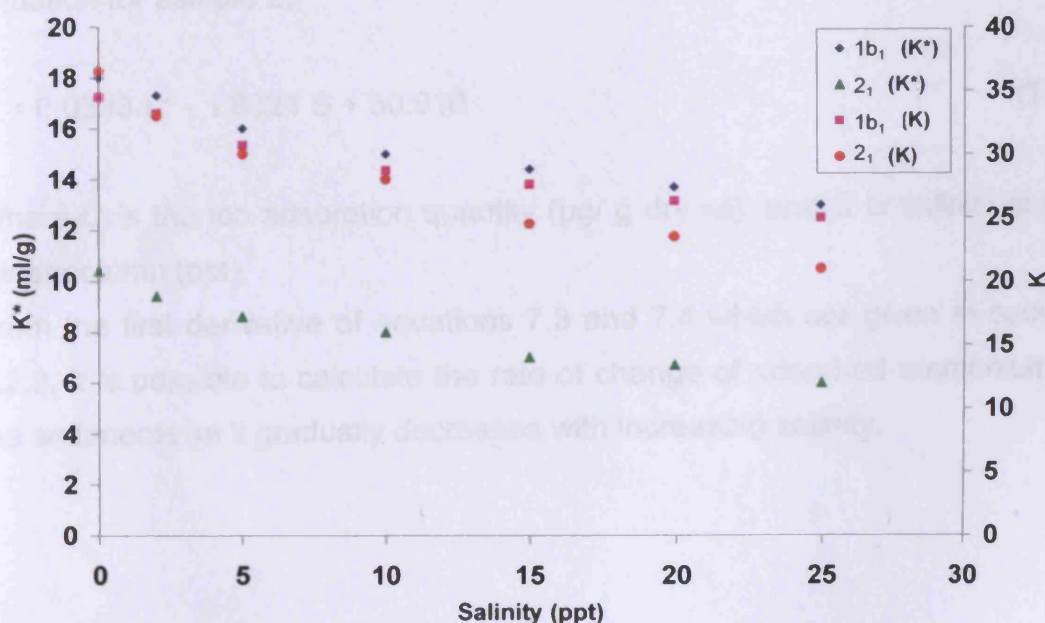


Figure 7.17 Ammonium adsorption for samples from sites 1b₁ and 2₁ under varying salinity concentrations

Experiments were then undertaken with sediment samples to investigate the effects of salinity on the adsorption of ammonium on the bed sediments (see Sections 6.4.2 and 6.4.4). This experiment was based on using the same

ammonium concentration of 6 mg/l in the water column, for samples from sites 1b₁ and 2₁. Figures 7.18 and 7.19 show the difference in the ammonium adsorption under different salinity conditions and based on the same initial ammonium concentration. Equation 7.1 relates to site 1b for sample 1b₁ and Equation 7.2 refers to site 2 for sample 2₁. The ammonium adsorption amount in the sediments for samples 1b₁ and 2₁ gradually decreased with increasing Salinity levels, varying from 86.5 µg/g at 0 ppt to 64 µg/g at 25 ppt and 45.5 µg/g at 0 ppt to 28.5 µg/g at 25 ppt respectively, and was found to be best represented by the following equations: The equations below present the effect of salinity on the ammonium adsorption on the sediment samples for the salinities range (2, 5, 10, 15, 20, 25 ppt).

Equation for sample 1b₁:

$$Q = 0.0098 S^2 - 1.0756 S + 85.477 \quad (7.1)$$

Equation for sample 2₁:

$$Q = 0.0393 S^2 - 1.8321 S + 50.916 \quad (7.2)$$

Where Q is the ion adsorption quantity (µg/ g dry wt); and S is salinity in the water column (ppt).

From the first derivative of equations 7.3 and 7.4 which are given in section 7.2.3, it is possible to calculate the rate of change of adsorbed ammonium in the sediments as it gradually decreases with increasing salinity.

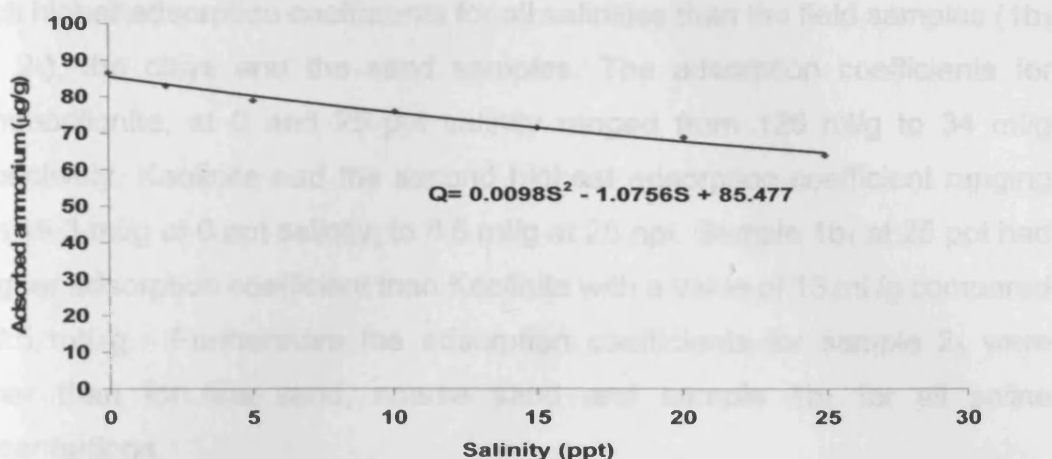


Figure 7.18 Salinity dependent ammonium adsorption in the sediments for sample 1b₁, Q (µg/ g dry wt); S (ppt)

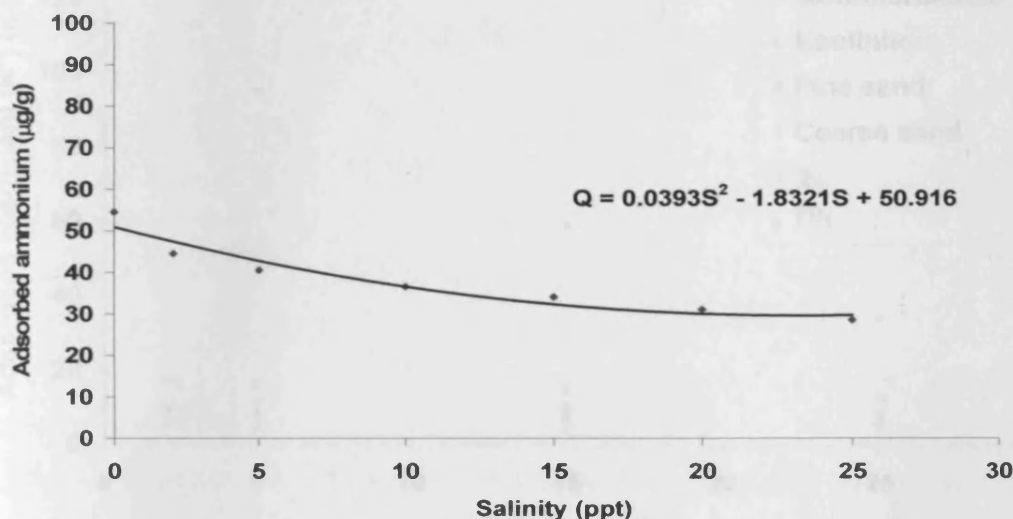


Figure 7.19 Salinity dependent ammonium adsorption in the sediments for sample 2₁, Q (µg/ g dry wt); S (ppt)

7.1.7 Comparison of adsorption coefficients of field data and clean clays (Montmorillonite, Kaolinite) and sand (fine and coarse)

Figure 7.20 shows the adsorption coefficient of the field data, taken at both sites 1b and 2 and for clean clays (i.e. Montmorillonite and Kaolinite) and sand both (fine and coarse) under different salinity conditions. For all samples it can be seen that the adsorption coefficients decreased gradually with increasing salinity concentrations. Also, the results indicated that Montmorillonite had

much higher adsorption coefficients for all salinities than the field samples ($1b_1$ and 2_1), the clays and the sand samples. The adsorption coefficients for Montmorillonite, at 0 and 25 ppt salinity ranged from 126 ml/g to 34 ml/g respectively. Kaolinite had the second highest adsorption coefficient ranging from 19.3 ml/g at 0 ppt salinity, to 8.5 ml/g at 25 ppt. Sample $1b_1$ at 25 ppt had a higher adsorption coefficient than Kaolinite with a value of 13 ml/g compared to 8.5 ml/g. Furthermore the adsorption coefficients for sample 2_1 were higher than for fine sand, coarse sand and sample $1b_1$ for all saline concentrations.

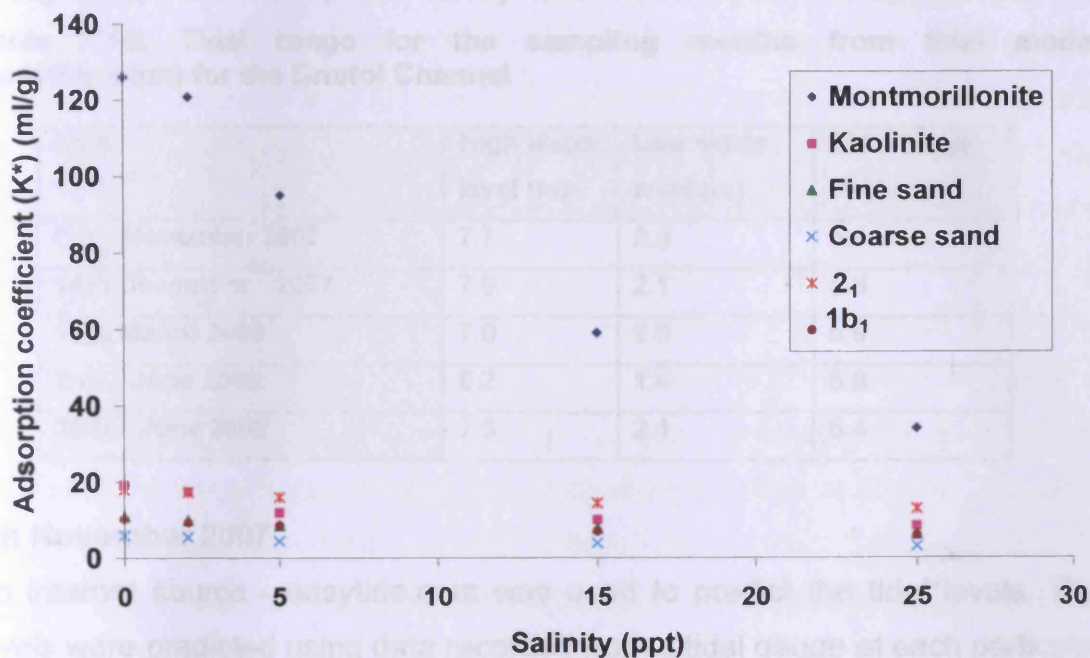


Figure 7.20 Comparison of adsorption coefficients of field samples $1b_1$ & 2_1 and clean clays (Montmorillonite & Kaolinite) and sand (fine and coarse)

7.1.8 Field data from the Loughor Estuary

As mentioned in section 7.1, The Loughor Estuary, located in the Bristol Channel in the UK, is made up of a land–sea transitional area which is an environmentally vulnerable zone.

Water and bed sediment samples were obtained from four cross-sections along the Loughor Estuary as indicated in Figure 7.2. This sampling programme ran from 7th November 2007 until 30th June 2008. Sediments and

water samples were collected on 7th November 2007, 14th December 2007, 13th March 2008, 2nd June and 30th June 2008.

The admiralty chart number 1179 for the Bristol Channel was used to indicate heights of spring and neap tides using the closest location to the Loughor Estuary namely, Barry Port. The tidal range for spring and neap tides at this location varies between 7.5m and 3.6m above chart datum, respectively. High and low water levels and the tidal range for each of the sampling dates are shown in Table 7.10. This section presents the physical and biochemical parameters of the water and sediment samples collected during rising and falling tides, with results presented by date and shown in Tables 7.11 -7.37.

Table 7.10: Tidal range for the sampling months from tidal model (easytide.com) for the Bristol Channel

Date	High water level (m)	Low water level (m)	Tidal range (m)
6th November 2007	7.7	2.3	5.4
14th December 2007	7.9	2.1	5.8
13th March 2008	7.9	2.0	5.9
2nd June 2008	8.2	1.4	6.8
30th June 2008	7.5	2.1	5.4

6th November 2007

An internet source - easytide.com was used to predict the tidal levels. The levels were predicted using data recorded from a tidal gauge at each particular location. The tidal predictions for 6th November 2007 show that the tide was close to a neap tide, which ranged between 2.3m at 10:10am and 7.7m at 4:08pm (See Table 7.10), and sampling started 1 hour 50 minutes after low tide, covering as incoming tide event. Tables 7.11 - 7.16 show the results of the water samples collected on this day for sites 1a, 1b, 2 and 3. Salinity was highest at 26.9 ppt at 4:00 pm at site 1b during high tide and lowest at 0.69 ppt at 12:00 pm at site 2 during low tide. Site 3, located in the village of Pontarddulais, upstream in the estuary, represents the input of nutrients via the Loughor river and an outfall from sewage treatment works STWs (Pontarddulais), located 6.86 km from site 3 (see Figure 6.2). Site 3 had the lowest salinity of 0.14 ppt, and was located above the tidal limit during this

nearly neap tide event, where it was not influenced by sea water ions. The pH of the water samples ranged from 6.9 to 7.3, i.e. approximately neutral. The water temperature of the samples ranged from 14.3 °C to 16.5 °C.

Ammonium, nitrate and nitrite concentrations in the water column were determined according to the methods described in Sections 6.4.5 and 6.4.6.2. Ammonium in the water column was found to be zero at sites 1a, 2 and 3 at low and high tides. Ammonium was found at site 1b in samples collected at 2:00 pm and 3:00 pm at 0.260 mg/l and 0.086 mg/l, coinciding with salinities of 18.31 ppt and 16.62 ppt, respectively. These ammonium concentrations only occurred half way through the incoming tide event. It was assumed that the source of pollution was from the Llanelli STWs located 1.9 km downstream from sampling point 1b. The highest nitrate concentrations were measured at sites 1b at 2 pm and 3 at 1:00 pm at 5.3 mg/l and 5.18 mg/l respectively. At site 1b₁ this increase in nitrate could be the result of release of nitrate into the water column from the sediment with increasing concentrations of salinity ions present in the water column. In addition, this high concentration of nitrate at site 1b came from downstream, hence outfall from the sewage treatment works between sites 1a and 1b, is the likely source of ammonium and nitrate. The higher concentration at site 3 of 5.18 mg/l did not reach site 2, which might be due to dilution effects, or because of attachment to the sediment. Dissolved inorganic nitrogen ($\text{DIN} = \text{NH}_4^+ + \text{NO}_3^- + \text{NO}_2^-$) ranged from 0.002 mg/l to 5.56 mg/l. DIN is dominated by nitrate concentrations and was highest at site 1b at 2:00 pm at 5.56 mg/l.

Table 7.11: Physical and biochemical water parameters measured on 6th November 2007 (LW, 10:10am, 2.3m; HW, 4:08pm, 7.7m) at site 1a


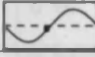
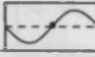
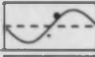
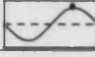
Site	Sampling time (GMT)	Tidal cycle	Salinity (ppt)	pH	Ammonium (NH_4^+) (mg/l)	Nitrate (NO_3^-) (mg/l)	Nitrite (NO_2^-) (mg/l)	Dissolved inorganic nitrogen (DIN) (mg/l)
1a	12:00		9.88	6.8	0	2.210	2	4.210
	13:00		8.79	7.3	0	1.660	0	1.660
	14:00		10.60	6.9	0	0.550	0	0.550
	15:00		17.21	7.0	0	0	0	0
	16:00		24.60	7.0	0	0.006	0.029	0.035

Table 7.12: Physical and biochemical water parameters measured on 6th November 2007 (LW, 10:10am, 2.3m; HW, 4:08pm, 7.7m) at site 1b

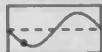
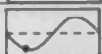
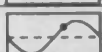
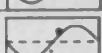
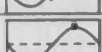
Site	Sampling time (GMT)	Tidal cycle	Salinity (ppt)	pH	Ammonium (NH ₄ ⁺) (mg/l)	Nitrate (NO ₃ ⁻) (mg/l)	Nitrite (NO ₂ ⁻) (mg/l)	Dissolved inorganic nitrogen (DIN) (mg/l)
1b	12:00		4.20	7.0	0	0	0	0
	13:00		3.60	7.0	0	0	0.009	0.009
	14:00		18.31	6.7	0.260	5.300	0	5.560
	15:00		16.62	7.2	0.086	1.200	0.007	1.467
	16:00		26.90	7.0	0	0.006	0.002	0.008

Table 7.13: Physical and biochemical water parameters measured on 6th November 2007, (LW, 10:10am, 2.3m; HW, 4:08pm, 7.7m) at site 2

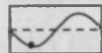
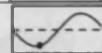
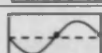
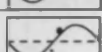
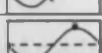
Site	Sampling time (GMT)	Tidal cycle	Salinity (ppt)	pH	Ammonium (NH ₄ ⁺) (mg/l)	Nitrate (NO ₃ ⁻) (mg/l)	Nitrite (NO ₂ ⁻) (mg/l)	Dissolved inorganic nitrogen (DIN) (mg/l)
2	12:00		0.69	7.0	0	0.55	0	0.55
	13:00		1.16	6.8	0	0	0.002	0.002
	14:00		10.60	7.0	0	3.32	0	3.320
	15:00		17.21	7.0	0	2.76	0.550	3.310
	16:00		24.60	7.0	0	2.21	0.004	2.214

Table 7.14: Physical and biochemical water parameters measured on 6th November 2007 (LW, 10:10am, 2.3m; HW, 4:08pm, 7.7m) at site 3

Site	Sampling time (GMT)	Salinity (ppt)	pH	Ammonium (NH ₄ ⁺) (mg/l)	Nitrate (NO ₃ ⁻) (mg/l)	Nitrite (NO ₂ ⁻) (mg/l)	Dissolved Inorganic nitrogen (DIN) (mg/l)
3	12:00	0.14	7.0	0	2.75	0	2.75
	13:00	0.14	6.8	0	5.18	0	5.18
	14:00	0.14	7.0	0	3.32	0	3.32
	15:00	0.14	7.0	0	1.10	0	1.10

Tables 7.15 and 7.16 show the physical and biochemical parameters of the sediments. Wet sediments were collected from depths of 0–3 cm at cross-sections of two sites (1b & 2) close to the water's edge, occasionally at high tide when this region was in the water (See Figure 6.2). It was found that the amount of ammonium adsorbed did not differ significantly between analytical methods using dry and wet sediment samples for all field data (See table 7.15 for results and differences). In this study, the results of the wet sediments will be used in the analysis of results according to Raaphorst et al. (1996) and Hou et al. (2003).

The measurements of ammonium adsorption on the bed sediments were obtained by potassium chloride (KCl) extraction according to the method described by Hou et al. (2003) and Abdulgawad et al. (2008) as detailed in Section 6.4.1. The amount of ammonium adsorption on the sediment was found to be higher in the samples collected at low tide towards the centre of the channel than at high tide when the samples were collected further away from the channel centre. In samples from site 2 at low tide and with salinity concentrations between 0.69 and 1.16 ppt, the amount of adsorbed ammonium was 30.4 µg/g and 24.3 µg/g, respectively. At site 1b and high tide, however, at a salinity concentration of 26.90 ppt, the amount of ammonium adsorbed on the sediment was only 2.4 µg/g.

The results of total carbon and organic carbon of the sediment samples for site 1b ranged from 0.92% to 7.79% and from 0.45% to 4.26% respectively, and for site 2 ranged from 2.40% to 11.94 % for total carbon and from 1.40% to 3.82% (organic carbon) of the total sample mass. This indicates that total carbon and organic carbon were higher for the samples that were collected at high tide than those collected during low tide. The total carbon content was determined by combustion, using a Leco Organic Carbon analyzer and the inorganic carbon (IC) content was determined after acidification with phosphoric acid, and was obtained using a SHIMADZU analyzer (as described in Chapter 6). The organic carbon content was evaluated from the difference between the two measured quantities. Details of these methods were given in Section 6.3.1.2. The median grain size decreased gradually with increasing distance from the channel centre at both sites 1b and 2. Maximum grain size was found

at low tide at 12:00 pm for both sites 1b and 2 at 170 μm . Minimum grain size was found at site 1b at 4:00 pm at 65 μm which was at high tide.

Table 7.15: Physical and biochemical sediment parameters measured on 6th November 2007 (LW, 10:10am, 2.3m; HW, 4:08pm, 7.7m) at site 1b



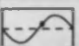
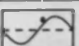
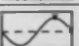
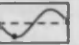
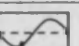
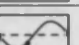
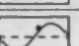
Site	Sampling time (GMT)	Tidal cycle	Salinity (ppt)	Ammonium (NH_4^+) (mg/l)	Adsorbed Ammonium (NH_4^+) ($\mu\text{g/g}$)		Total organic carbon (%)	Total carbon (%)	Median Grain Size (μm)
					Wet Sedi-ments	Dry Sedi-ments			
1b	12:00		4.20	0	23.50	21.77	0.45	0.92	170
	13:00		3.60	0	26.20	24.93	0.79	2.09	125
	14:00		18.31	0	7.30	6.88	3.75	4.61	120
	15:00		16.62	0	5.40	4.98	2.82	3.63	88
	16:00		26.90	0	2.40	2.00	4.26	7.79	65

Table 7.16: Physical and biochemical sediment parameters measured on 6th November 2007 (LW, 10:10am, 2.3m; HW, 4:08pm, 7.7m) at site 2

Site	Sampling time (GMT)	Tidal cycle	Salinity (ppt)	Ammonium (NH_4^+) (mg/l)	Adsorbed Ammonium (NH_4^+) ($\mu\text{g/g}$)		Total organic carbon (%)	Total carbon (%)	Median grain size (μm)
					Wet Sedi-ments	Dry Sedi-ments			
2	12:00		0.69	0	30.4	27.20	1.40	2.40	170
	13:00		1.16	0	24.3	21.23	1.53	2.55	165
	14:00		10.60	0	12.7	11.00	2.15	3.21	160
	15:00		17.21	0	8.5	7.65	3.82	11.94	145

14th December 2007

The tidal predictions for 14th December show that the tide was above neap tide conditions with tides ranging between 7.9 m at 8:48 am and 2.1 m at 3:12 pm (See Table 7.10). Sampling started 42 minutes after high tide conditions at 9.30 am, covering an outgoing tide. Tables 7.17 to 7.20 present the results of water samples collected on this day for sites 1a, 1b, 2, and 3.

The highest salinity measured was 21.67 ppt at 9:30 am at site 1a during high tide and the lowest salinity at 0.02 ppt was found at 3:00 pm at site 1b during

low tide. The pH of the water samples ranged from 6.7 to 7.3, i.e. approximately neutral. The temperatures of the water samples ranged from 6.3 °C to 7.8 °C.

The results indicate that the ammonium concentrations in the water column were zero at site 1a for all samples, and ranged from 0 to 0.531 mg/l at site 1b for low and high tide conditions, respectively. Highest NH_4^+ concentrations occurred at site 2 at 2.35 mg/l 2 hours after high tide at a salinity of 1.20 ppt and NH_4^+ was 0 mg/l at 9:30 am at high tide with salinity of 8.91 ppt, and 0 mg/l at 15:00 pm at low tide, respectively. These high concentrations of NH_4^+ could be due to the agricultural activities this section of the river (with farms directly next to the channel without fences) or due to the STWs outfalls along the Loughor or have come with the river input (see Site 3 has similar NH_4^+ concentrations). Site 3 was located above the tidal limit and would not be influenced by raising and falling tides. At site 3 ammonium concentrations ranged from 0 to 2.98 mg/l, due to input through the river and an outfall from a STWs (Pontarddulais) coming from upstream. These were the highest nitrate concentrations found along in the upper end of the estuary, i.e. sites 2, and 3. Nitrate concentrations further downstream in the estuary were lower at high tide than at low tide and ranged from 2.22 mg/l to 6.13 mg/l at site 1a and from 2.76 mg/l to 7.74 mg/l at site 1b, respectively, due to the dilution effect of low nitrate marine water inputs coming in during high tide. The highest nitrite concentration of 10.23 mg/l were found at site 1a and are likely to be due to the outfall of the Llanelli STWs which is located between sites 1a and 1b. They were found during outgoing tide conditions at lowest salinity (lowest dilution), in the water samples, which were higher at low tide than at high tide and ranged from 10.23 mg/l to 2.52 mg/l respectively. These concentrations of both nitrate and nitrite indicate that the nitrification rate must be high in the estuary at this time of the year, especially at site 1b and not just released from the sediment. This could potentially be the result of inputs from outfall of the Llanelli STWs but more likely results from diffuse source pollution can caused by agricultural across the catchments or from the sediment. DIN was dominated by nitrate and nitrite and ranged from 3.22 mg/l to 16.36 mg/l, which were the highest concentrations of all the dates where samples were collected and surveyed during the field programme. Overall, the highest concentrations were found at

sites 1a and 2 with values being generally high at site 1b throughout this falling tide.

Table 7.17: Physical and biochemical water parameters measured on 14th December 2007 (HW, 8:48am, 7.9m; LW, 3:12pm, 2.1m) at site 1a

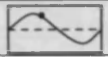
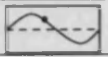
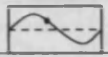
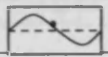
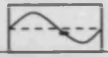
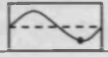
Site	Sampling time (GMT)	Tidal cycle	Salinity (ppt)	pH	Ammonium (NH_4^+) (mg/l)	Nitrate (NO_3^-) (mg/l)	Nitrite (NO_2^-) (mg/l)	Dissolved inorganic nitrogen (DIN) (mg/l)
1a	9:30		21.67	7.0	0	3.22	0	3.22
	11:00		19.84	6.7	0	3.01	2.52	5.53
	12:00		14.05	6.9	0	2.22	5.43	7.65
	13:00		10.08	7.0	0	2.32	7.40	9.72
	14:00		5.72	7.2	0	4.27	8.60	12.87
	15:00		3.00	7.2	0	6.13	10.23	16.36

Table 7.18: Physical and biochemical water parameters measured on 14th December 2007 (HW, 8:48am, 7.9m; LW, 3:12pm, 2.1m) at site 1b

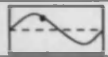
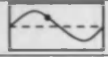
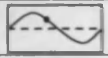
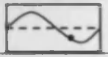
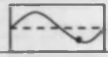
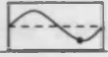
Site	Sampling time (GMT)	Tidal cycle	Salinity (ppt)	pH	Ammonium (NH_4^+) (mg/l)	Nitrate (NO_3^-) (mg/l)	Nitrite (NO_2^-) (mg/l)	Dissolved inorganic nitrogen (DIN) (mg/l)
1b	9:30		20.56	6.7	0.531	5.52	6.43	15.70
	11:00		13.37	6.8	0.351	3.56	6.22	10.13
	12:00		11.27	7.2	0.152	3.32	5.12	8.59
	13:00		3.32	7.4	0.089	2.76	0.61	3.46
	14:00		3.53	7.3	0	6.08	5.90	11.98
	15:00		0.02	7.5	0	7.74	7.11	14.85

Table 7.19: Physical and biochemical water parameters measured on 14th December 2007 (HW, 8:48am, 7.9m; LW, 3:12pm, 2.1m) at site 2

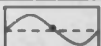
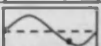
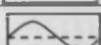
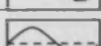
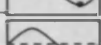
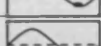
Site	Sampling time (GMT)	Tidal cycle	Salinity (ppt)	pH	Ammonium (NH ₄ ⁺) (mg/l)	Nitrate (NO ₃ ⁻) (mg/l)	Nitrite (NO ₂ ⁻) (mg/l)	Dissolved inorganic nitrogen (DIN) (mg/l)
2	9:30		8.91	7.2	0	2.21	1.12	3.33
	11:00		1.20	7.6	2.35	6.08	3.93	10.01
	12:00		1.10	7.5	2.10	4.36	4.33	8.69
	13:00		0.32	7.3	1.24	5.53	6.18	11.71
	14:00		0.39	7.3	1.26	7.18	6.04	13.22
	15:00		0.42	7.2	0	7.74	6.00	13.74

Table 7.20: Physical and biochemical water parameters measured on 14th December 2007, (HW, 8:48am, 7.9m; LW, 3:12pm, 2.1m) at site 3

Site	Sampling time (GMT)	Salinity (ppt)	pH	Ammonium (NH ₄ ⁺) (mg/l)	Nitrate (NO ₃ ⁻) (mg/l)	Nitrite (NO ₂ ⁻) (mg/l)	Dissolved inorganic nitrogen (DIN) (mg/l)
3	9:30	0.1	7.3	2.78	5.53	0.56	8.31
	11:00	0.1	7.2	2.65	6.63	0.51	7.14
	12:00	0.1	7.2	0	4.42	1.12	5.54
	13:00	0.1	7.3	0	4.52	0	4.52
	14:00	0.1	7.3	2.98	4.97	0.44	5.41
	15:00	0.1	7.2	0	3.82	0.35	4.17

Tables 7.21 and 7.22 present the physical and biochemical parameters of the sediments that were measured during outgoing tide. Wet sediment was collected next to the water's edge. The results indicate that the amount of ammonium adsorption was much lower at both sites 1b and 2 than on 7th November. Results of analysis of wet and dry samples were comparable again. The amount of ammonium adsorption was very low and ranged between 0.001 mg/l to 0.002 mg/l.

Total carbon in the sediment samples from sites 1b and 2 ranged from 2.63% to 8.32% and 1.33% to 9.32%, respectively. Total organic carbon for the sediment samples from sites 1b and 2 ranged from 0.65% to 4.81% and 1.29% to 5.23%, respectively. Median grain sizes for both sites 1b and 2 ranged from 90 μm to 155 μm , again with the smaller grain sizes occurring towards the centre of the channel; but this sorting effect of sediment sizes was less pronounced than on 7th November when the median sediment size ranged from 65 μm to 170 μm for both sites 1b and 2 at low and high tide respectively.

Table 7.21: Physical and biochemical sediment parameters measured at site 1b on 14th December 2007 (HW, 8:48am, 7.9m; LW, 3:12pm, 2.1m)

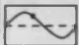
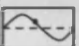
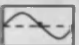
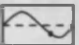
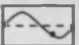
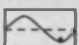
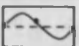
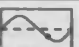
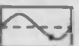
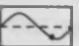
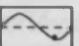
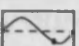
Site	Sampling time (GMT)	Tidal cycle	Salinity (ppt)	Ammonium (NH_4^+) (mg/l)	Adsorbed Ammonium (NH_4^+) ($\mu\text{g/g}$)		Total organic carbon (%)	Total carbon (%)	Median grain size (μm)
					Wet Sedi-ments	Dry Sedi-ments			
1b	9:30		20.56	0.612	0.000	0.000	4.81	5.19	150
	11:00		13.37	0.363	0.001	0.000	3.74	4.10	125
	12:00		11.27	0.198	0.002	0.001	2.82	2.92	90
	13:00		3.32	0.066	0.001	0.001	0.65	2.63	133
	14:00		3.53	0.002	0.000	0.000	3.46	7.79	131
	15:00		0.02	0	0.000	0.001	4.32	8.32	141

Table 7.22: Physical and biochemical sediment parameters measured at site 2 On 14th December 2007 (HW 8:48am, 7.9m; LW 3:12pm, 2.1m)

Site	Sampling time (GMT)	Tidal cycle	Salinity (ppt)	Ammonium (NH_4^+) (mg/l)	Adsorbed Ammonium (NH_4^+) ($\mu\text{g/g}$)		Total carbon (%)	Total organic carbon (%)	Median grain size (μm)
					Wet Sedi-ments	Dry Sedi-ments			
2	9:30		8.91	0	0.001	0.001	2.31	1.53	150
	11:00		1.20	2.21	0.000	0.001	1.60	1.39	155
	12:00		1.10	1.83	0.000	0.000	1.33	1.29	130
	13:00		0.32	1.16	0.001	0.000	5.63	4.03	137
	14:00		0.39	0.98	0.002	0.001	6.79	3.41	135
	15:00		0.42	0	0.000	0.001	9.32	5.23	139

13th March 2008

The tidal predictions for 13th March 2008 show that the tide was above neap tide which ranged between 7.9 m at 9:58 am and 2.0 m at 4:14 pm (see Table 7.10). Tables 7.23 to 7.25 present the results of water samples that were collected on this day for sites 1a, 1b and 3. Data collection from site 2 was cancelled due to the data of nutrient and sediment analysis measurements showing that there was not much difference between sites 1b and site 2. In addition site 2 is located in the muddy and quicksand area thus it was deemed unsafe to collect samples from it. The highest salinity of sites 1a and 1b was 24.44 ppt at 10:00 am at site 1a during high tide and lowest salinity was 3.03 ppt at site 1b at 3:00 pm. Site 3 was above the tidal limit for this tide. The pH of the water samples ranged from 6.7 to 7.8. The temperature of water samples ranged from 8.5 °C to 10 °C.

Sample collection commenced at the start of the outgoing tide. Table 7.23 indicates that ammonium concentrations for site 1a were negligible in the water column for all samples. The concentration of nitrate for site 1a ranged from 0 mg/l to 4.22 mg/l and the nitrite concentration ranged from 0 mg/l to 2.21 mg/l. Nitrate and nitrite concentrations were higher during low tide than high tide when there was less dilution with sea water. These concentrations of NO_3^- could have been released from the sediment during nitrification processes or could be the outfall of the Gowerton STWs which is just upstream of site 1a. Table 7.24 indicates that ammonium concentrations at site 1b ranged from 0 mg/l to 0.77 mg/l. The ammonium concentrations for site 3 ranged from 0 mg/l to 0.117 mg/l (see Table 7.24). Nitrate and nitrite concentrations for site 1b ranged from 0 mg/l to 5.33 mg/l and from 1.1 to 3.2 mg/l, respectively. Site 1b had higher concentrations of both nitrate and nitrite compared to site 1a this impacts on site 1a during outgoing tide. Nitrate and nitrite concentrations for site 3 ranged from 3.33 mg/l to 8.22 mg/l and from 1.19 mg/l to 5.00 mg/l, respectively. The highest concentration of nitrite was found at site 3 at 8.22 mg/l. This high concentration of nitrite observed in site 3, was attributed to nutrients from fertilisers which run off the fields and are transported by the rivers particularly during this time of the year at this time (during March, which is typical time for crop planting). In addition this could be the release from the

sediment due to the nitrification, even though the temperature is not favourable for nitrifying bacteria to oxidise the nitrite to nitrate. At this time, sampling was preceded by a period of a heavy rainfall that washed the nutrients resulting from the fertiliser and from the STWs into the receiving waters. Dissolved inorganic nitrogen was dominated by nitrate and nitrite at all sites and ranged from 0.002 mg/l to 13.30 mg/l. Dissolved inorganic nitrogen concentrations were increasing whilst the tide fell.

Table 7.23: Physical and biochemical water parameters measured at site 1a on 13th March 2008 (HW 9:58am, 7.9m; LW 4:14pm, 2.0m)

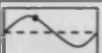
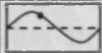
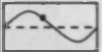
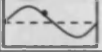
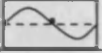
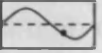
Site	Sampling time (GMT)	Tidal cycle	Salinity (ppt)	pH	Ammonium (NH_4^+) (mg/l)	Nitrate (NO_3^-) (mg/l)	Nitrite (NO_2^-) (mg/l)	Dissolved inorganic nitrogen (DIN) (mg/l)
1a	10:00		24.44	6.7	0	1.23	0	1.230
	11:00		24.38	7.0	0	0	0.002	0.002
	12:00		22.87	7.2	0	0	0	0
	13:00		17.07	7.4	0	2.76	1.980	4.740
	14:00		10.88	7.0	0	3.21	2.210	5.420
	15:00		4.77	6.7	0	4.22	1.980	6.200

Table 7.24: Physical and biochemical water parameters measured at site 1b on 13th March 2008, (HW 9:58am, 7.9m; LW 4:14pm, 2.0m)



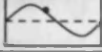
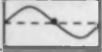
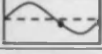
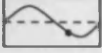
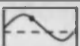
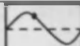
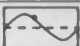
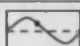

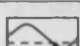
Site	Sampling time (GMT)	Tidal cycle	Salinity (ppt)	pH	Ammonium (NH_4^+) (mg/l)	Nitrate (NO_3^-) (mg/l)	Nitrite (NO_2^-) (mg/l)	Dissolved inorganic nitrogen (DIN) (mg/l)
1b	10:00		23.56	7.0	0.770	0.89	0	1.66
	11:00		22.83	7.0	0	1.03	0.32	1.35
	12:00		22.29	7.0	0.028	1.532	1.10	2.66
	13:00		17.42	7.0	0.030	2.32	0.89	3.24
	14:00		9.40	7.5	0.010	4.21	2.21	6.43
	15:00		3.03	7.8	0.115	5.33	3.20	8.64

Table 7.25: Physical and biochemical water parameters measured at site 3 on 13th March 2008, (HW, 9:58am, 7.9m; LW, 4:14pm, 2.0m)

Site	Sampling time (GMT)	Salinity (ppt)	pH	Ammonium (NH ₄ ⁺) (mg/l)	Nitrate (NO ₃ ⁻) (mg/l)	Nitrite (NO ₂ ⁻) (mg/l)	Dissolved inorganic nitrogen (DIN) (mg/l)
3	10:00	0.06	7.0	0.117	3.33	1.19	4.63
	11:00	0.06	7.4	0.115	4.21	2.00	6.32
	12:00	0.06	7.4	0	5.23	2.12	7.35
	13:00	0.06	7.4	0.114	4.41	3.10	7.62
	14:00	0.06	7.5	0.028	5.66	2.44	8.12
	15:00	0.06	7.3	0.086	8.22	5.00	13.30

Table 7.26 presents the biochemical and physical sediment parameters for site 1b. Wet sediment was collected close to the water's edge for all samples. Table 7.26 indicates that ammonium adsorption at site 1b of wet and dry samples ranged from 24.6 µg/g to 80.3 µg/g and 22.39 µg/g to 76.18 µg/g respectively. The difference of adsorbed ammonium between wet and dry sediment analysis was 5.4%. The highest amount of adsorbed ammonium was observed in the sample collected at 3:00 pm at low tide towards the centre of the channel. Sediment total carbon and organic carbon ranged from 1.1 % to 4.45% and 0.24% to 3.51%, respectively. These amounts of total carbon and organic carbon provide good adsorption sites for ammonium to adsorb on to the surface of the sediment. The results show that samples containing a high amount of total carbon and inorganic carbon have a high amount of ammonium adsorption. The results indicate that the sediment median grain size ranged from 65 µm to 120 µm. Median grain size was increasing gradually from samples collected at high tide at 10:00 am to samples collected at low tide at 2:00 pm meaning that samples collected at high tide further up the cross-section (see Figure 6.2) had smaller particle sizes than those collected at low tide.

Table 7.26: Physical and biochemical sediment parameters measured on 13th March 2008, (HW, 9:58am, 7.9m; LW, 4:14pm, 2.0m) at site 1b

Site	Sampling time (GMT)	Tidal cycle	Salinity (ppt)	Ammonium (NH ₄ ⁺) (mg/l)	Adsorbed Ammonium (NH ₄ ⁺) (µg/g)		Total carbon (%)	Total organic carbon (%)	Median grain size (µm)
					Wet Sediments	Dry Sediments			
1b	9:30		23.56	0.95	24.6	22.39	1.1	0.24	65
	11:00		22.83	1.09	37.3	36.22	1.22	0.98	79
	12:00		22.29	0.92	38.5	36.88	1.48	0.52	94
	13:00		17.42	0.86	45.7	43.79	3.46	1.38	80
	14:00		9.4	0.74	55.3	53.92	3.67	2.76	112
	15:00		3.03	0.46	80.3	76.18	4.45	3.51	120

2nd June 2008

The tidal predictions for 2nd June 2008 show that the tide was close to a spring tide which ranged between 1.4 m at 11:53am and 8.2 m at 5:51pm (see Table 7.10). Sample collection commenced at low tide. Tables 7.27 to 7.31 present the results of the water samples collected on this day for sites 1a, 1b and 3. The highest salinity found in samples from sites 1a and 1b of 26.33 ppt was measured at 4:45 pm at site 1a during high tide and the lowest of 1.3 ppt at 2:45 pm at site 1b during low tide. Site 3 was above the tidal limit for these tide conditions. The pH of the water samples ranged from 7.5 to 8. The temperature of water samples ranged from 17 °C to 19 °C. Ammonium was detected at all sites. Site 3 had the lowest amount of ammonium, ranging between 0.02 mg/l and 0.1 mg/l. At sites 1a and 1b, ammonium concentrations ranged from 0.87 mg/l to 4.12 mg/l. Ammonium concentrations at site 1b initially increased as the tide came in from 11:45 am to 13:45 pm. At site 1a for the sample collected at increasing tide (13:45 pm) and low salinity (9.58 ppt due to dilution influence from upstream) the ammonium concentration was highest at this site at 2.73 mg/l. The ammonium concentrations at site 1a were decreasing from 13:45 pm onwards with the incoming tide due to dilution effects of the sea water. In addition, the ammonium concentration was higher at site 1b than site 1a, pointing towards the impact of the outfall from the

results of the samples taken at different locations in the channel to the samples that were taken from the shore.

Suspended sediment concentrations were slightly higher in the mid-channel sample at 3.5%, than in the samples collected at 1/3 and 2/3 across the channel, which were at 0.7% and 1.9%, respectively. The channel at site b is narrower as a result of high velocity compared to site 1a, located in the large channel, thus velocity is slower. The water velocity of the channel is higher in the middle of the channel and gradually decreasing in shore direction. Shear stress is increasing in the shore as a result of reducing velocity of water inshore.

Suspended sediment concentrations were higher at site 1b than at sites 1a and 3 and ranged from 429 mg/l to 616 mg/l. The results show that there is not much difference in the amount of suspended sediment that was collected during high tide and low tide.

Table 7.27 Physical and biochemical water parameters measured on 2nd June 2008, British summer time (BST)(LW12:53am, 1.4m; HW 6:51pm, 8.2m) at site 1a

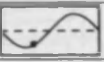
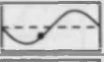

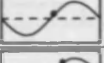
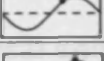
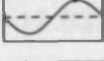
Site	Sampling time (GMT)	Tidal cycle	Salinity (ppt)	pH	Suspended sediment concentrations (SSC) (mg/l)	Ammonium (NH_4^+) (mg/l)	Nitrate (NO_3^-) (mg/l)	Nitrite (NO_2^-) (mg/l)	Dissolved inorganic nitrogen (DIN) (mg/l)
1a	11:45		12.22	7.2	548	2.23	0.002	0.006	2.33
	12:45		10.79	7.3	520	2.57	0.003	0.007	2.24
	13:45		9.58	7.2	523	2.73	0.004	0.002	2.85
	14:45		8.09	7.3	513	2.17	0.004	0	2.70
	15:45		21.95	7.2	587	2.03	0.001	0.002	2.14
	16:45		26.33	7.4	582	0.87	0.001	0	0.98

Table 7.28 Physical and biochemical water parameters measured on 2nd June 2008, (BST) (LW 12:53am, 1.4m; HW 6:51pm, 8.2m) at site 1b

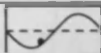
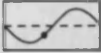
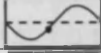
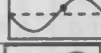
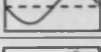
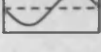
Site	Sampling time (GMT)	Tidal cycle	Salinity (ppt)	pH	Suspended sediment concentration (SSC) (mg/l)	Ammonium (NH_4^+) (mg/l)	Nitrate (NO_3^-) (mg/l)	Nitrite (NO_2^-) (mg/l)	Dissolved inorganic nitrogen (DIN) (mg/l)
1b	11:45		7.80	7.7	616	2.88	0.0004	0.0001	2.88
	12:45		4.50	8.4	615	3.31	0.0002	0.0007	3.31
	13:45		2.80	7.9	502	4.12	0.0003	0.0009	4.12
	14:45		2.70	7.7	507	3.99	0.0003	0.0009	3.99
	15:45		12.60	7.4	565	2.42	0.0003	0.0004	2.42
	16:45		26.81	7.5	479	0.89	0.0002	0.0002	0.89

Table 7.29 Physical and biochemical water parameters measured on 2nd June 2008, (BST) (LW, 12:53am, 1.4m; HW 6:51pm, 8.2m) at site 1b, unfiltered water samples

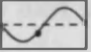
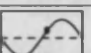
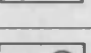
Site	Sampling time (GMT)	Tidal cycle	Salinity (ppt)	Ammonium (NH_4^+) (mg/l)	Nitrate (NO_3^-) (mg/l)	Nitrite (NO_2^-) (mg/l)	Dissolved inorganic nitrogen (DIN) (mg/l)	Suspended sediment concentration (mg/l)
1b	12:45 Mid of channel		3.24	3.31	0.0002	0.0006	3.31	534
	14:45 1/3 of channel		2.50	4.18	0.0001	0.0004	4.18	511
	14:45 2/3 of channel		2.40	4.25	0.0002	0.0005	4.25	505

Table 7.30 Physical and biochemical water parameters measured on 2nd June 2008, (BST) (LW, 12:53am, 1.4m; HW 6:51pm, 8.2m) at site 1b, unfiltered water samples

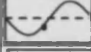
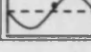
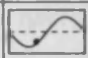
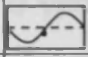
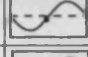
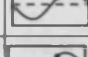
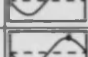
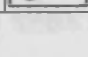
Site	Sampling time (GMT)	Tidal cycle	Salinity (ppt)	Ammonium (NH_4^+) (mg/l)	Nitrate (NO_3^-) (mg/l)	Nitrite (NO_2^-) (mg/l)	Dissolved inorganic nitrogen (DIN) (mg/l)	Suspended sediment Concentration (mg/l)
1b	12:45 shore		4.3	3.37	0.0003	0.0007	3.37	515
	14:45 shore		2.7	4.14	0.0003	0.0009	4.14	507

Table 7.31 Physical and biochemical water parameters measured on 2nd June 2008, (BST) (LW12:53am, 1.4m; HW 6:51pm, 8.2m) at site 3

Site	Sampling Time (GMT)	pH	Salinity (ppt)	Suspended Sediment Concentration-ion (mg/l)	Ammonium (NH_4^+) (mg/l)	Nitrate (NO_3^-) (mg/l)	Nitrite (NO_2^-) (mg/l)	Dissolved Inorganic Nitrogen (DIN) (mg/l)
3	11:45	7.7	0.16	431	0.11	0.0001	0	0.11
	12:45	8	0.16	433	0.05	0.0002	0.001	0.05
	13:45	8	0.16	436	0.02	0.0001	0.0002	0.02
	14:45	7.8	0.17	437	0.05	0.0002	0.0003	0.05
	15:45	7.5	0.17	434	0.10	0.0002	0.0001	0.10
	16:45	7.5	0.17	429	0.08	0.0001	0.0002	0.08

Table 7.32 presents the biochemical and physical sediment parameters for site 1b. Wet sediment samples were collected next to the water's edge. The results indicate that the ammonium adsorption was higher in the sediment samples collected close to the centre of the channel. The highest amount of adsorbed ammonium was in the sample collected at low tide and low salinity, and the lowest ammonium concentration was found in the sample collected during high tide, of $35.23 \mu\text{g/g}$ and $15.43 \mu\text{g/g}$, respectively. Sediment total carbon and organic carbon ranged from 2.18 to 5.05 and 0.78 to 3.15, respectively. Results indicate that sediment median grain size gradually decreases towards locations further up the cross-section of site 1b. The smallest median grain sizes were found in the samples collected during high tide conditions at 3:45 pm and the largest median grain size was found in the sample collected at low tide conditions at 11:45 am; median grain size ranged from $144 \mu\text{m}$ to $100 \mu\text{m}$ at low tide and high tide, respectively.

Table 7.32 Physical and biochemical sediment parameters measured on 2nd June 2008 (BST) (LW 12:53am, 1.4m; HW 6:51pm, 8.2m) at site 1b

Site	Sampling time (GMT)	Tidal cycle	Salinity (ppt)	Ammonium (NH ₄ ⁺) (mg/l)	Adsorbed Ammonium (NH ₄ ⁺) (µg/g)		Total carbon (%)	Total Organic carbon (%)	Median grain size (µm)
					Wet Sediments	Dry Sediments			
1b	11:45		7.80	3.3	25.21	24.45	2.46	0.89	144
	12:45		4.50	3.1	29.62	27.89	2.53	0.98	141
	13:45		2.80	3.2	32.41	29.77	4.27	2.39	131
	14:45		2.70	2.3	35.23	33.76	5.05	3.15	128
	15:45		12.60	3.7	18.8	16.38	2.23	0.78	100
	16:45		26.81	4.8	15.43	14.22	2.18	0.88	112

30th June 2008

The tidal predictions for 30th June 2008 show that the tide was close to neap tide conditions which ranged between 2.1 m at low tide at 10:30 am and 7.5 m at high tide at 4:32 pm (see Table 7.10). Tables 7.33 to 7.36 show the results of water samples collected on this day for sites 1a, 1b and 3. Sample collection started 1-5 hours after low tide at 12:00 pm. The highest salinity of 26.33 ppt was measured at 4:45 pm at site 1a during high tide and the lowest salinity measured at sites 1a and 1b was 1.7 ppt at site 1b at 1:00 pm. Site 3 is above the tidal limit during neap tides. The pH of the water samples ranged from 7.5 to 8.4. The temperature of water samples ranged from 18 °C to 21 °C. The results indicate that ammonium concentrations in the water column were negligible for all samples from all sites, implying that the nitrification and denitrification rates were high. Nitrate was present at all sampling sites and was higher during high tide than low tide conditions indicating its main source being the coastal waters. Nitrate concentrations ranged between 0.76 mg/l at site 1a at 1:00 pm and 5.3 mg/l at site 1b at 4:45 pm. Nitrate concentration increased during high tide because of high nitrification rates and it being released into coastal waters at this time of the year due to higher water temperatures in this summer season which ranged between 18 °C to 21 °C. This high concentration of nitrate could also come from downstream outfall

from STWs close to sites 1a and 1b. Site 3 was located above the tidal limit upstream of the estuary in Ponladudulais and had input of nutrient from the river and from STWs located upstream close to site 3; this could have come from outfall from STWs located downstream, during incoming tide. Dissolved inorganic nitrogen was dominated by nitrate at all sites and ranged from 1.1 mg/l to 5.3 mg/l. Dissolved inorganic nitrogen was higher at high tide than at low tide at sampling sites 1a and 1b. Nitrification was expected to be high at this time of the year, which is confirmed by the absence of ammonium and nitrite in the water column. In addition, the water temperature was higher and favourable to nitrifying bacteria to convert the nitrite to nitrate using dissolved oxygen, which was 11 mg/l.

Samples from sites 1a and 1b have a higher turbidity than from site 3 resulting from high suspended sediment concentrations which ranged for sites 1a, 1b and 3 from 594.0 mg/l to 668 mg/l, 624 mg/l to 668 mg/l and 552 mg/l to 563 mg/l at low tide and high tide respectively. Suspended sediment concentrations are affected and mainly caused by the tidal cycle, with their higher effect towards the end of the in-coming tide when velocities have been highest.

Table 7.35 presents the results of water samples for site 1b that were collected from approximately 1/3 into the channel. The results indicate that ammonium was low for all samples and not present at all in some of the samples. Nitrate concentrations ranged from 2.10 mg/l to 5.30 mg/l. This amount of nitrate was slightly lower (by 4%) than the nitrate concentrations of the water samples taken from the shore at the same time, which ranged from 0.99 mg/l to 4.2 mg/l. The results indicate that there are no major differences between 1/3 of channel samples and shore samples for nitrate concentrations. Use of near shore samples throughout the main part of the study was undertaken as these much safer to collect. Dissolved inorganic nitrogen was found to be higher in the high tide samples than in the low tide samples and was dominated by nitrate concentrations for all sampling sites. DIN for samples taken at site 1b from the 1/3 into the channel ranged from 2.10 mg/l to 5.30 mg/l. DIN was found to be higher by 6% at site 1b for samples collected from the shore than

Table 7.34 Physical and biochemical water parameters measured at site on 30th June 2008, (BST) (LW 11:30am, 2.1m; HW 5:32pm, 7.5m) 1b

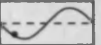
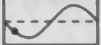

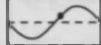
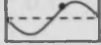
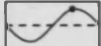
Site	Sampling time (GMT)	Tidal cycle	Salinity (ppt)	pH	Suspended sediment Concentration (mg/l)	Ammonium (NH_4^+) (mg/l)	Nitrate (NO_3^-) (mg/l)	Nitrite (NO_2^-) (mg/l)	Dissolved inorganic nitrogen (DIN) (mg/l)
1b	12:00		2.4	7.6	628.5	0	0.99	0	0.99
	13:00		2.2	7.8	624.0	0.03	2.11	0	2.14
	14:00		3.8	7.9	594.5	0.06	2.81	0	2.87
	14:45		13.4	7.8	647.0	0	3.50	0	3.50
	15:30		20.9	7.9	636.5	0	3.50	0	3.50
	16:45		24.1	8.1	668.5	0	4.2	0	4.20

Table 7.35 Physical and biochemical water parameters measured at site 1b (1/3 into the channel) on 30th June 2008, (BST)(LW 11:30am, 2.1m; HW 5:32pm, 7.5m)

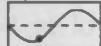
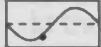
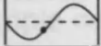
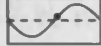

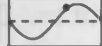
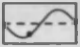
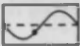
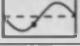
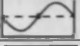
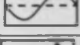
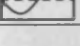
Site	Sampling time (GMT) (from 1/3 of channel)	Tidal cycle	Salinity (ppt)	pH	Suspended sediment Concentration (mg/l)	Ammonium (NH_4^+) (mg/l)	Nitrate (NO_3^-) (mg/l)	Nitrite (NO_2^-) (mg/l)	Dissolved inorganic nitrogen (DIN) (mg/l)
1b	12:00		2.2	8.2	604.0	0.0	2.10	0.0	2.10
	13:00		1.7	8.2	604.5	0.0	2.50	0.0	2.50
	14:00		4.8	8.3	505.0	0.002	2.70	0.0	2.70
	14:45		11.9	8.2	633.5	0.001	3.20	0.0	3.20
	15:30		20.7	8.2	620.5	0.0	3.80	0.0	3.80
	16:45		23.8	8.3	609	0.0	5.30	0.0	5.30

Table 7.36 Physical and biochemical water parameters measured at site 3 on 30th June 2008, (BST) (LW11:30am, 2.1m; HW 5:32pm, 7.5m)

Site	Sampling time (GMT)	Salinity (ppt)	pH	Suspended sediment Concentration (mg/l)	Ammonium (NH_4^+) (mg/l)	Nitrate (NO_3^-) (mg/l)	Nitrite (NO_2^-) (mg/l)	Dissolved inorganic nitrogen (DIN) (mg/l)
3	12:00	0.1	7.7	552.0	0.0	2.20	0.0	2.20
	13:00	0.1	7.7	553.5	0.0	3.30	0.0	3.30
	14:00	0.1	7.7	554.5	0.0	3.40	0.0	3.40
	14:45	0.1	7.6	554.0	0.0	4.70	0.0	4.70
	15:30	0.1	7.6	560.0	0.0	3.90	0.0	3.90
	16:45	0.1	7.5	563.0	0.0	5.20	0.0	5.20

Table 7.37 presents the physical and biochemical parameters of the sediments that were collected and measured during in-coming tide conditions. The results indicate that ammonium adsorption for both dry and wet sediment samples was lower during the high tide conditions samples compared to the low tide samples. The highest amount of ammonium adsorption was $30.2 \mu\text{g/g}$ at low tide in contrast with the lowest amount of ammonium adsorption, which was $8.3 \mu\text{g/g}$ at high tide. The highest amount of total carbon of 4.84% was found in sample collected at low tide at 12:00 pm, whereas the lowest amount was found at 1.75 % in the sample collected at 2:45 pm. Organic carbon was also higher in the sample collected at low tide and lower for the high tide sample at 2.44 % and 0.16 % respectively. Median grain sizes of the sediment were found to be decreasing towards samples collected at high tide conditions and ranged from $200 \mu\text{m}$ to $135 \mu\text{m}$.

Table 7.37 Physical and biochemical sediment parameters at site 1b on 30th June 2008, (BST) (LW 11:30am, 2.1m; HW 5:32pm, 7.5m)

Site	Sampling time (GMT)	Tidal cycle	Salinity (ppt)	Ammonium (NH_4^+) (mg/l)	Adsorbed Ammonium (NH_4^+) ($\mu\text{g/g}$)		Total carbon (%)	Total organic carbon (%)	Median grain size (μm)
					Wet Sediments	Dry Sediments			
1b	12:00		2.4	0	27.5	25.21	4.84	2.44	175
	13:00		2.2	0.001	30.2	28.63	3.66	1.26	200
	14:00		3.8	0.050	21.3	19.35	2.80	0.60	180
	14:45		13.4	0.020	17.4	16.66	1.75	0.39	135
	15:30		20.9	0	10.6	8.75	2.00	0.31	160
	16:45		24.1	0	8.3	7.16	1.84	0.16	145

7.2 Discussion of field work

This part of the chapter deals with the discussion of the adsorption isotherms and adsorption coefficients of ammonium for the sediments of the Loughor Estuary as well as discussion of the water quality and sediment parameters measured in this field work study and presented as previously. The effects of physical and biochemical water quality parameters on the nitrogen compounds in both the water and the sediment are also discussed here.

7.2.1 Adsorption isotherms adsorption coefficients and the effect of physical parameters on the ammonium adsorption

The ammonium ion adsorption in the sediments collected from the Loughor Estuary (as described in Chapter 7.1.5) was found to obey the Langmuir isotherm equation; in particular the study showed that the rate of adsorption by the sediments was found to be linear and fitted the Langmuir adsorption equation within the controlled range of ammonium concentrations present in the water column. The error analysis (Chi-squared and nonlinear regression) presented in Chapter 7.1.5 confirmed that ammonium adsorption data fits the Langmuir isotherm well. Figures 7.3 – 7.8 and Table 7.7 indicate that the

experimental data fitted well with the theoretical data of adsorption and there was found to be good agreement between the values for ammonium adsorption using both error analysis methods. Langmuir and Freundlich adsorption coefficients for site 2 were found to decrease during outgoing tide. The tide being higher at sample 2₁ (Langmuir coefficient, 0.111 and Freundlich coefficient, 25) and lower at sample 2₃ (Langmuir coefficient, 0.056 and Freundlich coefficient, 20.7). The Langmuir adsorption coefficient at Site 1b was higher at sample 1b₃ which was (0.182) and lower at sample 1b₂ (0.102). However the freundlich adsorption coefficient was higher for sample 1b₁ (42.6), and lower for sample 1b₂ (24.7).

The ammonium adsorption coefficient (K^*), which is defined as the ratio of the concentration of adsorbed ammonium to the equilibrium ammonium concentrations, was found to be very useful in highlighting the characteristics of ammonium adsorption on the sediments. K is the dimensionless equivalent of K^* (Berner, 1980), with K being larger than K^* , which is due to the sediment physico-chemical parameters. The sediment physico-chemical parameters are known to have a significant influence on the behaviour of ammonium adsorption (Morse and Morin, 2005). In the experiments carried out in this study, however, the mean grain size of the sediments was found not to have a significant influence on the amount of ammonium adsorption.

In related studies, Smallackin and Aller (1984) found that the ammonium adsorption coefficient had a significant correlation with the sediment porosity. In contrast, the present study showed that the ammonium adsorption coefficient did not appear to have any significant correlation with the sediment porosity. However, the adsorption coefficient was found to be highest in the sediments with comparatively high amounts of organic carbon.

Availability of organic matter was therefore considered to be one of the important factors controlling the degree of ammonium adsorption in the Loughor Estuary. The results show that ammonium adsorption increases with increasing organic carbon concentrations. Therefore, organic carbon content is believed to be one of the important factors controlling the ammonium adsorption on the sediment of the Loughor Estuary.

The result show that ammonium adsorption increases with increasing organic carbon concentrations. Therefore, organic carbon content is believed to be

one of the important factors controlling the ammonium adsorption on the sediment of the Loughor Estuary.

Figure 7.21 presents the influence of organic carbon on the adsorbed ammonium for samples from sites 1b and 2. It can be seen that the ammonium adsorption increases with increasing organic carbon content. Samples from site 1b were found to contain higher organic carbon content than samples from site 2 and correspondingly, higher ammonium adsorption when compared to the corresponding values measured at site 2.

This finding was attributed to the fact that site 1b was rich in organic carbon in comparison with site 2. Studies published by other authors have indicated that sediments with a high ammonium adsorption rate also have relatively large amounts of organic matter (Hou et al, 2003; Boatman and Murray, 1982; Mackin and Aller, 1984).

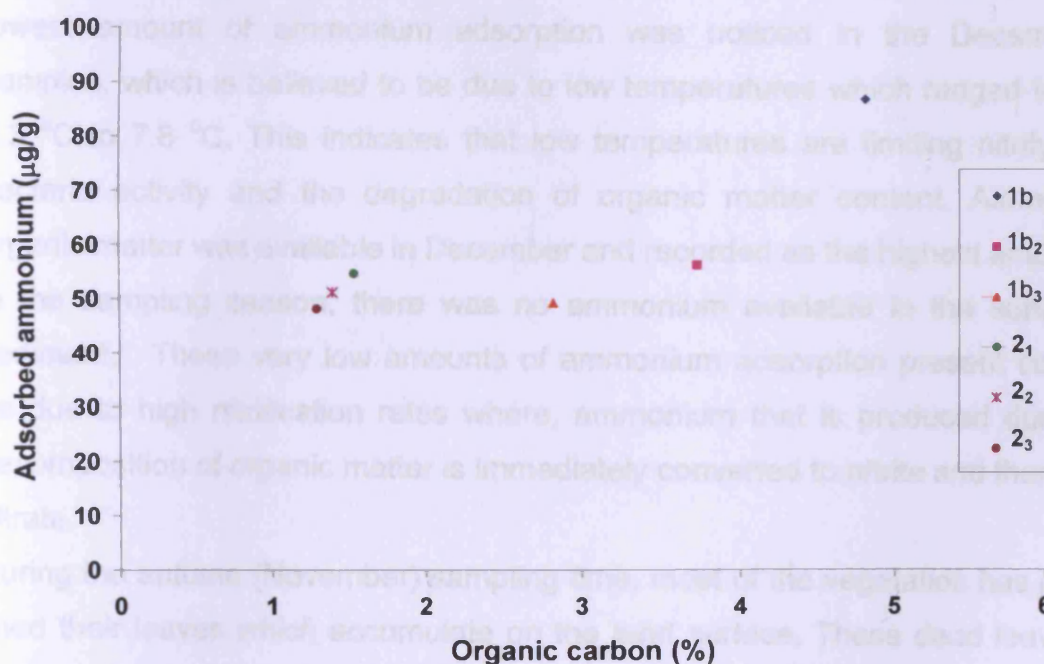


Figure 7.21 Correlation of ammonium adsorption with organic carbon content for the Loughor Estuary sediment samples at sites 1b and 2. The subscript numbers refer to the sampling time. These samples were collected on 14th December 2007

7.2.2 Seasonal effects on ammonium adsorption

Figure 7.22 presents the influence of seasonal difference on the adsorbed ammonium for sediment samples from the Loughor Estuary. It can be seen that the highest ammonium adsorption was measured during the month of March when the availability of organic carbon was highest. March in the early spring is the time of the year when farmers start applying fertilizer to their land, and also when there can be heavy rainfall periods which lead to washing of the nutrients resulting from the fertilizer and their running off the still bare fields into receiving water bodies. This introduces large amounts of nutrients from agricultural activities in addition to those from the outfalls from sewage treatment works (STWs) to the receiving waters. In related studies, Bockelmann-Evans et al (2007) found that the main nutrient loads after prolonged rain fall periods can be attributed to runoff from agriculture. The lowest amount of ammonium adsorption was noticed in the December samples, which is believed to be due to low temperatures which ranged from 6.3 °C to 7.8 °C. This indicates that low temperatures are limiting nitrifying bacteria activity and the degradation of organic matter content. Although organic matter was available in December and recorded as the highest amount in the sampling season, there was no ammonium available in the surface sediment. These very low amounts of ammonium adsorption present could be due to high nitrification rates where, ammonium that is produced during decomposition of organic matter is immediately converted to nitrite and then to nitrate.

During the autumn (November) sampling time, most of the vegetation has just shed their leaves which accumulate on the land surface. These dead leaves and plants are a source of organic matter and are transported with the rainfall runoff to the receiving waters of the catchment site of the Loughor Estuary. When the November samples were taken, the water temperature ranged from 14.3 to 16.5 °C, giving still good conditions for the decomposition of organic matter, thus producing ammonium ions.

The summer season is represented by the June samples. At this time of the year, organic matter is readily available, which can be transported to the catchment's receiving waters from the agriculturally used land resulting from run off with high nutrients loads caused by fertilisers. The elevated organic carbon content can provide good exchange sites for ammonium to adsorb on to. In addition, there is organic matter present, which is released from the sewage treatment works. Overall, the highest amount of ammonium adsorbed was 80.3 $\mu\text{g/g}$ found during spring time (March) and the lowest amount was 0.0 $\mu\text{g/g}$ found in December during winter time.

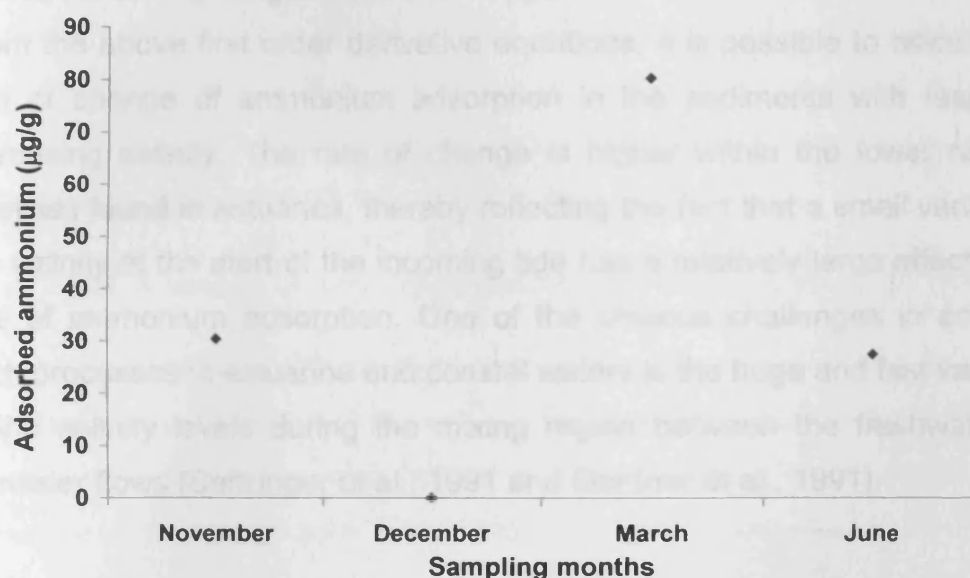


Figure 7. 22 Seasonal influence on ammonium adsorption

7.2.3 Salinity effect on ammonium adsorption

The difference in the adsorption isotherm of ammonium for the Loughor Estuary sediments showed that salinity affected the distribution of ammonium between the sediments and the water column. The ammonium adsorption coefficient was found to decrease with increasing salinity concentrations; meaning that lower salinity levels were found to be more favourable to ammonium adsorption by the sediments. The ammonium adsorption levels detected in the Loughor Estuary sediments, as taken from the sites 1b and 2

when linked to the salinity levels were fitted to Equations 7.1 and 7.2, which are presented in section (7.1.6), with the first derivative of this equation being given as: The first derivative equations present the adsorption coefficient for salinity range (2, 5, 10, 15, 20, 25 ppt).

Equation for sample 1b₁

$$dQ/dS = 0.0196S - 1.0756 \quad (7.3)$$

Equation for sample 2₁

$$dQ/dS = 0.0786S - 1.8321 \quad (7.4)$$

Where dQ/dS is the rate of change of the quantity of ammonium ($\mu\text{g g}^{-1}$ ppt); and S , the salinity ranged from 0 to 25 ppt.

From the above first order derivative equations, it is possible to calculate the rate of change of ammonium adsorption in the sediments with respect to increasing salinity. The rate of change is higher within the lower range of salinities found in estuaries, thereby reflecting the fact that a small variation in the salinity at the start of the incoming tide has a relatively large effect on the rate of ammonium adsorption. One of the obvious challenges in analysing such processes in estuarine and coastal waters is the huge and fast variations in the salinity levels during the mixing region between the freshwater and seawater flows (Seitzinger et al., 1991 and Gardner et al., 1991).

7.2.4 Sediment classification and composition

The sediment samples in the Loughor estuary from the two sites 1b and 2 are characterised by mean grain diameters of 83 μm to 155 μm . The majority of samples can thus be classified as fine sand due to their particle size according to the British Standard classification (see Tables 7.3 and 7.4). Sediments are a mixture of minerals with different grain sizes; quartz is the dominating mineral in the sea sediment although clay minerals are still present (Winterwerp, 2004). This agrees with the results from the Loughor Estuary samples showing it comprises of quartz and minor amounts of clay minerals. The sediments also contained comparatively large amounts of organic carbon

and small amounts of Kaolinite, especially at site 1b. The amount of adsorption appears to have been influenced by both the amount of organic matter and the mineralogy of the sediments. These results agree with Hou et al (2003) Mackin and Aller (1984) and Sugai (1992).

The highest organic carbon content was found to occur at Site 1b, in Sample 1b₁, which was collected during high tide at 9:30 am on 14th December 2007. A wet sediment sample was collected close to the water's edge. During high tide, when the sea water and fresh water mix, flocculation occurs and results in clay and organic matter accumulating to create slowly growing flocs (or suspended sediments of increasing particle size) which will partly deposit on the bed. Some of these sediments will be re-suspended from the bed, depending on the flow velocities and the resulting shear stresses during incoming tide. The creation, deposition and re-suspension of the sediments and organic matter are all heavily influenced by the tidal cycle and the prevailing hydrodynamic conditions (Geyer et al, 2004).

7.2.5 The influence of salinity on suspended sediment concentrations

Salinity changes constantly in the Loughor Estuary caused by the tidal cycle. The fluctuations of salinity in the estuary are caused by the tides, which cause major mixing processes and influence the adsorption behaviour and thus presence of nutrients such as ammonium, nitrate and nitrite. The salinity during the sampling in this study in the estuary ranges from 0.02 ppt during low tide at site 1b on 14th December 2007 to 26.9 ppt at high tide at site 1b on 6th November 2007. During incoming and outgoing tide, when the seawater and freshwater mix, and large velocities are present in the estuary some of the sediment will be resuspended from the bed, depending on the flow velocities and shear stresses and the suspended sediment concentrations will increase. In contrast at low and high tide conditions, vertical mixing reduces and there is an increase in deposition and a decrease in suspended solid concentration (Tanaka et al 2007; Schoellhamer, 2001). Incoming and outgoing flow conditions at spring tides cause the greatest vertical mixing and largest suspended sediment concentrations in the Loughor Estuary. This is reflected

in results shown in Tables 7.27 -7.31 and 7.33 – 7.36 for sampling dates of 2nd June which is spring tide and 30th June is neap tide, respectively. The highest suspended sediment concentration of 668.5 mg/l was noted just before incoming tide on 30th June at site 1b. In contrast the lowest concentration of suspended sediment of 479 mg/l was observed at site 1b on 2nd June, which was found in the sample collected at high tide. However increasing sediment concentration results in reducing the settling velocity of particles as found by Bogardi ,1974 and McNown and Lin 1952).

The suspended sediment concentration was found not to be affected with increasing salinity concentrations as can be seen in Figure 7.23 which presents the suspended sediment concentrations and salinities on 2nd and 30th June 2008; when samples were collected during the incoming tide on both dates. The suspended sediment concentration ranged from 594 mg/l at site 1a to 668.5 mg/l at site 1b on 30th June and from 479 mg/l at site 1b to 616 mg/l at site 1b on 2nd June respectively. The suspended sediment concentration increased towards the end of incoming tide for the 2nd of June samples at site 1a. This finding disagrees with Yang et al (2004), who found that suspended sediment concentrations decrease towards the end of incoming tides. In contrast in samples collected at the same time at site 1b, the suspended sediment concentration was lower at the end of the incoming tide, which agrees with Yang et al (2004). Overall, the amount of suspended sediment present in the Loughor Estuary appears to be independent of the velocities present. However, the velocities could impact suspended sediment size distribution, which was not measured in this study.

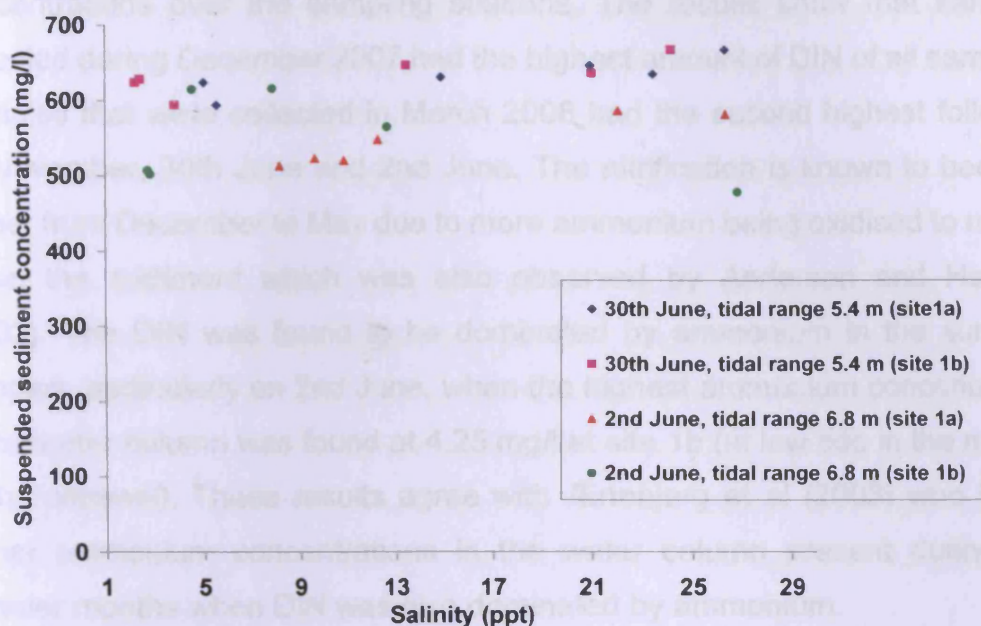


Figure 7.23 The influence of salinity on the suspended sediment concentrations in the Loughor Estuary

7.2.6 Nitrogen compounds

During this study nitrogen fluxes from the sediment to the water column in the form of dissolved inorganic nitrogen (DIN) were found to occur in autumn and spring as can be seen in Figure 7.24 and 7.25. These fluxes were dominated by nitrate and nitrite. These maximum amounts of nitrate at 1b and nitrite of 5.33 mg/l and 3.20 mg/l can be interpreted as resulting from decomposition of organic matter as well as being caused by discharges from various outfalls in the estuary. During the autumn and spring, the sediment oxygen demand is lower than in the summer due to lower temperatures, decreased biological activity and respiration rate of organisms and the decreased rate of decomposition of organic matter. This causes the oxygen content of the sediment to increase. Accordingly, nitrification was observed to be higher in samples collected on the 6th November, 14th December, and 30th June than on 2nd June. It is believed that ammonium released from the sediment is immediately converted to nitrite and subsequently to nitrate in the process of decomposition of organic matter in the summer (2nd June).

There is sufficient organic carbon present in the estuary to support nitrification and denitrification processes through the year. Figure 7.24 presents the DIN

concentrations over the sampling seasons. The results show that samples collected during December 2007 had the highest amount of DIN of all samples. Samples that were collected in March 2008 had the second highest followed by November, 30th June and 2nd June. The nitrification is known to become higher from December to May due to more ammonium being oxidised to nitrate within the sediment which was also observed by Anderson and Hansen (2003). The DIN was found to be dominated by ammonium in the summer samples, particularly on 2nd June, when the highest ammonium concentration in the water column was found at 4.25 mg/l at site 1b (at low tide in the middle of the channel). These results agree with Ærtebjerg et al (2003) who found higher ammonium concentrations in the water column present during the summer months when DIN was also dominated by ammonium.

Figure 7.25 shows the nitrate concentrations during the sampling months. The results indicate that the highest nitrate concentrations of up to 8.22 mg/l were found in the water column at 15:00 hours at site 3 in March at the fresh water boundary (River Loughor). In the tidally impacted samples the highest nitrate concentration of 7.74 mg/l was found in the water column at 15:00 hours at site 1b on 14th December at low tide. This nitrate is likely to be result from agricultural practices, with nitrates reaching the receiving waters with the rainfall runoff. This might have been caused by rainfall events, which could have well preceded this sampling date. The elevated nitrate content in the March samples reveals a higher increased level of 5.33 mg/l at 1b which is likely result from a decrease in the uptake by phytoplankton and an increase in the decomposition of organic matter which can have a significant influence on the amount of nitrate present in the water column (good source of nitrate). The lowest concentrations of nitrate and nitrite when comparing samples collected on 6th November 2007, 14th December 2007, 13th March 2008 and 2nd and 30th June 2008 were found on 2nd June 2008 at three locations. These low concentrations may be due to several factors:

- The rise in water temperature in the summer which ranged from 17 °C to 19 °C

- Increases in biological activity and these lower concentrations of NO_3^- and NO_2^- can mostly result from their assimilation by phytoplankton and aquatic plants during this time of the year.
- Low nitrate concentrations are caused by denitrification processes.

These results agree with *Ærtebjerg et al (2003)*, who found low nitrate concentrations and less dissolved oxygen in the water column in the summer months (June, July and August), which were caused both by nitrification and denitrification. In contrast nitrate was present on 30th June at all sampling sites compared to the results from all other sampling dates. In addition, at 30th June the nitrate concentrations at sites 1a and 1b increased with the incoming tide. This could be due to:

- High nitrate concentrations further out in the estuary; these appear to be present in the coastal water of the entire region.
- There is sufficient organic matter in the estuary to support nitrification process by which ammonium is oxidized to nitrite and subsequently to nitrate.
- Presence of suitable temperatures ($18\text{ }^{\circ}\text{C}$ to $21\text{ }^{\circ}\text{C}$; temperature on 2nd of June $17\text{ }^{\circ}\text{C}$ to $19\text{ }^{\circ}\text{C}$) which is suitable for organic matter degradation and for nitrification process.
- Sufficient dissolved oxygen (DO) concentration in the estuary because of the water movement, which has to be $> 1\text{ mg/l}$ to support biological activity of nitrification processes.

In comparison to the other sampling seasons, higher nitrite concentrations of 10.23 mg/l were observed at low tide at 15:00 hours at site 1a at the December sampling date. This could be caused by the Llanelli STWs outfall discharging to the Loughor Estuary. In addition, these high concentrations of nitrite can also indicate that the nitrification was high in the estuary. Table 7.38 indicates that the Loughor Estuary has high concentrations of nitrite and ammonium compared to many other estuaries in England and Wales. The lowest annual mean averages of ammonium and nitrite concentrations were observed in the Humber and the Conwy at 0.081 mg/l and 0.009 mg/l

respectively (Dong et al, 2004). The highest annual mean averages of nitrate concentrations of 8.10 mg/l and 17.3 mg/l were recorded at two Humber sites (Dong et al, 2004). Mortimer et al (1998) found that the Humber Estuary contained a nitrate concentration of 31.00 mg/l, which is the highest concentration measured in all UK estuaries. This was attributed to intensive fertiliser usage and large sewage inputs in the Humber catchment. The Loughor Estuary has a high nitrate concentration (maximum value) of 7.74 mg/l compared to the annual mean averages of nitrate concentration for the Conwy Estuary, where it is recorded as 1.20 mg/l. Overall, the nitrate concentration in the water column in the Loughor Estuary of 7.74 mg/l is high compared to maximum concentrations of < 6.2 mg/l measured for most other estuaries in UK except the Humber Estuary, which has the highest nitrate concentrations (Mortimer et al, 1998). In addition maximum ammonium and nitrite concentrations measured in the Loughor Estuary of 4.25 mg/l and 10.23 mg/l are higher than the annual mean averages of ammonium and nitrite concentrations measured for the other UK estuaries.

Table 7.38 Comparison of measured nitrate, nitrite and ammonium concentrations in UK estuaries

Estuary	NO ₃ ⁻ (mg/l)	NO ₂ ⁻ (mg/l)	NH ₄ ⁺ (mg/l)	Source
Humber (water column nitrate concentration) (Maximum)	31	-	-	Mortimer et al (1998)
Trent (Humber) (Annual means)	17.3	0.014	0.081	Dong et al (2004)
Humber (from Humber Bridge to Spurn Head)(Annual means)	8.10	0.018	0.160	Dong et al (2004)
Conwy (North West Wales)(Annual means)	1.20	0.009	0.219	Dong et al (2004)
Loughor (South west Wales)(Maximum concentration)	7.74	10.23	4.25	This study

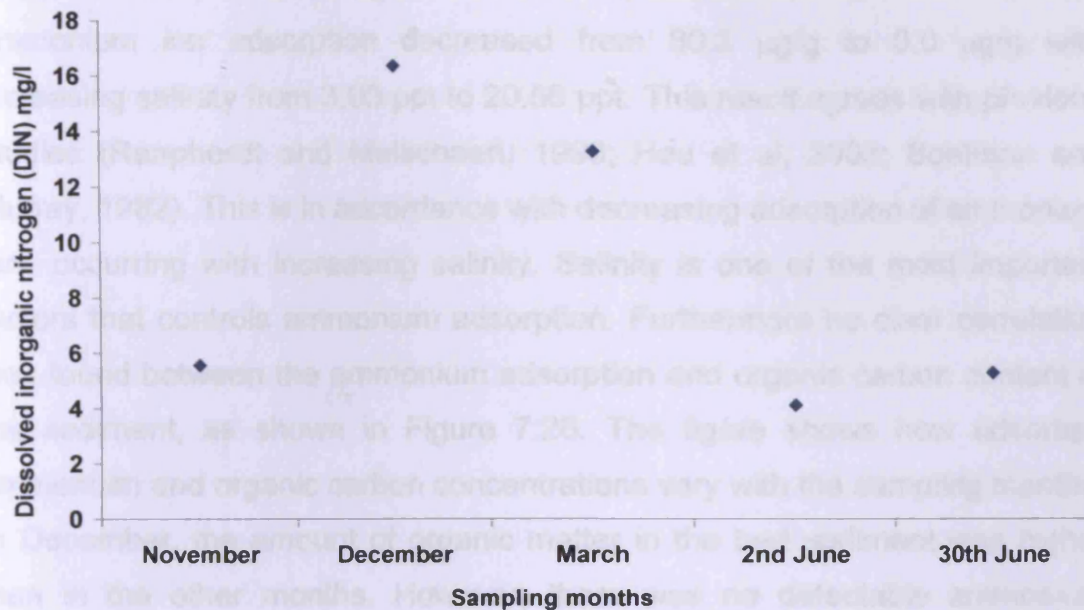


Figure 7.24 Concentrations of Dissolved Inorganic Nitrogen (DIN) over sampling season

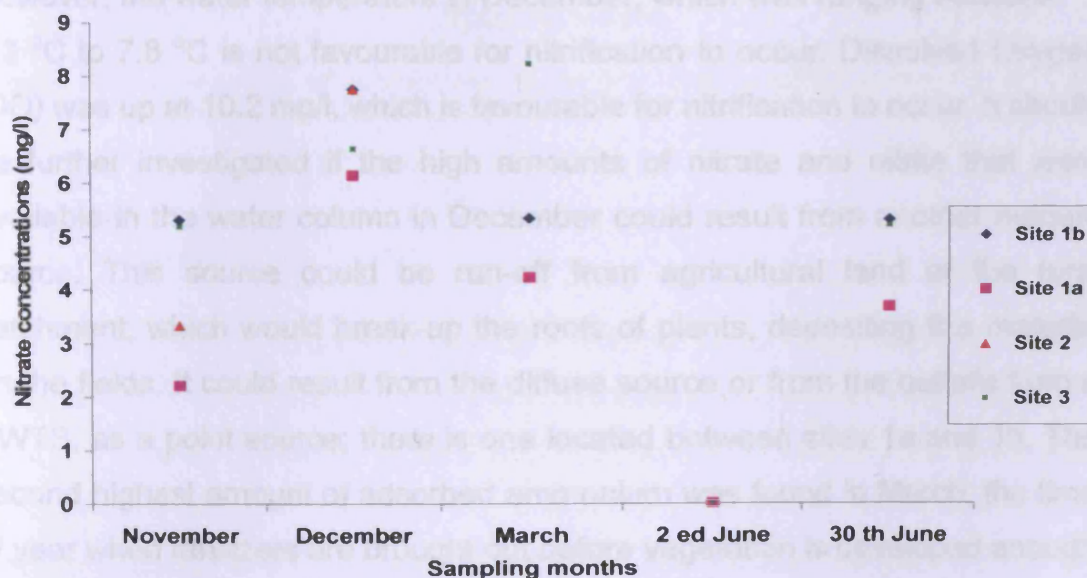


Figure 7.25 Nitrate concentrations during sampling season

Ammonium adsorption was found to be higher at low salinity concentrations. The highest amount of adsorbed ammonium during the sampling season was found during March 2008 at site 1b, at 80.3 $\mu\text{g/g}$. At this date, the bed sediment was characterised by a high amount of organic carbon of 3.51%; this

sample was collected during low tide at 15:00 hours. The results indicate that ammonium ion adsorption decreased from 80.3 $\mu\text{g/g}$ to 0.0 $\mu\text{g/g}$ with increasing salinity from 3.03 ppt to 20.56 ppt. This result agrees with previous studies (Raaphordt and Malschaert, 1996; Hou et al, 2003; Boatman and Murray, 1982). This is in accordance with decreasing adsorption of ammonium ions occurring with increasing salinity. Salinity is one of the most important factors that controls ammonium adsorption. Furthermore no clear correlation was found between the ammonium adsorption and organic carbon content of the sediment, as shown in Figure 7.26. The figure shows how adsorbed ammonium and organic carbon concentrations vary with the sampling months. In December, the amount of organic matter in the bed sediment was higher than in the other months. However, there was no detectable ammonium adsorbed in the sediment, but it was present in the water column at this time. This is believed to be attributed to ammonium produced during decomposition of organic matter which is being converted to nitrite and nitrate due to high denitrification and nitrification rates, occurring during this time of the year.

However, the water temperature in December, which was ranging between 6.3 °C to 7.8 °C is not favourable for nitrification to occur. Dissolved Oxygen (DO) was up at 10.2 mg/l, which is favourable for nitrification to occur. It should be further investigated if the high amounts of nitrate and nitrite that were available in the water column in December could result from another nutrient source. This source could be run-off from agricultural land of the rural catchment, which would break-up the roots of plants, depositing this material on the fields. It could result from the diffuse source or from the outfalls from a SWTS, as a point source; there is one located between sites 1a and 1b. The second highest amount of adsorbed ammonium was found in March; the time of year when fertilizers are brought out before vegetation is developed enough to prohibit the run-off of fertilizer with the often heavy rainfall still present in the late winter.

Ammonium is adsorbed onto the sediments due to the adsorption at cation exchange sites. These sites are present on the surface of clays and organic matter (Berner, 1980 and Morin et al., 1999). Therefore, the adsorption of ammonium ions by sediments has an important influence on nitrogen cycling

which is linked closely with nitrification and denitrification processes of nitrogen in sediments. Overall, it was observed that the amount of adsorbed ammonium was higher in the bed sediments that are exposed to fresh water compared to sediments from estuarine waters.

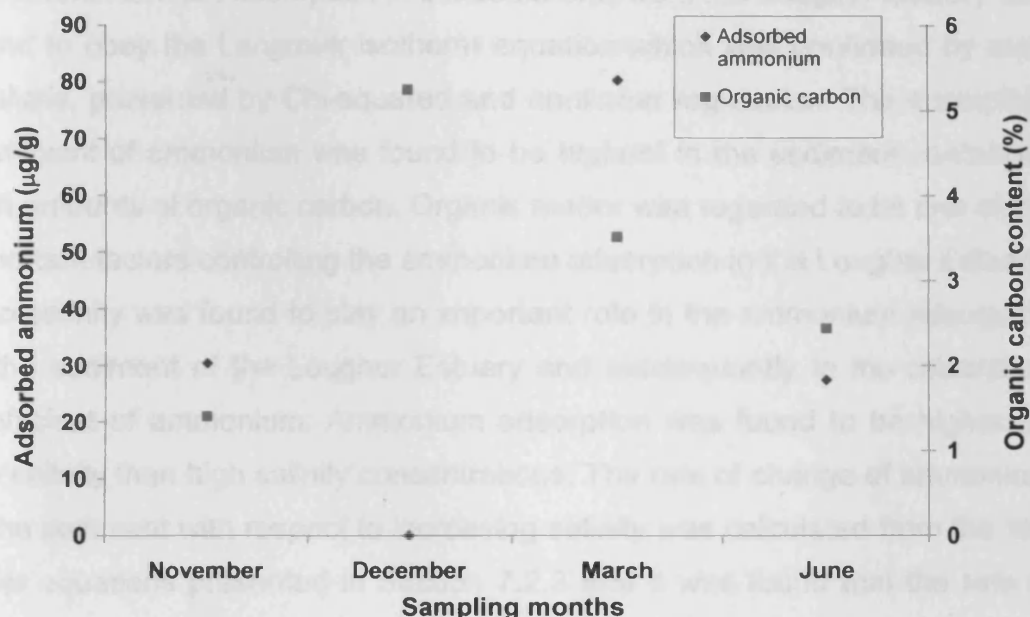


Figure 7.26 Correlation of ammonium adsorption with organic carbon in the field samples over the sampling months

7.3 Summary

This chapter shows and discusses the results of the physical and biochemical parameters of the sediments and water samples collected from sites along the Loughor Estuary. Porosity, particle and bulk density of the bed sediment were measured in order to calculate the adsorption coefficient for the ammonium adsorbed on the sediment. It was found that the particle and bulk density are influenced by the mineralogy of the sediment and the organic matter content. The grain size has an effect on the porosity of the solids samples as was observed in the various ranges of grain sizes investigated for sediment samples from the Loughor Estuary.

Organic, inorganic and total carbon content of the sediment samples was also measured. The highest amount of organic carbon was found in the bed

sediment sample collected at high tide at site 1b in 14th December 2007. In contrast, the lowest amount of organic carbon was found in a sample collected at low tide at site 1b in 30th June 2008. X-ray diffraction results for the field samples show that sediment samples mainly comprise of quartz followed by calcite and minor amounts of clay minerals (Holloysite and Kaolinite).

The ammonium ion adsorption in the sediments from the Loughor Estuary was found to obey the Langmuir isotherm equation which was confirmed by error analysis, presented by Chi-squared and nonlinear regression. The adsorption coefficient of ammonium was found to be highest in the sediment containing high amounts of organic carbon. Organic matter was regarded to be one of the important factors controlling the ammonium adsorption in the Loughor Estuary. Also salinity was found to play an important role in the ammonium adsorption in the sediment of the Loughor Estuary and subsequently to the adsorption coefficient of ammonium. Ammonium adsorption was found to be higher for low salinity than high salinity concentrations. The rate of change of ammonium in the sediment with respect to increasing salinity was calculated from the first order equations presented in Section 7.2.3 and it was found that the rate of change is higher within the lower range of salinity.

The results from suspended sediment analysis for the Loughor Estuary show that suspended concentrations were higher for low tidal ranges (neap tides) than high tidal ranges (spring tides), which could be due to the dilution effect of sea water. In addition, it was found that the settling velocity of the suspended sediment seems to be independent of the velocities present in the estuary resulting from different tides. This finding is contrary to other published literature sources which indicate that high velocity leads to increased suspended sediment concentrations.

The results of sampling data of the Loughor Estuary show that DIN during autumn and spring was dominated by nitrate and nitrite. The highest concentration of nitrate measured within the sampling season was 8.22 mg/l, which was measured at the fresh water boundary (River Loughor). The second highest concentration of nitrate, of 7.74 mg/l was measured in the water column of the Loughor Estuary at site 1b in December at low tide. Also nitrate concentrations ranging from 0.67 mg/l to 5.30 mg/l were present on 30th June at all sampling sites and increased with the incoming tide. The main source of

this concentration of nitrate appears to come from further out in the estuary - these appear to be present in the coastal water of the whole region during the summer months. In summer, DIN was dominated by ammonium and the highest ammonium concentration measured in the water column was 4.25 mg/l in the low tide sample. The concentrations of nitrate of up to 8.22 mg/l in the water column of the Loughor Estuary were higher compared to mean concentrations of <6.2 mg/l recorded for most other estuaries in the UK except the Humber Estuary (where concentrations up to 31 mg/l were measured. This was the highest concentration of nitrate measured for UK estuaries)(Mortimer et al, 1998). The results show that the highest ammonium and nitrite concentrations of 4.25 mg/l and 10.23 mg/l respectively, for UK estuaries were measured in the Loughor Estuary.

These results have wide implications for compliance with the EU Nitrate Directive, Bathing water Directive and Shellfish Directive in the following context:

- i. The EU Directive (91/676/EEC) seeks to protect water bodies from nitrate pollution from agricultural sources. High nitrate levels were observed in the Loughor Estuary in the summer and spring months with the highest in the latter. The high nitrate levels were due to the cumulative effect from sewage and agricultural sources. This leads to algal growth in the estuarine water which then leads to the well known degradation of water quality linked to eutrophication. The Loughor Estuary has been considered regularly over the past years to be considered as a polluted water body under the Nitrate Directive.
- ii. The aim of the EC Shellfish Directive (79/923/EC) is to protect or improve shellfish waters in order to support shellfish life and growth, therefore contributing to high quality of shellfish products directly edible by man. The main thrust of the directive for the Loughor Estuary is to protect aquatic habitat of cockles and scallops etc. As shown in the results from this study, high eutrophication is present in the Loughor Estuary which can affect the aquatic life of the shellfish population particularly during summer months. For instance cockle fishing had to be suspended in Bury Port which is an inlet to the Loughor Estuary in 2001/2002 owing to an outbreak of shellfish poisoning which might be

due to high nutrient levels since they depend on planktons for their food (Agnew et al, 2006). The Loughor Estuary may not meet the standards set in this Shellfish Directive.

These results are significant for the Environment Agency Wales, whose aims are to protect and conserve water resources under its jurisdiction and of which the Loughor Estuary forms a part. As indicated in the results reported herein there are high levels of pollution coming from the high ammonium and nitrate levels (from agricultural and sewage treatment), especially in the summer months which can affect public health. It is in the interest of the Environment Agency Wales to prevent this amount of pollution, so as to protect the habitats, shellfisheries and attract locals and tourists to the estuary.

8 Conclusions and Future work

The main conclusions drawn from this study and the future work recommendations are presented in this chapter.

8.1 Ammonium adsorption equation in QUAL2E

Water quality modelling deals with the prediction of water pollution transport processes using mathematical formulations and computational simulation techniques. Water quality models consist of a collection of formulations representing physical and biochemical processes that determine the fate and transport pollutions in the water body. However, there are limitations in using these models due to the uncertainties associated with various processes and variables. The water quality model QUAL2E (Brown et al, 1987) is widely used to evaluate surface water quality and is based on biochemical formulations for water quality. However, QUAL2E is related to water quality processes present mainly in the water body and does not cover the processes of the sediment interaction.

Ammonium adsorption processes are investigated in this study and have been included in the nitrogen cycle of the QUAL2E model. The adsorption equation of ammonium is based on the linear relationship between equilibrium concentration of ammonium and adsorbed ammonium one of the main aims of this study was to calculate the total concentration of ammonium in the water column. This has been carried out and is presented in individual equations which were developed by adding the equilibrium concentration of ammonium to the adsorbed ammonium.

8.2 Laboratory experiments

This study showed that the ammonium adsorption by clays (Montmorillonite, Kaolinite) and sand (coarse, fine) was almost linear and fitted to the Langmuir adsorption isotherm within different ranges of concentrations of ammonium in both distilled and artificial sea water.

The adsorption results from this study show that the Montmorillonite has the highest amount of adsorption compared to Kaolinite, fine and coarse sand. Over all, the ammonium adsorption was found to be effected by the particle size and salinity. The adsorption of ammonium in Montmorillonite, Kaolinite, fine and coarse sand was higher in distilled water than artificial sea water.

The adsorption coefficient (K^*) was calculated in this study from the regression line of adsorbed ammonium plotted against the ammonium equilibrium concentration. The result shows that the adsorption coefficient was affected by the particle size, the sediment characteristics and the salinity of the water. The adsorption coefficient of ammonium was found to be higher for distilled water and lower for artificial sea water for Montmorillonite, Kaolinite, fine and coarse sand, respectively. Ammonium has shorter resident time in estuarine sediment compared with fresh water sediment due to competition for exchange sites from sea water cations and ammonium anion. In addition Montmorillonite was found to have the highest adsorption coefficient in both distilled water and artificial sea water conditions.

In estuarine waters where there are constant tidal changes between fresh water (from the river) and sea water (from the ocean) conditions, regular deposition of suspended sediment is occurring including clays, in particular Montmorillonite. The small particle sizes encourage the attachment of ammonium. Although ammonium has a short residence time in estuaries, which can increase the flushing of ammonium attached to the sediment, ammonium may still being found in the water column. The implications are therefore that a high nutrient content can occur in the estuary, which leads to eutrophication and an increase in the water turbidity. This high eutrophication affects the fauna and flora and lead to non-compliance of the EU Habitats Directive (992/43/EEC), which seeks to conserve and protect these natural resources.

Ammonium adsorption was found to decrease gradually for all adsorbents over time when mixing the samples with artificial sea water. Montmorillonite, Kaolinite and fine sand with their comparatively small particle sizes reached the equilibrium after 70 minutes whereas coarse sand had reached equilibrium after 60 minutes. This result shows that in estuarine waters sand particles will

be deposited on the bed faster than clay particles due to turbulence. Thus, clay particles will be suspended in the water column for longer thereby increasing turbidity. This has serious implications for the water quality of an estuary with a high presence of clay suspended sediments.

Kaolinite was found to have the highest amount of ammonium release from the sediment at ammonium concentrations of 2 and 6 mg/l at 80% and 49%, respectively. Montmorillonite showed the highest ammonium release at an ammonium concentration of 10 mg/l at 57%. The equilibrium for all the samples did not occur before 60 minutes. The kinetic experiment gave a good picture of processes occurring in estuarine waters when sea water mixed with fresh water. This study has not previously been reported for the different types of clay (Montmorillonite, Kaolinite) and sand (fine, coarse). Also, if the bed sediments contain a lot of clay, then more ammonium will be released during turbulence owing to the high sea water cations competing for the ammonium on the surface of the clay. These results showed that the quantity of ammonium released to the water column will be higher if the ammonium concentration on the bed is higher. However, the percentage of ammonium released to the water column will be higher for situations where the clay has a low concentration of ammonium than where the clay has relatively a high concentration. The implications are that a high concentration of nutrients will take much longer to be released to the atmosphere in the form of nitrogen gas and thereby eutrophication levels will be increased in the estuarine waters.

Nitrate adsorption on Kaolinite in deionised water was found to obey the Langmuir adsorption isotherm. Nitrate was used in the nitrate adsorption isotherm experiments due to the positive charges on the edges of Kaolinite particles which can facilitate adsorption of negatively charged nitrate ions.

The types of clay minerals present in the sediments can influence anion adsorption which is the dominant mechanism affecting nitrate movement across the water, sediment interface. Thus, Kaolinite particles can demobilise the movement of nitrate into the water column, which otherwise would have been transported to the surface waters. The EU Nitrate Directive has established an upper limit of 50 mg/l for nitrates in drinking water and the

directive aims to reduce water pollution caused by fertilizer application on farmland. The implications of the findings from this study are that the presence of Kaolinite in the bed sediments can have positive effect on the water quality. It was found in this study that salinity can influence nitrate adsorption on Kaolinite during mixing of deionised water and artificial sea water. Artificial sea water anions compete with nitrate ions for adsorption onto the Kaolinite clay, reducing nitrate adsorption with increasing salinity. The adsorption of nitrate was found higher in deionised water than in artificial seawater. The amount of nitrate adsorbed was found to be reduced by up to 47.5%.

The nitrate adsorption coefficient was calculated for both deionised water and artificial seawater. The adsorption coefficient was found to be lower in artificial sea water than in deionised water at 7 mg/l and 3.6 mg/l, respectively. This finding has not previously been addressed in the literature. The implications of these results are that in the estuaries where the bed sediments contain Kaolinite clay minerals then nitrate will be adsorbed during low tide (where fresh water dominates) and an increased amount of nitrate will be in the water column during high tide (where sea water may dominate). The water quality in terms of nitrate levels will depend upon the movement of the tide, particularly salinity levels, which in turn influence the adsorption coefficient of nitrate, as found in this study.

8.3 Recommendations and future work resulting from laboratory study

The outcomes of this study have led to the following further research considerations that exceeded the scope of this work.

- Further investigation of the ammonium and nitrate adsorption processes within the sediment pores and comparison with the adsorption processes on particle surfaces.
- Further study is recommended to find the influence of pH and temperature on the NH_4^+ adsorption on Montmorillonite, Kaolinite and fine and coarse sand.

- Further investigation is recommended to determine the adsorption isotherm of NH_4^+ and NO_3^- on the sediment sample under different flow rates. This may be done by batch reactor and controlled of the ammonium concentrations, the amount of the sediments and use of different stirring velocities.
- Further investigation of the nitrate adsorption on the sediment and determination of the effect of the different concentrations of salinity and the influences of pH, temperature and organic matter is recommended.

8.4 Field experiments

Physical and biochemical water quality parameters for the Loughor Estuary have been analysed. The majority of sediment samples in the Loughor Estuary are classified as fine sand according to the British Standard Classification. These investigations showed that salinity fluctuations in the estuary caused by tides have major influence on the behaviour of nitrogen compounds (ammonium, nitrate and nitrite). The observed concentration of salinity at site 1b for example, ranged from 0.02 ppt to 26.9 ppt.

Deposition and resuspension of sediment and organic matter are influenced by the tidal cycle. It was observed that the median grain size did not show any influence on the ammonium adsorption behaviour. Salinity was found to influence suspended sediment concentrations. Suspended sediment concentrations of the Loughor Estuary increased with increasing salinity concentrations, and varied between neap and spring tides. The influence of salinity on the suspended sediment was higher at low tidal range (neap tides) than at high tidal range (spring tides), with the suspended sediment concentrations being higher at low tidal range conditions for all salinity concentrations. The amount of suspended sediment concentrations during neap tides and spring tides ranged from 594 mg/l to 668.5 mg/l at site 1a and from 479 mg/l to 616 mg/l at site 1b respectively. At high tide the suspended sediment was lower due to dilution effects of the incoming sea water. The dilution effect was found to be stronger than the larger flow velocities.

During neap tide conditions, the volume of water at high tide conditions will be less than the volume of water during spring tides at high tide. At the same time the maximum velocities present during spring tides will be higher than during neap tides causing higher turbulence during spring tides than during neap tides. The suspended sediment concentrations were not found to be affected with increasing salinity concentrations as measured in this study.

The ammonium ion adsorption in the sediments collected from the Loughor Estuary was found to obey the Langmuir isotherm equation. The error analysis (Chi-squared and nonlinear regression) confirmed that ammonium adsorption data fits the Langmuir isotherm well. The adsorption coefficient of ammonium was found to be highest in the sediments with comparatively high amounts of organic carbon. Organic matter was therefore considered to be one of the important factors controlling the degree of ammonium adsorption in the Loughor Estuary.

Salinity affected the distribution of ammonium between the sediment and the water column. Ammonium adsorption was found higher for low than high salinity concentrations. It is possible to calculate the rate of change of ammonium adsorption in the sediment with respect to increasing salinity from the first order Equations 7.3 and 7.4 which were developed in this study and are presented in Section 7.2.3. It was found that the rate of change is higher within the lower range of salinity concentrations (0 ppt to 25 ppt).

The measured nitrogen compound concentrations of NH_4^+ , NO_3^- and NO_2^- during incoming and outgoing tides show that:

- During the autumn and spring dissolved inorganic nitrogen (DIN) was dominated by nitrate and nitrite, showing that nitrification rates are high during these seasons. The highest concentration of nitrate measured in the water column was 8.22 mg/l at site 3 on 13th March above the fresh water boundary (river Loughor). The source for this nitrate load could be from agricultural practices and from STWs outfalls from upstream from site 3.

- The highest nitrite concentration found was 10.23 mg/l at low tide at site 1a in December 2007.
- The DIN was dominated by ammonium in summer and the high ammonium concentrations found in the water column was 4.25 mg/l at site 1b at low tide from a sample collected 2/3 into the channel.
- The concentrations of nitrate and ammonium in the Loughor Estuary ranged between 0 mg/l to 8.22 mg/l for nitrate and 0 mg/l to 4.25 mg/l for ammonium. In contrast, the highest nitrate concentration in the water column of the Loughor Estuary was measured at site 1b of 7.74 mg/l.
- The nitrate concentrations in the water column of the Loughor Estuary were found higher compared to mean nitrate concentrations of <6.2 mg/l recorded for other estuaries in UK (Mortimer et al (1998). However, the maximum NO_3^- concentration of 31 mg/l in the Humber Estuary indicates the highest amount of nitrate that was found in literature to have been measured within UK estuaries. The Loughor Estuary has the highest ammonium and nitrite concentrations of 4.25 mg/l and 10.23 mg/l found for all UK estuaries. It is therefore implied that the Loughor Estuary water may not meet the standards set by the EC Habitats, Shellfish and Nitrates Directives due to the high concentrations of nutrients on the form of (ammonium, nitrite and nitrate). These high levels of nutrients are prone to leading to algal growth and subsequently eutrophication, which has strong effect on the estuary water quality.
- The highest ammonium concentration adsorbed on bed sediment was found at 80.3 $\mu\text{g/g}$. This sample was collected in March 2008, at low tide during low salinity concentration in the water column of 3.03 ppt. It was observed that organic carbon has an important influence in ammonium adsorption. Ammonium adsorption was found higher in the sample with high amount of organic carbon.
- Ammonium adsorption coefficients and salinity influences for different types of clays and sand as shown in this study have not previously been reported in the literature.
- The suspended sediment concentrations present in the Loughor Estuary appear to be independent of the velocities present and not

sensitive to the difference in velocities. This usual finding could be due to the suspended sediment size distribution present in the Loughor Estuary which was not measured in this study.

- Finding of higher nitrogen concentrations in the coastal waters as a source back into the Estuary during incoming tidal conditions during the summer months

8.5 Recommendations and the future work resulting from field work

The outcomes of this study have led to the following recommendations for further studies:

- Measurement of velocities present in the Loughor Estuary along the estuary for different tides is recommended
 - i) To calibrate the solute transport within the hydrodynamic model DIVAST.
 - ii) To determine travel time of pollution.
- Future investigation of the nitrification and denitrification processes within the bed sediment, under both aerobic and anaerobic conditions in fresh water and saline water. Also more studies of microbial degradation of organic matter within the sediments.
- More sampling, further out in the estuary, to investigate the concentrations of nitrogen compounds such as nitrate within the coastal waters as a nitrogen source, especially in the summer months when elevated concentrations were found.
- Further investigation of the suspended sediment of the estuary including size distribution analysis to analyse the ammonium adsorption and desorption on the suspended sediment particles and determine the adsorption isotherms of ammonium for different sediment size ranges.
- More research is recommended to determine the nitrate concentrations and adsorption for suspended sediments and bed sediments under different conditions such as sediment organic matter content and for different grain sizes.

- Further research is recommended to investigate the effect of reed beds presented in the Loughor Estuary on the ammonium and nitrate concentrations and adsorption processes and the influence of reed beds on the nitrogen cycle in the water column. The reed beds are located close to site 2 opposite on the opposite shore.

References:

Abdulgawad, F., Bockelmann-Evans, B.N., Sapsford, D., Williams, K.P. and Falconer, R.A. 2008. Ammonium ion adsorption on clays and sand under freshwater and sea water conditions. Proceedings of the 16th IAHR-APD and the 3rd IAHR-ISHS Conference, Hohai, China.

Abrishamchi, A., Ebrahimian, A., Tajrishi, M. and Marino, M.A. 2005. Case study: Application of multicriteria decision making to urban water supply, Journal of Water Resources Planning and Management, vol.131, no.4, pp. 326–335.

Agnew, D., C. Grieve, P. Orr, G. Parkes and N. Barker. 2006. Environmental benefits resulting from certification against MSC's Principles and Criteria for Sustainable Fishing'. Marine Resources Assessment Group (MRAG) and MSC, May 4. Available at:

http://www.msc.org/documents/environmental-benefits/MSC_Environmental_Benefits_Report_Phase1_FINAL_4Ma.pdf

[accessed 6 March 2010]

Ærtebjerg, G., Andersen, J. H. and Hansen, O. S. (eds) (2003) Nutrients and Eutrophication in Danish Marine Waters. A Challenge for Science and Management. National Environmental Research Institute, 126 pp.
<http://eutro.dmu.dk/>

[accessed 14 July 2008]

Ambrose, R. B, Jr., Wool, T. A., and Martin, J. L. 1993a. The Water Quality Analysis Simulation Program, WASP5; Part A: Model Documentation. U.S. Environmental Protection Agency, Environmental Research Laboratory, Athens, Georgia, 202 pp.

- Ambrose, R. B, Jr., Wool, T. A., and Martin, J. L. 1993b. The Water Quality Analysis Simulation Program, WASP5; Part B: The WASP5 Input Dataset, Version 5.00. U.S. Environmental Protection Agency, Environmental Research Laboratory, Athens, Georgia, 80 pp.
- Anggara-Kasih, G. A. and Kitada, T. 2004. Numerical simulation of water quality response to nutrient loading and sediment resuspension in Mikawa Bay, central Japan: quantitative evaluation of the effects of nutrient-reduction measures on algal blooms.
- Ayers, RS., Westcot, DW. 1994. Water quality for agriculture. FAO irrigation and drainage paper, vol. 29. Rome: FAO; 174 pp.
- Avery, AA. 1999. Infantile methomogolebinemia re-examining the role of drinking water nitrates. Environmental health perspectives, vol.107, pp 583-586
- Allred, B.J., Bigham, J.M., Brown, G.O, 2007. The impact of clay mineralogy on nitrate mobility under unsaturated flow conditions. Soil Sci. Soc. Am, vol. 6, pp. 212-232.
- Arnold, J. G., and Allen, P. M. 1999. Automated methods for estimating base flow and groundwater recharge from stream flow records. J. American Water Resour. Assoc. vol. 35, no, 2, pp. 411 - 424.
- B.Bockelmann-Evans., F. Abdulgawad., X. Wang., R. Falconer. 2008. Sampling and modeling water and sediment nutrient concentrations along the salinity gradient in the upper Loughor Estuary, ECSA Symposium 'The Severn Estuary; Cardiff, Walls, UK.
- B.Bockelmann-Evans., Schnauder.I., Fenrich.E and Falconer.R. 2007. Development of a catchment - wide nutrient model. Water management 160 (MA4), pp. 35-42.

- Berner, R. A. 1980. Early diagenesis - A theoretical approach. Princeton Series in Geochemistry, Princeton University Press, Princeton, NJ
- Berelson, W.M., Heggie, D., Longmore, A., Kilgore, T., Nickolson, G., Skyring, G. 1998. Benthic nutrient recycling in Port Phillip Bay, Australia. *Estuarine and Coastal Shelf Science*, vol. 56, pp. 917-934
- Beven, k. 1989. Changing ideas in hydrology-the case for physically-based models. *Journal of Hydrology*, vol. 106, pp. 157-172.
- Binkley, D., Burnham, H., Allen, H.L. 1999. Water quality impacts of forests fertilization with nitrogen and phosphorus. *Forest ecology and management*, vol. 121, no. 3. Publisher: Elsevier Science, Amsterdam, Netherlands.
- Boynton, W. R, and Kemp. W. M. 1985. Nutrient regeneration and oxygen consumption by sediments along an estuarine salinity gradient. *Marine Ecology Progress Series*, vol. 23, pp 44-55.
- Boorman, D.B. 2003. Climate Hydrochemistry and Economics of surface water systems (CHESS): Adding a European dimension to the catchment modelling experience developed under LOIS. *sci. Total Environment*, 314-316, 411-437. Retrieved October 2005, from ScienceDirect database.
- Boatman, C.D. and Murray, J.W. 1982. Modelling exchangeable NH_4^+ adsorption in marine sediments: process and controls of adsorption. *Limnology and Oceanography*, vol. 27, pp. 99-110
- Brown, L., Barnwell, T.O., Jr. 1987. The enhanced stream water quality models QUAL2E and QUAL2E-UNCAS: Documentation and user manual. Report EP/600/3-87/007. US. Environmental Protection Agency, Athens, GA.
- Burt, T., and Johnes, P. 1997. Managing water quality in agricultural catchments. *Transactions- Institute of British Geographers*, ns. 22, pp. 61-68.

- Caddy, John. F. 1993. "Contrast Between recent Fishery Trends and Evidence from Nutrient Enrichment in Two Large Marine ecosystems: The Mediterranean and the Black Seas", "in Kenneth Sherman, et al. (eds), Large Marine Ecosystems: Stress, Mitigation and Sustainability, Washington, D.C; American Association for the Advancement of Science, pp. 137-147.
- Caraco, N.F. and Cole, J.J.1999. Human impact on aquatic nitrogen loads: A regional scale study using large river basins. *Ambio*, vol. 28, pp.167-170.
- Carpenter, E.J., Dunham, S.1985. Nitrogenous nutrient uptake, primary production, and species composition of phytoplankton in the Carmans River estuary, Long Island, New York. *Limnol. Oceanogr*, vol. 30, pp 513-526.
- Camerom. A. C., Trivedi, P.K. 2005. Microeconometrics – methods and applications. Cambridge University Press.
- Chapra, S.C. 1997. Surface Water-Quality Modeling, McGraw-Hill, New York, pp.844.
- Chapra,S.C. 2003. Engineering water quality models and TMDLs, *Journal of Water Resources Planning and Management*, no.129, vol. 4, pp. 247–256
- Chapra, S. C., Pelletier, G. J and Tao, H. 2005. QUAL2K: A modeling framework for simulating river and stream water quality. Version 2.02: documentation and users manual. Civil and Environmental Engineering Department, Tufts University, Medford, Maryland.
- Chapra, S and Pelletier,G. 2003. QUAL2K: A modeling framework for simulating river and stream water quality: Documentation and users manual, Civil and environmental engineering department., Tufts University, Medford, MA.
- Cheremisinoff, P. N. and Ellerbusch, F. 1978. "Carbon adsorption handbook", Ann Arbor Science Publishers, Mich. pp 55.

Campbell, NS., D'Arcy B., Frost CA., Novotny, V., Sansom AL. 2004. Diffuse Pollution – An Introduction to the Problems and the Solutions. IWAP, London. ISBN 1900222531

Casey, T. J. 1992. Unit treatment processes in waster and wastewater engineering, Wiley series, New York, January - International Conference on Water and the Environment (World Meteorological Organisation, Dublin/Ireland

Department of Water Affairs and Forestry (DWAF).1995. Water Quality Management series. Crocodile River Catchment Eastern Transvall.

Water Quality Situation Assessment, Department of water Affairs and Forestry, Pretoria, Volumes 1-9.

DEFRA, 2002.The Goverment's Strategic Review of diffuse water pollution from agriculture in England: Agriculture and water: A Diffuse Pollution Review.

Dong, L. F., Nedwell, D. B., Colbeck, I., Finch, J. 2004. Nitrous oxide emission from some English and Welsh rivers and estuaries. Water air and soil pollution, vol. 4,pp. 127-134.

<http://www.defra.gov.uk/environment/water/quality/diffuse/agri/reports/pdf/dwpa01-b.pdf>. accessed 10 April 2009.

Eaton,A,D., Clesceri,L,C., Greenberg,A,E (ed). 1995. Standard Methods for the Examination of Water and Wastewater, 19th edition, American Public Health Association, Washington, DC.USA

Erisman, J.W and Draaijers,G.P.J. 1995, Atmospheric deposition in relation to acidification and eutrophication, Elsevier. Amsterdam.

EUROHARP. 2006. Towards European harmonised procedures for quantification of nutrient losses from diffuse sources. Available at: euroharp.org/pd/pd/index.htm#5. Accessed 5 June 2009.

Eyre, B.D. and Ferguson, A.J.P. 2002. Comparison of carbon production and decomposition, benthic nutrient fluxes and denitrification in seagrass, phytoplankton, benthic microalgae- and macroalgae-dominated warm-temperate Australian lagoons. *Marine Ecology Progress Series*, vol. 229, pp. 43-59.

Falconer R A, Lin B L, Kashefipour S M. 2001. Bathing water quality in riverine systems: a combined data analysis and modelling approach, *Proc 3rd Int Symp on Environmental Hydraulics*

Falconer, R.A. 1992. Flow and water quality modelling in coastal and inland waters. *Journal of Hydraulic Research, IAHR*, no. 30, vol. 4, pp. 437–452

Falconer, R.A and Owens, P.H. 1990. Numerical modeling of suspended sediment fluxes in estuarine, *Coastal and Shelf Science*, vol. 31, pp. 745-762

Fevre, N. M. L. and Lewis, G. D. 2003. The role of resuspension in enterococci distribution in water at an urban beach. *Water Science and Technology* 47(3), pp. 205-210

Freundlich, H. 1906. Über die Adsorption in Lösungen. *Physical chemistry*, vol. 57, pp. 385–470

Galloway, J.N., Schlesinger, W.H., Lery, I.H., Michaels, A., Schnoor, J.L. 1995. Nitrogen fixation: Anthropogenic enhancement-environmental response. *Global Biogeochemical Cycles*, vol. 9, pp. 235-252.

Gardner, W.S., Seitzinger, S.P., Malczyk, J.M. 1991. The effects of sea salts on the forms of nitrogen released from estuarine and freshwater sediments: does ion pairing effect ammonium flux? *Estuaries*, vol. 14, pp. 558-568

Gardner, W. S., McCarthy, M. J., An, S., Sobolev, S., Sell, K.S., Brock, D. 2006. Nitrogen fixation and dissimilatory nitrate reduction to ammonium (DNRA) support nitrogen dynamics in Texas estuaries. *Limnol, Oceanogr.*, vol. 51, pp. 558-568

Gurbutt, P.A. (1993) Ituna: a Model of the Solway Firth. Lowestoft: Ministry of Agriculture, Fisheries and Food, Directorate of Fisheries Research, Fisheries Research Technical Report, 93, 13 pp.

Crittenden, B.; Thomas, W. J. 1998. Adsorption Technology and Design. Butterworth-Heinemann: Oxford, U.K..

Harris, G. G., Bately, P., Jerakoff, B., Newell, D., Fox, R., Molloy, J., Parslow, S., Walker, D., Hall, A., Murray, and G, Skyring. 1996. Port Phillip Bay environmental study final report. CSIRO, Canberra, Australia.

Hassanin, S. 2007. Evaluation of water quality of elnasr-3 main drain in Egypt using QUAL2K model, Eleventh international water technology conference, IWTCII 2007 Sharm el-sheikh, Egypt.

Heathwaite, A. L., Fraser, A. I., Johnes P. J., Hutchins M., Lord E. & Butterfield D. 2003. The Phosphorus Indicators Tool: a simple model of diffuse P loss from agricultural land to water. Soil Use and Management, vol. 19, pp. 1-11.

Heggie, D. T., Skyring, G. W., Orchard, J., Longmore, A. R., Nicholson, G. J., Berelson, W M. 1999. Denitrification and denitrifying efficiencies in sediments of Port Phillip Bay: direct determinations of biogenic N₂ and N-metabolite

Horn AJ, Goldman CR. 1983. Limnology. University of California Press, Berkeley

Hingston, F.J., A.M. Posner, and J.P. Quirk. 1972. Anion adsorption by goethite and gibbsite. I. The role of the in determining adsorption envelopes. J. Soil Sci, vol. 23, pp. 177–192.

Hou, L., Liu, M., Jiang, H. Y., Xu, S. Y., Ou, D. N., Liu, Q. M., Zhang, B. L. 2003. Ammonium adsorption by tidal flat surface sediments from the Yangtze. Environmental Geology, vol. 45, pp. 72 -78

James, R.T., Martin,J., Wool,T., Wang, P.F. 1997. A sediment resuspension and water quality model of lake Okeechobee, American water resources association,vol. 33, No .3

Jeon.B-H, Dempsey.B.A, Burgos.W.D, Royer.R.A.2001. Reactions of ferrous iron with hematite. Colloids and Surfaces A: Physicochem.Engineering Aspects, vol. 191, pp. 41-55

John Postgate (ed) 1987, Nitrogen fixation, Edward Arnold, Australia.

Jenne, E. A. 1995, 'Metal adsorption and desorption from sediments: I. Rates', in H. E. Allen (ed.),Metal Contaminated Aquatic Sediments, Ann Arbor Press, Inc., Ann Arbor, MI, pp. 81–110.

Jianlong,W., and K Jing. 2004. The characteristics of anaerobic ammonium oxidation (ANAMMOX) by granular sludge from an EGSB reactor, Process Biochemistry, no. 5, vol.40, pp.1973- 1978.

Jeff.M., John.M.1999. Ammonium release from resuspended sediment in the Lagona adre estuary. Marine Chemistry, vol. 65, pp. 97-110

Kirk, R.E and Othme,r D.F, 1947, Encydopolida of chemical technology. Mack printing Co., Easton, U.S.A, vol. 1, pp. 206-232

Kafkafi Uzi. 2007. Seven lectures on selected topics. Topics in fertilization and plant nutrition 1st. available on line
[http://departments.agri.huji.ac.il/plantscience/topics_irrigation/uzifert/1stmeet.
hm](http://departments.agri.huji.ac.il/plantscience/topics_irrigation/uzifert/1stmeet.htm). [accessed 18 July 2007]

Knisel, W.1992. Simulating process in nonpoint source pollution. Proceedings of the 1992 winter simulation Conference 1159-1165.

Kinjo and Pratt, 1971. T. Kinjo and P.F. Pratt, Nitrate adsorption: II. In competition with chloride, sulfate and phosphate. Soil Sci. Soc. Am, vol. 35 ,pp. 725–728.

Kroeze, C., Seitzinger, S.P, 1998. The impact of land use on N₂O emissions from watersheds draining into the Northeastern Atlantic and European Seas. Environmental Pollution 102 (1998) 149-158.

Krom M.D. and Berner R.A.1980. Adsorption of phosphate in anoxic marine sediments. Limnology and Oceanography, vol. 25, pp.797–806.

Langmuir, I.1918. The adsorption of gases on plane surface of glass, mica and platinum, J.AM.Chemistry. Soc,vol. 40,pp 1361-1402

Letey, J and Knapp ,K.C.1995. Simulating saline water management Strategies with application to arid-region agroforestry. Environmental quality, vol 24, pp. 934-940.

Lucas S and Cocero M. J.2002. report, Study and modeling of furfural adsorption and activated carbon under supercritical conditions, Univ. of Spain , www.iq.uva.es. accessed 12 July 2007.

Lucas, S. and Cocero, M.J.2004. Adsorption isotherms for ethylacetate and furfural on activated carbon from supercritical carbon dioxide. Fluid Phase Equilibria,vol. 219, pp 171-179.

Ludersen, A.L. 1983. Mass transfer in engineering practice, John Wiley and sons, New York

Liang, L.,Morgan, J.1990. Chemical aspects of iron oxide coagulation in water: Laboratory studies and implications for natural system. Aquatic sciences, no. 52, vol 1, pp. 32-55.

- Landen, A., Hall, P.O. 1998. Seasonal variation of dissolved and adsorbed amino acids and ammonium in a near-shore marine sediment. *Marine Ecology Progress series*, vol. 170, pp 67-84
- Lin, B., J. M. Wicks, R. A. Falconer and K. Adams. 2005. Integrating 1D and 2D hydrodynamic models for flood simulation. *Water management* 159, pp, 19-25
- Lin, B., and Falconer, R.A., (1997), "Tidal Flow and Transport Modelling using ULTIMATE QUICKEST Scheme", *Journal of Hydraulic Engineering (ASCE)*, Vol. 123, No. 4, pp. 303-314
- Martin R.J. and AL-Bahrani K.S, 1978, Adsorption studies using gas-liquid chromatography. Experimental factors influencing adsorption. *Water Research*, vol. 12, pp. 879-888
- Martin, R.J. and AL-Bahrani K.S, 1979, Adsorption studies using gas-liquid chromatography-iv. Adsorption from biosolute systems. *Water Research*, vol. 13, pp. 1301-1304,
- Milan Smisek, Slavoj Cerny. 1970. Active carbon: manufacture, properties and applications, Amsterdam, Elsevier Pub. Co
- Mangelsdorf, P.C., Wilson. T.R., Daniel, E. 1969. Potassium enrichments in interstitial waters of recent marine sediments. *Science*, vol. 165, pp. 71-174
- Mackin, J.E., Aller, R.C. 1984. Ammonium adsorption in marine sediment. *Limnol Oceanogr*, vol. 29, pp. 250-257
- MASM Modified Artificial Sea water
<http://www.ccap.ac.uk/media/recipes/MASM.htm>. [accessed 31 May 2007].
- Morin, J., Morse, W.J. 1999. Ammonium release from resuspended sediments in Laguna Madre estuary. *Marine Chemistry*, vol. 65, pp. 97-110

- Morse, J.W., Morin, J. 2005. Ammonium interaction with coastal marine sediments: influence of redox conditions on K*. *Marine Chemistry*, vol. 95, pp. 107-112
- Mortimer, R. J. G., Krom, M.D., Watson, P.G., Frickers, P.E., Davey, J. T and Clifton, R. J. 1998. Sediment-water exchange of nutrients in the intertidal zone of the Humber Estuary, UK. *Marine Pollution Bulletin*, vol.37, pp. 261-279
- Park, S.S and Y.S.Lee.2002. A water quality modeling study of the Nakdong River, Korea ,*Ecological modelling*, vol.152,pp.65-75.
- Paul, M. C. 2005. Environmental fluid dynamic code (EFDC) version 050712, dynamic solutions,LLC, USA
- Perry R.Hinton. 1995, *Statistics explained – A guide for social science students*. Routledge London. EC4P4EE.
- Pieterse,N.M., Bleuten, W and Jorgensen, S.E.2003.Contribution of point sources and diffuse sources to nitrogen and phosphorus loads in lowland river tributaries. *Hydrology*, vol. 271, pp. 213–225
- Poots, V.J.P., Mckay, O and Healy, J.J.1976a.The removal of acid dye from effluent using natural adsorbents-pear. *Water Research*, vol. 10, pp. 1061-1066
- Margesin, R (ed). 2008. *Soil Biology, Permaforst Soils*,Springer.
- Rao C. S.1994. *Environmental pollution control engineering 2nd Edition*, Wiley Eastern, India
- Read S, Elliott M, and Fernandes T. 2001. The possible implications of the Water Framework Directive and the Species & Habitats Directive on the Management of Marine Aquaculture. In: Read Pea, editor. *The implications of directives, conventions and codes of practice on the monitoring and regulation*

of marine aquaculture in Europe (MARAQUA). Aberdeen (UK) Fisheries Research Services p 58–74.

Raaphorst, W.V., Malschaert, J.F.P. 1996. Ammonium adsorption in superficial North Sea sediments, *Cont. Shelf Res*, vol 16, pp. 1415–1435

Rosenfeld, J. K. 1979. Ammonium adsorption in near shore anoxic sediments. *Limnology. Oceanogr*, vol. 24, pp. 356-364.

Rysgaard, S., Thastum, P., Dalsgaard, T., Bondo Christensen, P and Sloth, N.P. 1999. Effects of salinity on NH_4^+ adsorption capacity, nitrification, and denitrification in Danish Estuarine sediments. *Estuaries*, no.1, vol. 22, pp. 21-30.

Schoellhamer, D. H. 2001. Influence of salinity, bottom topography, and tides on locations of estuarine turbidity maxima in northern San Francisco Bay, pp. 343–357. In: W. H. McAnally, and A. J. Mehta [eds.], *Coastal and estuarine fine sediment transport processes*. Elsevier.

Schoellhamer, D.H. 1996. Factors affecting suspended- solids concentrations in South San Francisco Bay, California: *Journal of Geophysical Research*, no. C5, vol. 101, pp. 12087- 12095

Sips, R. 1948. On the Structure of a Catalyst Surface. *Physical chemistry*, vol.16, pp. 490–495.

Schnauder, B., Bockelmann-Evans, B. Lin. 2007. Modelling faecal bacteria pathways in receiving Estuary and Coastal waters. *Maritime Engineering*, 160 (MA4), pp. 143-153.

Sharkar, M and Acharya, P. K. 2006. Use of fly ash for the removal of phenol and its analogues from contaminated water *Waste Management*, vol.26, pp 559-570.

Suzuki m. and Kawazoi K. 1974. *J. of Chem. Eng. Of Japan*, vol. 7, No.5, pp. 346-349.

Suzuki, M. 1990. *Adsorption engineering*, Elsevier, Amsterdam.

- Nixon, G., Boicourt, W.C. 1996. The fate of nitrogen and phosphorous at the land-sea margin of the North Atlantic Ocean. *Biogeochemistry*, vol.35, pp 141 – 180
- Seitzinger, SP., Gardner, WS., Spratt, AK .1991. The effect of salinity on ammonium adsorption in aquatic sediments: implications for benthic nutrient cycling. *Estuaries*, vol.14, pp 167- 174
- Simon, N. S and Kennedy, M. M.1987. The distribution of nitrogen species and adsorption of ammonium in sediments from the tidal Potomac River and Estuary. *Estuarine, Coastal and Shelf Science*, vol. 25, pp 11-26
- Sayles M. A., K. Aagaard, and L. K. Coachman.1979. *Oceanographic Atlas of the Bering Sea Basin*. University of Washington Press, 158 pp.
- Sayles, F.L., and F. T.Manheim. 1975. Interstitial solutions and diagnosis in deeply buried marine sediments: Results from the Deep-Sea Drilling Project. *Geochim. Cosmochim. Acta*, vol. 39, pp.103-127.
- Schroder, J., Aarts,H., Ten Berge,H., Van keulen, H., and Neeston, J. 2003. An evaluation of whole- farm nitrogen balances and related ideas for efficient nitrogen use. *European Journal of Agronomy*, vol 20,pp. 33-44.
- Sokrut, N.2001. A distributed coupled model of surface and subsurface dynamics as a tool for catchment management, Royal Institute of Technology, Stockholm, Sweden.
- Singh, V. P.1996. *Kinematic wave modelling in water resources: surface water hydrology*, Wiley, New York.
- Sugai, S.F., Henrichs, S.M., 1992. Rates of amino acid decomposition in Resurrection Bay (Alaska) sediments. *Mar. Ecol. Prog. Ser.* 88, pp. 129–141
- Sparks., D.L.1995. *Environmental Soil Chemistry*. , Academic Press, San Diego, CA

Sparks, Tim, Diana Kountcheva, Bettina Bockelmann, and Roger Falconer. 2006. Physical and numerical modeling of groundwater and surface-water interactions with a conservative tracer. Proceedings of ISSMGE: 5 th International congress on environmental geotechnics Cardiff, Wales, UK, June 2006

Sparks, T., Namin,M., Bockelmann, B and Falconer, R.A.2005. Integrated modeling of 2-D surface water and groundwater flow with contaminant transport. Proceedings of XXXI International association of hydraulic engineering and research congress (IAHR Congress) Water engineering for the future – choices and challenges, Seoul Kores.

Tanaka, K and Kodama, M.2007. Effect of resuspended sediments on the environmental changes in the inner part of Ariake Bay, Japan. Bull . Fish. Res, no.19, pp.9-15

Thomas J and Crittenden BD, (1998), Adsorption Technology and Design, Butterworth-Heineman, 271 pp book, ISBN 0-7506-1959-7

Townsed, D.w.1998. Sources and cycling of nitrogen the Gulf of marine. University Maine, Sch Marine Science ,Orono, Me 04469. Journal of Marine Systems,no.3-4,vol.16,pp.283-295.Publisher:Elsevier Science, B.V., Amsterdam, Netherlands.

Toth.J.S.1964, The physical chemistry of soils in Bear.F.E (ed). Chemistry of the soil. Reinhold. Second edition.pp 2-155

United State Environmental Protection Agency [USEPA]. 1985. Guidelines for deriving numerical national water quality criteria for the protection of aquatic organisms and their uses. Washington DC: Office of Research and Development.

PB85–227049. [USEPA] US Environmental Protection

United States Environmental Protection Agency (USEPA). 1991. Guidance for Water Quality based Decisions: The TMDL Process. EPA 440/4-91-001, Office of Water, Washington, DC.

Vollenweider, R. A., Rinaldi, A. and Montanari, G. 1992. Eutrophication, structure and dynamics of a marine coastal system: results of ten-year monitoring along the Emilia-Romagna coast (Northwest Adriatic Sea). *Science of the Total Environment*, Supplement, 63–106

Wark, K. and Warner, C. F.: 1976, *Air pollution, It's origin and control*, Harper and Row Pub., New York.

Wang DQ, Chen ZL, Qian CP, Xu SY. 2002. Effect of salinity on ammonium exchange behavior at the sediment–water interface in east Chongming tidal flat. *Mar Environ Sci*, vol. 21, pp 5-9

Weber, W.J.1972. *Physiochemical processes for water quality control*, Wiley-Inter science, New York

Wild , Alan. 1993. *Soils and the environment: an introduction*. Cambridge University press. ISBN. 0-521-43859-4

Winterwerp, J.C., van Kesteren, W.G.M., 2004. *Introduction to the Physics of Cohesive Sediment in the Marine Environment*, Elsevier, Amsterdam, Netherlands.

WHO. 2004. *Nitrates and Nitrites in Drinking-Water*. WHO/SDE/WSH/04.08/56. Rolling revision of the WHO guidelines for drinking-water quality. Draft for review and comments. Geneva:World Health Organization.

Available:

http://www.who.int/water_sanitation_health/dwq/chemicals/en/nitratesfull.pdf

[accessed 4 june 2009].

Yang, S.L., Zhang.J., Zhu. J. 2004. Response of suspended sediment concentration to tidal dynamics at a site inside the mouth of an inlet: Jiaozhou Bay (China). Hydrology and earth system sciences, vol. 8,no.2, pp. 170-182.

Zhang. X., Rygwelski, K. R., Rossmann, R., Pauer, J.J., Kreis, R.G. Jr. 2008. Model construct and calibration of an integrated water quality model (LM2-Toxic) for the Lake Michigan Mass Balance Project, Ecological Modelling, 219,92-106.

Appendix 1 Mineralogy of the sediment (XRD analysis)

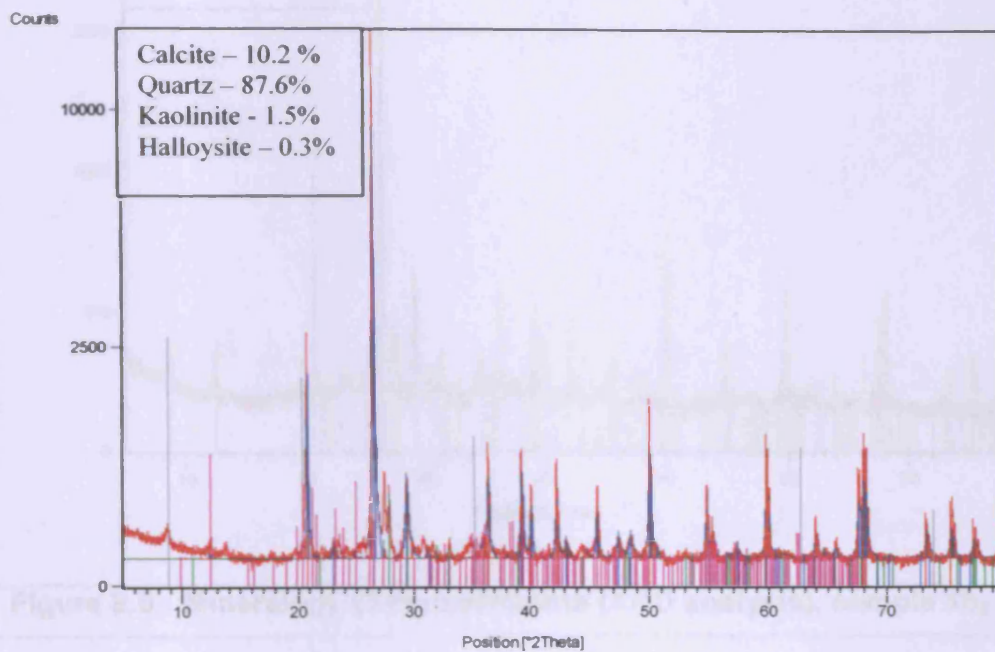


Figure 8.3 Mineralogy of the sediment (XRD analysis) ,sample 1b₁

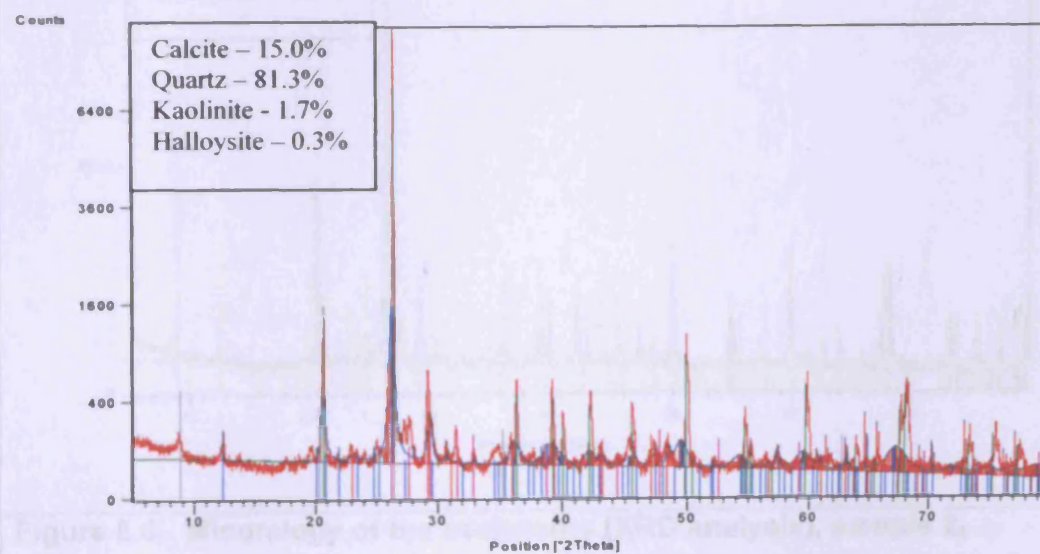


Figure 8.4 Mineralogy of the sediments (XRD analysis), sample 1b₂

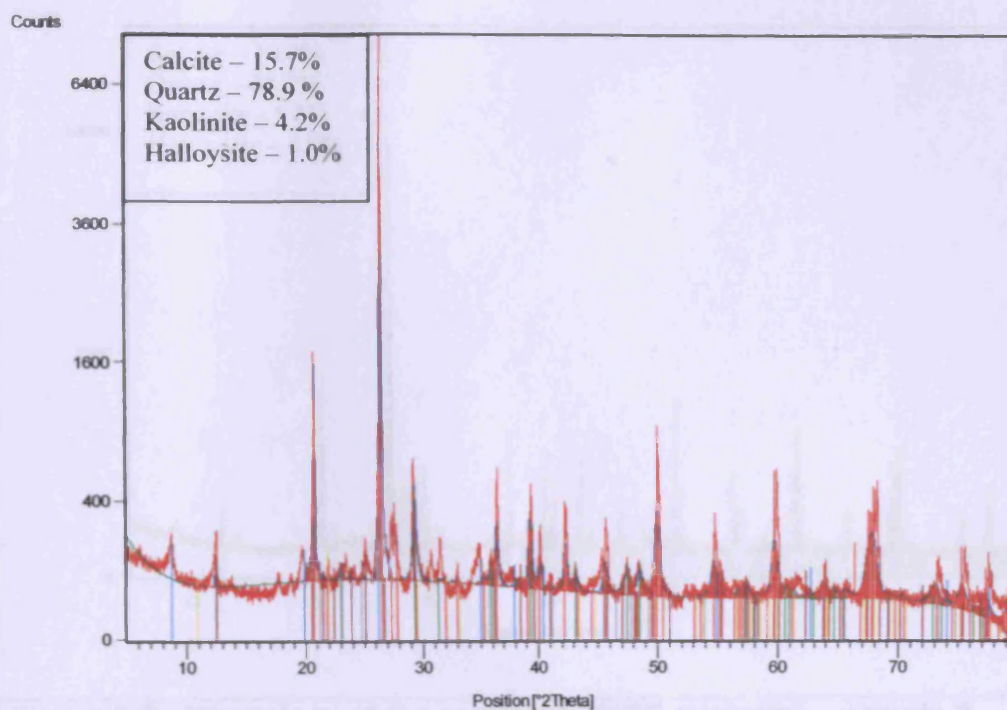


Figure 8.5 Mineralogy of the sediments (XRD analysis), sample 1b₃

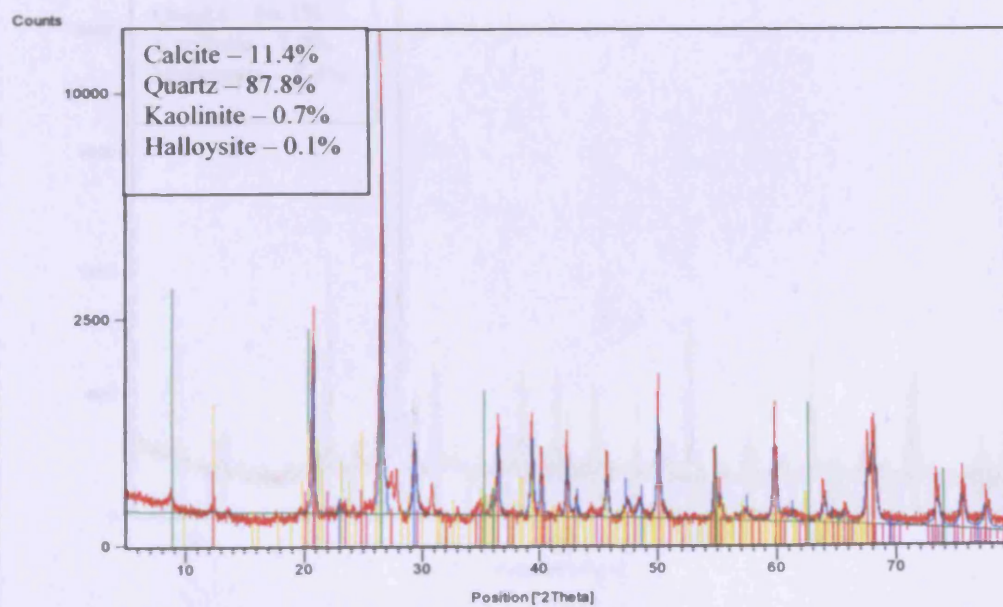


Figure 8.6 Mineralogy of the sediments (XRD analysis), sample 2₁

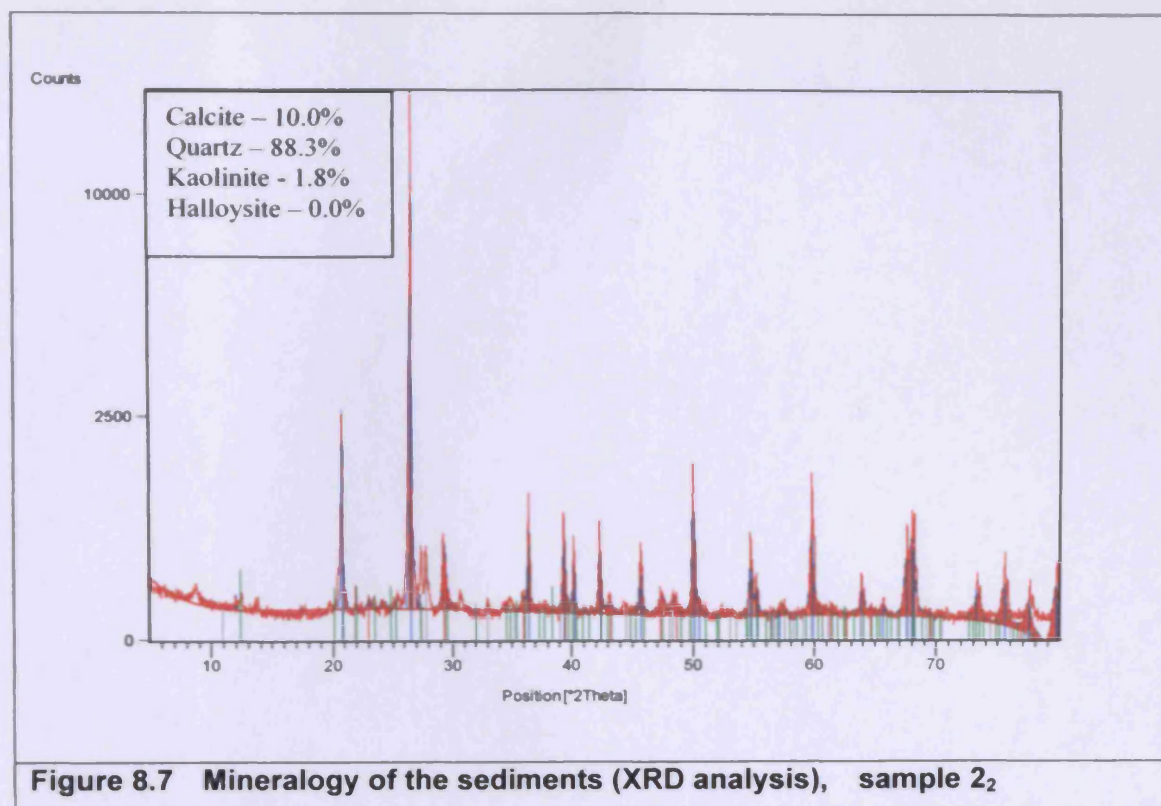


Figure 8.7 Mineralogy of the sediments (XRD analysis), sample 2₂

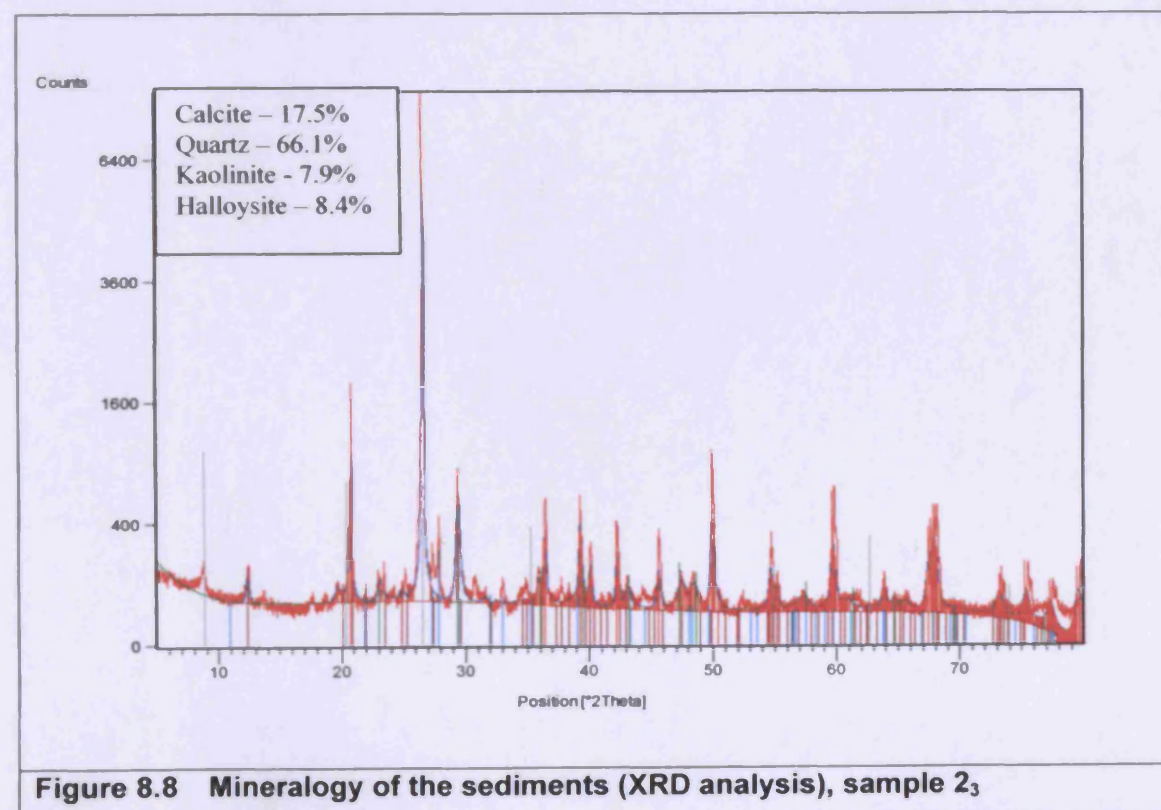


Figure 8.8 Mineralogy of the sediments (XRD analysis), sample 2₃